

# Investigating the impact of OCT transporter genotype on metformin- induced vitamin B<sub>12</sub> deficiency

Thesis submitted in accordance with the requirements of  
the University of Liverpool for the degree of  
Doctor in Philosophy

by

**Lewis Anthony Green**

September 2015

## **Declaration**

This thesis is the result of my own work. The material contained within this thesis has not been presented, nor is currently being presented, either wholly or in part for any other degree or qualification.

Lewis Anthony Green

This research was carried out in the Department of Molecular and Clinical Pharmacology, in the Institute of Translational Medicine, at the University of Liverpool.

# Acknowledgements

Firstly, I would like to thank my supervisors, Munir Pirmohamed and Kevin Park for their support and guidance. I would also like to thank the BBSRC and AstraZeneca for funding the work in this thesis. Special thanks must go to Dan Carr and Fabio Miyajima for their knowledge and additional support throughout this PhD. Equally I'd like to thank Steven Lane for his continuous help with the statistics throughout this thesis.

I would like to thank my industrial supervisors Glynis Nicholls, Tracy Mills, Amy Cheung, Colin Howes, for their support, expertise and enthusiasm which made my time at AstraZeneca enjoyable. Additional thanks goes to all the people within the DMPK, Genetics and Pharmacometrics departments for making me feel welcome.

I'd like to collectively thank all my colleagues at the Wolfson Centre for Personalised Medicine and the Department of Molecular and Clinical Pharmacology at the University of Liverpool. I've truly met some wonderful people there and will be leaving with many fond memories. An honourable mention goes out to Jon, who is still my friend after Blackpool beat Liverpool FC during their brief spell in the premier league, twice. I'd like to thank my work wife Andrew, my doppelganger according to the department; although not quite as handsome as me. It's been a pleasure to share the PhD experience with you.

I would also like to acknowledge the patients who kindly donated their blood for this project, without which this thesis would not exist.

Thanks to Mum, Dad and Steph for support and encouragement. I would also like to express my gratitude to my new extended family for their support.

And finally, thanks to my best friend and my wife, Helen, for constant support, encouragement and endless love throughout the duration of my studies and for supporting my still ongoing, endless mission to still be a student. But most importantly, thanks for not going in to labour before I submit this thesis; you may now give birth. And lastly, thanks to Tess, truly a man's best friend.

# Contents

<b>ACKNOWLEDGEMENTS</b> .....	III
<b>PUBLICATIONS AND COMMUNICATIONS</b> .....	V
<b>ABSTRACT</b> .....	VII
<b>ABBREVIATIONS</b> .....	VIII
<b>CHAPTER 1: GENERAL INTRODUCTION</b> .....	1
<b>CHAPTER 2: IDENTIFICATION OF GENETIC VARIATIONS IN METFORMIN DRUG TRANSPORTERS <i>SLC22A1</i> AND <i>SLC22A2</i></b> .....	49
<b>CHAPTER 3: ASSESSING THE IMPACT OF GENETIC VARIATIONS ON METFORMIN TRANSPORT USING <i>IN SILICO</i> STRUCTURAL MODELS OF OCT1 AND OCT2</b> .....	84
<b>CHAPTER 4: DEVELOPMENT AND VALIDATION OF A HYDROPHILIC INTERACTION LIQUID CHROMATOGRAPHY – TANDEM MASS SPECTROMETRY METHOD FOR THE DETERMINATION OF METFORMIN IN HUMAN PLASMA IN T2DM PATIENTS</b> .....	111
<b>CHAPTER 5: POPULATION PHARMACOKINETIC MODELLING OF METFORMIN IN T2DM PATIENTS</b> .....	143
<b>CHAPTER 6: INVESTIGATION OF FACTORS INFLUENCING METFORMIN-INDUCED VITAMIN B<sub>12</sub> DEFICIENCY</b> .....	171
<b>CHAPTER 7: FINAL DISCUSSION</b> .....	195
<b>APPENDICES</b> .....	205
<b>BIBLIOGRAPHY</b> .....	220

# Publications and communications

## Manuscripts in preparation

**Green L.A.**, Lane S., Constable S., Antoine D.J., Park B.K., Pirmohamed M. (2015). METFORMIN AND VITAMIN B<sub>12</sub> DEFICIENCY IN PATIENTS WITH TYPE 2 DIABETES MELLITUS: ASSOCIATION WITH DOSE BUT NOT SYSTEMIC EXPOSURE.

**Green L.A.**, Nicholls G., Constable S., Antoine D.J., Park B.K., Pirmohamed M. (2015). DEVELOPMENT AND VALIDATION OF A HILIC-MS/MS METHOD FOR DETERMINATION OF METFORMIN IN T2DM PATIENTS.

## Oral Presentations

“Investigating the impact of polymorphic drug transporters on metformin induced vitamin B<sub>12</sub> deficiency”. Pharmacology postgraduate seminar day, 20 June 2014, Liverpool, UK.

“The characterisation of model systems to investigate the impact of genetic variation and expression in drug transporters on drug safety and efficacy”. Drug Transporters DMPK Group Meeting, 29 February 2012, AstraZeneca, Manchester, UK.

“The characterisation of a model system to investigate the impact of genetic variation and expression in *SLC22A* drug transporters on metformin drug safety and efficacy”. European Medicines Research Training Network Workshop, 23-26 February 2012, Manchester, UK.

“The identification of genetic variations in *SLC22A1* and *SLC22A2* – potential link to vitamin B<sub>12</sub> deficiency in metformin treated T2DM”. External Collaborations Genetics Research Day, 21 January 2011, AstraZeneca, Manchester, UK.

## **Poster presentations**

**Green L.A.,** Nicholls G., Mills T., Antoine D.J., Park B.K., Pirmohamed M.:

THE CHARACTERISATION OF MODEL SYSTEMS TO INVESTIGATE THE IMPACT OF GENETIC VARIATION AND EXPRESSION IN DRUG TRANSPORTERS ON DRUG SAFETY AND EFFICACY. 2<sup>nd</sup> External Science DMPK Collaborations Day, 17<sup>th</sup> November 2010, AstraZeneca UK.

**Green L.A.,** Nicholls G., Mills T., Antoine D.J., Park B.K., Pirmohamed M.

NOVEL OCT1 & OCT2 GENETIC VARIATIONS – POTENTIAL LINK TO METFORMIN ASSOCIATED VITAMIN B12 DEFICIENCY DURING DIABETES. British Toxicology Society (BTS) Annual Congress, 27-30 March 2011, Durham, UK.

**Green L.A.,** Nicholls G., Mills T., Antoine D.J., Park B.K., Pirmohamed M.

STRUCTURAL MODELLING OF OCT-1,-2 &-3 – ASSESSING THE IMPACT GENETIC VARIATIONS ON METFORMIN TRANSPORT. In Vitro Toxicology Society, 8-9 November 2011, Liverpool, UK.

# Abstract

Metformin is the first-line therapy for the treatment of Type 2 Diabetes Mellitus (T2DM) and is the most widely prescribed anti-diabetic drug in the world. A common and potentially hazardous side-effect of metformin treatment is vitamin B<sub>12</sub> deficiency. OCT1 (*SLC22A1*) and OCT2 (*SLC22A2*) are highly polymorphic drug transporters responsible for the hepatic and renal uptake of metformin, respectively. Studies have documented that variants in OCT1 and OCT2 can have an effect on transporter function altering the pharmacokinetic profile of metformin, which leads to inter-individual variability in metformin response. To date, there is no reported correlation between the systemic concentration of metformin, metformin dose, and vitamin B<sub>12</sub> levels, and whether this is affected by OCT gene polymorphisms. Thus, the overall aim of the studies described in this thesis was to explore the relationship between metformin pharmacokinetic parameters, OCT genetic variants and vitamin B<sub>12</sub>. To investigate this, we used biological samples from a cohort of 75 T2DM patients receiving metformin.

In order to quantify metformin in human plasma, we designed and developed a sensitive and transferable hydrophilic interaction liquid chromatography (HILIC) method for both UV and mass spectrometric detection. This was successfully used to quantify metformin plasma levels in our cohort which ranged from 49 to 4908 ng/mL with a mean of 1879 ng/mL.

To genotype patients for OCT1 and OCT2 polymorphisms, the *SLC22A1* AND *SLC22A2* genes were sequenced using Sanger sequencing. Fifty genetic variants were identified within the 5' untranslated region (5'UTR), 3'UTR, exon and exon-intronic boundaries across both genes. Two novel single nucleotide polymorphisms (SNPs) were identified in *SLC22A1* (g.-59C>T, c.+14 A>G). The potential effect of these variants on transporter function was explored using bioinformatic algorithms and *in silico* 3D structural modelling and ligand docking techniques.

The metformin plasma concentrations and genetic data was collated with other clinical and biological data and incorporated into a population pharmacokinetic (PopPK) model to assess the influence genetic variants on metformin pharmacokinetics. Serum urea levels were the biggest predictor of metformin clearance. Only one genetic variant, the rs113569197 insertion was shown to be a significant influence on the predicted population metformin clearance in a univariate model. The rs113569197 variant was of particular interest as it represented an 8 bp insertion across an exon-intron boundary in *SLC22A1*, which we predicted to result in a premature stop codon and truncated protein. However, in multivariate PopPK modelling, this variant dropped out possibly because of lack of power.

Multivariate linear regression analysis was used to explore the effect of metformin clinical variables and OCT genetic variants on vitamin B<sub>12</sub> concentrations. Metformin dose, mg/kg of body weight ( $P < 0.0001$ ) and serum folate levels ( $P = 0.048$ ) contributed independently to explain 32% ( $P < 0.0001$ ) of the variance in serum vitamin B<sub>12</sub> concentrations, but there was no effect of metformin plasma concentration ( $P = 0.08$ ) or genetic variants in *SLC22A1* and *SLC22A2*. These data show that decreased serum vitamin B<sub>12</sub> concentrations in patients with T2DM are driven more by metformin dose than exposure indicating that the mechanism by which metformin causes vitamin B<sub>12</sub> deficiency is due to its effects at the level of the intestine, rather than systemically.

In conclusion, the work presented in this thesis demonstrates that the mechanism of metformin-induced vitamin B<sub>12</sub> deficiency is related to the dose, but not the plasma concentration of metformin. Genetic variants in *SLC22A1* and *SLC22A2* did not influence vitamin B<sub>12</sub> levels in this patient group. Further work is required to define whether metformin specific drug transporters expressed in the intestine are responsible for metformin-induced vitamin B<sub>12</sub> deficiency in order to better understand the pathogenesis.

# Abbreviations

## Acronym

ADME	Absorption, distribution, metabolism, excretion
aa	Amino-acid
AMPK	AMP-activated protein kinase
AMP	Adenosine monophosphate
AP	Apical
ARE	AU-rich elements
ATP	Adenosine triphosphate
AUC	Area under the curve
BL	Basolateral
BMI	Body Mass Index
BNF	British National Formulary
bp	Base pair
BSV	Between subject variability
C <sub>18</sub>	Octadecyl carbon chain
cDNA	Complementary DNA
CL	Clearance
CL <sub>CR</sub>	Creatinine clearance
C <sub>max</sub>	Maximum (peak) serum concentration
CV	Coefficient of variance
ddNTP	Dideoxyribonucleotide triphosphate
DNA	Deoxyribonucleic acid
dNTP	Deoxyribonucleotide triphosphate
DOPE	Discrete optimised protein energy
EC	Evolutionary conserved
ECM	Extra Cellular Matrix
EDTA	Ethylendiaminetetraacetic acid
EU	Evolutionary unconserved
FDA	U.S. Food and Drug Administration
GFR	Glomerular filtration rate
GI	Gastrointestinal
Hb	Haemoglobin
HbA1c	Glycosylated haemoglobin A1c
HCT	Haematocrit
HET	Heterozygous
HILIC	Hydrophilic interaction liquid chromatography
HOM	Homozygous
HPLC	High performance liquid chromatography
hr	Hour
HWE	Hardy-Weinberg equilibrium
IBW	Ideal body weight
IF	Intrinsic factor

Ka	Absorption constant
kb	Kilo base
kDa	kiloDalton
L	Litre
LacY	Lactose permease
LBW	Lean body weight
LD	Linkage disequilibrium
LLOQ	Lower limit of quantification
LOD	Limit of detection
M	Molar
<i>m/z</i>	Mass-charge ratio
MAF	Minor allele frequency
MATE	Multi-drug And Toxic compound Extrusion
MCV	Mean Corpuscular Volume
MeCN	Acetonitrile
mg	Milli grams
min	Minute
mL	Milli litre
mM	Milli molar
MPP <sup>+</sup>	1-methyl-4-phenyl-pyridinium
mRNA	Messenger RNA
MS	Mass spectrometry
Mw	Molecular weight
NaDS	Sodium dodecyl sulfate
NCBI	National Centre for Biotechnology Information
ND	Not determined
ng	nanogram
NHS	National Health Service
NICE	National Institute for Health and Care Excellence
NONMEM	Non-linear Mixed Effect Modelling
NSAID	Non-steroidal anti-inflammatory
nsSNP	Nonsynonymous single nucleotide polymorphism
OCT	Organic Cation Transporter
OFV	Objective function Value
OGTT	Oral glucose tolerance test
PCR	Polymerase chain reaction
PD	Pharmacodynamic
pg	Picogram
PK	Pharmacokinetic
PMAT	Plasma membrane monoamine transporter
PopPK	Population pharmacokinetic
PPARs	peroxisome proliferator-activated receptors
PPI	Proton pump inhibitor
QC	Quality control

RP	Reverse phase
rpm	Rotations per minute
rs	Reference SNP
RSE	Relative standard error
RT	Reverse transcriptase
SAS	Splicing acceptor site
SD	Standard deviation
SDS	Splicing donor site
SLC	Solute carrier family
SNP	Single-nucleotide polymorphism
SS	Steady-state
T1DM	Type I diabetes mellitus
T2DM	Type II diabetes mellitus
TBS	tris-buffered saline
TEA	Tetraethylammonium
Tmax	Time at which the Cmax is observed
TMD	Transmembrane Domain
TMG	Tetramethyl guanidine
TV	Typical value
U	Activity unit
UK	United Kingdom
ULOQ	Upper limit of quantification
UTR	Untranslated region
UV	Ultra violet
V <sub>d</sub>	Volume of distribution
WHO	World Health Organisation
WT	Wild-type
VPC	Visual predictive check
μM	Micro molar

# **Chapter 1**

## **General Introduction**

## Contents

<b>CONTENTS.....</b>	<b>4</b>
<b>1.1 DIABETES .....</b>	<b>4</b>
1.1.1 TYPE I DIABETES.....	4
1.1.2 TYPE II DIABETES.....	4
<b>1.2 PATHOPHYSIOLOGY .....</b>	<b>5</b>
1.2.1 LONG TERM COMPLICATIONS .....	6
<b>1.3 EPIDEMIOLOGY .....</b>	<b>7</b>
<b>1.4 ECONOMIC COSTS .....</b>	<b>7</b>
<b>1.5 DIAGNOSIS .....</b>	<b>8</b>
<b>1.6 MANAGEMENT .....</b>	<b>9</b>
1.6.1 LIFESTYLE CHANGES.....	9
1.6.2 ANTI-DIABETIC THERAPIES.....	10
1.6.2.1 <i>Insulin secretagogues</i> .....	10
1.6.2.2 <i>Thiazolidinediones</i> .....	10
1.6.2.3 <i>Alpha-glucosidase inhibitors</i> .....	11
1.6.2.4 <i>dipeptidyl-peptidase-IV inhibitors</i> .....	11
1.6.2.5 <i>Insulins</i> .....	11
1.6.2.6 <i>Biguanides</i> .....	12
<b>1.7 METFORMIN .....</b>	<b>13</b>
1.7.1 MECHANISM OF ACTION.....	14
<b>1.8 CLINICAL PHARMACOLOGY OF METFORMIN .....</b>	<b>15</b>
1.8.1 ADMINISTRATION .....	15
1.8.2.1 <i>Absorption</i> .....	16
1.8.2.2 <i>Therapeutic range</i> .....	17
1.8.2.3 <i>Distribution</i> .....	17
1.8.2.4 <i>Elimination</i> .....	18
<b>1.9 ADVERSE EVENTS AND TOXICITY .....</b>	<b>20</b>
1.9.1 METFORMIN ASSOCIATED LACTIC ACIDOSIS .....	20
1.9.2 GASTROINTESTINAL SIDE EFFECTS .....	21

<b>1.10 VITAMIN B<sub>12</sub></b> .....	<b>21</b>
1.10.1 SOURCES VITAMIN B <sub>12</sub> .....	21
1.10.2 VITAMIN B <sub>12</sub> FUNCTION .....	23
1.10.3 VITAMIN B <sub>12</sub> HOMEOSTASIS .....	24
1.10.4 SIGNS AND SYMPTOMS OF VITAMIN B <sub>12</sub> DEFICIENCY.....	25
1.10.5 DIAGNOSIS OF VITAMIN B <sub>12</sub> DEFICIENCY .....	27
1.10.5.1 <i>Total serum vitamin B<sub>12</sub></i> .....	27
1.10.5.2 METHYLMALONIC ACID.....	28
1.10.5.3 HOMOCYSTEINE .....	28
1.10.5.4 HOLO-TRANSCOBALAMIN II.....	29
1.10.5.5 THE SCHILLING TEST.....	29
1.10.6 VITAMIN B <sub>12</sub> REFERENCE RANGE.....	30
1.10.7 METFORMIN & VITAMIN B <sub>12</sub> .....	30
<b>1.11 METFORMIN DRUG TRANSPORTERS</b> .....	<b>34</b>
1.11.1. SLC TRANSPORTER FAMILY.....	34
1.11.1.1 <i>Organic Cation transporter 1</i> .....	35
1.11.1.2 <i>Organic Cation transporter 2</i> .....	37
1.11.1.3 <i>Organic Cation transporter 3</i> .....	37
1.11.2 SLC22A TRANSPORTER GENETICS .....	38
1.11.3 OTHER METFORMIN DRUG TRANSPORTERS.....	40
1.11.3.1 <i>Multidrug And Toxin Extruders</i> .....	40
1.11.3.2 <i>Plasma membrane monoamine transporter</i> .....	40
<b>1.12 METFORMIN DRUG-DRUG INTERACTIONS</b> .....	<b>41</b>
<b>1.13 METHODS</b> .....	<b>43</b>
1.13.1 DNA SEQUENCING .....	43
1.13.2 MOLECULAR MODELLING .....	43
1.13.3 HPLC-MS/MS.....	44
1.13.4 POPULATION PHARMACOKINETICS .....	45
<b>1.14 AIMS OF THE PROJECT</b> .....	<b>47</b>

## 1.1 Diabetes

The term diabetes mellitus describes metabolic disorders with multiple aetiologies characterised by chronic hyperglycaemia as a result of disturbances in carbohydrate, fat and protein metabolism due to defects in insulin action, secretion, or combination of both. Typical symptoms include thirst, polyuria, blurry vision, lethargy and weight loss. These symptoms are commonly not severe, or may be absent, and consequently hyperglycaemia sufficient to cause pathological and functional changes may be present for a long time before the diagnosis is made.

There are two main types of diabetes; Type I diabetes mellitus (T1DM) previously known as insulin-dependent diabetes or juvenile diabetes, and Type II diabetes mellitus (T2DM), previously known as noninsulin-dependent diabetes mellitus.

### 1.1.1 Type I Diabetes

T1DM is a chronic autoimmune disorder that arises from the destruction of insulin producing  $\beta$ -cells in the pancreas. This is characterised by the presence of autoimmune antibodies specific to islet cells or insulin, which leads to  $\beta$ -cell destruction (Samuelsson et al., 1994). The detection of these antibodies and the C-peptide assay, which measures endogenous insulin production, help distinguish T1DM from T2DM (Atkinson and Eisenbarth, 2001). The exact cause of T1DM is unknown, but a number of explanatory theories include genetic susceptibility, environmental factors and/or exposure to an antigen from precipitating events such as viral or bacterial infection (Van Belle et al., 2011).

### 1.1.2 Type II Diabetes

T2DM is the most common form of diabetes and is characterised by disorders of insulin secretion and insulin action, either of which may be the predominant feature leading to insulin resistance. Both are usually present at the time that this form of diabetes is clinically manifest. In general, most cases of T2DM have

an unknown aetiology, but there are some other forms where specific factors are involved in causation including gestational diabetes and Maturity Onset Diabetes of the Young (Simha and Garg, 2008). This thesis is only concerned with T2DM, and thus, further discussion will focus on this form of diabetes only.

## 1.2 Pathophysiology

Under normal physiological conditions, glucose from the diet, or breakdown products of carbohydrates in the gut, are absorbed into the bloodstream elevating blood glucose levels. This rise in glucose levels stimulates the endocrine secretion of insulin from the  $\beta$ -cells of the pancreas, which binds to specific cellular receptors and facilitates entry of glucose into the cell. The cell then uses the glucose for energy. The increase in insulin secretion and the cellular glucose utilisation results in a decrease in blood glucose levels. A decrease in glucose levels is mirrored by a decrease in insulin production and secretion. Normal glucose levels can be maintained if hepatic gluconeogenesis matches insulin mediated glucose uptake in peripheral tissue. However, when insulin resistance creates an imbalance, T2DM can ensue (Shah et al., 2000).

A number of pathogenetic processes lead to the development of T2DM. These include mechanisms that lead to insufficient insulin production and thus secretion through the destruction of  $\beta$ -cells of the pancreas, and mechanisms that lead to insulin resistance in peripheral tissues; predominately liver, muscle and adipose tissue. This collectively results in high blood glucose levels or hyperglycaemia. Insulin is the only hormone that can lower blood glucose levels. However there are several counter-regulatory hormones which act to increase blood glucose levels, such as glucagon, growth hormone, catecholamines, thyroid hormones, and glucocorticoids (Mealey and Ocampo, 2007). These pathological processes can lead to an increased risk of other comorbidities including cardiovascular, peripheral vascular and cerebrovascular disease.

### 1.2.1 Long term complications

Long-term complications of diabetes mellitus include progressive development of complications that can be categorised as micro-vascular or macrovascular. Micro-vascular complications include nervous system damage or neuropathy, renal system damage or nephropathy and retinopathy (Stratton et al., 2000). Macro-vascular complications lead to cardiovascular disease and stroke in addition to peripheral vascular disease. In individuals with diabetes, >65% of individuals die as a result of these long-term complications (Nathan et al., 2009b). Risk factors for cardiovascular disease amongst people with diabetes are the same as in patients without diabetes including hypertension, hypercholesterolemia, obesity, lack of exercise and smoking, but the overall effect is compounded by the presence of diabetes (Espeland et al., 2007). Diabetes contributes to atherosclerosis partly because of elevated lipid levels; up to 97% of diabetic patients exhibit dyslipidaemia (Mazzone et al., 2008). Elevated plasma low density lipoprotein and decreased plasma high density lipoprotein levels lead to lipid deposition in large vessels which can accelerate atherosclerosis in T2DM.

Diabetic retinopathy is the most common micro-vascular complication in people who have T2DM; this can ultimately lead to blindness (Williams et al., 2004, Klein, 2002). More than 60% of T2DM patients will have some evidence of diabetic retinopathy during their lifetime (Williams et al., 2004). Hyperglycaemia can cause death of retinal intramural pericyte cells and thicken basement membranes. This blood-retinal barrier is particularly vulnerable to poor glucose control since the accumulation of glucose can increase the permeability of the barrier impairing vision (Stratton et al., 2000).

Diabetic nephropathy occurs in around 30% of T2DM individuals (de Zeeuw et al., 2004). It is diagnosed by unrelenting proteinuria. The most common test is the urine albumin:creatinine ratio which quantifies microalbuminuria for the early detection of nephropathy (Gross et al., 2005). The exact aetiology is unknown but hyperglycemia may cause hyperfiltration and renal injury,

advanced glycation products, and activation of cytokines which all lead to impaired kidney function (Jermendy and Ruggenti, 2007). High blood pressure is a major risk factor for nephropathy in T2DM, and hence there is a need to control blood pressure very strictly in diabetics. Other risk factors for nephropathy in T2DM are smoking, obesity, and genetic factors (Jermendy and Ruggenti, 2007).

Diabetic peripheral neuropathy is a frequent complication seen in approximately 30-50% of persons with diabetes (Vinik et al., 2003, Sun et al., 2005, Tesfaye et al., 1996). The function of neurons and blood vessels are intertwined; blood vessels require normal neuronal function while neurons require adequate blood flow. Narrowing of peripheral blood vessels can lead to neuronal dysfunction which correlates closely with hypoxia. Risk factors include age, duration of diabetes, smoking and hypertension (Teskaye et al., 2005). People with diabetic peripheral neuropathy are at risk of foot ulceration and neuropathic arthropathy which may lead to lower-extremity amputation (Singh et al., 2005).

### **1.3 Epidemiology**

Globally, diabetes is one of the commonest chronic diseases. It affects 9% of the world's population (World Health Organization, 2014). T2DM diabetes accounts for up to 85% of this total in both adults and children. In the UK, it affects 1.8 million people with an estimated 1 million currently undiagnosed (Diabetes UK, 2015). This figure is expected to rise in the coming decades because of the increased tendency of the population towards a sedentary lifestyle.

### **1.4 Economic costs**

It is currently estimated that about £10 billion is spent by the NHS on diabetes equating to roughly 10% of the NHS budget (Hex et al., 2012). The total cost, including direct and indirect costs, associated with diabetes in the UK currently

stands at £24 billion and this is predicted to rise to £40 billion by 2035 (Hex et al., 2012). In England 2012, 42 million prescription items for diabetes were dispensed in primary care units at a net ingredient cost of £768 million (The Health and Social Care Information Centre, 2013). What these estimated costs fail to take into account is the considerable costs to the individual in terms of loss of earnings and decreased quality of life.

## 1.5 Diagnosis

The diagnosis of diabetes is performed using two biochemical tests, glucose and/or glycosylated haemoglobin A1c (HbA1c) (Selvin et al., 2004). Fasted glucose measurements are more commonly used in practice - see Table 1.1 for interpretive results. Two separate fasted glucose levels outside the normal range with the individual presenting with symptoms of diabetes can be indicative of diabetes, with high glucose levels reflecting poor glycaemic control. However, if after two fasting glucose measurements the results are equivocal then an oral glucose tolerance test (OGTT) should be performed. This requires the patient to be fasted, a fasting blood sample is then taken (0 minutes), and then a glucose load (75g glucose - Polycal in 250-300 mL water) is given and a second glucose sample taken after 2 hours (120 minutes) (Stumvoll et al., 2000).

High serum glucose results in glucose non-enzymatically binding (glycating) to HbA1c. Thus a glycated HbA1c level can reflect the average glucose red blood cells have been exposed to in their lifetime: 115 days (>3 months) with 50% of HbA1c levels from the period preceding 30 days (Goldstein et al., 2004, Nathan et al., 2009a). The test result is independent of fasting status and does not require special test preparations as with the oral glucose test. As of 2011 the World Health Organisation (WHO) recommended glycosylated HbA1c for the diagnosis of diabetes and to screen an individual at high risk of diabetes (WHO, 2011). A glycosylated HbA1c of 48 mmol/mol is recommended as the cut-off point for diagnosing diabetes.

**Table 1.1 Values of glucose and glycosylated HbA1c for diabetes mellitus and other categories of hyperglycemia.**

	Glucose concentration mmol/L	Glycosylated HbA1c mmol/mol
Normal		<42
Fasting and 2 hrs*	<6.1 <7.8	
Diabetes Mellitus		42-47
Fasting <b>or</b> 2 hrs*	≥7.0 ≥11.1	
Impaired Glucose Tolerance		42-47
Fasting <b>and</b> after 2 hrs *	<7.0 ≥7.0-<11.1	
Impaired Fasting Glucose		≥48
Fasting <b>and</b> after 2 hrs *	6.1-6.9 <7.8	

\*Following the oral glucose test involving ingesting 75 g anhydrous oral glucose. Fasting is defined as no food for 10 hours prior to sample being taken, water is allowed. Glycosylated HbA1c levels are independent on fasting status and time following oral glucose tolerance test.

## 1.6 Management

T2DM can be managed in several ways, from dietary and lifestyle changes through to therapeutic interventions. Since the 1920s when diabetes was initially treated with porcine insulin (Banting et al., 1923), there are now 15 described classes of anti-glycaemic drugs available (Kahn and Buse, 2015). All share a common goal to reduce and maintain glucose within normal concentrations for as long as possible post diagnosis to prevent the development of complications.

### 1.6.1 Lifestyle changes

There is evidence to suggest that T2DM can be prevented by lifestyle changes in adults with impaired glucose tolerance such as changes in weight, physical activity or dietary factors (Gillies et al., 2007, Penn et al., 2009). Weight reduction and increase in exercise are also beneficial to slow the progression of diabetes and its complications (Boule et al., 2001). Although these lifestyle changes are proven to be effective, almost 50% of individuals will require the addition of oral hypoglycaemic drugs and/or insulin within 6yrs of diagnosis (Inzucchi, 2002).

## 1.6.2 Anti-diabetic therapies

There are five main groups of therapies used to control hyperglycaemia: insulin secretagogues, thiazolidinediones,  $\alpha$ -glucosidase inhibitors, insulins and the biguanides.

### 1.6.2.1 *Insulin secretagogues*

These are one of the most commonly prescribed class of antidiabetic drugs comprising of two distinct drug groups, the sulphonylureas and meglitinide analogues (Agarwal et al., 2014). Both classes primarily act to increase pancreatic insulin secretion. The sulphonylureas stimulate insulin secretion by binding to sulphonylurea receptors on the pancreatic  $\beta$ -cell plasma membrane, causing membrane depolarisation through potassium influx, and exocytosis and release of insulin (Turner et al., 1998, Campbell et al., 1991). The meglitinides also bind to the sulphonylurea receptors through a different mechanism to the sulphonylureas but result in a shorter duration of action, and are therefore used to control postprandial hyperglycaemia. As the efficacy of sulphonylureas decreases over time and is associated with a decrease in insulin secretion, combination therapy has focused mainly on implementing insulin-sensitising medications, including metformin and thiazolidinediones (Campbell et al., 1991). Insulin secretagogues are associated with weight gain as the increased insulin concentration leads to anabolic effects (Turner et al., 1998).

### 1.6.2.2 *Thiazolidinediones*

Otherwise known as the 'glitazones', this group of drugs are insulin sensitisers which activate peroxisome proliferator-activated receptors (PPARs) (Inzucchi, 2002). These are primarily expressed in adipose tissue and to a lesser extent the liver. When activated, these nuclear receptors increase the expression of insulin-sensitive genes. The downstream effects include increasing adipocyte lipogenesis, decreasing circulating free fatty acids and increasing glucose utilisation (Saltiel and Olefsky, 1996).

### *1.6.2.3 Alpha-glucosidase inhibitors*

Alpha-glucosidase inhibitors are competitive inhibitors of enzymes responsible for digesting carbohydrates (Lebovitz, 1998). This results in a delay in carbohydrate and glucose absorption thereby lowering postprandial blood glucose levels. They are only used in patients with non-insulin dependent diabetes.

### *1.6.2.4 dipeptidyl-peptidase-IV inhibitors*

Incretin hormones are defined as intestinal hormones that are released in response to carbohydrates (glucose) ingestion, from the intestinal mucosa of substances that enhance insulin secretion beyond the release caused by the absorbed glucose itself (Gautier et al., 2005). In humans, the incretin effect is mainly caused by two peptide hormones, glucose-dependent insulin releasing polypeptide, and glucagon-like peptide-1 (Vilsboll and Holst, 2004). Both of these hormones are both rapidly degraded into inactive metabolites by the enzyme dipeptidyl-peptidase-IV (DPP-IV). Thus, DPP-IV known as or gliptins, can be used as hypoglycemic medication in T2DM. Examples of which are Sitagliptin and Vildagliptin (Scheen, 2012).

### *1.6.2.5 Insulins*

Although insulin therapy is critical in T1DM, it also plays an important role in the treatment of with T2DM individuals and is usually indicated with the failure to achieve glycaemic control with oral hypoglycaemic drugs, exercise or diet. Between 2013-2014 there were 6.5 million insulin items prescribed, representing 14.3 % of items prescribed for T2DM (The Health and Social Care Information Centre, 2013).

Insulin is categorised in the British National Formulary (BNF) into three groups; short-acting (rapid onset), intermediate-acting and long-acting (Home et al., 2008). However, these exhibit different immunogenicity, pharmacokinetic and pharmacodynamic properties. The rapid-acting human insulin analogues have a faster onset but shorter duration (0.5-1 hr) of action than soluble insulin; as a result, compared to soluble insulin, fasting and preprandial blood-glucose

concentrations are higher, with postprandial blood glucose concentration being marginally lower.

Intermediate and long-acting insulins have an onset of action of approximately 1–2 hours and a duration of 16–42 hours. Some are taken twice daily in combination with short-acting insulin, and others are given once daily, particularly in elderly patients (Home et al., 2008).

Using insulin in combination with oral anti-diabetic therapies improves glucose levels in patients with poorly controlled glycaemia despite maximal and prolonged administration of oral anti-diabetic drugs (Mayfield and White, 2004).

#### 1.6.2.6 Biguanides

The French lilac (*Galega officinalis*) was firstly used for medicinal purposes in the 17<sup>th</sup> century when it was proposed to possess anti-diabetic properties (Patade and Marita, 2014). This plant contained high levels of galegine and guanidine, both of which exhibit anti-diabetic properties.

This interest in the therapeutic properties of guanidine ultimately led to the development of a class of compounds in the early 1900s called biguanides for the management of type II diabetes mellitus (Slotta and Tschesche, 1929). Anti-hyperglycemic biguanide therapies which share this class include metformin, buformin and phenformin (Figure 1.1).

Metformin is the only biguanide in use as both phenformin and buformin were discontinued from use in the 1970s due to their ability to lead to lactic acidosis - see section 1.9.1 (Irsigler et al., 1979). This thesis will now predominantly focus on metformin.

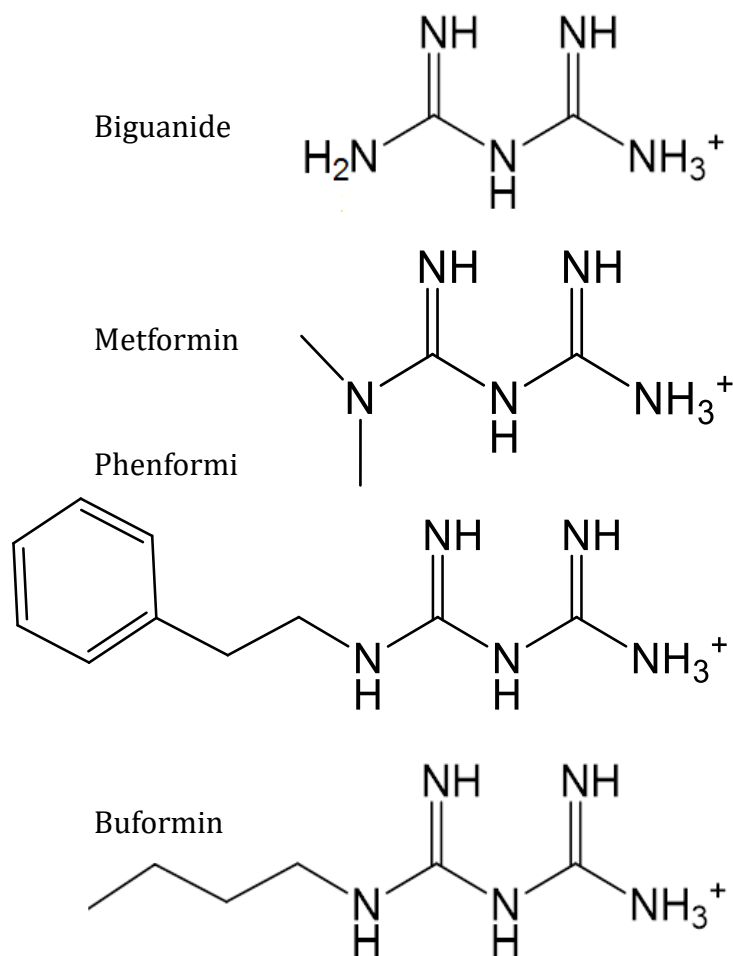


**Figure 1.1 Structure of metformin and related compounds.**

Top to bottom, biguanide, metformin, phenformin, buformin. All share a common structural feature; the biguanide backbone,  $\text{HN}(\text{C}(\text{NH})\text{NH}_2)_2$ . Structures drawn with ChemBioDraw.

## 1.7 Metformin

Metformin, *N,N*-dimethyl imidodicarbonimidic diamide, is the most commonly prescribed oral antidiabetic drug for T2DM globally and in the UK (Agarwal et al., 2014, Srinivasan et al., 2008). Between 2012 and 2013, over 16 million metformin items were prescribed in the UK (Prescribing and Primary Care team, 2013). Although metformin is the most commonly prescribed antidiabetic drug in the UK, it has a relatively low cost in comparisons to insulin therapies. NICE recommends that this drug should be the first choice for oral antidiabetic therapy (Home et al., 2008).

### 1.7.1 Mechanism of action

Metformin's primary action is to decrease hyperglycaemia, primarily through suppressing hepatic and skeletal gluconeogenesis and opposing the action of glucagon which has a pharmacological endpoint of reducing glucose levels (Wiernsperger and Bailey, 1999, He et al., 2009, Kirpichnikov et al., 2002). One study found that individuals with T2DM had twice the normal rate of gluconeogenesis and metformin reduced this rate by 24% (Hundal et al., 2000). The exact mechanism by which metformin suppresses gluconeogenesis still remains elusive. However, at the centre of metformin's mechanism of action is the alteration of energy metabolism of the cell. There are a number of proposed mechanisms by which metformin exerts its effects, including the inhibition of the mitochondrial respiratory chain (complex I), and activation of protein kinase A (PKA). The most widely accepted and studied mechanism is the activation of AMP-activated protein kinase (AMPK) (Foretz et al., 2010, Chen et al., 2013, Marcil et al., 2013). Other research suggests metformin does not directly activate AMPK but this is secondary to metformin's effect on the mitochondria, specifically inhibiting the mitochondrial respiratory-chain complex 1. Although the exact mechanism by which metformin inhibits the respiratory-chain complex 1 remains unknown, it is thought to decrease the hepatic energy state which indirectly activates AMPK (Um et al., 2007, Foretz et al., 2010). The downstream effects of this are dependent on the target organ or tissue. The summary of the clinical effects of metformin are summarised in Figure 1.2.

A genome-wide association study (GWAS) found common variants near the ataxia telangiectasia mutated (*ATM*) gene associated with glycaemic response to metformin in T2DM (Zhou et al., 2011). The *ATM* gene encodes a 370 kDa protein that is a serine/threonine protein kinase of the atypical phosphoinositide 3-kinase-related protein kinase family (van Leeuwen et al., 2012). This is involved in Deoxyribonucleic acid (DNA) repair and cell cycle control and crucially plays a role in the effect of metformin upstream of AMPK. It has been suggested that AMPK is an effector of the *ATM* gene and that

activation or inhibition of ATM alters AMPK activation (Sun et al., 2007, Lewis et al., 2009).

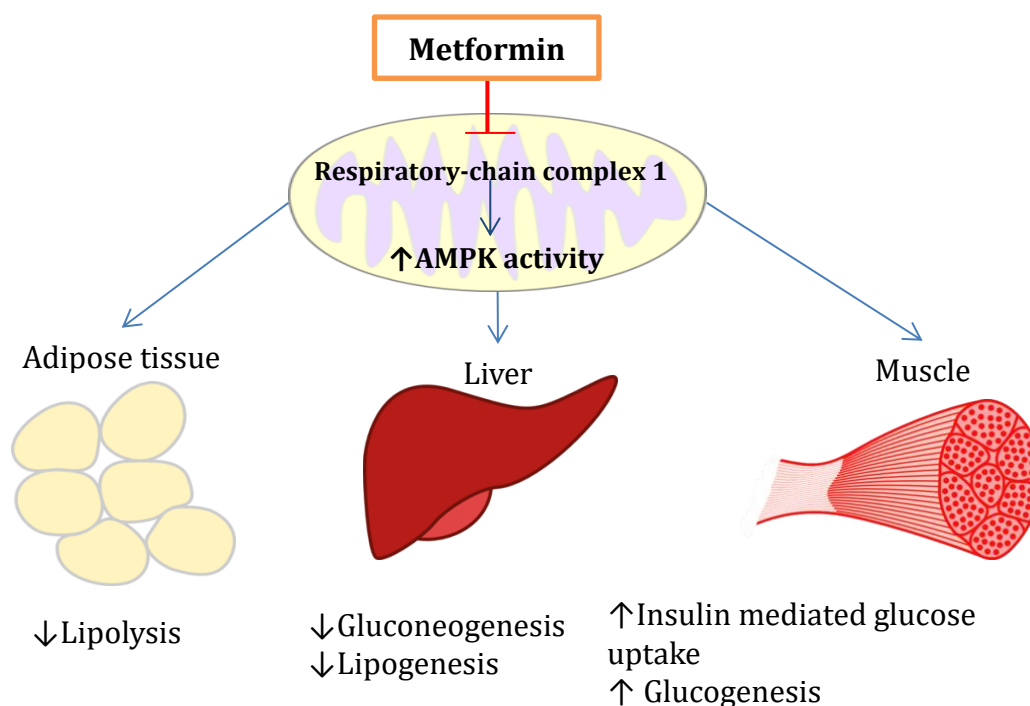


**Figure 1.2 Summary of metformin's mechanism of action**

Metformin's site of action is the mitochondria in liver, muscle and adipose tissue. Through the inhibition of the respiratory-chain complex I, AMPK is activated and performs downstream signaling effects which ultimately leads to countering insulin resistance and decrease gluconeogenesis.

## 1.8 Clinical Pharmacology of Metformin

### 1.8.1 Administration

Although metformin is primarily administered orally, intravenous dosing studies have revealed that metformin is rapidly cleared from the body with an intravenous plasma half-life ranging from 1.7 to 4.5 hr (Graham et al., 2011). Following intravenous administration, the majority of metformin was excreted in the urine unchanged, with 35-85% of metformin being recovered (Pentikainen et al., 1979, Tucker et al., 1981). Metformin's renal clearance is >4-fold higher than creatinine clearance; indicating metformin is actively secreted into the urine (Tucker et al., 1981). Sum et al (Sum et al., 1992) found no acute

effect of IV metformin on hepatic glucose production or peripheral glucose disposition, implying that a chronic persistent effect is more important than an immediate effect upon changes in the plasma metformin level. Metformin is not detected in faeces following intravenous administration (Tucker et al., 1981).

The oral daily doses of metformin range from 0.5-3 g (British National Formulary, 2015) which are administered as a hydrochloride salt (Mw 165.63); however metformin exists in its protonated state in the body (Mw 129.16). Normal dosing is dependent on severity of glycemic control in T2DM but normal dosing starts at 0.5 g with dose escalated if not HbA1c levels are not responding to treatment (British National Formulary, 2015). Exposure of oral metformin is dose proportional (Cullen et al., 2004). The pharmacokinetics of metformin and data presented in this thesis encompasses orally administered metformin.

#### *1.8.2.1 Absorption*

Oral metformin is absorbed predominantly from the small intestine (ileum). The bioavailability is unexpectedly high (40-60%), given its hydrophilicity and positive charge at all physiologic pH values (Scheen, 1996, Graham et al., 2011, Pentikainen et al., 1979). Metformin bioavailability is dose-disproportional, meaning there is a decrease in bioavailability with increasing dose. This has been observed by Tucker et al (1981) who found that the bioavailability of a 1.5 g dose of metformin was approximately 9-24% lower than that of a 0.5 g dose. Additionally, Sambol et al (1996) observed 12% lower bioavailability with a 0.85 g dose of metformin than with a 0.5 g dose. One possible hypothesis for the dose-disproportionality in absorption is because metformin is hydrophilic and largely ionised in the gastrointestinal (GI) tract, its permeability is limited, perhaps increasingly as it transcends the tract. Proctor et al. (2008) found that the major route of metformin absorption was not through cellular transport but through the tight junctions of ileal cells using paracellular proteins called claudins. Their *in vitro* studies found that metformin was taken up by cells in the apical membrane but not transferred through the basolateral membrane. They have suggested the 'sponge' hypothesis to describe the absorption of

metformin from the gut: as the basolateral membrane restricts cellular transport of metformin, it subsequently sequesters in the cell, and as luminal metformin concentration decrease and falls below the intracellular concentration, metformin is transported back into the intestinal lumen.

The peak plasma concentration ( $T_{max}$ ) is reached within 1-3 hr after oral intake of immediate release tablets and within 4-5 hr after oral intake of extended release tablets (Graham et al., 2011, Tucker et al., 1981). The delivery of metformin in the gut is considered to be the rate-limiting step in its absorption (Vidon et al., 1988). Steady-state metformin concentrations are reached within 24 to 48 hours (Scheen, 1996, Charles et al., 2006, Graham et al., 2011). Unlike the majority of therapeutic drugs, metformin is not metabolised (Hardie, 2007).

#### *1.8.2.2 Therapeutic range*

Despite metformin being in routine use for over 50 years, there is no definitive therapeutic range. A systematic review of metformin therapeutic concentrations found that cited concentrations ranged from 0.13 to 90  $\mu\text{g}/\text{mL}$  with the lowest and highest boundaries ranging from 0 and 1800  $\mu\text{g}/\text{mL}$ , with the majority of ranges proposed between 0.1 – 4  $\mu\text{g}/\text{mL}$  (Kajbaf, 2015). They concluded that cited concentrations were conceptual rather than based on scientific basis and advised that metformin therapeutic concentrations should be related to efficacious dose, and blood glucose control in long-term treated patients. The most common therapeutic concentrations range cited is between 1-2  $\mu\text{g}/\text{mL}$  (Dell'Aglio et al., 2009, Kruse, 2001, Graham et al., 2011, Scheen, 1996). Conversely, concentrations below 2.5  $\mu\text{g}/\text{mL}$  have been suggested to minimise the risk of metformin accumulation and the development of metformin associated lactic acidosis (Graham et al., 2011, Vecchio et al., 2014).

#### *1.8.2.3 Distribution*

Metformin absorption in the body is fast, but exhibits a slow transfer to other peripheral compartments (Pentikainen et al., 1979, Tucker et al., 1981). In

humans, metformin has been found to accumulate in the small intestine (Wang et al., 2002), liver (Graham et al., 2011, Nies et al., 2011b) and in the kidney (Kimura et al., 2005b, Kimura et al., 2005a). At the cellular level, localisation of metformin has been observed in rat cells in which 75% of metformin localised in the cytosolic compartment with the remainder found in other organelles such as mitochondrial and plasma membrane fractions (Wilcock et al., 1991). Metformin does not bind to plasma proteins, reflected by its high volume of distribution, of which is around 300 L (Scheen, 1996, Graham et al., 2011). Metformin is also taken up and accumulates in erythrocytes, contributing to a longer elimination half-life (Robert et al., 2003, Tucker et al., 1981). See Table 1.2 for a summary of metformin pharmacokinetics.

#### *1.8.2.4 Elimination*

The principle route of metformin elimination is through active tubular secretion in the kidney. Metformin is excreted unchanged in the urine; the population mean for renal clearance ( $CL_R$ ) is  $510 \pm 120$  mL/min (Graham et al., 2011, Pentikainen et al., 1979, Tucker et al., 1981). Approximately >80% of the oral dose is recovered in the urine following oral administration.

Graham et al (2011) concluded metformin's high clearance is attributed to three factors;

1. Metformin is a small polar molecule that does not bind to plasma proteins, and thus is readily filtered at the glomerulus.
2. Metformin is a substrate for OCT, MATE1 and MATE2K (see section 1.11.3.1).
3. Passive resorption should be minimal due to its low lipid solubility.

Renal function strongly correlated with the renal clearance rates observed with metformin treatment (Tucker et al., 1981); therefore, sufficient renal function is

**Table 1.2. Summary of pharmacokinetic parameters for oral metformin in humans.**

	units	Pentikainen (1979)	Tucker et al (1981)		Pentikainen (1986)	Timmins (2005)	Sambol (1996)
N		3	4	4	6	15	9
Dose	g	0.5	0.5	1.5	1.0	1.0	0.85
C <sub>max</sub>	mg/mL	1.55 (0.24)	1.02 (0.34)	3.1 (0.93)	1.58 (0.1)	1.32 (0.23)	1.51 (0.2)
T <sub>max</sub>	h	1.9 (0.43)	2.2 (0.3)	1.5 (0.4)	2.25 (0.4)	-	3.28 (0.4)
AUC	mg/h/L	9.08 (1.54)	6.71 (1.82)	18.4 (6.52)	-	-	11.7 (1.3)
CL <sub>R</sub>	mL/min	444 (23)	525 (125)	519 (278)	542 (78)	1265 (274)	1130 (457)
V <sub>D</sub>	L	69 (4.5)	276 (68)	-	-	559 (163)	1211 (690)
F	%	60 (8)	55 (15)	50 (21)	33	-	-

Pharmacokinetic parameter values are expressed as mean with the standard deviation in parenthesis. (N), the number of patients; C<sub>max</sub>, the maximal plasma metformin concentration; T<sub>max</sub>, is the time to the maximal plasma drug concentration; AUC, represents the area under curve of the metformin plasma concentration as a function of time; CL<sub>R</sub>, represents the renal clearance; V<sub>D</sub>, apparent volume of distribution; F, oral bioavailability (absorption).

essential to eliminate the drug (Jones et al., 2003). In cases where renal function is impaired, such as in diabetic nephropathy (see section 1.2.1), metformin can accumulate in the plasma and may lead to possible adverse reactions (see section 1.9). NICE recommends that the dose should be reviewed if estimated glomerular filtration rate (eGFR) less than 5 mL/minute/1.73 m<sup>2</sup> and to avoid if eGFR less than 30 mL/minute/1.73 m<sup>2</sup> (Home et al., 2008). Intravascular administration of iodinated contrast agents can cause renal failure, which can increase the risk of lactic acidosis with metformin (Goergen et al., 2010).

## **1.9 Adverse Events and Toxicity**

### **1.9.1 Metformin Associated Lactic Acidosis**

Metformin's most severe adverse effect, and that of other biguanides, is lactic acidosis (Graham et al., 2011, Brown et al., 1998, Kruse, 2001, Hulisz et al., 1998). However, unlike phenformin and buformin, the risk of developing lactic acidosis with metformin is lower (rate of 10 per 100,000) (Brown et al., 1998). Lactic acidosis is characterised by elevated blood lactate concentration (>5.0 mmol/L), decreased blood pH (<7.35), and electrolyte disturbances with an increased anion gap. The mortality rate of metformin associated lactic acidosis (MALA) is approximately 50% (Graham et al., 2011). This is predominately observed in high-risk patients such as those with significant renal impairment or acute renal failure (Brown et al., 1998). Therefore it is common that metformin should only be prescribed if patients' CL<sub>CR</sub> or eGFR is above a defined low limit. Other risk factors include old age associated with reduced renal function and metformin doses >2 g/day (Salpeter et al., 2003). Furthermore, individuals with T2DM may be more prone to MALA for a number of reasons, including their microvascular disease and risk of diabetic nephropathy (Hulisz et al., 1998, Jones et al., 2003). One study found metformin plasma concentrations of 20–107 mg/L in around 50% of patients with lactic acidosis (Lalau and Race, 1999).

The exact mechanisms of MALA are not fully understood. Metformin inhibits hepatic gluconeogenesis, which results in lactate formation (Wiernsperger and Bailey, 1999). Under normal physiological conditions, excess lactate is cleared by the kidneys and other biological processes. When impaired renal function is present, however, clearance of both lactate and metformin is reduced, leading to increased levels of both, thus resulting in an accumulation of lactic acid (Lalau and Race, 1999). Additionally metformin decreases liver uptake of lactate.

### **1.9.2 Gastrointestinal Side Effects**

The most common adverse effect of oral metformin is GI irritation, with symptoms including diarrhoea, cramps, nausea, vomiting, and increased flatulence (Scheen, 1996, Graham et al., 2011). The rates of GI intolerance range from 5 to 54%, with premature discontinuation of therapy in 4% of cases (Tarasova et al., 2012, Scheen, 1996, Bray et al., 2012, Haupt et al., 1991). These rates make metformin the most common antidiabetic drug associated with GI side effects (Garber et al., 1997). GI symptoms can be minimised through slowly incrementing dosage over a period of weeks (Scarpello, 2001).

## **1.10 Vitamin B<sub>12</sub>**

Vitamin B<sub>12</sub> was first described in 1926 by Minot and Murphy (Minot and Murphy, 1926) as a substance present in the liver which reversed pernicious anaemia. The vitamin was first isolated from liver and given the name vitamin B<sub>12</sub> in 1948 (Rickes et al., 1948). Vitamin B<sub>12</sub> belongs to the group of biologically active compounds chemically classified as cobalamins. Structure is illustrated in Figure 1.3.

### **1.10.1 Sources Vitamin B<sub>12</sub>**

As vitamin B<sub>12</sub> is only synthesised by bacteria, humans must obtain vitamin B<sub>12</sub> from dietary sources. However, some animals can source vitamin B<sub>12</sub> synthesised by their own bacterial colonic flora. Humans can obtain vitamin B<sub>12</sub> from foods of animal-origin, such as dairy products, eggs, fish and meat. The

recommended dietary reference intake for an adult in the UK is 1.5  $\mu\text{g}$  daily (National Health Service NHS, 2012).

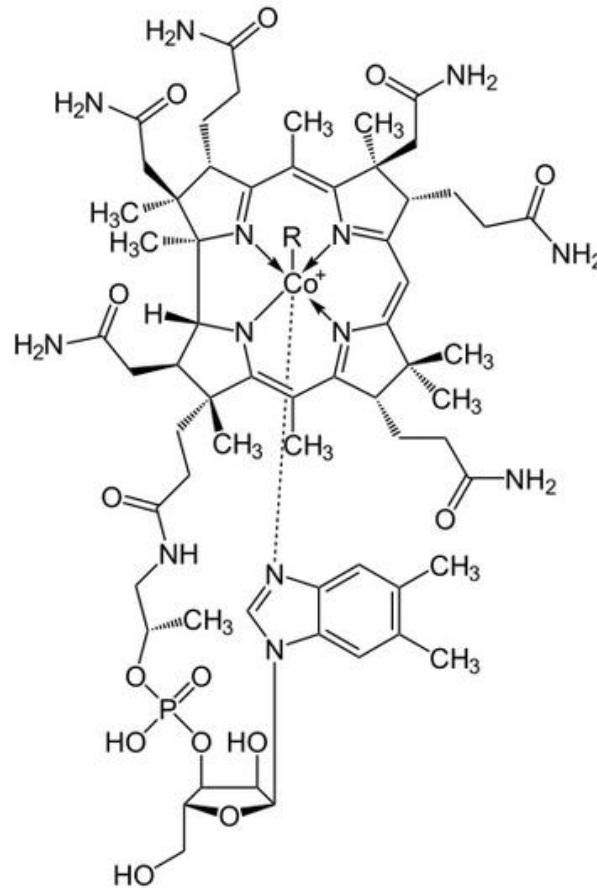


**Figure 1.3. structure of vitamin B<sub>12</sub>.**

The basic structure is a tetrapyrrole ring, a corrin, with a central cobalt atom and a purine nucleotide. The cobalamins differ in the side chain (R-) attached to the cobalt and are named by the organic ligand, Cyanocobalamin (-CN), 5'-deoxyadenosyl, Methyl (-Me), Hydroxycobalamin (-OH). The biologically active compounds methylcobalamin and deoxyadenosylcobalamin are labile, whereas hydroxycobalamin and cyanocobalamin, which are used therapeutically, are more stable, but must be converted to the former two to function as enzyme cofactors. The labile forms are converted to cyanocobalamin when the serum concentration of vitamin B<sub>12</sub> is quantified.

However, the Food and Drug Administration (FDA) recommends higher amounts, 2-3  $\mu\text{g}$  daily (Fankhanel and Gassmann, 1998). Vitamin B<sub>12</sub> can also be provided through supplements in multi-vitamin pills and processed foods, including energy drinks (Selvakumar and Thakur, 2012)].

### 1.10.2 Vitamin B<sub>12</sub> function

The highly reactive C-Co bond in vitamin B<sub>12</sub> acts in two main enzymatic reactions in humans: the methionine synthase reaction and the methylmalonyl-CoA mutase reaction (Figure 1.4).

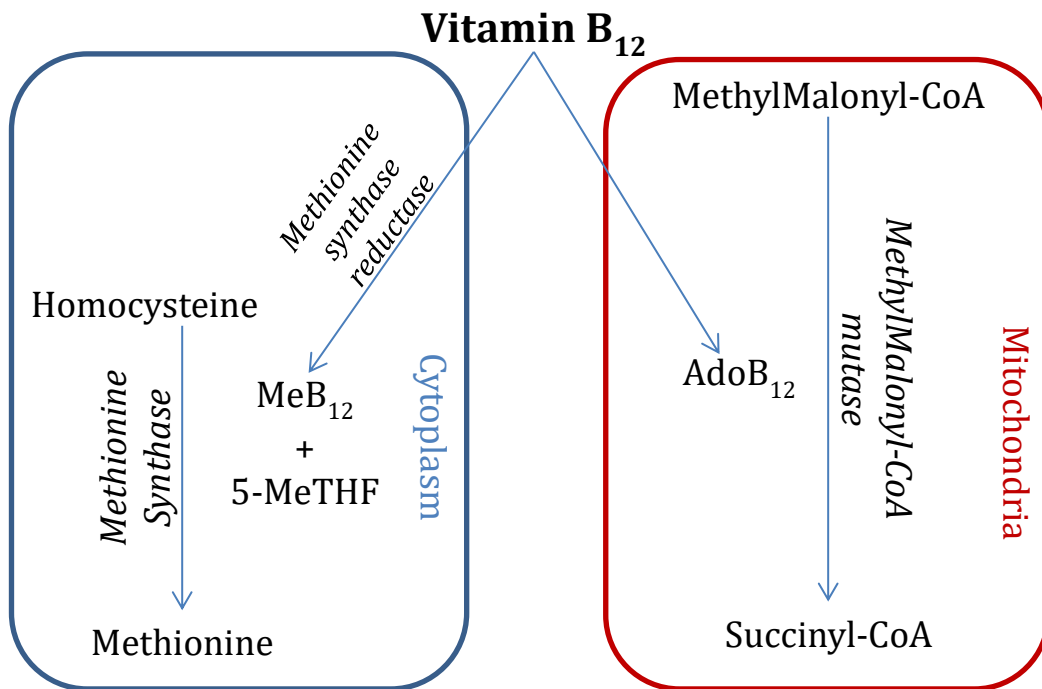


**Figure 1.4 Summary of vitamin B<sub>12</sub> in the methionine synthase and methylmalonyl-CoA mutase reactions.**

Vitamin B<sub>12</sub> is essential for the metabolism of homocysteine and methylmalonyl-CoA. Methionine synthase catalyses the conversion of homocysteine to methionine and requires the cofactor methylcobalamin (MeB<sub>12</sub>) as a methyl group donor. The metabolism of methylmalonyl-CoA to succinyl-CoA is accomplished by the enzyme methylmalonyl-CoA mutase and requires the presence of adenosylcobalamin (AdoB<sub>12</sub>). A lack of vitamin B<sub>12</sub> can potentially cause an increase in homocysteine and methylmalanoic acid.

The methionine synthase reaction occurs in the cytoplasm where methylcobalamin serves as an intermediate, to transfer a methyl group from 5-methyl-tetrahydrofolate (5-MeTHF) from folate. This then converts homocysteine to methionine (Figure 1.4). The production of 5-methyl-tetrahydrofolate from folate is irreversible, and in vitamin B<sub>12</sub> deficiency, traps folate; this is known as the methyl-folate trap (Sauer and Wilmanns, 1977). Thus DNA production is impaired due to shortage of this functional form of folate. Simultaneously, homocysteine accumulates due to impaired methionine synthesis.

The methylmalonyl-CoA mutase reaction occurs in mitochondria where adenosylcobalamin (AdoB<sub>12</sub>) is required as a coenzyme for methylmalonyl-CoA mutase (Allen et al., 1993). Vitamin B<sub>12</sub> deficiency causes accumulation of methylmalonic acid, the effects of which are explained later in section 1.10.5.2.

### 1.10.3 Vitamin B<sub>12</sub> homeostasis

Absorption of dietary vitamin B<sub>12</sub> is a complex process involving several parts of the GI tract. Around 1% of the ingested vitamin B<sub>12</sub> is thought to be absorbed by passive diffusion (Birn, 2006). After ingestion, vitamin B<sub>12</sub> is released from dietary protein by the acidic environment and peptic digestion in the stomach, followed by binding to haptocorrin, a glycoprotein secreted in saliva and gastric juice. In the duodenum, pancreatic secretion raises intraluminal pH and facilitates degradation of haptocorrin by pancreatic proteases, releasing vitamin B<sub>12</sub>. The absorption of vitamin B<sub>12</sub> is dependent on binding to the Intrinsic factor (IF), a glycoprotein, produced by parietal cells of the gastric mucosa in the stomach. This vitamin B<sub>12</sub>-IF complex is recognised by the multi ligand apical membrane protein, Cubam, which endocytoses the complex into the epithelium of the terminal ileum (Fyfe et al., 2004, He et al., 2005). Cubam is composed of the extracellular protein cubilin (460 kDa) and the transmembrane protein amnionless (45 kDa) (Andersen et al., 2010). Amnionless is responsible for membrane anchorage, biosynthetic processing, and trafficking to the plasma membrane of the receptor whereas cubilin contributes to the recognition and binding of the vitamin B<sub>12</sub>-IF complex. More specifically the CUB5-8 domains of cubilin bind with high affinity to the vitamin B<sub>12</sub>-IF complex in a Ca<sup>2+</sup>-dependent manner (Andersen et al., 2010). Vitamin B<sub>12</sub> is then released into the bloodstream and binds to its transport proteins, transcobalamin, and haptocorrin. Normally no free B<sub>12</sub> is present in the circulation (Birn, 2006, Bor et al., 2004). Serum transcobalamin concentrations are around 1 nM of which 10% is saturated with vitamin B<sub>12</sub>. Serum haptocorrin is similar to that of transcobalamin but 75% is saturated with vitamin B<sub>12</sub> (Nexo and Andersen, 1977). Although transcobalamin binds only 25% of the circulating vitamin, it is responsible for the delivery of B<sub>12</sub> to most tissues.

Around 50% of the body's total vitamin B<sub>12</sub> store is located in the liver, with the remaining amounts stored in other tissues including muscle and kidneys (Birn et al., 2002). It has been estimated that a normal person's body store of 1-3 mg would be sufficient to meet the body's needs for 3-6 years under normal conditions (Allen, 2008).

Vitamin B<sub>12</sub> is excreted predominantly through faecal and biliary secretion when concentrations are within the normal range with urinary excretion levels being minimal (Birn, 2006). However, under excess, urinary excretion increases. There is increasing evidence demonstrating the contribution of the kidney to vitamin B<sub>12</sub> homeostasis. Vitamin B<sub>12</sub> has been shown to be filtered in the glomeruli and reabsorbed in the renal tubular system to prevent its urinary loss (Birn et al., 2003, Nielsen et al., 2001). The megalin receptor is essential for the reabsorption of filtered transcobalamin-B<sub>12</sub>-complex in the proximal tubule (Birn et al., 2002). The receptors megalin and cubilin receptors are heavily expressed in the proximal renal tubular cells (Moestrup et al., 1996). After endocytosis into the proximal tubular cells, vitamin B<sub>12</sub> may be metabolised, stored or released. Significant amounts of vitamin B<sub>12</sub> accumulate in lysosomes of the proximal tubular cells, suggesting a storage role of the kidney for vitamin B<sub>12</sub> (Birn, 2006).

#### **1.10.4 Signs and symptoms of vitamin B<sub>12</sub> deficiency**

Vitamin B<sub>12</sub> deficiency can cause a wide range of signs and symptoms dependent on the extent of the deficiency and the stage at which the clinical manifestation arises. Most commonly vitamin B<sub>12</sub> deficiency is associated with both macrocytic and megaloblastic forms of anaemia leading to symptoms such as fatigue, shortness of breath and light-headedness. In practice there is a plethora of effects, conditions and signs and symptoms vitamin B<sub>12</sub> deficiency can cause (see Table 1.3 for a summary).

A more serious and irreversible effect of vitamin B<sub>12</sub> deficiency is peripheral neuropathy, a result of demyelination of axons in the peripheral and central nervous system which can lead to neurological problems and in severe cases can lead to death (Bell, 2010).

**Table 1.3. Clinical signs and symptoms of vitamin B<sub>12</sub> deficiency**


---

Haematological
Anaemia, macrocytic and megaloblastic
Haemolytic anaemia
Neutrophil hyper-segmentation
Leukopenia
Thrombocytopenia
Neurological
Peripheral polyneuropathy - myelopathy
Paraesthesia
Muscle weakness
Ataxia
Optic neuritis
Autonomic neuropathy
Cognitive
Dementia
Memory impairment
Psychosis- depression
Delirium
Gastroenterological
Reduced appetite
Weight loss
GI pain or disorders
Lingual atrophy

---

Table constructed from reviews by (Wong, 2015, Moridani, 2006)

Vitamin B<sub>12</sub> deficiency is typically characterised by macrocytic and megaloblastic anaemia. Impaired DNA synthesis in rapidly dividing cells of bone marrow origin is the underlying mechanism. DNA synthesis is decreased due to inadequate formation of thymidine triphosphate because of impaired methionine synthase reaction, which needs vitamin B<sub>12</sub> as a cofactor (see Figure 1.4).

At earlier stages, clinical manifestations are subtle and highly variable, but neurological disorders occur only during the later stages of vitamin B<sub>12</sub> deficiency and cognitive defects may occur in the absence of haematological signs (Allen et al., 1998, Lindenbaum et al., 1988).

Vitamin B<sub>12</sub> deficiency also causes peripheral neuropathy. Common symptoms include paraesthesia and numbness, muscle weakness and in advanced stages, symptoms of autonomic neuropathy (Aaron et al., 2005, Bell, 2010, Tesfaye et al., 1996). Cerebral disorders due to vitamin B<sub>12</sub> deficiency include cognitive

impairment ranging from mild concentration impairment to dementia and psychosis (Girdwood, 1968, Reynolds, 2006)

There have been several mechanisms suggested to explain the pathogenesis of neurological and cognitive manifestations from vitamin B<sub>12</sub> deficiency. Impaired methylmalonyl CoA mutase activity can cause a decrease in succinyl CoA, which may decrease myelin production and subsequently lead to the incorporation of abnormal fatty acids into neuronal lipids (Chrast et al., 2011, Weir and Scott, 1995). The other alternative hypothesis is that impaired activity of methionine synthase decreases the production of S-adenosylmethionine, and leads to myelin sheath damage and disrupted neurotransmitter metabolism (Briani et al., 2013).

### **1.10.5 Diagnosis of vitamin B<sub>12</sub> deficiency**

There is no precise or gold standard test for the diagnosis of vitamin B<sub>12</sub> deficiency. The diagnosis is usually based on identifying a low level of serum vitamin B<sub>12</sub> with clinical evidence of deficiency, which responds to vitamin B<sub>12</sub> replacement therapy (Wong, 2015). The diagnostic approach to vitamin B<sub>12</sub> deficiency includes, firstly, the demonstration that the deficiency exists and, secondly, the identification of the cause of the deficiency.

#### *1.10.5.1 Total serum vitamin B<sub>12</sub>*

This is the standard and most common measurement for diagnosing vitamin B<sub>12</sub> deficiency as it is widely available. Serum vitamin B<sub>12</sub> levels are most commonly measured using competitive immunoassays using direct chemiluminescence (Morovat et al., 2006). Vitamin B<sub>12</sub> from the patient sample competes with vitamin B<sub>12</sub> labelled with acridinium ester, for a limited amount of purified intrinsic factor. The assay uses sodium hydroxide to release the vitamin B<sub>12</sub> from the endogenous binding proteins in the sample.

The sensitivity and specificity of the serum total vitamin B<sub>12</sub> concentration for the diagnosis of vitamin B<sub>12</sub> deficiency is questionable, and ranges from 30-100% and 60-95%, respectively (Lindenbaum et al., 1990, Oosterhuis et al., 2000, Moridani, 2006). The interpretation of the assay results is affected by

many circumstances. Serum total vitamin B<sub>12</sub> does not directly reflect the vitamin B<sub>12</sub> status in tissues. This is because the majority of vitamin B<sub>12</sub> is bound to plasma proteins, with around 20% bound to transcobalamin and is thus biologically active (Bor et al., 2004, Seetharam, 1999). Conversely, the vitamin B<sub>12</sub> status in tissues may be inadequate even though the serum total vitamin B<sub>12</sub> concentration is in the reference range (Obeid et al., 2013). Falsely increased vitamin B<sub>12</sub> levels are caused by liver diseases and moderate alcohol intake (Baker et al., 1998, Ermens et al., 2003).

#### **1.10.5.2 Methylmalonic acid**

In vitamin B<sub>12</sub> deficiency, methylmalonic acid (MMA) accumulates due to decreased methylmalonyl-CoA mutase activity (Figure 1.1). Increased serum MMA concentration is a sensitive and very specific marker of vitamin B<sub>12</sub> deficiency (Kooy et al., 2013, Lindenbaum et al., 1990, Wong, 2015). MMA can be quantified in both serum and urine; however, serum MMA has a greater sensitivity and specificity (Moridani, 2006). Renal insufficiency can falsely raise serum MMA but not urine MMA results (Loikas et al., 2007). MMA has been suggested to be used as a screening tool in cases where the elderly, who are prone to B<sub>12</sub> deficiencies, have few recognisable symptoms (Bailey et al., 2011). MMA testing may not be suitable for monitoring because it is subject to variation and results do not reliably respond to B<sub>12</sub> treatment.

#### **1.10.5.3 Homocysteine**

As shown in Figure 1.4, vitamin B<sub>12</sub> and 5-MeTHF are required for the conversion of homocysteine to methionine by methionine synthase. Homocysteine accumulates both in vitamin B<sub>12</sub> and folate deficiency. Homocysteine concentration is an independent risk factor for cardiovascular disease, especially among individuals with T2DM (Carlsen et al., 1997, Welch and Loscalzo, 1998). Elevation of homocysteine is a sensitive indicator of vitamin B<sub>12</sub> deficiency. However, the specificity is poor (38-68%) because the concentration is increased by numerous other factors (Moridani, 2006). For example, folate and vitamin B<sub>6</sub> deficiencies raise homocysteine (Selhub, 2002).

Additionally, there is high variation in homocysteine levels contributed to by pre-analytical factors, renal impairment and other diseases or conditions (Loikas et al., 2007, Nauck et al., 2001).

#### **1.10.5.4 Holo-transcobalamin II**

Holo-transcobalamin II (HC) is a measure of vitamin B<sub>12</sub> directly available to cells as only this bound fraction of vitamin B<sub>12</sub> enters the cells and thus is biologically active (Hvas and Nexo, 2003, Birn, 2006). HC is thought to reflect the immediate changes in vitamin B<sub>12</sub> status (Nexo and Andersen, 1977). HC has excellent sensitivity and specificity, 100% and 89% respectively (Hvas and Nexo, 2003). Additionally HC is regarded as an early marker of changes in vitamin B<sub>12</sub> homeostasis (Baker et al., 1998).

#### **1.10.5.5 The Schilling test**

Although there is no gold standard, the Schilling test is a useful test to diagnose several causes of vitamin B<sub>12</sub> deficiency. The Schilling test is a dynamic functional investigation used for patients with vitamin B<sub>12</sub> deficiency (Schilling et al., 1951, Schilling, 1953). The primary objective of the test is to determine whether the patient has pernicious anaemia through malabsorption of vitamin B<sub>12</sub>. The patient is given radiolabelled vitamin B<sub>12</sub>. The most commonly used radiolabels are <sup>57</sup>Co and <sup>58</sup>Co. An hour later an intramuscular injection of unlabelled vitamin B<sub>12</sub> is administered. This is not enough to replete or saturate body stores of B<sub>12</sub>. The purpose of the single injection is to temporarily saturate B<sub>12</sub> receptors in the liver with enough unlabelled vitamin B<sub>12</sub> to prevent labelled vitamin B<sub>12</sub> being taken up in the liver and other tissues. Therefore if vitamin B<sub>12</sub> is absorbed from the intestine, it will be cleared and excreted into the urine. The patient's urine is then collected over the next 24 hours to assess the level of absorption. Under normal conditions, the ingested radiolabelled vitamin B<sub>12</sub> will be absorbed from the intestine into circulation. However, as the body is saturated with vitamin B<sub>12</sub>, a large proportion of the ingested labelled vitamin B<sub>12</sub> will be excreted in the urine. The Schilling test is less commonly used nowadays but has been utilised to show that metformin induces vitamin B<sub>12</sub>

malabsorption (Tomkin, 1973, Andres et al., 2003, Berger et al., 1972, Mazokopakis, 2012).

### **1.10.6 Vitamin B<sub>12</sub> reference range**

Published reference ranges for serum vitamin B<sub>12</sub> and sensitivity and specificity for the diagnosis of clinically significant vitamin B<sub>12</sub> levels is variable. Pieters et al., 2009 used the Bhattacharya technique to calculate the reference range. This technique allows estimates of reference values, to be not affected by disease or treatment. Using a cut-off of 2.5% at both ends of values produced a vitamin B<sub>12</sub> range of 150 to 630 pmol/L. Marks et al., 2004 used a hazard ratio and found that 90% to 95% of patients with vitamin B<sub>12</sub> deficiency had levels <148 pmol/L (200 pg/mL), 5-10% patients had levels 148-221 pmol/L (200-300 pg/mL) and < 1% levels >221 pmol/L (300 pg/mL). The most accepted lower limit of normal is considered to be <148 pmol/L (200 ng/L) (Pieters et al., 2009, Carmel et al., 2003, de Jager et al., 2010, Mazokopakis and Starakis, 2012). Additionally some groups report a borderline deficiency range of 150-220 pmol/L (Marks et al., 2004, de Jager et al., 2010, Lindenbaum et al., 1990, Snow, 1999). The reported upper limit of normal is more variable than the lower limit, but concentrations >900 ng/L are generally accepted as highly elevated (Lindenbaum et al., 1990, Mazokopakis and Starakis, 2012, de Jager, 2014). Levels that exceed the upper limit are rarely suspicious in terms of aetiology, although patients with myeloproliferative disorders, can exhibit normal to high serum concentrations (Gauchan et al., 2012).

### **1.10.7 Metformin & vitamin B<sub>12</sub>**

A common, potentially damaging, and well documented complication of metformin is vitamin B<sub>12</sub> deficiency (Anfossi et al., 2010, Liu et al., 2006). Metformin was first described as a potential cause for vitamin B<sub>12</sub> absorption in 1969 (Berchtol.P et al., 1969). However, the first report of metformin induced vitamin B<sub>12</sub> malabsorption was in 1971 when 30% of patients receiving metformin for more than 2 years exhibited metformin-induced vitamin B<sub>12</sub> malabsorption (Tomkin et al., 1971). This was identified through conducting the

previously described Schilling test. Since then there have been more than 85 publications on metformin-induced vitamin B<sub>12</sub> deficiency. Table 1.4 displays a few selected studies of vitamin B<sub>12</sub> levels in metformin treated T2DM populations.

Metformin-induced vitamin B<sub>12</sub> deficiency is poorly recognised and not currently screened for or treated by the majority of physicians who prescribe metformin. Approximately 10-30% of patients with prolonged use of metformin develop vitamin B<sub>12</sub> deficiency (<200 pmol/L) (de Jager et al., 2010, Ting et al., 2006, Bell, 2010, Liu et al., 2006, Leung et al., 2010). Metformin dose and treatment duration appear to be the most consistent risk factors for vitamin B<sub>12</sub> deficiency in patients with T2DM (Kang et al., 2014, Ting et al., 2006). A significant reduction in vitamin B<sub>12</sub> levels can occur as quickly as 3-4 months after the initiation of the metformin therapy (Bauman et al., 2000), while symptomatic deficiency may take as long as 5-10 years to manifest. Given the estimate that a normal person's body store of 1-3 mg would be sufficient to meet the body's biochemical needs for 3-6 years, under normal conditions (Allen, 2008), metformin appears to exert its effects more rapidly perhaps influencing the storage of vitamin B<sub>12</sub> in the liver.

A meta-analysis conducted by Niafar et al., 2015 used 29 studies incorporating a total of 8,089 patients and observed an increased incidence of vitamin B<sub>12</sub> deficiency in metformin users (Odds ratio = 2.45) (mean difference -88 ng/mL, P<0.0001). They concluded that metformin treatment is significantly associated with an increase in incidence of vitamin B<sub>12</sub> deficiency. Liu et al., 2014 compiled a smaller systematic review using 6 randomised controlled trials incorporating 816 patients. Serum vitamin B<sub>12</sub> concentrations were significantly lower in patients treated with metformin (Mean difference -74 ng/mL P<0.0001). They concluded metformin reduced vitamin B<sub>12</sub> levels in a dose-dependent manner.

**Table 1.4. Comparison of studies investigating vitamin B<sub>12</sub> levels in metformin vs placebo T2DM patients**

Reference	Country	Group <sup>a</sup>	Duration of T2DM (Years)	Number	Male %	Age (years)	Metformin dose (mg)	Duration of metformin treatment	Vitamin B <sub>12</sub> (ng/L)
de Jager et al., (2010)	Netherlands	M	14±9	194	42	64±10	2050 daily	52 months	392±176
		P	-	191	50	59±11	850 tds	-	515±183
Bauman et al., (2000)	New York, USA	M	6.9±6.1	14	100	49±10	2050 daily	3 months	227±22
		P	6±3.6	7	100	54±5	-	-	375 ± 90
Leung et al., (2010)	Canada	M	>1	10	50	(67-91)	-	3 months	183
		P	-	10	50	(67-91)	-	-	471
Liu et al., (2006)	Hong Kong	M	-	56	45	80±6	-	-	382±333
		P	-	78	36	81±7	-	<3 years	516±62
Kos et al., (2012)	Illinois, USA	M	-	142	30	67±14	1500 daily	>4 years	496±282
		P	-	205	30	67±14	-	-	637±352
Chen et al., (2012)	Cardiff, UK	M	14.1±7.1	152	57	66±11	1900±578 daily	8.5±5.4 years	219±106
		P	-	50	52	69±12	-	-	281±95
Romero et al., (2012)	Spain	M	-	81	31	72±12	1779 (425-2550) daily	43 months	394±184
		P	-	28	43	75 ±8	-	-	509±176
Obeid et al., (2013)	Germany	M	8 (4-20)	49	47	64 (54-78)	-	-	347 (188-505)
		P	12.5 (2-32.4)	43	40	67 (52-82)	-	-	414 (259-642)
Wile & Toth., (2010)	Canada	M	5.5±3.3	59	71	67±12	3390 g	>6 months	659 (1169)
		P	4.7±2.9	63	76	65±12	-	-	313 (465)

<sup>a</sup> Groups, M, metformin; P, placebo. Values represent mean±SD, while ranges are in parenthesis. Tds, three times daily; bd, twice daily.

The majority of the clinical studies demonstrating that metformin leads to vitamin B<sub>12</sub> deficiency refer to the work of Schafer, 1976 as an explanation for the mechanism behind the association between metformin and vitamin B<sub>12</sub> deficiency. The findings of this study suggest that the binding of biguanides causes a positive shift of a membrane's surface charge. Metformin induces a positive charge to the surface of the ileal membrane, which would act to displace divalent cations such as calcium. Therefore metformin could impair calcium availability and interfere with the calcium-dependent process of vitamin B<sub>12</sub> absorption. The only evidence to suggest that metformin impairs calcium availability is from a clinical study which illustrated that metformin-induced vitamin B<sub>12</sub> deficiency was reversed with dietary supplements of calcium carbonate (Bauman et al., 2000).

An *in vivo* study by Greibe et al., 2013 explored potential alternate malabsorption mechanisms for vitamin B<sub>12</sub> caused by metformin. This study used rats injected subcutaneously with either metformin or control for 3 weeks. Following this exposure period the amount of vitamin B<sub>12</sub> was located and regionalized using radio-labelled B<sub>12</sub>. They speculated the reduced serum vitamin B<sub>12</sub> was attributed to a 36% increase of vitamin B<sub>12</sub> observed in the livers of metformin treated rats, in comparison to controls. Interestingly their study showed that the total amount of absorbed vitamin B<sub>12</sub> in both populations (metformin vs. control) were comparable, further suggesting that there is no metformin-induced malabsorption but rather a redistribution of the vitamin to the liver. These data may reflect the findings in humans receiving metformin, where the decrease in serum vitamin B<sub>12</sub> is due to an increased displacement of vitamin B<sub>12</sub> from serum to the liver. However, the study has several limitations, most crucially was the intravascular administration of metformin, thereby removing the GI system.

The most common method for treatment of vitamin B<sub>12</sub> deficiency in the UK is the use of intramuscular hydroxocobalamin injections (British National Formulary, 2015). This is used both in a loading regimen followed by a maintenance administration for long term treatment (Mazokopakis and Starakis, 2012). The efficacy of oral vitamin B<sub>12</sub> use to correct its deficiency has

resulted in comparable treatment success to that of the intramuscular route (Mazokopakis and Starakis, 2012). However, others suggest the amount available in general multivitamins (6 µg) may not be enough to correct the deficiency in T2DM patients (Reinstatler et al., 2012).

## **1.11 Metformin drug transporters**

Membrane transporters are responsible for the sustainability of cell homeostasis and can be major determinants of a drug's safety, efficacy and pharmacokinetic profile. Physiologically transporters play an important role in the absorption, distribution and elimination of cationic compounds, metabolites and toxins (Giacomini et al., 2010). There are many families of drug transporters including ATP binding cassette (ABCs) organic anion transporters (OATs); and organic anion transporting polypeptides (OATPs); and the organic cation transporters (OCTs) (Hediger et al., 2004). As this thesis interests are in metformin drug transporters, the rest of this introduction will focus of the OCTs.

### **1.11.1. SLC Transporter Family**

The solute carrier (SLC) family consists of over 360 members in 52 gene families in humans which fall under the largest group of secondary membrane transporters in eukaryotes, the major facilitator family (MFS) (Saier, 2000, Zhou et al., 2007b).

One subset of the SLC family is the *SLC22A* family; three sub-types of this class of transporters have been identified; Organic Cation Transporter 1 (OCT1), OCT2 and OCT3 (Giacomini et al., 2010). All share a common structure of 12 transmembrane alpha-helix domains (TMDs), a large extracellular loop with glycosylation sites and a large intracellular loop with phosphorylation sites hypothesised to be involved in intracellular signalling. The model OCT substrates for the OCTs include MPP<sup>+</sup> (1-methyl-4-phenyl-pyridinium), TEA (tetraethylammonium), biogenic amines, and a number of clinically used drugs (Wright and Dantzler, 2004).

Metformin, is a substrate for all OCTs (Nies et al., 2009, Chen et al., 2010a, Yoon et al., 2013). As metformin does not undergo any known form of metabolism, the most important factors contributing to its pharmacological action are the drug transporters that distribute metformin to its target organs (Kimura et al., 2005a, Nies et al., 2009). These transporters share >48% sequence identity and >65% sequence similarity and are thought to have evolved from a common ancestor (Saier, 2000). Unlike the majority of membrane transporters, OCTs perform bidirectional transport of substrates; therefore the expression of OCTs whether they are expressed apically or basolaterally governs their function. Although these transporters display similar selectivity and activity for some substrates (MPP<sup>+</sup>) they have distinct selectivity for others (cimetidine) (Kerb et al., 2002, Shu et al., 2003). The TMDs are most likely to be the sites of substrate specificity and recognition where conserved residues account for similar substrates affinities. OCTs transport a large number of diverse organic cations including primary, secondary, tertiary and quaternary amines with a net positive charge on the amine nitrogen atom at physiological pH (Zhang et al., 2005). See Figure 1.5 for an illustrative summary of metformin drug transporters.

#### *1.11.1.1 Organic Cation transporter 1*

OCT1 is expressed at the sinusoidal membrane of hepatocytes with lower levels in the adrenal gland, lung epithelium, neurons, placental tissue and the spleen (Wang et al., 2002). OCT1 translocates a broad array of organic cations and drugs including histamine, serotonin, tetraethylammonium and metformin (Zair et al., 2008). As the liver is the target organ of metformin, OCT1 is regarded as the primary transporter that allows metformin to exert its pharmacological action in lowering peripheral blood glucose levels. There is conflicting evidence as to whether OCT1 is located in enterocytes of the GI tract. Previous reports have suggested, but not provided evidence, that *SLC22A1* (OCT1) is expressed on the basolateral membrane of enterocytes and thus aids in the cellular transport of metformin from the cell to the blood (Mulgaonkar et al., 2013, Koepsell et al., 2007, Jonker and Schinkel, 2004). In contrast, Han et al 2013 (Han et al., 2013), discovered OCT1 was not expressed on the basolateral

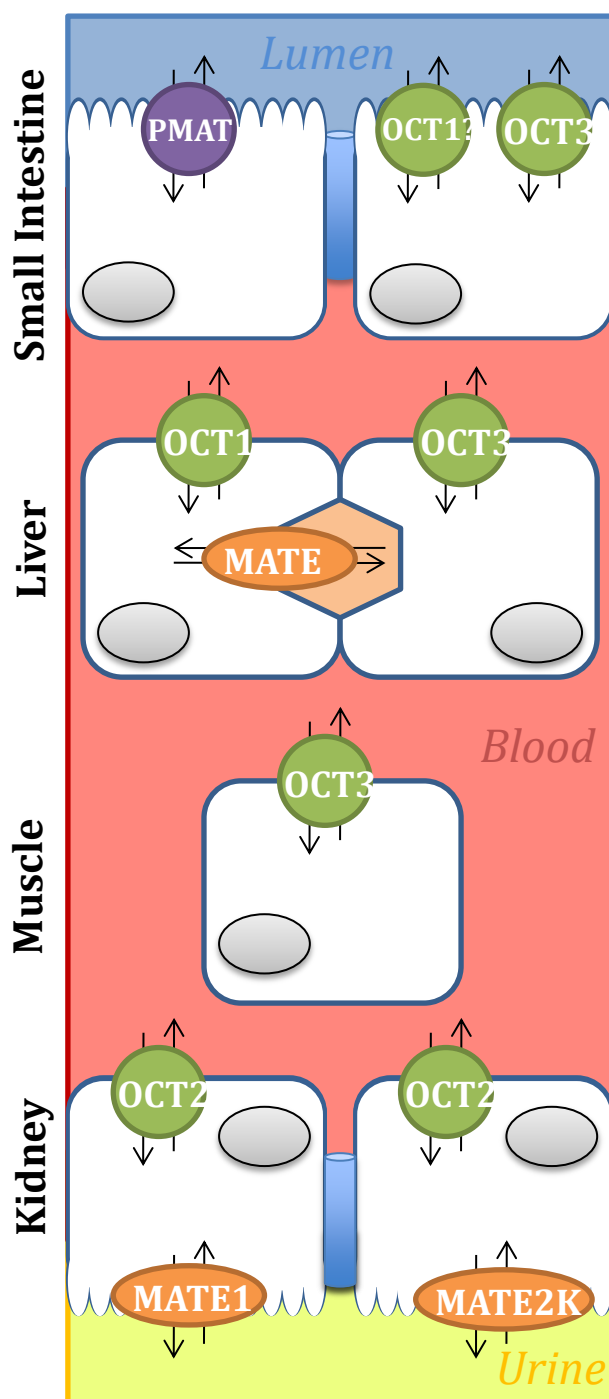


**Figure 1.5 Summary of Cationic transporters for metformin disposition in humans.**

PMAT, OCT1 and OCT3 are present on the lumen apical membrane (AP) and facilitate intestinal accumulation of metformin. OCT1 and OCT3 mediate uptake into hepatocytes, where MATE1 facilitates the biliary excretion of metformin. OCT3 is also expressed on skeletal muscle cells and may be important in the disposition and efficacy of metformin. In the proximal tubule cells of the kidney, OCT2, located on the basolateral membrane (BL) mediates uptake of metformin from the blood, while MATE1 and MATE2K, located on the apical membrane, rapidly efflux metformin directly into the urine. There is conflicting evidence to the expression and location of these transporters, this figure represents a summary of the majority of expression studies.

membrane of human and mouse enterocytes, but in fact was on the apical membrane, and inhibition of the transporter did not influence basolateral transport of known OCT1 substrates. They and others have however found OCT1 to be located on the apical membrane of the Caco-2 cell line (Han et al., 2013, Han et al., 2015, Proctor et al., 2008). However due to the heterogeneity of the cell line there is a possibility that cell lines may behave differently as compare to primary cells and express different drug transporters as compare to primary cells (Sambuy et al., 2005).

#### *1.11.1.2 Organic Cation transporter 2*

OCT2 is expressed in the distal renal tubules. OCT2 facilitates the uptake of a variety of cationic compounds including cimetidine and metformin from the circulation into renal epithelial cells (Zair et al., 2008). OCT2 has been established to have a greater affinity and capacity for metformin than OCT1 and thus to be able to rapidly eliminate metformin into the urine (Kimura et al., 2005a). As illustrated in Figure 1.5, OCT2 expressed in the basolateral membrane of proximal tubule cells of the kidney, and mediates uptake of metformin from the blood, while Multidrug And Toxin Extruders 1 (MATE1) and MATE2K, located on the apical membrane, rapidly efflux metformin directly into the urine (see section 1.11.3). Human OCT2 protein expression has not been identified in the human jejunum (Muller et al., 2005).

#### *1.11.1.3 Organic Cation transporter 3*

OCT3 is expressed in a variety of tissues, primarily in skeletal muscle. Its strongest expression was found in skeletal muscle, kidney, placenta, brain, and heart (Nies et al., 2009). A significant contribution in the handling of organic cations at the periphery has been confirmed in knock-out mice in which the *SLC22A3* gene was disrupted. These mice showed impaired uptake activity of a monoamine OCT3 substrate in brain, heart and embryos (Zwart et al., 2001, Vialou et al., 2004). It has recently been acknowledged that muscle tissue is an important site for metformin to exert its pharmacological effects (Chen et al., 2010a). Other studies have data suggesting OCT3 variants can affect their

activity and may contribute to inter-individual variation in cation distribution and clearance (Sakata et al., 2010, Chen et al., 2010a, Nies et al., 2011b).

### 1.11.2 SLC22A Transporter genetics

Genetic polymorphisms in cation-selective transporters have been identified and may have implications in metformin pharmacokinetics and dynamics (Giacomini et al., 2010). As metformin is not metabolised and excreted in its unchanged form in the urine, drug transporters are primarily responsible for the pharmacokinetics of metformin and their polymorphic variants may therefore be responsible for metformin side effects and the inter-individual variability observed in its efficacy. For example, genetic factors contribute to over 90% of the variability observed in metformin renal clearance (Leabman and Giacomini, 2003). The most widely studied polymorphisms involve single-nucleotide polymorphisms (SNPs) for OCT1 and OCT2 that alter transport of metformin and other cationic compounds. *SLC22A1* and *SLC22A2* genes are regarded to be highly polymorphic with >90 and >40 registered SNPs resulting in altered amino acid changes, respectively, on the NCBI database.

*SLC22A1* and *SLC22A2* genes are located on chromosome 6q26. *SLC22A1* consists of 11 exons spanning 37 kb, the translated protein consists of 554 amino acids. Adjacent to the *SLC22A1* gene is *SLC22A2* which also consists of 11 exons spanning 42 kb; the translated protein consist of 555 amino acids. The two human proteins share 70% homology with each other and are conserved across species showing at least 74% and 82% homology with characterised mammalian orthologs.

SNPs in these genes have been extensively characterised at different frequencies in ethnically diverse populations, (Shu et al., 2007, Shu et al., 2003, Kerb et al., 2002, Leabman et al., 2002, Itoda et al., 2004). Furthermore, Shu et al determined that several nonsynonymous SNPs (nsSNP) of OCT1 decreased metformin uptake *in vitro* (Shu et al., 2007). Therefore it is hypothesised that one or multiple nsSNP may lead to decreased metformin uptake in hepatic cells *in vivo* leading to decreased metformin action which may then alter the pharmacokinetic profile of metformin, leading to inter-individual variability to

metformin response. It should be noted that a GWAS did not find any significant association between metformin transporter genes and metformin response (Zhou et al., 2011).

**Table 1.5 Examples of non-synonymous mutations in OCT1 & OCT2 and effects of transport function.**

	Exon	SNP identifier	Nucleotide Change <sup>a</sup>	Protein Variation	Transport Activity <sup>b</sup>		Prevalence (n=494)	Ethical Bias <sup>c</sup>	
					MPP <sup>+</sup>	Metformin			
SLC22A1 (OCT1)	1	rs34447885	41 C>T	S14F	↓	↓	0.013	AA	
	1	rs12208357	181 T>C	R61C	↓	↓	0.031	CA/ME	
	1	rs35546288	253 C>G	L85F	ND	ND	0.004	AA	
	1	rs55918055	262 T>C	C88R	↓	↓	0.005	EA	
	2	rs683369	480 C>G	F160L	↔	↔	0.032	AA/CA/ME	
	3	Rs34104736	566 C>T	S189L	↔	↓	0.002	CA	
	3	Rs36103319	659 G>T	G220V	↓	↓	0.002	AA	
	4	Rs4646277	953 C>T	P283L	↓	ND	0.0011	JP	
	6	rs2282143	1022 C>T	P341L	↓	↓	0.047	AA/AS	
	6	rs34205214	1025 G>A	R342H	ND	ND	0.012	AA	
	7	Rs34130495	1201 G>A	G401S	↓	↓	0.008	AA/CA	
	7	rs628031	1222 A>G	M408V	ND	↓	0.682	AA/CA/AS	
	7	rs202220802	1256 ATGdel	M420del	↔	↓	0.105	AA/CA/ME	
	8	Rs35956182	1320 G>A	M440I	↔	ND	0.002	AA	
	8	rs34295611	1381 G>A	V461I	↔	ND	0.004	AA	
	9	rs34059508	1393 G>A	G465R	↓	↓	0.016	CA	
	9	rs35270274	1493 G>T	R488M	↔	↑	0.02	AA	
	SLC22A2 (OCT2)	1	rs8177504	160C>T	P54S	↔	ND	0.002	AA
		2	rs45591037	481T>C	F161L	↔	ND	0.002	CA
2		rs45520136	493A>G	M165V	↓	ND	0.002	AA	
2		rs8177507	495G>A	M165I	ND	↓	0.004	AA	
4		rs316019	808G>T	A270S	↓	↓	0.127	CA/AS/AA	
5		rs45592541	890C>G	A297G	ND	ND	0.002	CA	
7		rs8177516	1198C>T	R400C	↓	↓	0.006	AA	
8		rs8177517	1294A>C	K432Q	↓	↑	0.006	AA	

<sup>a</sup> Complementary DNA (cDNA) numbers are relative to the ATG start site and based on the cDNA sequence from GenBank accession numbers NM\_003057.2 (OCT1) NM\_003058 (OCT2). <sup>b</sup> Transport activity of 1-methyl-4-phenylpyridinium (MPP<sup>+</sup>) and Metformin, ↓, decrease; ↑, increase; ↔, similar; ND: Not determined. <sup>c</sup> AA: African-American; AS: Asian-American; CA, Caucasian; JP: Japanese; ME: Mexican-American; PA: Pacific Islander. Table constructed using data collated from (Shu et al., 2007, Shu et al., 2003, Kerb et al., 2002, Leabman et al., 2002, Itoda et al., 2004).

### 1.11.3 Other metformin drug transporters

#### 1.11.3.1 Multidrug And Toxin Extruders

Metformin is a known substrate of the Multidrug And Toxin Extruders (MATEs), MATE1 (*SLC47A1*) and MATE2K (*SLC47A2*). Both isoforms function as bidirectional cation-selective transporters (Otsuka et al., 2005; Masuda et al., 2006). Human MATE1 has a higher affinity (apparent  $K_m$  values) for metformin than MATE2K (Tanihara et al., 2007).

Multidrug and toxin extrusion 1 (MATE1), *SLC47A1*, is located on the luminal side of the renal proximal tubules and bile canaliculi of hepatocytes (Boyer, 2013). MATE1 is involved in transportation of metformin out of hepatocytes and renal cells into the bile and urine, respectively. MATE1 directly excrete metformin in its unchanged form into the urine. Several studies have shown genetic variants in the *SLC47A1* gene leads to alterations in metformin elimination in the urine (Toyama et al., 2011, Choi et al., 2011) and can interplay with *SLC22A2* (OCT2) in the elimination of metformin, but genetic factors could interfere with this interplay (Schwabedissen et al., 2010).

A protein homologous of MATE1, MATE2-K, *SLC47A2-K*, is also expressed on the apical membrane of distal renal tubules, and with MATE1, directly excretes metformin in its unchanged form into the urine. Several studies have examined the effect of MATE genetic variants on metformin treatment response. They found promoter variants are associated with the pharmacokinetics and response to metformin in both healthy volunteers and diabetic patients (Stocker et al., 2013, Choi et al., 2011, Chung et al., 2013). Additionally two nsSNPs in MATE2K (Lys64Asn and Gly211Val), exhibited decreased transport activities, and Gly211Val resulting in complete loss of transport activity due to loss of protein expression on the cell surface (Kajiwara et al., 2009).

#### 1.11.3.2 Plasma membrane monoamine transporter

The *SLC29A4* gene codes for the plasma membrane monoamine transporter; (PMAT). First identified in 2004, PMAT is a 55 kDa metformin transporter comprising of 530 aa and 11 TMDs (Engel et al., 2004, Engel and Wang, 2005).

PMAT has been found to be expressed in a variety of tissues including intestine, brain and kidney (Engel et al., 2004, Xia et al., 2007, Chen et al., 2013, Han et al., 2015). In the intestine, PMAT is expressed on the tips of the mucosal epithelial layer and transports metformin in a pH dependent manner. Under acidic conditions (Zhou and Wang, 2006) found decreased metformin transport with PMAT. Conversely, Xia et al., 2007 observed PMAT to be located on the apical surface of Madin-Darby canine kidney (MDCK) cells and exhibited increased MPP<sup>+</sup> transport under acidic conditions. PMAT exhibits striking functional similarity to the OCTs in sharing a large portion of its substrate and inhibitor specificity with the OCTs (Engel and Wang, 2005, Chen et al., 2013, Han et al., 2015). PMAT is less polymorphic than the other metformin transporters, OCTs and MATEs (Ho et al., 2012). The only study to investigate the effect of genetic variants in PMAT on metformin PK was from Duong et al., 2013. They investigated the effect of 11 PMAT SNPs on the population pharmacokinetics of metformin in T2DM patients. However, they found no association between PMAT polymorphisms and predicted metformin clearance.

## 1.12 Metformin drug-drug interactions

Metformin is commonly administered in combination with other drugs to both achieve glycaemic control and to treat other comorbidities associated with T2DM such as hypertension, cardiovascular disease and dyslipidaemia. This use of multiple drugs may lead to drug-drug interactions and alter the pharmacokinetics and efficacy of the drugs. As metformin is not metabolised in the liver, drug-drug interactions through the inhibition of metformin transporters can be clinically relevant. Recent drug-drug interaction studies suggest that proton pump inhibitors (PPIs) can inhibit OCT-mediated metformin transport *in vitro* which may lead to interference with metformin pharmacokinetics (Nies et al., 2011a). Metformin and PPIs have both been independently implicated in decreasing levels of vitamin B<sub>12</sub> levels (Atwell et al., 2012). Long et al (Long and Atwell, 2012) found PPIs and metformin alone were not associated with a significant difference in vitamin B<sub>12</sub> deficiency, but

that the combination was associated with a significant increase in vitamin B<sub>12</sub> deficiency.

The Food and Drug Administration recognises that cimetidine significantly influences the excretion and disposition of metformin through transport with SLC22A2; however they do state this interaction could be partly mediated by MATE-1/MATE-2K transporters which are also expressed in the proximal tubule of the kidney.

The H<sub>2</sub> blocker, cimetidine, is associated with reduced renal tubular secretion and increased systemic exposure to metformin when both drugs are co-administered (Somogyi et al., 1987). Table 1.6 provides a list of FDA recognised OCT inhibitors. Inhibition of MATEs, but not OCT2, is the likely mechanism underlying the drug–drug interactions with cimetidine in renal elimination (Gong et al., 2012, Wang et al., 2008). Additionally, some anti-retrovirals have been shown to inhibit OCT1 and OCT2 transport in vitro. (Moss et al., 2013, Moss et al., 2015).

**Table 1.6. FDA recognised Major Human Transporters.**

Gene	Transporter	Tissue Expression	Substrate	Inhibitor
<i>SLC22A1</i>	OCT1	Liver	acyclovir, amantadine, desipramine, ganciclovir, metformin	Disopyramide, midazolam, phenformin, phenoxybenzamine, quinidine, quinine, ritonavir, verapamil
<i>SLC22A2</i>	OCT2	Kidney, brain	Amantadine, cimetidine, memantine	Desipramine, phenoxybenzamine, quinine
<i>SLC22A3</i>	OCT3	Skeletal muscle, basolateral ileum	cimetidine	Desipramine, prazosin, phenoxy-benzamine

Depending on the affinities for the OCTs, some substrates can act as inhibitors for other compounds. For example, phenformin is also a substrate of OCT1 but can inhibit other substrates due to its high binding affinity.

## 1.13 Methods

### 1.13.1 DNA Sequencing

In 1977 Frederick Sanger presented a DNA sequencing technique that would still be use nearly 40 years later (Sanger et al., 1977). This method uses dideoxy terminator DNA with automated gel electrophoresis and fluorescent terminator chemistry, later capillary gel-based systems (Valencia et al., 2013).

Firstly, millions of copies of the sequence to be determined are purified or amplified using traditional polymerase chain reaction (PCR) methods. Reverse strand synthesis is performed on these copies using a known priming sequence upstream of the sequence to be determined and a mixture of deoxyribonucleotide triphosphates (dNTPs) and dideoxyribonucleotide triphosphates (ddNTPs). ddNTPs are modified nucleotides missing a hydroxyl group at the third carbon atom of the sugar which when incorporated in PCRs, terminate the extension reaction. The dNTP and ddNTP mixture causes random, non-reversible termination of the extension reaction; creating from the different copies molecules extended to different lengths. Following clean-up of free nucleotides, primers and the enzyme, the resulting molecules are sorted by their molecular weight, corresponding to the point of termination, and the fluorescent label attached to the terminating ddNTPs is read out sequentially in the order created by the sorting step. Sequencing allows all genetic variants to be identified within an amplicon when compared to a reference sequence.

### 1.13.2 Molecular modelling

Molecular modelling is a method for analysing 3D structures of proteins. There are only a few crystal structures available from the thousands of all known human protein sequences including transporters. 3D computer models can be derived from known protein crystal structures. One challenge of modelling membrane transporters is the generation of robust models using low levels of sequence identity; however it is appreciated membrane topologies are highly conserved, such as number of amino acids in transmembrane helices. Thus, low

sequence homology structural templates can be used to predict the 3D structure of a protein from a primary sequence. The predicted models can offer a useful insight into the underlying mechanisms of drug transport across the plasma membrane. Additionally the effect of protein variants can be analysed in to determine if they induce a structural effect leading to a conformational change or influence ligand binding. Structural modelling can contribute to the understanding of drug transport through elucidating the substrate binding regions, determining how substrates bind, and which residues are essential for substrate binding (Chang et al., 2006). The application of 3D computational modelling techniques and algorithms to gain insight into drug transporters function has increased over the past decade because of the availability of high-quality crystal structures, validated modelling algorithms and insights into evolutionary conservation. The importance of 3D structure-based molecular techniques has also been recognised and discussed in the International Transporter Consortium's white paper (Giacomini et al., 2010).

### **1.13.3 HPLC-MS/MS**

High-performance liquid chromatography (HPLC) coupled to mass spectrometry (MS) is a routine technique for the quantification of analytes from a biological matrix. The HPLC-MS technique functions in two main parts, separation from the analyte from a matrix, using HPLC followed by detection and quantification of the analyte, using mass spectrometry (MS) or ultraviolet (UV) (Lough and Wainer, 1995).

HPLC in itself is a technique in used to separate component and analytes in a heterogeneous mixture. It relies on pumps to pass an pressurised liquid solvents containing the analyte through a column filled with a solid material, known as the stationary phase. Each component in the sample interacts differently with the stationary phase, causing different flow rates for the different components and leading to the separation of the components as they flow out the column.

Mass spectrometers operate by converting the analyte molecules to a charged (ionised) state, with subsequent analysis of the ions and any fragment ions that

are produced during the ionisation process, on the basis of their mass to charge ratio ( $m/z$ ) (Pitt, 2009). These analytes and other compounds are detected in proportion to their abundance; thus a mass spectrum of the molecule is thus produced. This technology is routinely used as the gold standard of measuring compounds in industry, academia and clinical laboratories.

### **1.13.4 Population Pharmacokinetics**

Pharmacokinetic (PK) studies examine the time course of absorption, distribution, metabolism and elimination (ADME) of a drug or compound in the body in an attempt to explain biologic processes with mathematical expressions. PK is considered as 'what the body does to the drug' (Lin and Lu, 1997). Pharmacodynamics (PD) is considered to be 'what the drug does to the body' (Bonate, 2011).

It is common knowledge that subjects receiving the same dose of a drug exhibit high PK variability, drug efficacies and toxicities. The population approach attempts to understand such PK/PD differences among a sub population and determine and classify the sources of variability. Population pharmacokinetics (PPK) can be defined as the study of the sources of variability in drug concentrations among individuals who are the target patient population receiving clinically relevant doses of a drug of interest. This knowledge can be applied to develop rational guidelines for individualised drug dosage regimens which can significantly increase efficacy and safety of a drug.

Traditionally, the pharmacokinetics of a compound or drug were derived from intensive experimentation in healthy volunteers or highly selected patients in rich sampling data-studies. However, it is not always feasible to obtain such data (extensive sampling) in relevant patient populations. Consequently, data analysis techniques that are capable of utilising sparse data sets to obtain the relevant and representative pharmacokinetic information of target population are of great interest and their use is increasing. This type of analysis or the population approach has been applied to pharmacokinetic and pharmacodynamic data analysis since the 1970s.

PPK has been widely used in a number of drug studies over a wide range of drug classes during drug development including anticoagulants, antibacterial and anti-cancer drugs (Lee et al., 2012, Zhao et al., 2012, Menon et al., 2006).

PPK aims to understand the mean population response and identify and explain the variability using demographic and biological data to derive information about an individual which may not be obtained from each individual directly. A nonlinear mixed-effects modelling approach is used to analyse data as a single-stage approach. Instead of modelling data from each individual separately, data from all individuals are modelled in parallel meaning this method allows sparse data collection. It has become widely accepted to the extent that the term population pharmacokinetics is commonly used synonymously with nonlinear mixed effects models.

NONMEM® (ICON Development Solutions, Ellicott City, MD) is a software package developed by S. Beal and L. Sheiner in the 1970s for population PK modelling and is regarded as the 'gold standard' both in academia and the pharmaceutical industry (Beal and Sheiner, 1980, Sheiner and Beal, 1983). The NONMEM software is a regression program that specializes in non-linear systems. A non-linear system is when the response variable changes non-linearly with changes in the predictor variable. An example of a non-linear system is the basic pharmacokinetic equation:

$$C(t) = \frac{Dose}{V} \times e^{-\frac{CL}{V} \times t}$$

The response variable (C) changes with the predictor variable (t), non-linearly as (t) is exponential. Unlike linear equations, non-linear systems often do not have exact solutions, and therefore numerical integrators are required to perform regressions.

The mixed-effects model is defined as including both a fixed effect and a random effect. Fixed effects are defined as known or observable properties of a subject that cause the descriptors to vary across the population. There are two types of random effects that arise from pharmacological data, inter-individual (between-subject) variability and residual error (noise). Residual error is the difference

between the measured observed value and the models predicted values. Therefore it is also known as intra-individual (within-subject) variability which can arise from errors in the quantification assays, drug dosing and human error.

### **1.14 Aims of the project**

Despite metformin being used for decades and being the most commonly prescribed anti-diabetic medication in the world today, there is a considerable number of unknown questions about the mechanisms surrounding vitamin B<sub>12</sub> deficiency, the interaction with OCT1 and the pharmacokinetics of metformin. OCT1 (*SLC22A1*) and OCT2 (*SLC22A2*) are highly polymorphic drug transporters responsible for the hepatic and renal uptake of metformin, respectively. Studies have documented that variants in OCT1 and OCT2 can have an effect on transporter function altering the pharmacokinetic profile of metformin, which leads to inter-individual variability in metformin response. To date, there is no reported correlation between the systemic level of metformin, metformin dose, and vitamin B<sub>12</sub> levels with a particular OCT functional mutation. It is interesting to note that metformin is distributed in the liver and kidneys which are sites of vitamin B<sub>12</sub> storage and regulation respectively. Pharmacokinetic, biological, clinical and genetic data relating to OCT1 will be acquired to determine if there is a specific genotype associated with metformin induced vitamin B<sub>12</sub> deficiency, with an overall aim to develop a genetic screen for susceptibility.

Using biological samples from a cohort of T2DM patients receiving metformin, this project aims to:

1. Sequence the polymorphic metformin drug transporters, *SLC22A1* and *SLC22A2*, genes to detect potentially new and existing genetic variants.
2. Explore the potential effect of new and existing genetic variants on transporter function using bioinformatic algorithms and *in silico* 3D structural modelling and ligand docking techniques.
3. Develop and validate a high performance liquid chromatography (HPLC) method to quantify the levels of metformin in human plasma.
4. Incorporate the data generated from aims 1, 2 & 3 along with other associated biological and clinical data in a population pharmacokinetic model to assess the impact genetic variants have on metformin pharmacokinetics.
5. Collate all the data to determine whether there is an association between metformin parameters, genetic variants in *SLC22A1* and *SLC22A2*, and serum vitamin B<sub>12</sub> levels.

# Chapter 2

Identification of genetic variations in  
metformin drug transporters *SLC22A1* and  
*SLC22A2*

## CONTENTS

<b>2.1 INTRODUCTION.....</b>	<b>51</b>
<b>2.2 MATERIALS &amp; METHODS.....</b>	<b>53</b>
2.2.1 STUDY SUBJECTS .....	53
2.2.2 ISOLATION OF HUMAN GENOMIC DNA .....	53
2.2.3 GENE SEQUENCES AND POLYMERASE CHAIN REACTION (PCR) .....	54
2.2.4 POST AMPLIFICATION PURIFICATION .....	55
2.2.5 GENDER DETERMINATION .....	56
2.2.6 VARIANT IDENTIFICATION/SEQUENCING .....	57
2.2.7 BIOINFORMATIC ANALYSIS.....	58
<i>Prediction of transcription factor binding sites.....</i>	<i>58</i>
<i>Prediction of functional consequences of mutations .....</i>	<i>58</i>
<i>SIFT .....</i>	<i>58</i>
<i>PolyPhen .....</i>	<i>59</i>
<i>SNPs3D .....</i>	<i>59</i>
<i>Evolutionary conservation of variant.....</i>	<i>59</i>
<i>Prediction of potential splicing aberrations.....</i>	<i>60</i>
<i>Prediction of potential mRNA stability .....</i>	<i>60</i>
2.2.8 HAPLOTYPE ANALYSIS.....	60
<b>2.3 RESULTS.....</b>	<b>61</b>
2.3.1 <i>SLC22A1</i> .....	61
2.3.2 <i>SLC22A2</i> .....	61
2.3.3 5'UTR VARIANTS .....	69
2.3.4 PREDICTION OF POTENTIAL SNP FUNCTIONALITY .....	69
2.3.5 HAPLOTYPE ANALYSIS.....	73
<b>2.4 DISCUSSION .....</b>	<b>74</b>

## 2.1 Introduction

The importance of genetic polymorphisms in drug metabolising enzymes influencing the pharmacology of a drug has been extensively studied and well established (Evans and McLeod, 2003). More recently the significance of drug transporters has been recognised to underlie the inter-individual differences in the pharmacology and ADMET of a drug. For example, the MHRA Drug Safety Update (May 2012) highlighted changes to simvastatin usage which can increase the risk of myopathy and rhabdomyolysis dependent on genetic polymorphisms in the membrane transporter *SLCO1B1*, encoding for OATP1B1. This transporter controls statin uptake from the blood into the liver and genetic polymorphisms have been associated with statin-induced myopathy (Carr et al., 2013, Niemi, 2010).

Absorption, distribution and excretion of most endogenous compounds and drugs are controlled by polymorphic and polyspecific membrane transporters expressed in a wide range of tissues including intestine, liver, kidneys, skeletal muscle, white blood cells and endothelial blood-brain barrier (Giacomini et al., 2010). The largest superfamily of membrane transporters, the solute carrier family include OCT1 and OCT2 which are responsible for hepatic and renal uptake of metformin, respectively (Kimura et al., 2005a). The transporters are encoded by the *SLC22A1* and *SLC22A2* genes located on chromosome 6q26. *SLC22A1* consists of 11 exons spanning 37 kb, the translated protein consists of 554 amino acids. Adjacent to the *SLC22A1* gene is *SLC22A2* which also consists of 11 exons spanning 42 kb, the translated protein consists of 555 amino acids (Giacomini et al., 2010, UniProt, 2015). The two human proteins share 70% homology with each other and are conserved across species showing at least 74% and 82% homology, respectively, with characterised mammalian orthologs (UniProt, 2015).

Human OCT1 is primarily expressed at the sinusoidal membrane of hepatocytes with decreasing levels in the adrenal gland, lung epithelium, neurons, placental tissue and the spleen (Nies et al., 2009). OCT1 translocates a broad array of organic cations and drugs including histamine, serotonin, tetraethylammonium

and metformin (Zair et al., 2008). As the pharmacological target organ of metformin is the liver, OCT1 is regarded as the primary transporter that allows metformin to exert its pharmacological action in lowering peripheral blood glucose levels.

Human OCT2 is primarily expressed in the distal renal tubules (Aoki et al., 2008). OCT2 facilitates the uptake of a variety of cationic compounds including cimetidine and metformin from the circulation into renal epithelial cells (Zair et al., 2008). OCT2 has greater affinity and capacity for metformin than OCT1 and thus is able to rapidly eliminate metformin into the urine (Kimura et al., 2005a).

Both *SLC22A1* and *SLC22A2* genes are regarded to be highly polymorphic with 100 registered nsSNPs resulting in altered amino acid changes on the NCBI database. These SNPs have been extensively characterised at different frequencies in ethnically diverse populations, (Chapter 1, Table 1.5) (Shu et al., 2007, Shu et al., 2003, Kerb et al., 2002, Leabman et al., 2002, Itoda et al., 2004). Furthermore, Shu et al (2003) determined that several nsSNPs of OCT1 decreased metformin uptake *in vitro* (Shu et al., 2007). Therefore it is hypothesised that one or multiple nsSNPs may lead to decreased metformin uptake in hepatic cells *in vivo* leading to decreased metformin action to decrease peripheral blood glucose levels.

Both genes are polymorphic and there are many known variants across both genes. Therefore sequencing these genes will potentially find both new and rare variants as both genes. In this chapter both *SLC22A1* and *SLC22A2* were sequenced including all exons, including intron-exon boundaries plus up to 2 kb of 5'UTR in a Caucasian population. The results obtained from this chapter will be used as covariates in population PK modelling.

## 2.2 Materials & Methods

### 2.2.1 Study Subjects

Seventy-five patients (45 male and 30 female; mean age 64 years; range 42-80 years) receiving metformin treatment for T2DM were chosen for this study. Ethical approval for the study was obtained from the Liverpool Ethics Research Committee, University of Liverpool, all subjects gave informed written consent before participating. Relevant information on demographics, admission and clinical history was collected for each patient and recorded in an anonymised case report proforma. Table 2.1 displays summary of demographic, clinical and biological data for the patients used for this thesis. Blood samples were collected in EDTA vacutainers from 09/2005 – 10/2007 and were stored for DNA preparation at -20 °C until analysis in 11/2010.

The time of day of metformin dosing ranged from 02:00 to 12:50 with a median time of 08:17. The first of the blood samples taken ranged from 08:37 to 15:10 with a median time of 11:19. Time from the dose received and blood sample taken ranged from 4 min to 9 hr 5 min with a median time of 3 hr. Time between the first sample of blood taken and the last ranged from 45 to 195 minutes with a median time of 80 min. A summary of individual patient sampling times can be displayed in appendix figure A2.1. A total of 218 plasma samples were collected from 75 T2DM patients with up to three blood samples per individual were collected at random time intervals.

### 2.2.2 Isolation of human genomic DNA

Extraction was performed on the Chemagic Magnetic Separation Module I apparatus (Chemagen Auto-Q Biosciences, Germany), according to the manufacturer's instructions. Five millilitres of blood was used per extract. Extracts were subsequently quantified and stored at 4°C. Yield average was 183 ng/μL (range 25 – 333 ng/μL) yielding 91 μg DNA/sample (range 4.5 – 166 μg), (Average 260/280: 1.9; 260/230: 2.96). All DNA samples were diluted to 25 ng/μL with 1x TE buffer.

**Table 2.1 Summary of clinical variables**

	Mean (SD)	Median	Range
<b>Demography</b>			
Age (years)	64 (9.7)	65.39	42.3 - 80.6
Height (m)	1.67 (0.1)	1.67	1.45 - 1.91
Weight (kg)	91 (18.2)	92	51.2 - 140
BMI (kg/m <sup>2</sup> )	32.6 (5.1)	31.96	22.2 - 43.6
Ideal body weight (kg)	62 (11)	63	39 - 84
Lean body weight (kg)	55 (6)	56	41 - 70
Body surface area (m <sup>2</sup> )	2.00 (0.24)	2.03	1.46 - 2.61
<b>Biochemistry &amp; Haematology</b>			
Vitamin B <sub>12</sub> (ng/mL)	237 (96)	238	52 - 547
Folate (µg/ml)	8.6 (4.8)	7.8	1.6 - 20
Lactate (mmol/L)	2.10 (0.75)	1.75	0.8 - 3.9
Haemoglobin (g/dL)	13.2 (1.64)	13.3	8.8 - 16.1
Haematocrit (%)	38.9 ( 4.6)	39.2	26 - 48.2
Mean Corpuscle volume (fL)	88.4 (4.8)	88.9	74.9 - 99.3
<b>Kidney function</b>			
Creatinine (µmol/L)	90.4 (27.8)	84	75 - 195
Urea (mmol/L)	6.8 (2.2)	6.4	3.3 - 13.6
CL <sub>CR</sub> (mL/min)	90.8 (33)	85	37 - 174
eGFR (mL/min)	74 (21)	73	33 - 138
<b>Liver function</b>			
Albumin (g/L)	42 (3.5)	42	32 - 48
Alanine aminotransferase (g/L)	25 (15)	22	10 - 117
Alkaline phosphatase (g/L)	76 (24)	74	40 - 167
Gamma GT (U/L)	36 (31)	27	7 - 171
Bilirubin (µmol/L)	9 (5)	8	3 - 34
<b>Metformin parameters</b>			
Metformin total daily dose (mg)	2125 (793)	2000	500 - 3000
Metformin single dose (mg)	793 (222)	850	500 - 1000
Metformin total daily dose (mg/kg)	24 (10)	23	5 - 59
Metformin cumulative dose (kg)	6.99 (6.31)	5.10	0.15 - 31.24
Metformin plasma level (ng/mL)	1894 (1027)	1744	30 - 5387
Duration of metformin treatment (years)	8.05 (6.04)	6.44	0.41 - 29.03
Duration of T2DM (years)	10.17 (6.85)	8.55	0.41 - 31.67

N=75, Ethnicity: 73; White British, 1; White/Chinese, 1; Black Caribbean

### 2.2.3 Gene sequences and polymerase chain reaction (PCR)

The reference genomic and cDNA sequences of *SLC22A1* and *SLC22A2* were obtained from GenBank (NCBI Reference Sequence: NM\_003057.2 and NM\_003058.3, respectively) (Lander et al., 2001, Mungall et al., 2003). Primers were designed manually using the DNASTAR Laser gene SeqBuilder program to sequence all exons, including intron-exon boundaries plus up to 2 kb of 5'UTR sequence to capture variants in nearby regulatory elements (Table 2.2).

Each region was amplified using 25 ng of genomic DNA using 0.25  $\mu$ M of each primer as listed in Table 2.1 with Reddy-PCR Master Mix, 2.0 mM MgCl<sub>2</sub> (Thermo Scientific AB-0608/LD/A). The PCR set up was performed in a pre-PCR laboratory, free from PCR products and amplified using MJ Research PTC 240 Tetrad 2 thermal cycler. The conditions were as follows: Lid control set constant at 105°C; 95°C for 10 min followed by 40 cycles of 94°C for 0.5 min, 58°C for 0.5 min, 72°C for 1 min followed by a final extension of 72°C for 10 min. Each set of primers were initially tested with Roche DNA to ensure primers could amplify the required regions. All PCR products were run on a gel in a post PCR laboratory to confirm amplification. Three  $\mu$ L of each post-PCR product was run on a 2% agarose gel (EMBITec GE-4572) at 150 V, 400 mA for 40 min including a 100 bp ladder (Thermo Scientific, Superladder-Low 100 bp Ladder SL-100/LD). The buffer used was 1x TAE (EMBITec EC-1018)The gel was visualised using a UVP benchtop UV transilluminator. Primers were tested with reference DNA to check amplification (Appendix Figure A2.1).

### 2.2.4 Post Amplification Purification

Post PCR amplification products were treated with ExoSAP-IT reagent (Affymetrix) in order to remove unincorporated primers and dNTPs that may interfere with sequence analysis. ExoSAP-IT contains Exonuclease I and Shrimp Alkaline Phosphatase to degrade primers and dephosphorylate dNTPs respectively unconsumed in the PCR amplification reaction. To each 13  $\mu$ L reaction volume, 2  $\mu$ L of a 1:10 dilution of ExoSAP-IT was added. This was treated for 60 min at 37°C followed by 15 min at 85°C to inactivate enzymes.

**Table 2.2. Primers used for the sequence analysis of SLC22A1 and SLC22A2.**

Amplified and sequenced region	Forward Primer (5' -3')	Reverse Primer (5'-3')	Amplified length (bp)	
<i>SLC22A1</i> (OCT1)	5'UTR 1	AGCATGTCAGGCTGCTGAGC	GTTCAAACAAGTTATGGAAGG	507
	5'UTR 2	TAGTCAATATGTTTACACACAGG	TAAGGTCATAAACTGCTTTGGC	453
	5'UTR 3	TCCAGCATAGCTAGGGCAGG	CCATAGGTTTTGAGGGAACAGG	525
	5'UTR 4	GGTGCAGTGTATACTGCTTGG	CCCTATGGTGCTGGTTTCAGG	463
	5'UTR 5	TTAGACCCCACTGACTCGCTC	CAACCTGCTCCAGAATGTCATC	326
	Exon 1.1	GATGTTTCACACTTGGACAGC	CCTGGCACTGTATAGTTTCAGC	396
	Exon 1.2	TTCACACCTGACCACCACTGC	GATATGGAAGTGAAGTTCATAGG	402
	Exon 2	ATGGAAGGGTGTAGTCCCTGAC	CACCACTGAGAACAGATTCCG	298
	Exon 3	GCATCCCACCATGCATGTCTG	CCATTCTAGCCCATGTCTCTGC	414
	Exon 4	AGAAGCCTGGGAGCAGGTGAG	ATGCGTTATGCATGTGGACACC	507
	Exon 5	AGAAGCCTGGGAGCAGGTGAG	TGCTTCACACCCATGACAAGG	399
	Exon 6	AGGTGGCTCTGCTCATGACAG	CACCTGAGTATTCCTACTGTCTC	254
	Exon 7	CTTCAGTCTCTGACTCATGCC	CCTCATCTTTGTTCTCATTCC	408
	Exon 8	ATAGTCCAAGCATGACCCACC	AACTGAGCAATGCTTGGCTGC	354
	Exon 9	TGAGCACTGGACAGCCACAG	GTACTIONCACACTCAGTTCCACC	357
	Exon 10	TCCTCTCTTTGGCTGGCTGTG	TTCCTCATAGCAGTTCTGGGAG	391
Exon 11*	GTGTACAACCTTTGCAACAGTTCC	GATACCAATAGCACCAACAGC	444	
<i>SLC22A2</i> (OCT2)	5'UTR 1	ACGAAGCAGAGTGCCTCTGTG	TTCCTGTATCTGTGGGTCTTC	578
	5'UTR 2	TAAGGCTCACGGCCAACACC	AGCAGCTCGTGGAACAGAC	452
	5'UTR 3	CCACTGTTACACAGAAAGGCAG	AAGAGCCGTCGGGATGCATG	525
	5'UTR 4	ACTTCAGGGTTGAAACGCAGG	TGAGCTCACTCCCAGGATGC	510
	5'UTR 5	ATGGGCCAGCACTCAGATTCC	CATGATCCTGCAGGCAGGAG	394
	Exon 1	GTGCACCTTTGAAGTCAGCTG	TGCAGGCCAAAGAGATGTCCAG	747
	Exon 2	TACCCTAGCTGAGTTATGTCC	ATGAAGGCCAGGAGATTGTGG	358
	Exon 3	CTATCAGTCTGTGCCTCCTGG	TTTGGCAGCGAGGTTGCTTTG	389
	Exon 4	GTTCTAGTTTCTGATAGCTGG	CATGGAATTGGGCTCTTTGTG	429
	Exon 5	GAGATCCAAGTATTAACATCC	TTTGATACTTAAGGCCCTGGC	287
	Exon 6	GTTATTCCCTATGTGACCCAGG	AGCGCTAATACCGGGATGAGG	321
	Exon 7	CTAGCAAGGAGATGGTCACAG	GGTTTTCTATCAATGGGCC	456
	Exon 8	GTCCTTACAGTCCCCTCTGG	GGTAAGATATCCTTTGTCTGCAC	323
	Exon 9	GAGCAGTGTACTATAGCTC	GTTACTAATAGGCATGACACC	380
	Exon 10	GGAAACTCTAATTATAGACCTTG	GTATGGTGTGAAGTATAAAGTC	309
	Exon 11	GAGAACCACCACTCAGAACAC	TTGGCAGGATCTGGTCCCATG	448
	3'UTR 1	GAGACCGTTGCTGCTGTCATG	TCACCTGTGTTACTGAAAGGC	409
	3'UTR 2	GTTGTCCAGAATGTATGTCAAG	GTAGAGGTGAAATAGGGCAAGG	446

Promoter Regions covered 2 kb upstream of 5'UTR. Each forward primer included the M'13 tag (ACTGTAAAACGACGGCCAGT) and the reverse included (ACCAGGAAACAGCTATGACC). Amplified length includes region, primer and M'13 universal tag. Each region was amplified to include a 5' and 3' 100 bp flanking sequence.

### 2.2.5 Gender determination

Quality control measures consisted of determining the sex of each sample and matching it with the patient's clinical data using the amelogenin gene where expression differs between the X and Y chromosome. The amelogenin gene in

the X chromosome expresses a 6 bp deletion in intron 1 relative to the Y chromosome. Gel electrophoresis resolves two bands (112 and 106 bp) for male gDNA whereas one is resolved for female gDNA (Appendix Figure A2.2). Genomic DNA was amplified using primers and visualised on a 2 % agarose gel (EMBITec GE-4572) at 150 V, 400 mA for 25 min as a marker for each sex to compare against gender recorded for each clinical sample.

### **2.2.6 Variant identification/Sequencing**

The PCR products were amplified using the ABI PRISM Big Dye\* Terminator v3.1 Cycle Sequencing Ready Reaction Kit (Applied Biosystems). In brief, 1 µL of purified PCR product per sample was added to 9 µL of sequencing mastermix which comprised of 1 µL BigDye Terminator reaction mix V3.1; 7 µL sequencing buffer; 1 µL of primer at 3.2 pM. Primers from table 2.2 with M'13 tags were used for the sequencing reaction. Forward primer included the M'13 tag (ACTGTAAAACGACGGCCAGT) and the reverse tag included (ACCAGGAAACAGCTATGACC). The reactants were amplified using a Tetrad 2 thermal cycler with the following conditions, lid control set constant at 105 °C; 25 cycles of 96 °C for 10 sec, 50 °C for 5 sec and 60 °C for 4 min. Each PCR product was sequenced in both forward and reverse directions. Sequencing reaction products were purified by gel filtration using Performa® DTR 384-well gel filtration plates. Sequences were delineated with a ABI PRISM Sanger 3730XL DNA analyser and data acquired on the ABI PRISM 3100 Data Collection Software Version 1.01. Sequencing reads ranged from 274-767 bp. Chromatograms were aligned and analysed using Consed Command line (version 16.0) program and variants recorded manually in an Excel spreadsheet. All variants were verified through evaluating each chromatogram using the Chromas Lite 2.1.1. software (Technelysium Ltd) using the forward and reverse sequence directions. Novel SNPs were re-sequenced or if a SNP was not visible in both forward and reverse directions. Variants were assigned a refSNP cluster identifier (rs#) using the National Centre for Biotechnology (NCBI) website using the GRCh38 (NC 000006.12) assembly.

## 2.2.7 Bioinformatic Analysis

### *Prediction of transcription factor binding sites*

Mutations identified in the 5'UTR promoter regions were assessed to determine if they were expressed in predicted transcription factor putative-binding sites. The 5'UTR sequence was submitted to two databases to predict TF binding sites: BioBases' TRANSFAC® (<http://www.biobase-international.com/product/transcription-factor-binding-sites>) and Motif (<http://www.genome.jp/tools/motif/>). TRANSFAC uses positional weight matrices (PWMs) to search DNA sequences for potential transcription factor binding sites (Wingender et al., 2000). Motif utilises dynamic programming to find the best alignment between a query sequence and each profile entry in the PROSITE database (Sigrist et al., 2002).

### *Prediction of functional consequences of mutations*

For novel and known mutations identified in both *SLC22A1* and *SLC22A2*, four *in silico* algorithms were used to predict the effect coding SNPs had on protein function; the Grantham Matrix, the SIFT algorithm, the PolyPhen algorithm and the SNP3D algorithm. For each analysis, reference protein sequences for *SLC22A1* and *SLC22A2* were obtained from the UniProt database for analysis (accession numbers O15245 and O15244 respectively). All results were then collated in one table (Table 2.5) which applied a novel colour intensity to reflect the effect on protein function and compare the five algorithms.

#### *The Grantham Matrix*

This predicts the effect of substitutions between amino acids based on physical and chemical properties, including polarity, composition and molecular volume. An increasing/greater score is indicative of increasing chemical dissimilarity between the substituted amino acids (Grantham, 1974).

#### *SIFT*

Sorting Intolerant from Tolerant [<http://sift.jcvi.org/> (Ng and Henikoff, 2001)] predicts the functional effect of an amino acid substitution based on the alignment of highly similar orthologs determining whether the amino acid is

evolutionarily conserved in protein families and calculates whether the biochemical parameters of the exchanged amino acids are similar or disparate. Conservation of amino acids has been indicative of normal transporter function. SIFT scores range from 0 to 1, scores near 0 reflect evolutionary conservation and intolerant amino acid substitutions whereas scores near 1 reflect evolutionary unconserved residues and thus tolerant to substitution.

### *PolyPhen*

Polymorphism Phenotyping [<http://genetics.bwh.harvard.edu/pph2/> (Sunyaev et al., 2001)] predicts the functional effect of substitutions using physical and comparative considerations such as the level of sequence conservation between orthologs, the phylogenetics of the protein, the physical and chemical properties of the substituted amino acid and the proximity of the substitution to predicted functional domains and characteristic structural features within the protein sequence. PolyPhen scores of less than 1.5 indicate functionally normal variants; scores between 1.5 and 2.0 are categorized as possibly deleterious and greater than 2.0 are categorized as probably deleterious.

### *SNPs<sub>3D</sub>*

This incorporates two previously developed methods to assess the impact of nsSNPs on protein function. The first identifies which amino acid substitutions significantly destabilize the folded state of the protein. The second analyses the extent of evolutionary conservation at the site of the altered amino acid. A negative score predicts a SNP to be deleterious and a higher score relates to a higher confidence in prediction [<http://www.snps3d.org/> (Yue et al., 2006)].

### *Evolutionary conservation of variant*

Shu et al., 2003 have established that determining evolutionary conservation of orthologous sequences to assess the impact of non-synonymous SNPs was a more accurate predictor of protein function. This study therefore determined whether the substituted amino acid residue is evolutionary conserved (EC) or evolutionary unconserved (EU) through alignments using NCBI BLAST software and the Gerhard and Wolff study (Burckhardt and Wolff, 2000) to label a residue EC or EU. A residue was classified EC based on sequence alignments

with 4 or 5 mammalian orthologs and highlighted red in Table 2.5 The orthologs used were mouse, rat, rabbit, porcine and bovine. All orthologs were at least 74 % and 82 % identical for *SLC22A1* and *SLC22A2* to the human sequence, respectively.

#### *Prediction of potential splicing aberrations*

All intronic and intronic flanking coding mutations were analysed for their potential effect on splicing (pre-mRNA splicing) using the intronic splice site consensus sequence (Strachan and Read, 2011). SNPs located in a splice donor, acceptor or branch sites could influence alternative splicing and thus affect protein levels or functionality.

#### *Prediction of potential mRNA stability*

To determine if any SNPs located in the 3'UTR were expressed in adenylate-uridylylate-rich elements (AU-rich elements; AREs), the 3'UTR of *SLC22A1* and *SLC22A2* were submitted to AREsite, an online resource for the investigation of AU-rich elements (ARE) in vertebrate mRNA UTR sequences, [<http://rna.tbi.univie.ac.at/cgi-bin/AREsite.cgi>](Gruber et al., 2011)]. ARE contain the core motif, AUUA and are recognised ARE-binding proteins to determine RNA stability.

### **2.2.8 Haplotype analysis**

The pattern of pairwise linkage disequilibrium (LD) between SNPs was visualised using the HaploView software version 4.1 (Barrett et al., 2005). HaploView calculates several pairwise measures of LD, which it uses to create a graphical representation. HaploView estimates the maximum-likelihood values of the four gamete frequencies, from which the multi-allelic  $D'$ , LOD and  $r^2$  calculations derive. Conformance with Hardy-Weinberg equilibrium is computed using an exact test. The minor allele frequency (MAF) cut-off was defined as 0.05 rather than 0.01 due to the small sample size ( $n = 75$ ).

## 2.3 Results

To identify variants in *SLC22A1* and *SLC22A2* we sequenced all 11 exons per gene including 50-100 bp intronic flanking sequence as well as sequencing the 3'UTR and 2 kb of the 5'UTR.

### 2.3.1 *SLC22A1*

Twenty-five variants were identified including some which had not been reported at the time. Overall 6 were located in the 5'UTR, 7 were intronic and 12 were exonic comprising 9 nonsynonymous, 2 synonymous and a 3 bp del resulting in a methionine deletion. The novel variant was g.IVS8+14 A>G (Figure 2.1). The variants are summarised in Table 2.3. The 12 coding SNPs (cSNPs) are displayed in Figure 2.2. The topology diagrams were produced using the transmembrane protein display software TOPO2 (UCSF), transmembrane protein display software available at <http://www.sacs.ucsf.edu/TOPO2>. This was produced through uploading primary OCT protein sequences with their respective known TMDs. OCT TMDs were predicted using the TMHMM Server v. 2.0.

### 2.3.2 *SLC22A2*

Twenty-five variants were identified with 7 being located in the 5'UTR, 4 intronic, 7 exonic comprising 3 nonsynonymous and 4 synonymous, and 7 in the 3'UTR. The SNPs are summarised in Table 2.4. The 7 cSNPs are displayed in Figure 2.4.

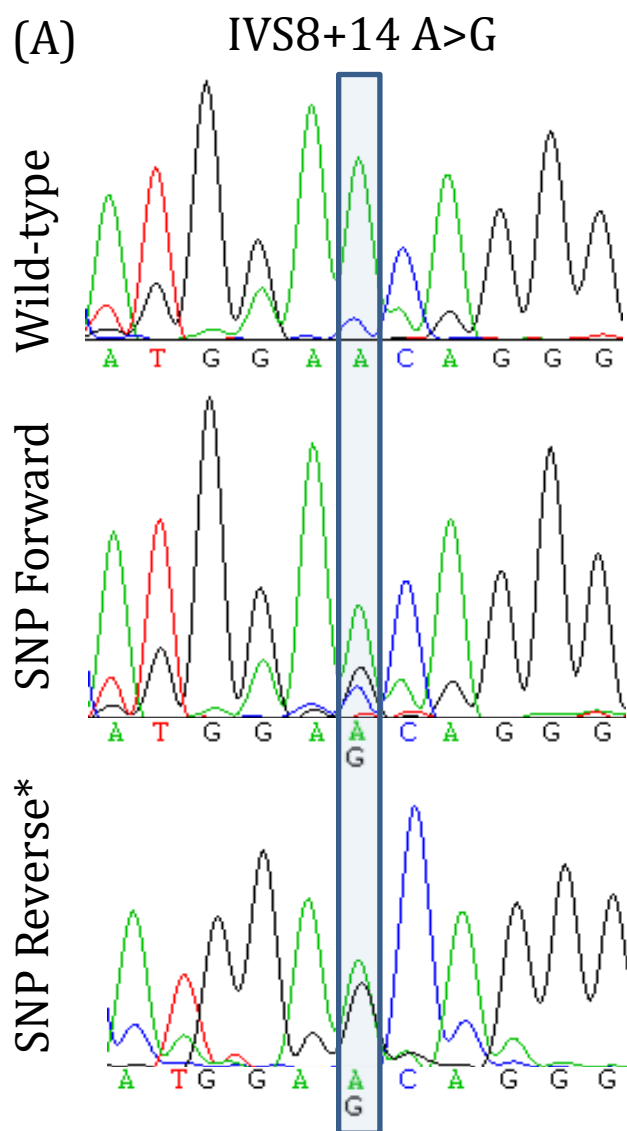


**Figure 2.1 Chromatograms of novel SLC22A1 SNP**

(A) g.IVS8+14A>G Chr6:160143663. Box highlights nucleotide position. Each PCR products were sequenced in both directions. \*Chromatogram is reverse direction post complimented using Chromas Software for an illustrative comparison.

**Table 2.3. Summary of variants in *SLC22A1* gene in 75 Caucasian patients receiving metformin for treatment of T2DM.**

	Nucleotide Location <sup>a</sup>	Chromosomal position (GRCh38)	Reference <sup>b</sup>	Nucleotide Change	$\alpha\alpha$ change <sup>d</sup>	$\alpha\alpha$ location <sup>e</sup>	HET	HOM	WT
5'UTR	-1620	160120316	rs9457840	T>A	-	-	0.013	-	0.987
	-1419	160120517	rs12110656	T>A	-	-	0.026	-	0.974
	-1198	160120738	rs57504133	A>G	-	-	0.013	-	0.987
	-605	160121331	rs182178700	G>A	-	-	0.013	-	0.987
	-430	160121506	rs73598465	T>A	-	-	0.026	-	0.974
	-59	160121877	rs536113777	C>T	-	-	0.013	-	0.987
Exon 1	181	160122116	rs12208357	C>T	p.R61C*	ECM	0.184	-	0.816
Exon 2	480	160130172	rs683369	C>G	p.L160F	TMD	0.395	0.053	0.553
Intron 2	IVS2-26	160132206	rs45584532	C>T	-	-	0.276	0.013	0.711
Exon 3	558	160132274	rs34134157	C>T	p.N186N	TMD	0.013	-	0.987
Exon 3	566	160132282	rs34104736	C>T	p.S189L	TMD	0.013	-	0.987
Intron 5	IVS5-7	160136537	rs7762846	C>T	-	-	0.276	0.013	0.711
Exon 6	1022	160136611	rs2282143	C>T	p.P341L*	CYTO	0.013	-	0.987
Intron 6	IVS6+22	160136672	rs35235578	C>T	-	-	0.013	-	0.987
Exon 7	1201	160139792	rs34130495	G>A	p.G401S*	CYTO	0.026	-	0.974
Exon 7	1222	160139813	rs628031	A>G	p.M408V	TMD	0.553	0.289	0.158
Exon 7	1238	160139829	rs144322387	C>T	p.A413V*	TMD	0.013	-	0.987
Exon 7	1260	160139849-51	rs202220802	ATGdel	p.M420del	TMD	0.224	0.026	0.750

**Table 2.3 (continued). Summary of variants in *SLC22A1* gene in 75 Caucasian patients receiving metformin for treatment of T2DM.**

	Nucleotide Location <sup>a</sup>	Chromosomal position (GRCh38)	Reference <sup>b</sup>	Nucleotide Change	$\alpha$ change <sup>d</sup>	$\alpha$ location <sup>e</sup>	HET	HOM	WT
Exon 7	IVS7+7	160139866-73	rs113569197	TGGTAAGTins	-	-	0.566	0.171	0.263
Intron 7	IVS7+34	160139901	rs9457843	C>T	-	-	0.250	0.013	0.737
Exon 8	1320	160143584	rs35956182	G>A	p.M440I	TMD	0.026	-	0.974
Intron 8	IVS8+14	160143663	<i>Novel</i>	A>G	-	-	0.013	-	0.987
Exon 9	1393	160154805	rs34059508	G>A	p.G465R*	TMD	0.040	-	0.961
Exon 10	1503	160155979	rs41267797	G>A	p.V501V	TMD	0.026	-	0.974
Intron 10	IVS10- 21	160158495	rs622591	C>T	-	-	0.342	0.066	0.592

<sup>a</sup> Location of nucleotide relative to ATG start site. <sup>b</sup> Obtained from NCBI database (GRCh38 assembly). <sup>c</sup> Number indicates location on amino acid in sequence. <sup>d</sup> Predicted location of amino acid in protein, ECM, extracellular matrix; TMD, transmembrane domain; CYTO, cytoplasmic. Note, no SNPs were found in the 3'UTR. MAF; minor allele frequency.

**Table 2.4. Summary of variants in *SLC22A2* gene in 75 Caucasian patients receiving metformin for treatment of T2DM.**

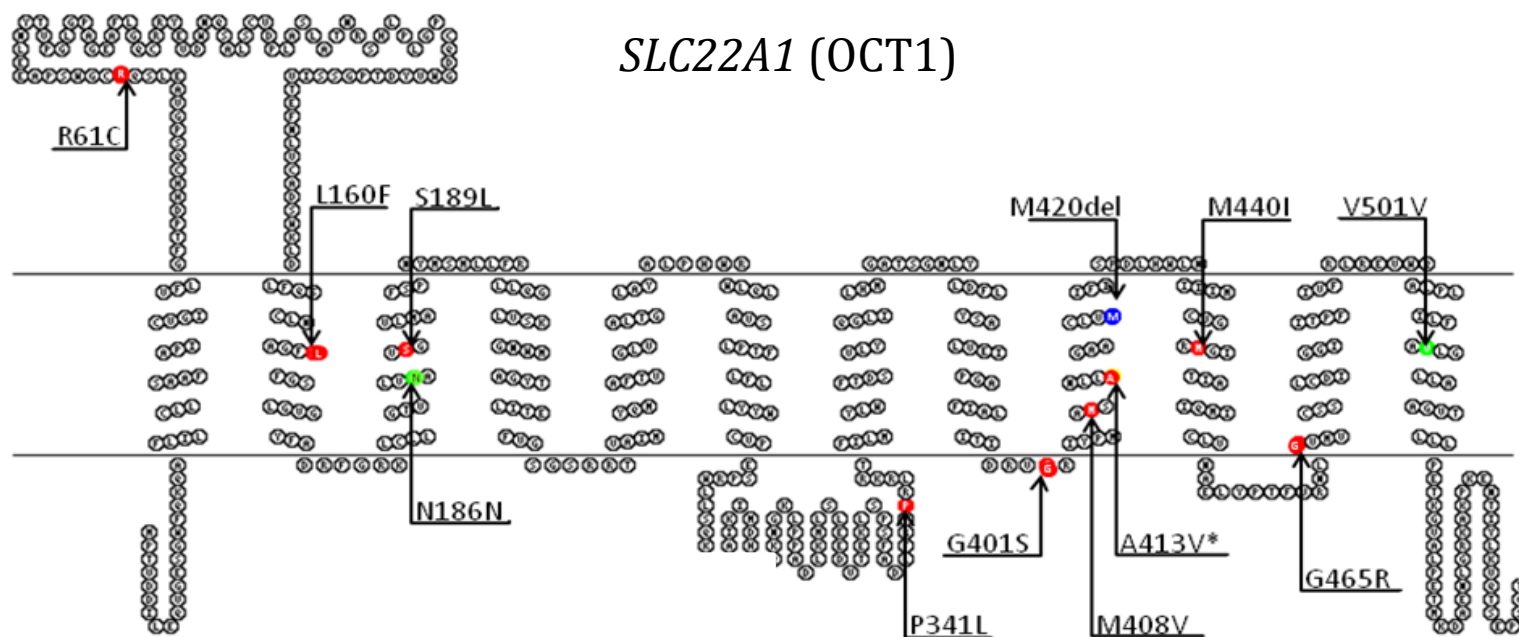
	Nucleotide location <sup>a</sup>	Chromosomal position (GRCh38)	Reference <sup>b</sup>	Nucleotide Change	αα change <sup>c</sup>	αα location <sup>d</sup>	HET	HOM	WT
	-1604	160260361	rs3127573	T>C	-	-	0.240	0.013	0.747
	-1525	160260282	rs316023	A>G	-	-	0.440	0.120	0.440
	-1222	160259979	rs148965379	A>T	-	-	0.013	-	0.987
5'UTR	-1189	160259946	rs146811048	C>T	-	-	0.013	-	0.987
	-956 - 954	160259711-13	rs34129302	GAA/-	-	-	0.280	0.013	0.707
	-922	160259681	rs183436020	G>C	-	-	0.027	-	0.973
	-246	160259003	rs55920607	C>T	-	-	0.013	-	0.987
Exon 1	390	160258368	rs624249	T>G	p.T130T	ECM	0.493	0.387	0.120
Intron 2	IVS2+32	160256582	rs2774230	C>G	-	-	0.400	0.547	0.053
Intron 2	IVS2- 18	160250720	rs8177511	T>C	-	-	0.013	-	0.987
Intron 2	IVS2-3	160250705	rs512275	C>A	-	-	0.027	-	0.973
Exon 3	599	160250641	rs376744152	A>G	p.M194V	TMD	0.013	-	0.987
Exon 4	808	160249250	rs316019	G>T	p.A270S	TMD	0.173	-	0.987
Intron 4	IVS4-59	160247357	rs2279463	T>C	-	-	0.293	0.013	0.693
Exon 7	1214	160243656	rs368002099	G>A	p.D399N	CYTO	0.013	-	0.987
Exon 7	1222	160243648	rs8177515	C>T	p.I401I	CYTO	0.013	-	0.987
Exon 10	1525	160224800	rs316003	G>A	p.V502V	TMD	0.387	0.067	0.547
Exon 10	1594	160224731	rs139737555	C>A	p.T525T	CYTO	0.027	-	0.973
	1686 + 108	160217325	rs8177524	C>A	-	-	0.053	-	0.947
	1686 + 361	160217072	rs3127594	A>T	-	-	0.293	0.013	0.693
3'UTR	1686 + 389	160217044	rs3103353	G>A	-	-	0.293	0.013	0.693
	1686 + 462	160216971	rs3127593	T>A	-	-	0.293	0.013	0.693
	1686 + 490	160216943	rs2450975	C>A	-	-	0.400	0.067	0.533

**Table 2.4 (continued). Summary of variants in *SLC22A2* gene in 75 Caucasian patients receiving metformin for treatment of T2DM**

	Nucleotide location <sup>a</sup>	Chromosomal position (GRCh38)	Reference <sup>b</sup>	Nucleotide Change	αα change <sup>c</sup>	αα location <sup>d</sup>	HET	HOM	WT
3'UTR	1686 + 575	160216858	rs694812	A>G	-	-	0.213	-	0.787
	1686 + 621	160216812	rs3127592	A>G	-	-	0.293	0.013	0.693

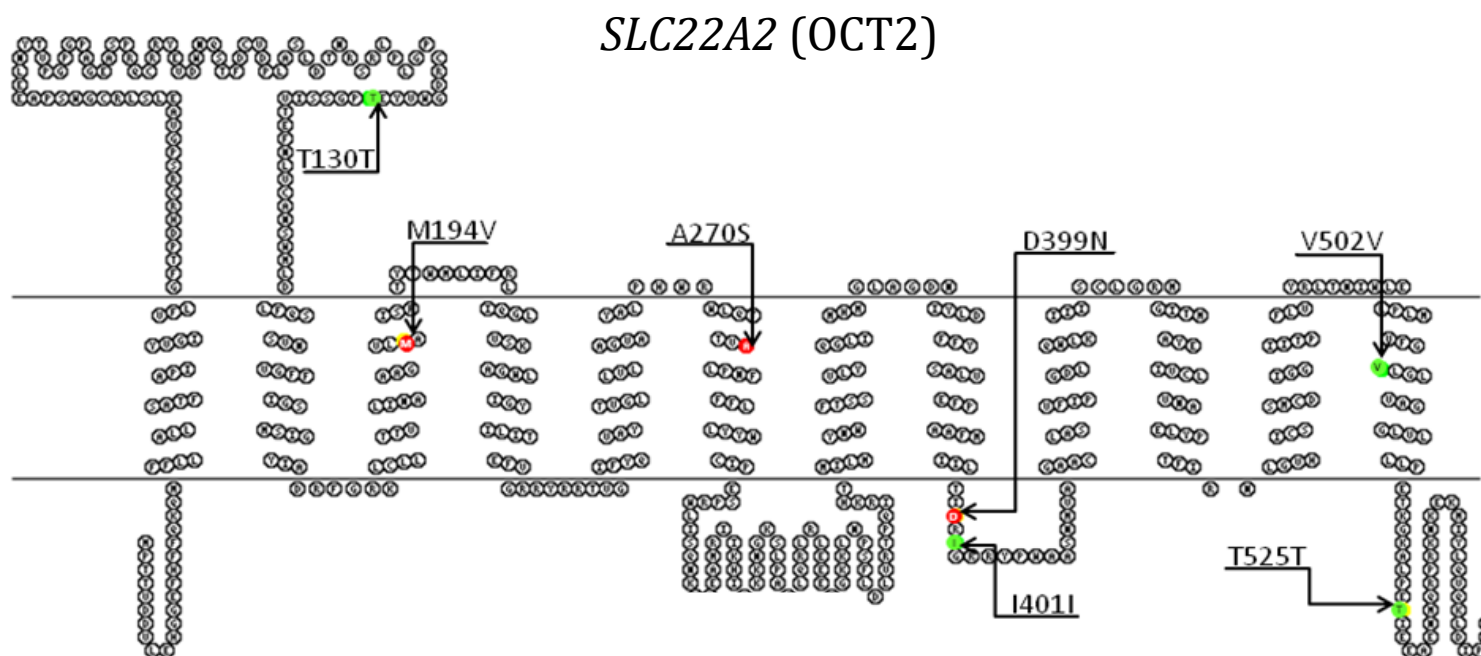
<sup>a</sup> Location of nucleotide relative to ATG start site. <sup>b</sup> Obtained from NCBI database (GRCh38 assembly). <sup>c</sup> Number indicates location on amino acid in sequence. <sup>d</sup> Predicted location of amino acid in protein, ECM, extracellular matrix; TMD, transmembrane domain; CYTO, cytoplasmic. MAF; minor allele frequency.

Figure 2.2. Predicted secondary structure and alignment of OCT1 with coding region SNPs.



Nonsynonymous amino acid changes are shown in red, synonymous changes in green and an amino acid deletion is shown in blue. The transporters are predicted to consist of 12 transmembrane domains with both N and C terminus located intracellularly with a large extracellular loop between TMDs 1 and 2. Note that the majority of SNPs are located in the transmembrane domains, the domains responsible for OCT substrate specificity.

Figure 2.3. Predicted secondary structure and alignment of OCT2 with coding region SNPs.



Nonsynonymous amino acid changes are shown in red, synonymous changes in green and an amino acid deletion is shown in blue. The transporters are predicted to consist of 12 transmembrane domains with both N and C terminus located intracellularly with a large extracellular loop between TMDs 1 and 2. Note that the majority of SNPs are located in the transmembrane domains, the domains responsible for OCT substrate specificity.

### 2.3.3 5'UTR variants

The 5'UTR was submitted to two transcription factor databases; TRANSFAC® and Motif, to identify potential transcription factor (TF) binding sites within *SLC22A1* and *SLC22A2* genes. TRANSFAC® identified two SNPs in potential *SLC22A1* transcription binding sites; rs57504133 (g.-1198A>G) and rs73598465 (g.-430T>A). No predictive binding sites near or containing a SNP were found using the MOTIF server. TRANSFAC® predicted rs57504133 to be present in a Zinc finger protein 333 (ZNF33) binding site ATAAT (Tian et al., 2002) and rs73598465 is present in POU class 6 homeobox 1 transcription site CTCATTAT (Messier et al., 1993). These SNPs could potentially lead to the loss of a transcription site. One potential TF binding site was identified in the *SLC22A2* 5'UTR, Churchill domain containing 1, a zinc ion binding protein. Its recognition site, CCCCCG, is located together with rs183436020 (g.-922G>C) (Lee et al., 2009a). Therefore this SNP could potentially lead to the loss of this transcription site. No SNPs present in both genes lead to the creation of a new binding site.

### 2.3.4 Prediction of Potential SNP Functionality

*Exonic variants*- This chapter applied four *in silico* algorithms: the Grantham Matrix, the SIFT algorithm, the PolyPhen algorithm and the SNP3D algorithm to predict the effect of each nSNP on protein function. These five algorithms were chosen based on popular use and citation number. The use of five algorithms displayed with colour intensities allowed for comparative analysis to determine if the results were similar between one another. Nine nsSNPs were identified in *SLC22A1*, but only five, p.R61C, p.P341L, p.G401S, p.A413V, and p.G465R, were predicted by all algorithms to have a significant negative effect on protein function. This was because the majority of scoring and predictive systems were in agreement that the change in amino acid residue would cause a damaging effect on protein function. Adjacently, p.L160F and p.M408V were predicted by all algorithms to not have a significant impact on protein function. p.M440I was predicted by three out of the five algorithms to have a

**Table 2.5. Summary of variant scoring systems**

Variant	Algorithm				
	Grantham	SIFT	PolyPhen	SNPs3D	Evolutionary Conservation
R61C*	180	0.02	2.018	-0.21	EC
L160F	22	0.66	0.132	0.08	EU
S189L	145	0.49	0.525	0.18	EC
P341L*	98	0.07	1.967	-1.96	EC
G401S*	56	0.19	1.124	-1.71	EC
M408V	21	0.27	0.617	0.66	EU
A413V*	64	0.01	1.754	-0.93	EC
M440I	10	0.12	2.203	0.31	EC
G465R*	125	0	2.539	-3.15	EC
M194V	21	0.83	0.539	-1.08	EC
A270S	99	0.69	1.138	0.24	EU
D399N	23	0.42	0.4	0.82	EC

The table displays the classification of scores this study has used. The addition of colour intensities to classifications shows more intense the colour, the more damaging the change is predicted to be to the protein. See Table 2.5 for colour intensities key. \* indicates amino acid change will alter protein function based on predictive scoring systems. EC, evolutionary conserved; EU, evolutionary unconserved. See table 2.6 for key to scoring.

negative effect, while conversely 3 out of 5 algorithms predicted S189L to not have a negative impact on protein.

Three nsSNPs were identified in the *SLC22A2* gene, p.M194V, p.A270S and p.D399N. As illustrated, the algorithms did not agree that there are differences in prediction. Nonetheless, the majority predicted that there was not likely to be a negative effect on protein function. p.M194V produced a negative SNPs3D score predicting that this substitution will have a deleterious effect on protein function. p.A270S was predicted to have some effect on altering protein function in Grantham and PolyPhen scores only.

**Table 2.6. Key to variant scoring systems**

Algorithm	Score	Classification
Grantham	0 – 50	Conservative
	51 – 100	Moderately Conservative
	101 – 150	Moderately Radical
	> 151	Radical
SIFT	0.00 – 0.05	Intolerant
	0.051 – 0.10	Potentially Tolerant
	0.101 – 0.2	Borderline Tolerant
	0.201 – 1.00	Tolerant
PolyPhen	0.00 – 0.99	Benign
	1.00 – 1.24	Borderline
	1.25 – 1.49	Probable Damaging
	1.50 – 1.99	Highly Probable Damaging
	> 2.00	Most Probable Damaging
SNPs3D	Negative score	Deleterious
	Positive score	Non-deleterious
Evolutionary Conservation	Evolutionary conserved (EC)	Deleterious
	Evolutionary Unconserved (EU)	Non-deleterious

Key to Table 2.5. Although they represent discrete data, SNPs3D scores and evolutionary conservation were highlighted red if the score was negative or conserved, respectively, indicating a deleterious substitution.

*Intronic variants* - Two variants located on the *SLC22A1*, IVS5-7C/T (rs7762846) and IVS7+9TGGTAAGT del (rs113569197), were located in splice acceptor and splice donor sites, respectively (Appendix Figure A2.3). IVS5-7 C/T was located in the splice acceptor site (SAS); this position does not have a specific preference for which pyrimidine (C or T) is present, and thus it is more likely to not cause a significant effect. The

The intronic 8 bp insertion IVS7+9 TGGTAAGTins is located over the 3' end of exon 7 and the splice donor site (SDS). Immediately after this 8 bp deletion is a repeat sequence TGGTAAGT. This leads to an alternative splicing site in the

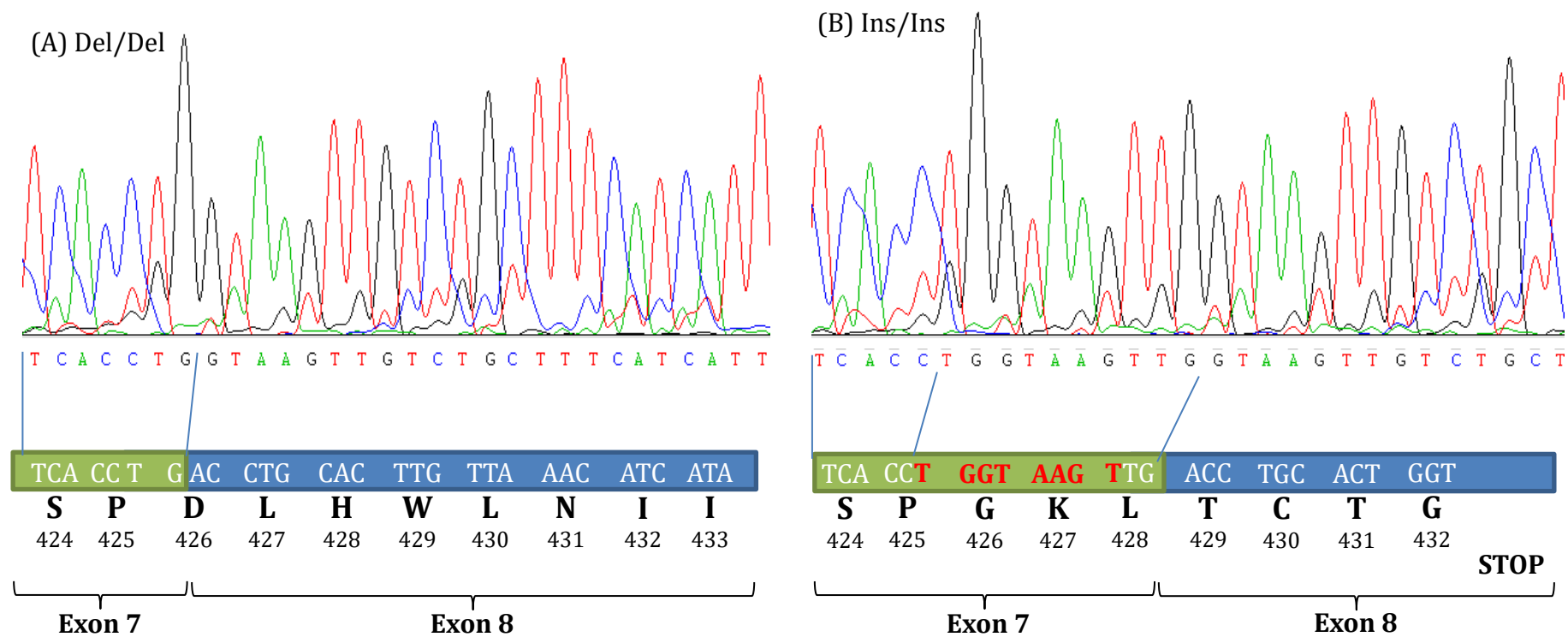


**Figure 2.4. 8 bp insertion in *SLC22A1* exon 7.**

(A) rs113569197 (del/del), location of amino acids across exon 7 and exon 8 boundary. Exon 7; green, exon 8; blue. (B) Alternative splicing of rs113569197 (ins/ins) with 8 bp insertion (red text) producing a longer length exon 7 leading to an alternative splice donor site and a premature stop codon in exon 8.

(ins/ins) genotype (Figure 2.4) leading to a premature stop codon. The premature stop codon produces a truncated protein 432 amino acids in length and 9 TMDs in comparison to the full length protein of 554 residues with 12 TMDs. Heterozygosity was common (57% of patients) with 17% and 26% homozygous for the insertion and deletion variant respectively.

*3'UTR variants* - 3'UTR SNPs were analysed to establish if any variants were located in AU-rich elements (ARE). ARE sites are cis-acting regulatory elements in the 3'UTR that are responsible for RNA stabilisation. There was no 3'UTR SNPs identified in the *SLC22A1* gene unlike *SLC22A2* where 8 variants were found. Analysis using the AREsite online resource identified 3 ARE in *SLC22A2* 3'UTR, but, none of the 8 SNPs found in this cohort were present in these AREs.

### 2.3.5 Haplotype analysis

The LD plot reveals there is a high degree of linkage disequilibrium across each gene, but little LD between the two genes. The only variant to exhibit a LD across both genes was the intronic GAA deletion (rs34129302) in *SLC22A2* which was in slight LD with M408V, R61C and L160F, of which the latter three were all in complete LD. There was strong LD between the majority of the seven 3'UTR SNPs in *SLC22A2*.

In order to elucidate whether our observed allele frequencies in the metformin cohort were representative and comparable to the frequencies of a wider Caucasian population, we compared frequencies with those available on the International HapMap project (release #28, Aug 2010, CEPH (Utah Residents with Northern and Western European Ancestry)). Allele frequencies for thirteen SNPs were available from the HapMap database for comparing MAF frequencies, including *SLC22A1* (rs683369, rs34134157, rs2282143, rs628031, rs622591) and *SLC22A2* (rs3127592, rs694812, rs3103353, rs316003, rs8177515, rs2279463, rs316019, rs624249). The comparison showed there were no significant deviations from Hardy-Weinberg equilibrium (HWE) either in the metformin group or the HapMap data (Chi-squared test ( $X^2$ )  $P > 0.05$ ); Appendix Figure A2.4.

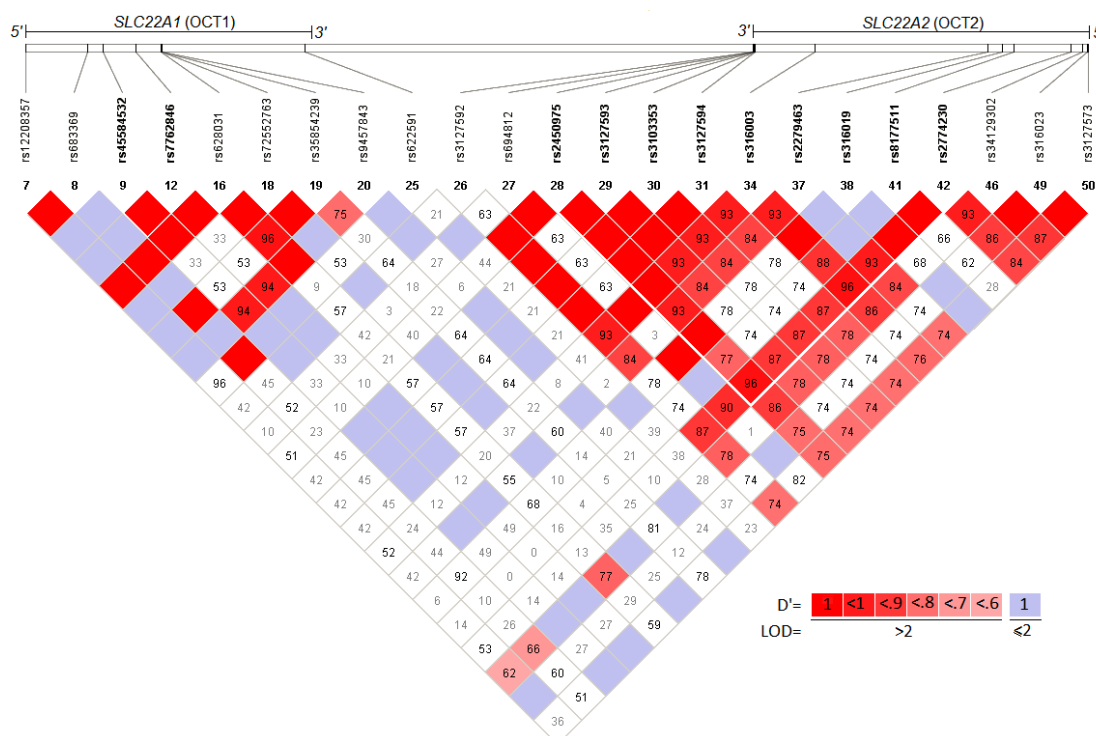


**Figure 2.5. Linkage Disequilibrium across *SLC22A1* and *SLC22A2* genes in the 75 metformin T2DM patients.**

Linkage disequilibrium plot shows *SLC22A1* on the left with *SLC22A2* on the right. LD pattern was generated using HaploView version 4.2 and strength of LD ( $D'$  measure) is shown in increasing shades of pink, as depicted by the bars on the bottom right.

## 2.4 Discussion

In total, fifty variants were identified in this study, though only 75 individuals were sequenced and not the entire genes (only flanking exonic, 5'UTR and 3'UTR). This highlights that *SLC22A1* and *SLC22A2* are highly polymorphic genes. As sequencing was performed in year 2010, variants were initially assigned 'rs' numbers using the GRCh37 assembly, release date (March 3<sup>rd</sup> 2009). The analysis first revealed 4 novel SNPs in OCT1 (g.-605G>A, g.-59C>T, c.1238C>T (p.Ala413Val) and IVS8+14A>G) and 6 novel SNPs in OCT2 (g.-1222A>T, g.-1189C>T, g.-922G>C, c.599A>G (p.Met194Val), c.1214G>A (Asp399Asn) and c.1594C>A (Thr525Thr)). In December 2013, NCBI updated the dbSNP following the inclusion of 1000 genomes phase 1 novel data dbSNP

141 Release 106, assembly GRCh38. Subsequently 9 of the 10 original novel SNPs were assigned RefSNP identifiers. This left one novel SNP; SLC22A1, IVS8+14A>G.

*Alignment ambiguity of rs113569197 and rs202220802 variants*

An issue arose during the analysis of the 8 bp variant located on the seventh exon-intron border. Upon assigning the 8 bp variant, a refSNP cluster identifier (rs#) from the Single Nucleotide Polymorphism Database (dbSNP) hosted by the National Centre for Biotechnology (NCBI) database there was two to choose from. Each conformed to different insertions, the first located at Chr6:160139866 TGGTAAGT (rs113569197) whereas the second was located 2 bp downstream Chr6:160139868 GTAAGTTG (rs35854239). From viewing the Sanger sequencing chromatograms, it is impossible to determine which is the true location of the 8 bp variant, as both rs113569197 and rs35854239 are possible (Figure 2.6). Sequencing traces from heterozygous samples read up to the end base of GTAAGTTG (rs35854239), however as there is a tandem repeat the true point where the insertion occurs is indeterminable.

To determine the true location of the 8 bp insertion we used the UCSC Genome Browser to analyse if any of the base pairs or region are evolutionarily conserved. The analysis revealed that TGGTAAGT (rs113569197) was not conserved in any other mammalian species, including primates, whereas the last two bp of GTAAGTTG (rs35854239) 'TG' were conserved in pig (*porcus, porca*), alpaca (*Vicugna pacos*) and Bactrian camel (*Camelus ferus*) only (Figure 2.7). The evolutionary conservation, within the region, dictates that the true deletion is more likely to be TGGTAAGT (rs113569197), and not GTAAGTTG (rs35854239).

The same ambiguity of a deletion can be applied to the 3 bp deletion in exon 7; M420del located just 17 bp upstream of rs113569197. The 3 bp deletion is registered as both ATGdel rs202220802 (Chr6:160139849) and GATdel rs72552763 (Chr6:160139851) which from viewing individual chromatograms are both possible deletions (Figure 2.6). Interestingly both options confer a Methionine deletion at position 420 despite differing in location by 2 bp.

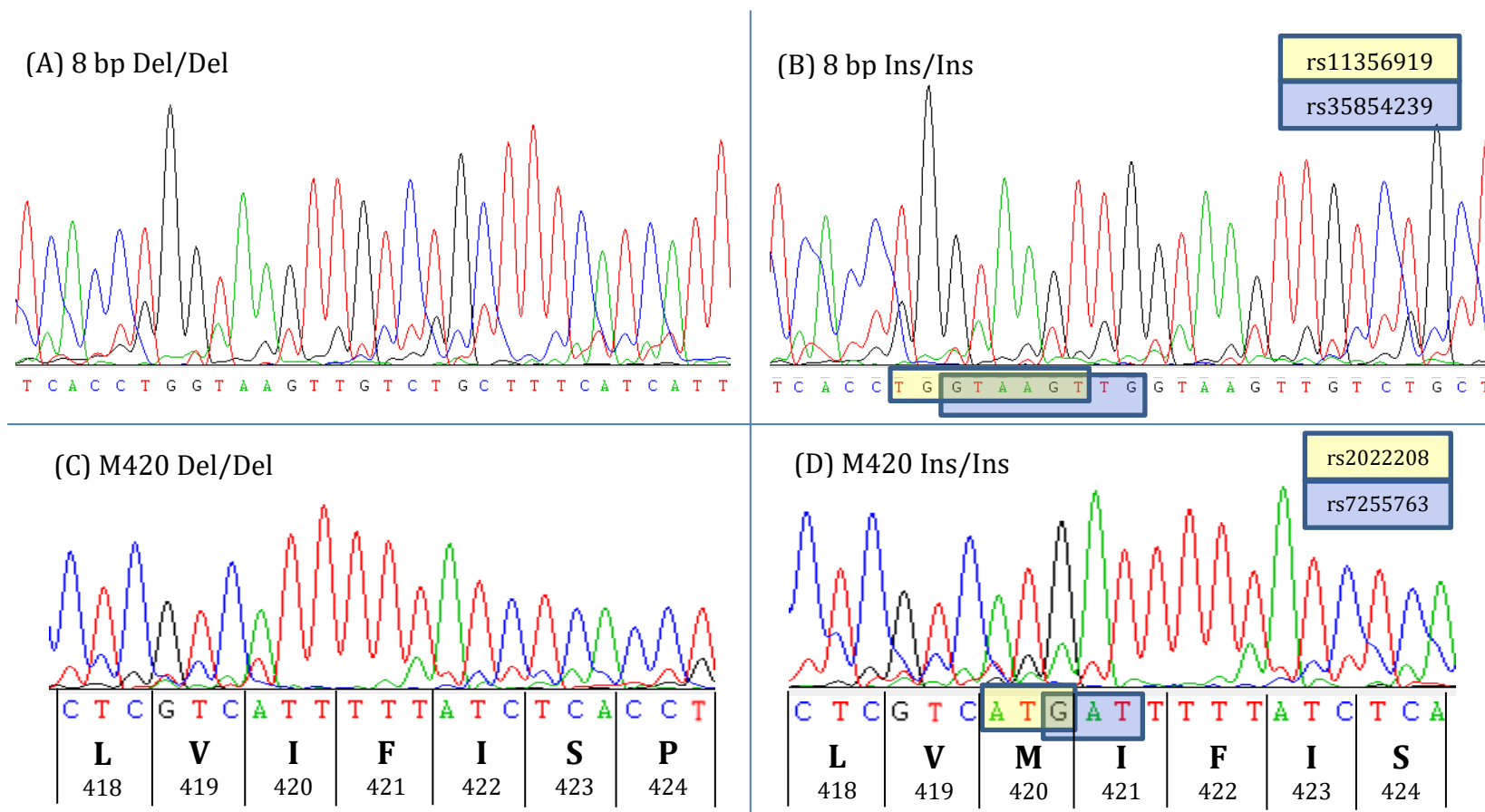


**Figure 2.6. Ambiguity alignment of 8 bp insertion and M420del**

(A) 8 bp (del/del), (B) 8 bp (ins/ins) highlighting rs113569197 (TGGTAAGT) in yellow and the alternative rs35854239 (GTAAGTTG) in blue. Both rs numbers show that either is possible according to the sanger sequencing. (C) M420 (del/del). (D) M420 (ins/ins) highlighting rs202220802 (ATG del) in yellow and the alternative rs7255763 (GAT del) in blue, both deletions result in a methionine deletion at position 420.

Alignment ambiguity arose in both TGGTAAGT (rs113569197) and ATGdel rs202220802 as the first two base pairs of the deletion were repeated following the deletion.

Alignment ambiguity in a number of genes has been previously reported in phylogenetic studies. There are several methods which can distinguish between ambiguous deletions/insertions without the need to conduct cDNA experiments including fragment-level alignment and the Elison method (Lee, 2001). However alignment ambiguity does not seem to be evaluated within human sequences. Alignment ambiguity arose as the first two base pairs of the deletion were repeated following the deletion, resulting in two feasible deletions. The ambiguity of deletions has been hypothesised to contain hierarchical signals and may be phylogenetic.

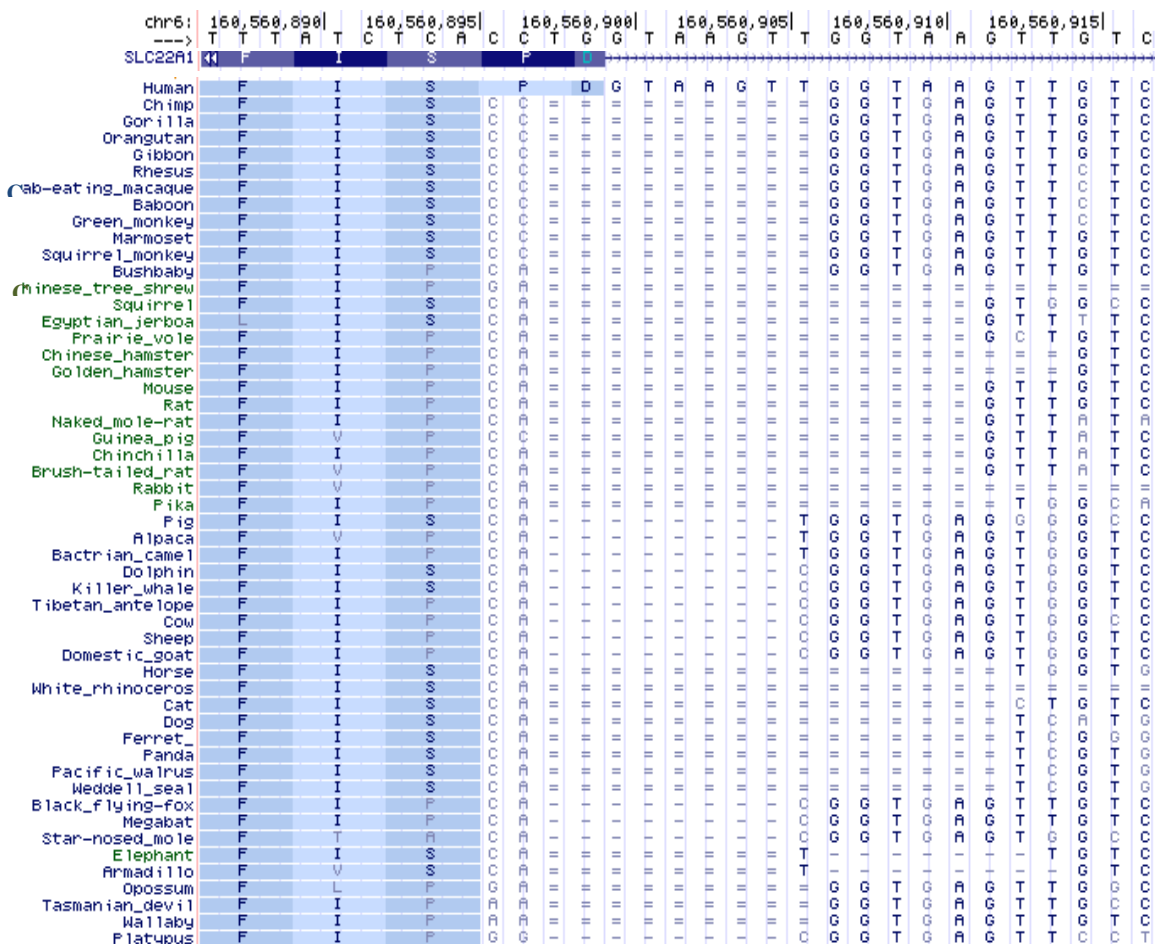


**Figure 2.7. Evolutionary conservation of SLC22A1 exon 7 - intron 7 boundary** The conservation of this region across a wide range of mammalian species shows TGGTAAGT (rs113569197) is not conserved in any other mammalian species, including primates. This strongly suggests the true variant is TGGTAAGT and not GTAAGTTG (rs35854239).

*Significance of the rs113569197 insertion*

On first inspection, the presence of the 8 bp insertion appears to not influence the amino acid sequence of OCT1 due to the presence of a repeat 8 bp sequence (TGGTAAGT) immediately following the 8 bp insertion. However, the 8 bp insertion is located at the 3' end of exon 7 and the splice donor site (SDS), and thus may influence alternative splicing through extending exon 7 by 8 bp conforming to a new SDS. The new SDS site is then predicted to produce a premature stop codon 6 amino acid residues downstream from the insertion. This would produce a truncated OCT1 protein of 432 amino acids in length in comparison to the full length transcript of 554 residues. The possible effects of the 8 bp insertion on OCT1 expression levels has been previously determined by only one group, (Grinfeld et al., 2013), who analysed and compared *SLC22A1* mRNA levels in individuals expressing rs113569197 variants. They amplified exon 7 through to the start of exon 8 in *SLC22A1* cDNA. They found the 8 bp insertion produced a longer transcript length, suggesting the insertion is included in the mRNA which would produce a premature stop codon, leading to a truncated OCT1 protein. Interestingly they found that the (ins/ins) variant was associated with impaired responses to imatinib, an OCT1 substrate, in patients with chronic myeloid leukaemia. It is also worth noting that poor responses to imatinib were also observed in patients expressing p.M420del which was expressed *in cis* with the 8 bp insertion (Giannoudis et al., 2013, Grinfeld et al., 2013).

The 8 bp insertion has also been previously documented by Tarasova et al., 2012, who described the insertion using the rs36056065 (GTAAGTTG) and not rs113569197 (TGGTAAGT) (refer to Figure 2.6). Note that rs35854239, as described in this chapter, and rs36056065 both refer to GTAAGTTG. Interestingly they found a significant association between rs36056065 (ins/ins) and the presence of metformin induced gastrointestinal side effects. These side effects included diarrhoea, flatulence, abdominal pain and vomiting within 1 year after starting metformin therapy. Given the findings of Grinfeld et al (2013) together with our prediction of the 8 bp insertion leading to a truncated OCT1 protein, one could hypothesis the 8 bp insertion may lead to metformin induced

gastrointestinal side effects through lack of OCT1 protein expression or reduced level of function from a truncated OCT1 transcript. They state that rs36056065 and rs628031 (p.M408V) are in strong LD with each other and were both statistically associated with GI side effects. It is therefore possible that their findings could be caused by any of the variants, or a combination of both. The observed MAF for rs113569197 in this study (0.40) was comparable to what was observed in the previously reported studies by Grinfeld et al and Tarasova et al (0.39 and 0.42 respectively).

### *Predictive power of algorithms*

Non-synonymous SNPs can be interpreted through the use of algorithms which analyse variants using specific criteria such as evolutionary conservation, location within the protein sequence, functional domains and physical and chemical properties of the substituted amino acid residue. The algorithms may permit the choice of which SNPs to choose to determine the effect on transporter function in future studies. The four algorithms were chosen based on popular use and citation number. The use of four algorithms and evolutionary conservation analysis allowed for comparative analysis and to determine if the results were similar between one another. In OCT1, p.R61C, p.P341L, p.G401S, p.A413V and p.G465R were predicted to negatively affect protein function whereas p.L160F and p.M408V were not. The algorithms were not in agreement with p.S189L and p.M440I predictions; nonetheless the general consensus was that p.S189L was not detrimental to protein function and p.M440I was. The bioinformatic analysis in this study denotes that not all algorithms agree that a particular amino acid change will or will not significantly affect protein function. However, the novel application of colour intensity to the predictive scores in this chapter illustrates the majority of scoring systems are in agreement with the effect each nsSNPs has on protein function. In regards to this study, evolutionary conservation appears to be a simple and accurate method for predicting nsSNPs on OCT1 protein function. This is supported by Rudd et al., 2005 who revealed that the EC as well as

Grantham scores were accurate predictors of transport function in OCT1 variants.

Shu et al., 2007 have observed the effect of OCT1 variants in HEK293 cells and measured the activity of metformin uptake. The nsSNPs predicted to be detrimental to protein function in OCT1 (p.R61C, p.P341L, p.G401S and p.G465R) exhibited reduce metformin uptake. This demonstrates that the prediction algorithms give an accurate evaluation of protein function.

Scoring systems can only predict the functional effect of SNPs, and thus functional studies are necessary to determine the effect they can have on transporter activity. Furthermore the scoring systems do not take into account multiple nsSNPs in proteins which could have an additive or co-regulatory effect on protein function. For example, in this cohort there was high LD between p.R61C and p.L160F and between p.M420del and p.M408V in *SLC22A1*. The effect of the co-expression of these variants in one protein on function cannot be predicted using the algorithms. Similarly in *SLC22A2*, p.M194V and p.A270S were found in a single individual, although both variants were not predicted to be detrimental to protein function. Therefore the combination of two or more amino acid variants on the same transporter could significantly alter the scores predicted with the algorithms. Shu et al., 2007 has examined the effect of combinations of variants in OCT1 transport uptake of 1-methyl-4-phenylpyridinium (MPP<sup>+</sup>). The results appear to suggest that if one variant in the combination is predicted to be detrimental to protein function, then the OCT1 transport activity is significantly decreased. Therefore, assessing if one amino acid is predicted to be detrimental to protein function may be an accurate predictor of protein function, in a transporter expressing multiple variants. However, this needs to be assessed with other variants across other proteins using predictive algorithms.

Of the 21 exonic variants identified across both genes, six were synonymous; i.e. SNPs which do not change the amino acid. However, it must not be assumed that a synonymous SNP will not affect protein function or expression. It is known that sSNPs can affect mRNA splicing, stability and protein folding (Hunt et al.,

2009). Additionally Se'mon et al., 2006 have discovered that usage of specific tRNAs varies significantly between tissues. For example, rs316003 (p.V502V) in *SLC22A2* is a GTG to GTA variant which human tRNA levels are 46% and 12%, respectively (as a fraction; codon levels per amino acid) (Nakamura et al., 2000). Therefore the introduction of a rare codon may affect protein levels due to lack of translational machinery which can lead to a misfolded or truncated protein. However Se'mon et al., 2006 state the effect is very weak in that variability in synonymous codon usage between tissues accounts for 2.3% of the total variability. Therefore although sSNPs are predictably inert, they could potentially affect transporter expression.

Although no bioinformatic analysis could be applied to p.M420del (*SLC22A1*), its evolutionary conservation could be determined to predict its function. Examination of orthologs identified M420 to be conserved in 4 of 5 mammalian species analysed in this study (unconserved in rabbit). Therefore this deletion could have a significant impact on protein function. Furthermore M420 has a predicted location in transmembrane domains, which are regarded as important for OCT1 substrate specificity and activity.

#### *Potential effect of 5'UTR variants*

In total, 13 SNPs were identified within the 5'UTR of both genes. The transcription factor database, Transfac, predicted rs57504133 to be present in a Zinc finger protein 333 (ZNF333) binding site ATAAT (Tian et al., 2002). rs73598465 was present in POU class 6 homeobox 1 transcription site CTCATTAT (Messier et al., 1993). ZNF333 is highly expressed in the heart and to a lesser extent the liver (Tian et al., 2002), and therefore rs57504133 may have an impact on *SLC22A1* expression in the liver through disrupting ZNF333 binding. Conversely POU6 mRNA expression is absent in liver or kidney tissue, but present in skeletal and brain tissue (Messier et al., 1993).

In *SLC22A2* rs183436020 may be located within the TF Churchill recognition site, but, it has only been found to be expressed in liver and not the primary site

of *SLC22A2* expression, the kidneys (Lee et al., 2009a). Therefore we predict that rs183436020 will not have a significant impact on OCT2 expression.

To date, there are a few known TFs or promoters for the *SLC22A* genes. The most widely investigated to a *SLC22A1* promoter is regulation by Hepatocyte nuclear factor-4 alpha (HNF-4 alpha) (Saborowski et al., 2005, Saborowski et al., 2006, Kajiwara et al., 2008). This has been shown to trans activate the *hOCT1* promoter in a dose-dependent manner. Two putative binding sites for the liver-enriched hepatocyte nuclear factor are located between nucleotides -1479 and -1441 upstream of the transcription initiation site (Saborowski et al., 2006). However, the nearest 5'UTR SNP near these regions was rs12110656 (g.-1419), 22 bp from -1441.

In adjacent, peroxisome proliferator agonist receptor (PPAR), a murine *SLC22A1* TF, has been shown to influence OCT1 expression (Nie et al., 2005). Additionally, functional assays treated with PPAR agonists displayed significant increases in OCT1 transport uptake, through transcriptionally increasing *SLC22A1* expression. As this was identified in mice, the TF may not be responsible for human *SLC22A1* expression. The PPAR regulatory element (PRE) is located 2392 bp upstream from the ATG start codon. In this study we didn't analyse this region as we sequenced only the first 2 kbp upstream from the start codon.

Interestingly DNA methylation of the promoter region for the OCT2 has been shown to contribute to OCT2 expression (Aoki et al., 2008). *Aoki et al* have discovered a CpG site at -85 bp from the ATG start site which is hypomethylated in kidney tissue and thus enhances gene transcription. However, all the 5'UTR variants in this study were identified between -246 and -1604bp from ATG and not near the CpG sites.

In conclusion, this chapter identified 50 genetic variants in *SLC22A1* and *SLC22A2* genes including 1 novel SNP. There is little known about the significance of the 8 bp insertion and its potential effect on truncating OCT1 which may lead to decreased transporter function or expression. Based on previous studies, findings with rs113569197 (Grinfeld et al., 2013) and our predictions, this presents itself as a potential variant which may drastically

influence metformin pharmacokinetics and potentially vitamin B<sub>12</sub> levels in our metformin cohort. Further studies are warranted to confirm this prediction and to assess the impact of multiple variants on a single transporter. The genetic data generated will be used in subsequent chapters as covariates for population pharmacokinetic modelling and statistical analysis.

# **Chapter 3**

**Assessing the impact of genetic variations  
on metformin transport using in silico  
structural models of organic cation  
transporters 1 and 2**

## CONTENTS

<b>3.1 INTRODUCTION.....</b>	<b>86</b>
<b>3.2 MATERIALS &amp; METHODS.....</b>	<b>88</b>
3.2.1 TARGET TEMPLATE ANALYSIS.....	88
3.2.2 SEQUENCE ALIGNMENT & ANALYSIS.....	88
3.2.3 3D-STRUCTURAL MODELLING .....	90
3.2.4 SIDE-CHAIN OPTIMISATION .....	90
.....	91
3.2.5 MODEL VALIDATION.....	91
3.2.5.1 <i>Modeller</i> .....	91
3.2.5.2 <i>Rampage</i> .....	92
3.2.5.3 <i>MolProbity</i> .....	92
3.2.5.4 <i>PDBeFold</i> .....	92
3.2.6 HELICAL WHEEL ANALYSIS.....	94
3.2.7 DOCKING.....	94
3.2.8 IMPACT OF GENETIC VARIANTS ON STRUCTURE AND DOCKING .....	95
3.2.9 POST TRANSLATIONAL MODIFICATION PREDICTION .....	95
3.2.8.1 <i>Glycosylation sites</i> .....	95
3.2.8.2 <i>Ubiquitination prediction</i> .....	95
<b>3.3 RESULTS.....</b>	<b>96</b>
3.3.1 MODEL VALIDATION.....	96
3.3.2 3D-STRUCTURAL ANALYSIS.....	99
3.3.3 <i>HELICAL WHEEL ANALYSIS</i> .....	99
3.3.4 DOCKING.....	99
3.3.5 IMPACT OF GENETIC VARIANTS ON STRUCTURE AND DOCKING .....	101
.....	103
3.3.6 POST TRANSLATIONAL MODIFICATION PREDICTION .....	103
3.3.6.1 <i>Glycosylation sites</i> .....	103
3.3.6.2 <i>Ubiquitination prediction</i> .....	103
<b>3.4 DISCUSSION .....</b>	<b>104</b>

### 3.1 Introduction

Membrane transporters are responsible for the sustainability of cell homeostasis and can be major determinants of a drug's safety, efficacy and pharmacokinetic profile. Physiologically transporters play an important role in the absorption, distribution and elimination of cationic compounds, metabolites and toxins (Giacomini et al., 2010).

The solute carrier (SLC) family in humans consists of over 360 members in 46 gene families which fall under the largest group of secondary membrane transporters in eukaryotes, the major facilitator family (MFS) (Saier, 2000, Zhou et al., 2007b). The *SLC22A* family all share a common structure of 12 transmembrane alpha-helices domains (TMDs), a large extracellular loop with glycosylation sites and a large intracellular loop with phosphorylation sites hypothesised to be involved in intracellular signalling. Three sub-types of this class of transporters have been identified, organic cation transporters (OCTs) 1-3. These transporters share >48% sequence identity and >65% sequence similarity and are thought to have evolved from a common ancestor (Saier, 2000). Unlike the majority of membrane transporters, OCTs perform bidirectional transport of substrates; therefore the expression of OCTs whether they are expressed apically or basolaterally governs their function. Although these transporters display similar selectivity and activity for some substrates (MPP<sup>+</sup>), they have distinct selectivity for other substrates (e.g. cimetidine) (Kerb et al., 2002, Shu et al., 2003). The TMDs are likely to be the sites for substrate specificity and recognition, where conserved residues account for similar substrates affinities. OCTs transport of a large number of diverse organic cations including primary, secondary, tertiary and quaternary amines with a net positive charge on the amine nitrogen atom at physiological pH (Zhang et al., 2005).

Metformin, a substrate for OCT1-3, is the most commonly prescribed anti-diabetic drug in the world today (Graham et al., 2011). As metformin does not undergo any known form of metabolism, the most important factors

contributing to its pharmacological action are drug transporters which distribute metformin to its target organs and enables its excretion via the kidneys (Kimura et al., 2005a, Nies et al., 2009).

OCT1 is expressed at the sinusoidal membrane of hepatocytes (Wang et al., 2002). As the liver is the target organ of metformin, OCT1 is regarded as the primary transporter that allows metformin to exert its pharmacological action. OCT2 is expressed in the distal renal tubules. OCT2 has a greater affinity and capacity for metformin than OCT1 and is thus able to rapidly eliminate metformin into the urine (Kimura et al., 2005a). These transporters are highly polymorphic and several variants alter the pharmacokinetic profile of metformin, with the potential to lead to inter-individual variability in metformin response.

The 3D structures of three members of the major facilitator superfamily LacY permease *E.coli* (Abramson et al., 2003), glycerol-3-phosphate transporter (GlpT) *E.coli* (Huang et al., 2003) and the oxalate transporter (OxlT) from *Oxalobacter formigenes* (Hirai et al., 2002) have been reported. Known crystal structures of transmembrane proteins have been used to predict the 3D structures of other proteins which share common structural properties. For example, the rat OCT2 structure has been predicted using the LacY permease crystal structure as a template (Zhang et al., 2005). Additionally these structures can be used to screen a large library of drugs and compounds, predicting potential substrates and inhibitors of transporters. 3D-models have been routinely and successfully used to screen large databases and identify possible transporter ligands through docking experiments and providing a rationale for drug design (Grant, 2009). This can also offer an insight to which amino acid residues are responsible for substrate recognition and provide an explanation of the effect of genetic variation on transporter activity. As the tertiary crystal structures of OCTs are unknown, this chapter aims to use computational modelling techniques to predict OCT structure and visually assess the impact genetic variants have on metformin transport. This may provide an illustrative mechanistic explanation of OCT function and metformin transport.

## 3.2 Materials & Methods

### 3.2.1 Target template analysis

In order to predict a 3D model from a primary protein sequence, a crystallised structure of a related protein is required to act as a template. OCT primary amino acid sequences were obtained from UniProtKB with the following accession numbers: hOCT1 (O15245) and hOCT2 (O15244) and used as probes to search for homologous sequences with acquired 3D structures using Phyre2 (Wass et al., 2010, Kelley and Sternberg, 2009). This server uses and combines several conformational and structural servers such as Psi-Pred (McGuffin et al., 2000), SSPro (Pollastri et al., 2002) and JNet (Cole et al., 2008) with algorithms described by Bennett-Lovsey et al., 2008. Top hit matches, and those used in the literature, were then physically investigated for structural similarity and used for further analysis (Table 3.1). Two proteins were identified which were appropriate templates, Lactose Permease (LacY) Protein Data Bank (PDB) code: 1PV6 and Glucose-3-phosphate transporter (GlpT), PDB code: 1PW4.

### 3.2.2 Sequence alignment & analysis

Although target-template servers provide 3D modelling structures, the models are commonly misaligned and exhibit poor structural properties. Primary sequences of OCTs and crystal structures listed in Table 3.1 were obtained from UniProtKB with the following accession numbers: hOCT1 (O15245), hOCT2 (O15244), hOCT3 (O75751), 1PW4 (P08194), 1PV6 (P02920), 3O7P (P11551), 3MKT (P18622), G2FP (Q2GFP1) and 2XUT (2XUT). Vector NTI Suite 8 (Invitrogen) and ClustalW (EMBL-EBI) were used for sequence alignment and analysis. Predicted TMDs were obtained using the TMHMM v2.0. server (Krogh et al., 2001). The sequences of respective TMDs and 10 residues flanking each end were aligned manually to ensure the model TMDs were aligned correctly with the TMDs of the crystal structures. Figure 3.1 demonstrates the alignments of template and OCTs.

**Table 3.1. Available crystal structures which can be potentially used as OCT templates**

Protein	PDB code	Organism	Number of TMDs	Crystal resolution (Å)	Sequence identity (similarity) with OCTs	Reference
Lactose Permease	1PV6	<i>E.coli</i>	12	3.5	13.7 (28.9)	(Abramson et al., 2003)
Glucose-3-phosphate transporter	1PW4	<i>E.coli</i>	12	3.3	14.4 (29.7)	(Huang et al., 2003)
Multidrug Transporter EmrD	2GFP	<i>E.coli</i>	12	3.5	13.9 (31.4)	(Yin et al., 2006)
Multidrug and Toxin Extrusion transporter	3MKT	<i>Vibrio cholerae</i>	12	3.65	10.5 (24.8)	(He et al., 2010)
L-fucose-proton symporter	3O7P	<i>E.coli</i>	12	3.2	13.1 (29.1)	(Dang et al., 2010)
Oligopeptide-proton symporters, PepT1	2XUT	<i>Shewanella oneidensis</i>	12	3.62	13.1 (22.8)	(Newstead et al., 2011)

The table displays membrane transporters which all have 12 TMDs. Interesting they all share common structural properties; TMDs 3, 6, 9 and 12 are all located within the plasma membrane and are not in contact with the binding cleft of the protein whereas the remaining TMDs, 1, 2, 4, 5, 7, 8, 10 and 11 all have a alpha-helices face orientated towards the substrate binding cleft.

### 3.2.3 3D-Structural Modelling

This study used LacY and GlpT as templates for the OCTs. As LacY and GlpT do not contain a large extracellular loop unlike the OCTs, the extracellular loop was not aligned to the templates and thus not included in the model. Target-template modelling of TMDs was subsequently performed using Modeller9v8 (Fiser and Sali, 2003) using the aligned sequences as described in section 4.2.2. Fifty models were produced per OCT per template for reviewing and evaluating. During the analysis, a log file generated in each model is continuously scanned for errors allowing the process to be iterated until an acceptable model is obtained. Modeller produces an estimated objective function score for each model to give an indication of how well the particular model satisfies the restraints used to calculate it. However, this value does not necessarily indicate the quality of the model. The models are generated as PDB files and were viewed with PyMOL (Seeliger and de Groot, 2010) and Chimera (Pettersen et al., 2004).

### 3.2.4 Side-chain optimisation

The orientation of the side-chains was optimised using SCWRL 4.0 (Bower et al., 1997, Canutescu et al., 2003). SCWRL uses dead-end elimination algorithms to predict the structure of side chains on a given protein backbone structure. Optimising the dihedral angle of side chains minimises the energy function to a discrete set of rotamers of fixed length. The side chains with the most favourable energy status would be chosen and the side chains of the models are adjusted accordingly.

Additionally Asn/Gln/His 180° flips were performed if needed with MolProbity (Chen et al., 2010b). Mis-orientation of the end of Asn, Gln and His side-chains by 180° is common because the electron density is symmetric. MolProbity can geometrically recognise and flip the residues into the correct state.

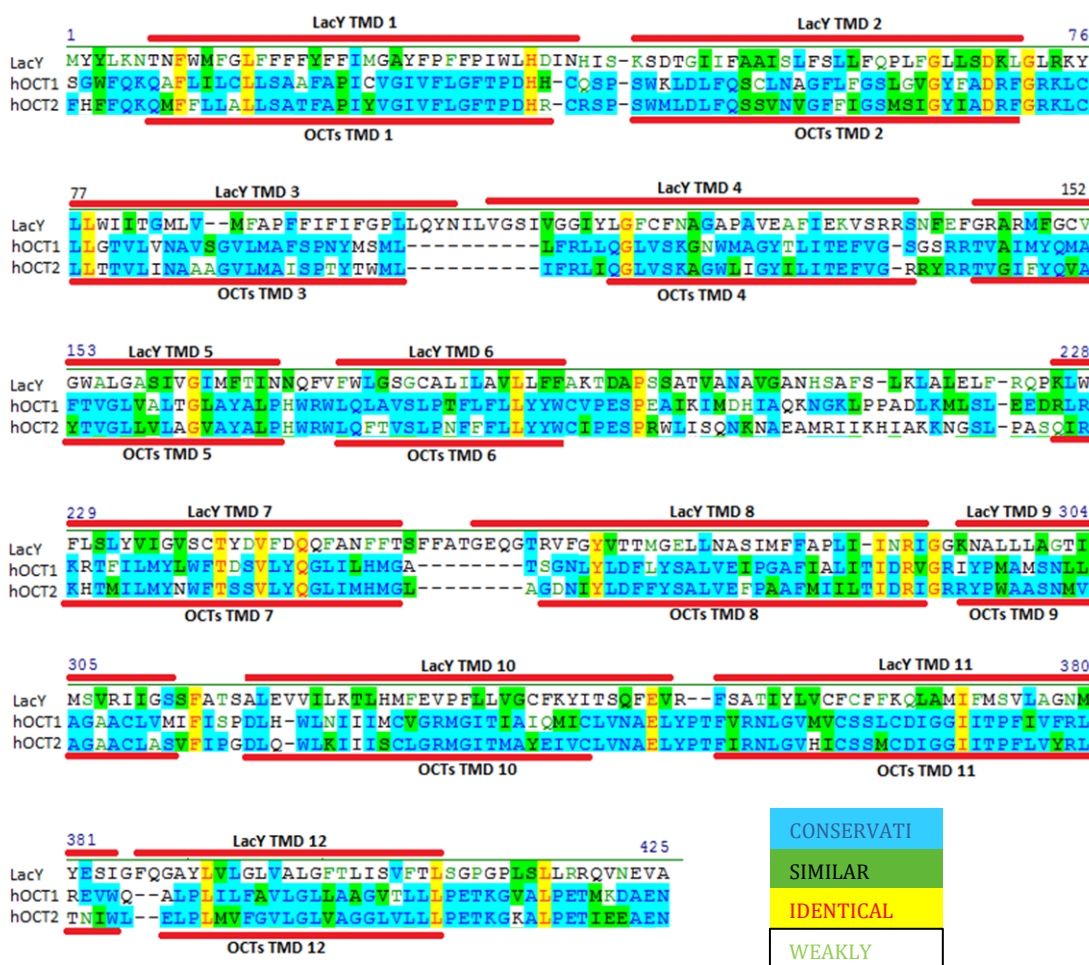


**Figure 3.1. Amino acid sequence alignment of the predicted TMDs domains of OCTs with the TMDs of LacY permease.**

Individual TMDs between the template and OCT were manually aligned to ensure TMDs were aligned correctly. Positions of TMDs are illustrated above and below the sequence alignment in red. Numbering of amino acids are in accordance with the LacY permease primary sequence. As LacY permease does not have a large extracellular loop the amino acids sequence encoding for this in OCTs were removed from the sequence alignment

### 3.2.5 Model Validation

#### 3.2.5.1 Modeller

Model accuracy was analysed using MODELLER, MolProbity, Ramachandran plots and PDBeFold SSM. Each structural model produced by Modeller 9v8 was assessed for accuracy and reliability using discrete optimised protein energy (DOPE) scores produced by Modeller 9v8. DOPE scores are the statistical potential based on the reference state corresponding to non-interacting atoms

to account for the spherical shape of the native structures. Figure 3.2 illustrates decision tree for computer modelling of transporters.

#### 3.2.5.2 *Rampage*

Ramachandran plots were produced using the RAMPAGE server (Lovell et al., 2003) which produced plots conforming to algorithms produced by Ramachandran et al., 1963. In brief, the plots assess backbone dihedral angles,  $\psi$ , against  $\phi$  of amino acid residues within a protein structure and acknowledge any residues fall within an acceptable region on the plot. Glycine and proline are residues which are of most concern when producing structural models. As glycine only has a hydrogen atom as its side chain (rather than  $\text{CH}_3$ ,  $\text{CH}_2$  or  $\text{CH}$  groups which exist in other amino acid side chains), the residue is less sterically restricting. On the contrary, proline contains a distinctive cyclic structure in its side chain which 'locks' its  $\phi$  backbone dihedral angle at approximately  $75^\circ$ , giving proline exceptional conformational rigidity within a proteins tertiary structure.

#### 3.2.5.3 *MolProbity*

MolProbity is a specific structure-validation web server to provide atom contact analysis, steric problems, and dihedral-angle diagnostics in order to validate and improve the quality of the structures (Chen et al., 2010b).

#### 3.2.5.4 *PDBeFold*

A comparative validation procedure between the template and the target was conducted using the PDBeFold SSM server (<http://www.ebi.ac.uk/msd-srv/ssm/>) for structural similarity. The SSM server compares 3D structures of the target and the template from the PDB database and calculates Root Mean Square Deviation (RMSD) values calculated between  $\text{C}\alpha$ -atoms of matched amino acid residues at best 3D superposition of the target and template. Therefore RMSD simply gives an indication of the positional accuracy of a pair

of matched C $\alpha$ -atoms. A large RMSD value indicates a low accuracy of the model (Krissinel and Henrick, 2004).

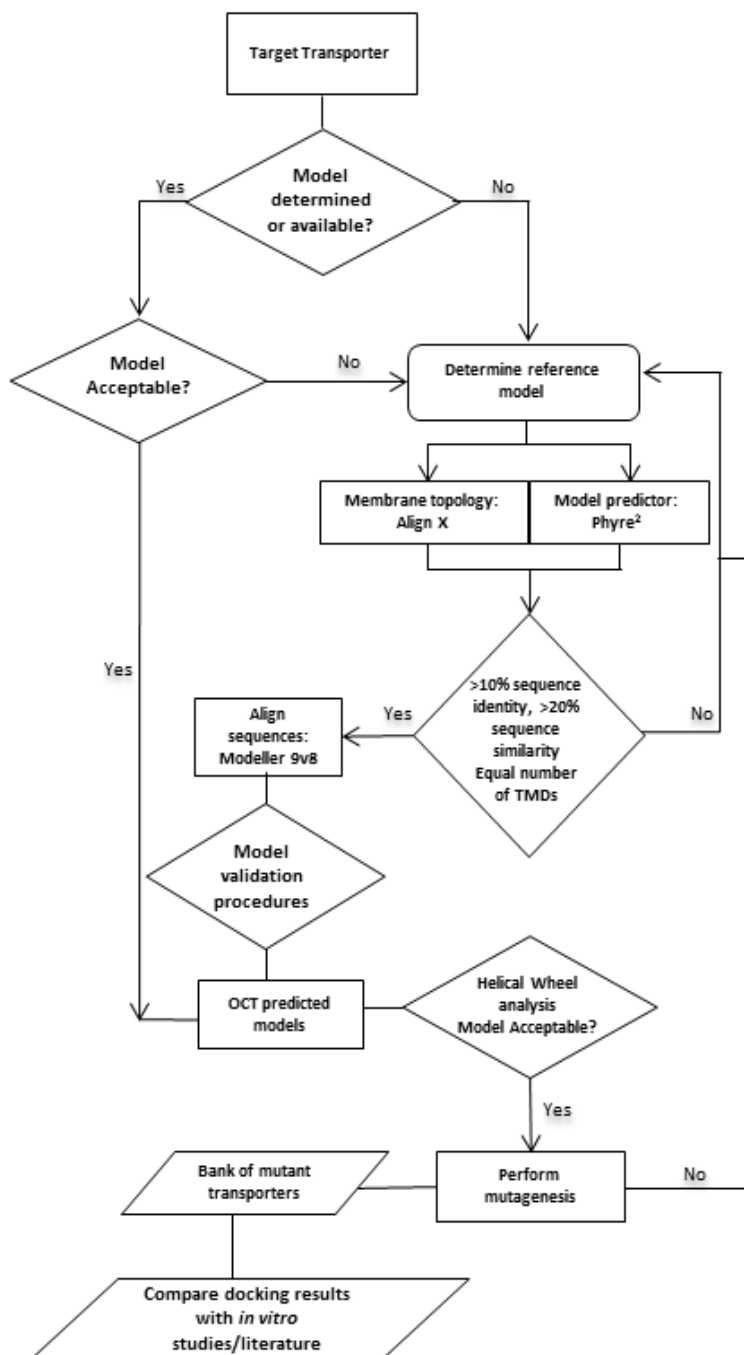


**Figure 3.2. Decision tree for structural computer modelling of OCT transporters**

Validation of models can be evaluated using a variety of different techniques and criteria. DOPE scores are often used but offer little insight into the true accuracy of a model. Ramachandran plots are a more accurate method to use, but we used manual methods to ensure the TMDs of OCTs were aligned correctly to the target-templates. Additionally helical wheel plots were used to confirm TMDs were in the correct orientation.

### 3.2.6 Helical Wheel Analysis

To assess if the TMDs important for substrate specificity are in the correct orientation and alignment, helical wheels plots for all TMDs were generated using the Helical Wheel Applet Projection (University of Virginia). Firstly TMDs were predicted using TMHMM Server V.2.0 (Sonnhammer et al., 1998). Predicted TMDs were then loaded into the Helical Wheel Applet available (<http://cti.itc.virginia.edu/~cmg/Demo/wheel/wheelApp.html>).

Transmembrane domains are assumed to take the conformation of standard  $\alpha$ -helices (3.6 residues/helical turn) roughly corresponding to residues existing at an angle of  $100^\circ$  to their neighbouring residues. This allows a projection of the positions of the residues on a plane perpendicular to the  $\alpha$ -helical axis. The plots then reveal whether hydrophobic residues are concentrated on one side of the helix with polar groups concentrated on the other. This arrangement is common with globular or transmembrane proteins where the hydrophobic face of the helix is orientated to the hydrophobic core or membrane and the hydrophilic face is orientated towards the solvent-exposed front or substrate binding cleft.

### 3.2.7 Docking

FlexX BioSolveIT LeadIT software (Gohlke et al., 2000) was used for docking experiments. FlexX is a computer program for predicting protein-ligand interactions. For a given protein and a ligand, FlexX predicts the geometry of the complex as well as an estimate for the strength of binding. Specific transmembrane regions located in the binding clefts were selected for docking of metformin. Ligand structures, including metformin and two OCT1 inhibitors; quinidine and cimetidine, were obtained from the PubChem website (<http://pubchem.ncbi.nlm.nih.gov/>). Ligands were flexible whilst the OCT models were modelled as a rigid structure. Appropriate residues were given charges relating to the protein existing in an environment with a pH of 7.35.

Docking was performed using a 20 Å sphere located in the binding cleft of the model. Top hit docking results were used for binding affinity assessment. Ligand

minimisation including changes to torsion angles, and orientation of hydrogens was permitted. Binding affinity was predicted considering hydrogen bonding interactions with hydrophobic and desolvation effects. The results provide three values for the protein-ligand complex; the estimated  $K_i$  of the ligand range (mM to nM), the calculated  $\Delta G$  kJ/mol and ligand efficiency ( $\Delta G$ /number of heavy atoms).

### 3.2.8 Impact of genetic variants on structure and docking

The impact of TMD genetic variants, as described in chapter 2, on potential 3D structure and metformin docking were assessed. Firstly the amino acid residues of the genetic variants were visualised to determine if the functional R-group or side chain is orientated into the binding cleft. Secondly the same residues were determined if they were within 10 Å of residues predicted to be involved with metformin docking as described in 4.2.7. Other previously known genetic variants proven to affect metformin transport *in vitro* were also included in the analysis (Leabman et al., 2002, Nies et al., 2011b) to determine if they were also located in binding cleft or within 10 Å of predictive metformin binding.

### 3.2.9 Post Translational modification prediction

Not all amino acid changing SNPs could be assessed as the structural models represented TMDs. Therefore we analysed if any nsSNPs were present on or near post translational sites.

#### 3.2.8.1 Glycosylation sites

N-linked and O-linked glycosylation sites in OCTs were predicted using Centre for Biological Sequence analysis NetNGlyc 1.0 and NetOGlyc 4.0 Servers respectively (Steentoft et al., 2013).

#### 3.2.8.2 Ubiquitination prediction

Ubiquitination sites were predicted using BDM-PUB, Prediction of ubiquitination sites with the Bayesian discriminant method. (<http://bdmpub.biocuckoo.org/>) A reduction in the number of ubiquitination sites may decrease the protein expression of OCTs.

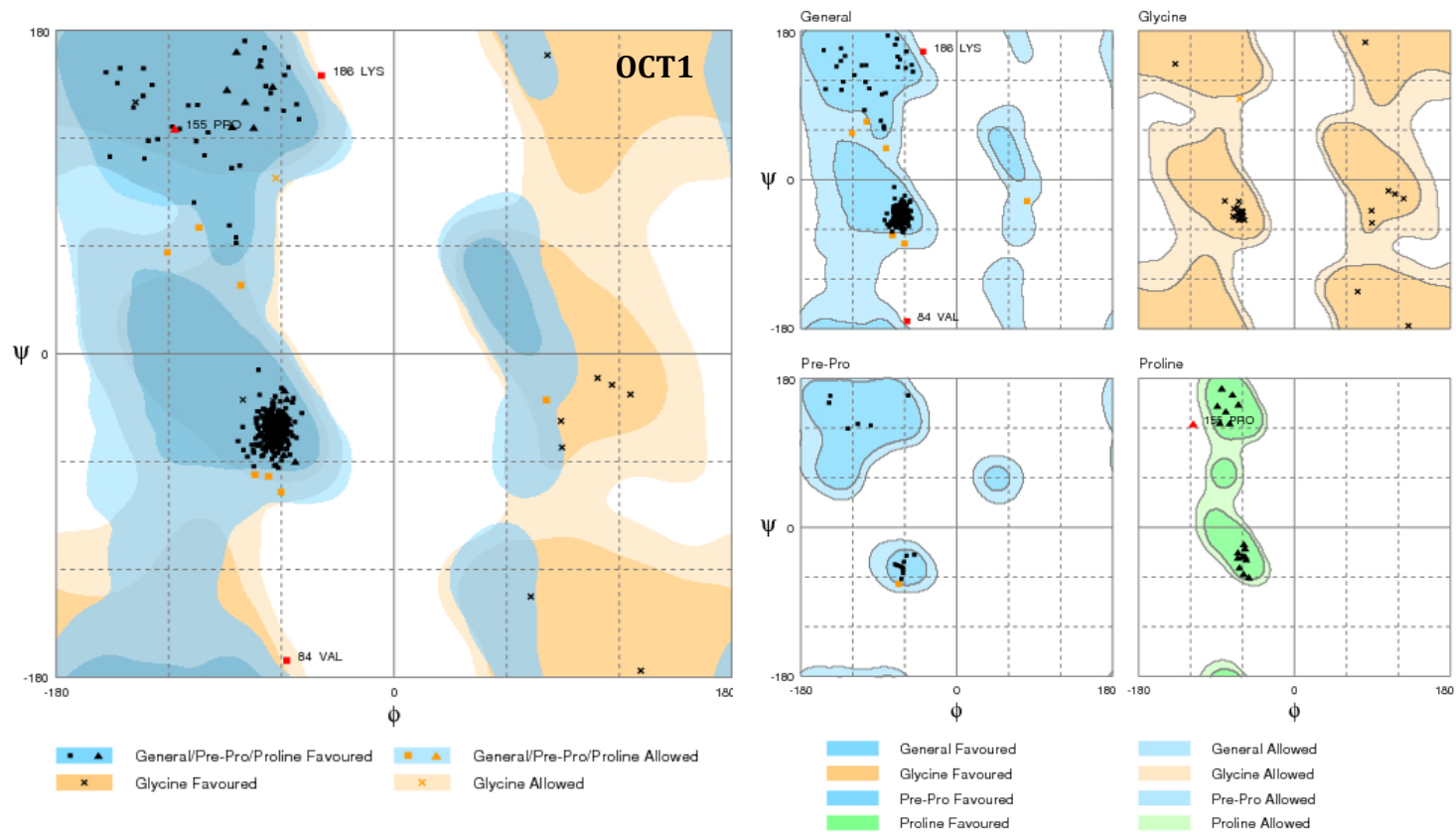
## 3.3 Results

### 3.3.1 Model Validation

All DOPE scores were less than -1 indicating that 80% of the C $\alpha$  atoms were within 3.5 Å of their correct positions. However, a more accurate method to assess a model is using Ramachandran plots to assess if the residues backbone dihedral angles,  $\psi$ , against  $\phi$  of amino acid residues within the model are acceptable. Figure 3.3 and 3.4 gives the Ramachandran assessments. The OCT1 model conformed to Ramachandran plot with 99.2% of the residues in the favoured and allowed regions of the Ramachandran plots according to RAMPAGE analysis. Of the total 398 residues built into the model, only 3 residues occupied phi/psi backbone torsion angles in disallowed regions; however, upon further analysis, these residues are located in loop regions not involved with TMDs or substrate binding cleft. Additionally 8 residues were in allowed regions and were all located in loop regions, with the exception of one S340 residue located in TMD11. The OCT2 model only had 2 residues in the outlier regions, but these residues were in intracellular loops. Table 3.4 gives summary results of the OCTs with the two templates used. LacY and GlpT sequence identity and similarity between these two templates and OCTs are >13% and >27% respectively. LacY was chosen as the best template for both OCTs and was subsequently used for further analysis.

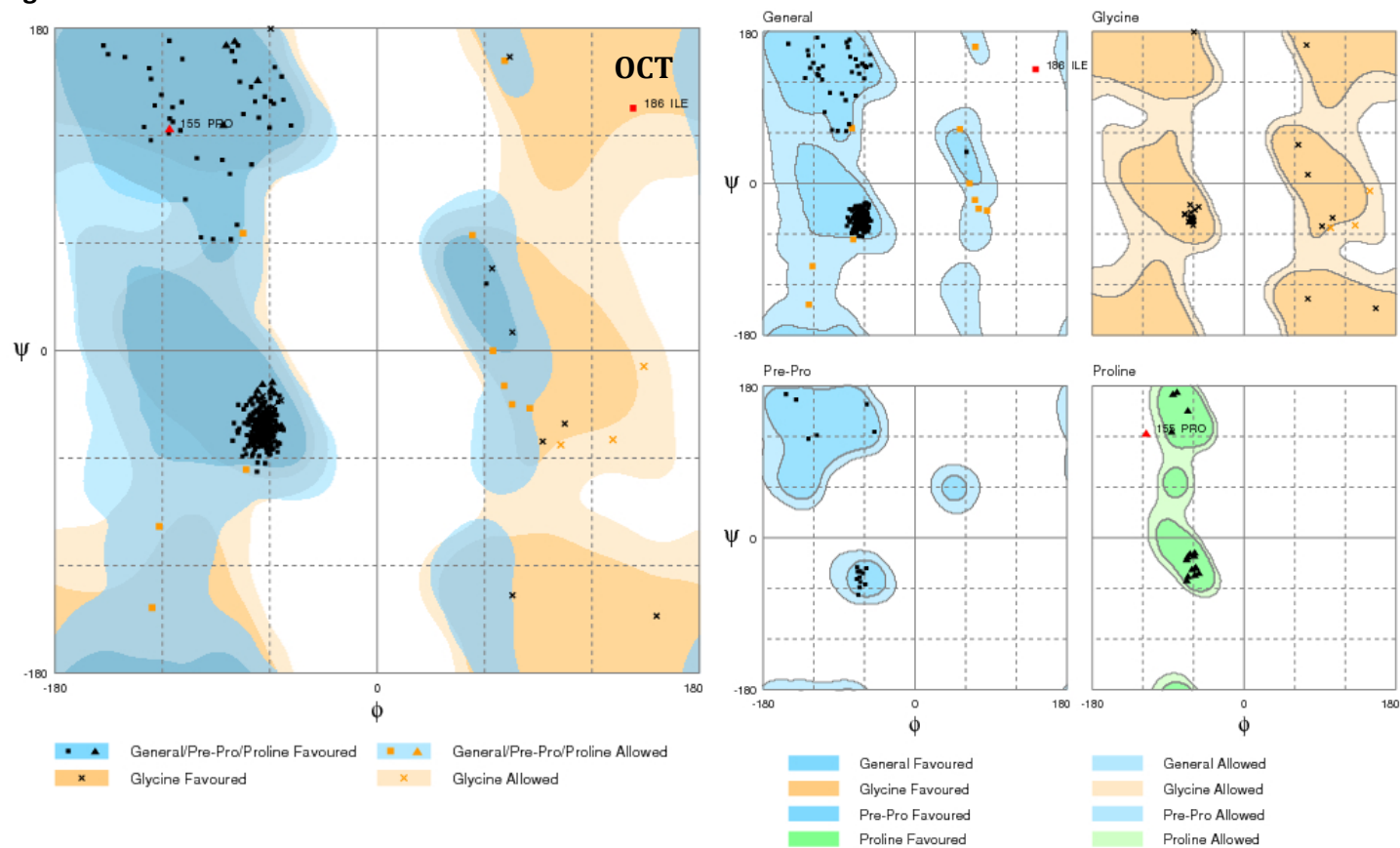
Some residues exhibit ambiguous orientations of side-chain amides, namely, Asn, Gln and His residues. Some of these orientations overlap with other residues in close proximity. MolProbity recommended flips for Asn, Gln, and His sidechains as part of its default run of adding hydrogens. This was performed in both models. This reduced the average number of bad backbone bonds from >0.73% to >0.38% in both transporters. The PDBeFold SSM server-produced RMSD values between the OCT1 and OCT2 models and the 1PV6 crystal structure was only 0.84Å and 3.51Å. This suggests the OCT1 model is a better constructed model than OCT2, but overall the validation results indicate the models are reasonably well constructed and acceptable.

Figure 3.3. Ramachandran assessment of final OCT1 model



Each peptide backbone dihedral angles,  $\psi$  and  $\phi$  within the models are plotted against each other and acknowledge any residues fall within a acceptable region on the plot. Overall 387 (97.2%) residues were in the favoured region, 8 (3.0%) were in the acceptable region and 3 (0.8%) were in the outlier region. Expected and desirable results are 98% residues within the favoured region with 2% within the acceptable region.

Figure 3.4. Ramachandran assessment of final OCT2 model



Overall 387 (96.3%) residues were in the favoured region, 13 (3.3%) were in the acceptable region and 2 (0.5%) were in the outlier region. Expected and desirable results are 98% residues within the favoured region with 2% within the acceptable region.

### 3.3.2 3D-Structural Analysis

Figure 3.5 illustrates a model of OCT using LacY as a template. The two different stereoviews show how the binding cleft is in an inward facing orientation towards the cytoplasm. The binding cleft measures  $>25.3$  Å wide and a depth of  $>36.4$  Å. Figure 3.5c shows the distribution of TMDs within the plasma membrane. TMDs 1, 2, 4, 5, 7, 8, 10 and 11 are all predicted to contribute to the binding cleft suggesting they are involved with substrate recognition and specificity. Conversely TMDs 3, 6, 9 and 12 are located within the plasma membrane suggesting they are not involved with substrate binding.

### 3.3.3 Helical Wheel Analysis

The wheel plots showed that the majority of TMDs 1,2,4,5,7,8,10 in both transporters exhibited specific hydrophobic and hydrophilic faces. To ensure the helical wheel plots correlated with the TMDs of the models, each TMD was assessed to evaluate whether the hydrophilic faces of the model were facing the binding cleft. Structural models correlated with the helical wheel analysis suggesting that they were correctly aligned with respect to the crystal structures. Unfortunately the models produced by the GlpT template appeared to have the TMDs incorrectly aligned in respect to the helical wheel plots. All helical wheel plots for OCT1 and OCT2 transporters are shown in appendix Figure A-3.1 and A-3.2 respectively.

### 3.3.4 Docking

Models produced from the LacY template were used in further docking experiments. This was due to the TMDs being correctly aligned and predicted to be in the correct orientation. In total  $>400$  docking results were produced for each model and ranked accordingly. The first 10 top hit docking results were then used for further study investigating predicted binding affinities. The top hit

docking results for OCTs are displayed in Figure 3.7. Although this figure displays the top hit for OCTs, there was a degree of overlap for residues involved in metformin binding for OCT1 and OCT2. For example conserved residues Asp(378/381;OCT1/OCT2) and Tyr(381/384) located on TMD 8 were predicted to bind to metformin in other top docking results. Metformin exhibited a binding affinity ( $\Delta G$ ) of -14 and -16 kJ/mol for OCT1 and OCT2 respectively.

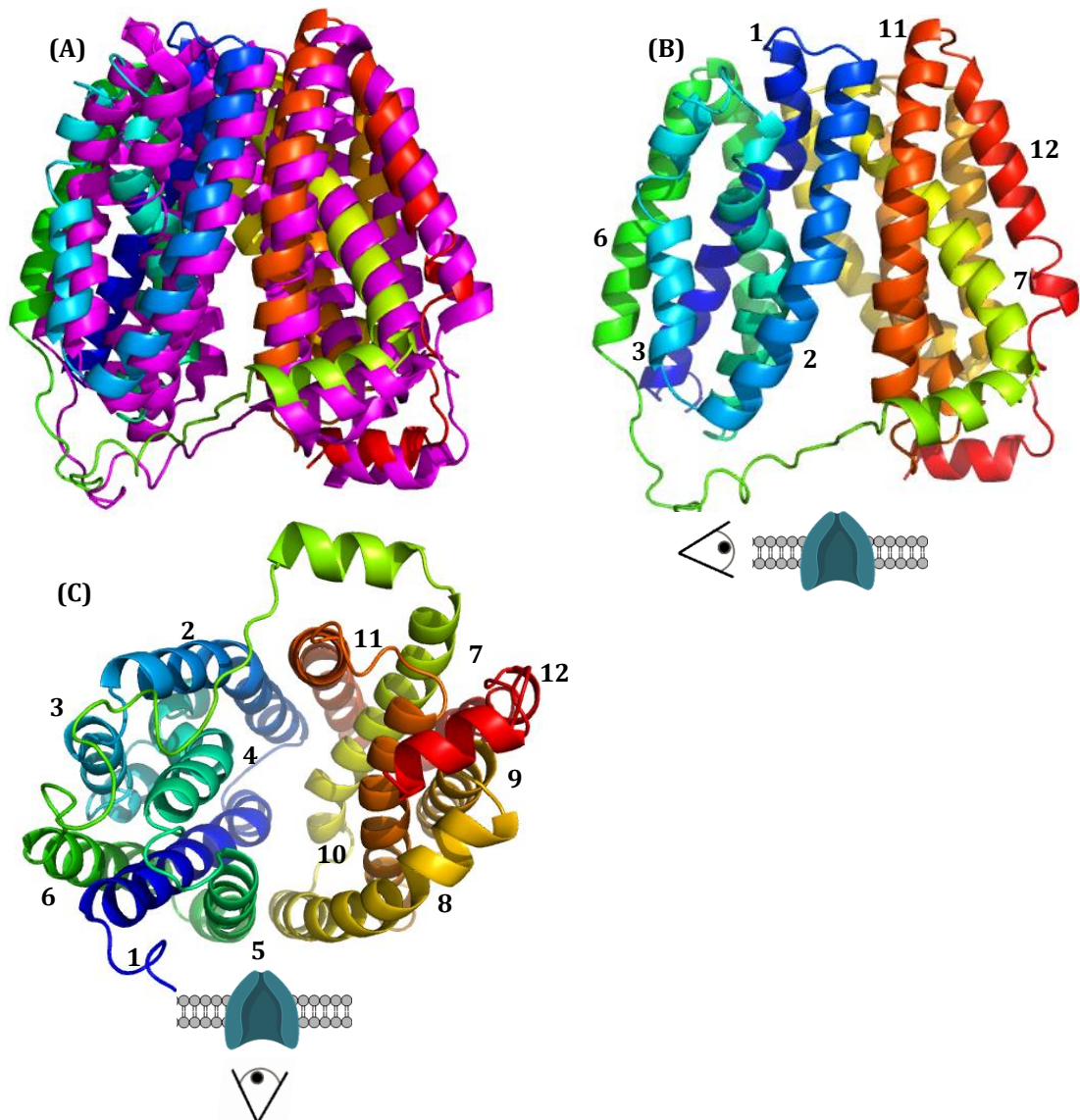


**Figure 3.5. Predictive structural model of hOCT1**

(A) This image displays the LacY permease transporter template (pink) overlapping the hOCT1 model in rainbow colours with each colour representing a TMD. (B) hOCT1 model, each colour represents a single TMD. This view is orientated to display hOCT1 on the X-axis to the plasma membrane showing the binding cleft facing the intracellular compartment. Numbers correspond to TMD number. (C) This view is orientated to display the binding region of hOCT1. TMDs are numbered accordingly. The transporter binding cleft measures at 25.3 Å wide by 36.4 Å depth. Note that TMDs 3, 6, 9 and 12 are predicted not to contribute to the binding pocket.

There was a degree of overlap for the OCT1 inhibitors with Asp156, Gln362 and Trp354 being involved in docking of both quinidine and cimetidine. The top quinidine docking result also shared the same residues involved in metformin binding (Tyr361, Asn156, Trp354 and Phe355). The predicted binding affinity for quinidine and cimetidine was greater than metformin with  $\Delta G$  of -25 and -19 kJ/mol, respectively.

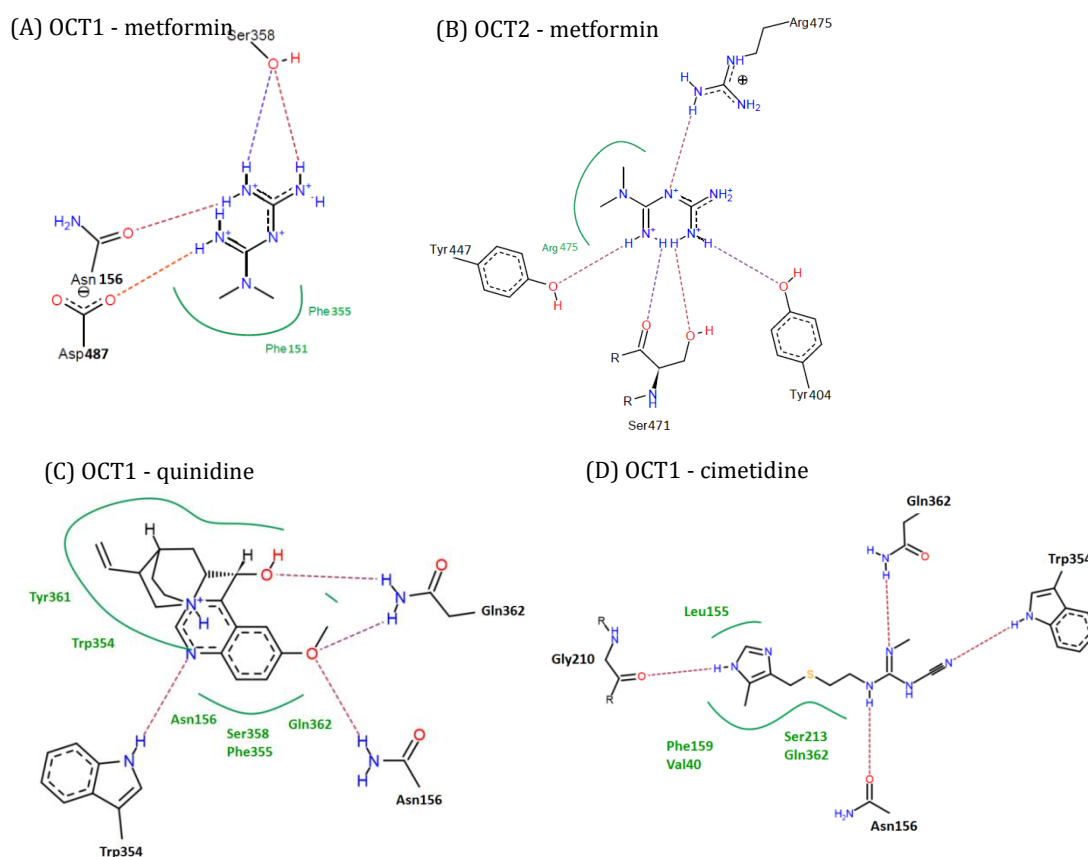


**Figure 3.6. Top hit docking results of ligands with OCT1 & 2**

(A) OCT1. Polar and charged groups contribute to metformin binding to OCT1 binding cleft. The hydrophobic residues are shown in green interacting with two  $\text{CH}_3$  groups on metformin. (B) OCT2. Four residues are contributing to metformin binding. All residues shown to interact with metformin binding were all within 4 Å of metformin. All docking results showed that polar or charged residues would dock to metformin contributing to the binding affinity. (C) OCT1 – quinidine. (D) OCT1 – cimetidine. Both OCT inhibitors and metformin shared specific amino acids contributing to binding.

### 3.3.5 Impact of genetic variants on structure and docking

Amino acid altering genetic variants were assessed to see if they were located near the predicted metformin docking sites or orientated into the binding cleft.

Three variants in OCT1 were orientated into the binding cleft, L160, M440 and G465R, Figure 3.7 shows the structural effect of G465R has on the binding cleft. However, L160 residue in OCT1 was the only amino acid within 10 Å of the area predicted to contribute to metformin binding. Only the M165 residue in OCT2 was orientated into the binding cleft and within 10 Å of residues involved in metformin binding. Table 3.2 summarises the results.

**Table 3.2. Common amino acid variants in OCT 1 and 2.**

	Residue	Effect on metformin transport	on TMD	Residue orientated into binding cleft?	Residue within 10Å of residues involved in binding?
SLC22A1 (OCT1)	L160F	Similar	2	Y	Y
	S189L	Decreased	3	N	N
	G220V	Decreased	4	N	N
	G401S	Decreased	9	N	N
	M408V	Decreased	9	N	N
	A413V	-	9	N	N
	M420del	Decreased	9	N	N
	M440I	Similar	10	Y	N
	G465R	Decreased	11	Y	N
SLC22A2 (OCT2)	M165I	Decreased	2	Y	Y
	M194V	-	3	N	N
	A270S	Decreased	6	N	N
	K432Q	Increased	10	N	N

All variants listed in the table are located in TMDs and the majority have been expressed *in vitro* to assess the impact they have on metformin transport. The table therefore provides a comparison to residues identified to potentially interact with metformin binding with results obtained *in vitro*. Polymorphic residues were identified to evaluate whether they are involved in the binding cleft or are in close proximity of residues predicted to bind to metformin. Y, yes; N, no. *In vitro* metformin transport results used to generate this table were acquired from (Leabman et al., 2002, Nies et al., 2011b).

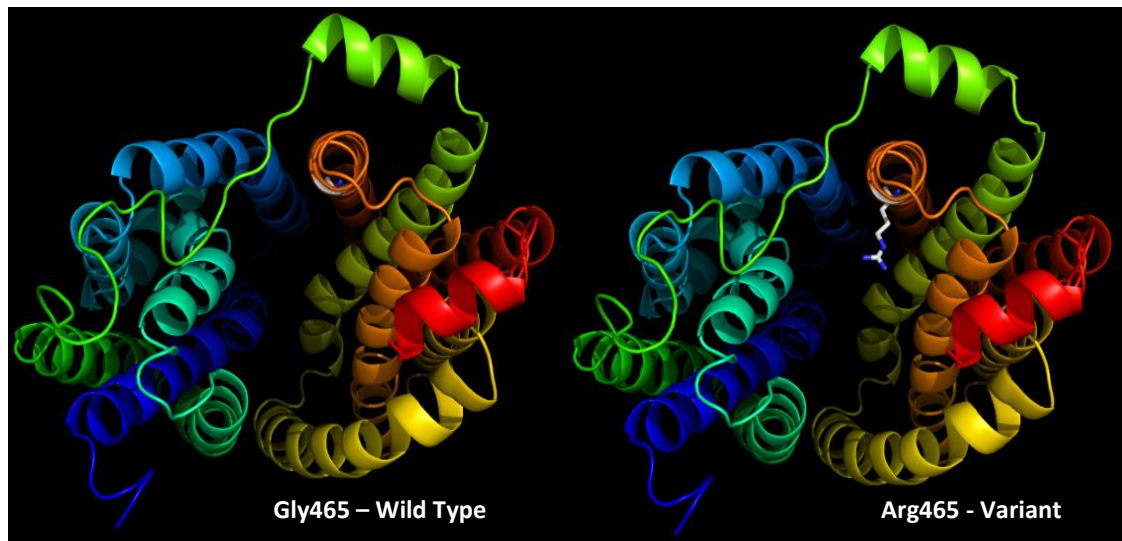


**Figure 3.7. G465R variant in OCT1**

The major allele Gly465 exhibits no bulky side chain within the substrate binding cleft, left. The minor allele variant Arg465 (right) has its bulky side chain orientated within the substrate binding cleft which would suggest could directly impact substrate binding.

### 3.3.6 Post Translational modification prediction

#### 3.3.6.1 Glycosylation sites

Four potential N and O-linked glycosylation sites were predicted within OCT1 on residues N72, N112, S52 and S108. These were not located near the identified R61C genetic variant. Three potential N-linked glycosylation sites were predicted within OCT2 on residues N72, N97 and N113. These were not located near any nsSNPs in OCT2. No O-linked sites were identified in OCT2.

#### 3.3.6.2 Ubiquitination prediction

The BDM-PUB server showed OCT1 had 11 potential ubiquitination sites on lysine residues. Residue 19 in first intracellular loop, residues 308, 311, 318, 345 in second loop and residues 517, 526, 534, 536, 538, 545 in the third loop. For OCT2 the BDM-PUB server revealed 9 potential ubiquitination sites with residues 304, 308, 309, 312, 329 in second loop and residues 518, 537, 539, 541 in the third loop. All ubiquitination sites were located in cytoplasmic loops. The two SNPs in OCT1 and two SNPs in OCT2 were not located on or near (within 10 residues) any predicted ubiquitination sites.

### 3.4 Discussion

Predicted 3D-structure models have been routinely and successfully used to screen large databases and identify possible transporter ligands through docking experiments and for enabling rational drug design. The 3D-structures of these transporters can be used for homology and comparative predictive modelling for other transporters that share sequence similarity and transmembrane domains. Ultimately they provide an illustrative mechanistic insight to the binding of ligands and possible transport mechanisms.

There are several online automatic structure prediction servers which can produce structural models through only inputting the amino acid primary sequence of the target protein including I-TASSER, SWISS-MODEL and Phyre2 which have been used to predict the structure of transporter proteins in publications (Giannoudis et al., 2013, Dickens et al., 2013). However initial analysis using the web based servers produced models which failed the validation procedures used in this chapter and were thus not biologically accurate models. A more stringent method in producing structural models is using programs such as MODELLER as implemented in this chapter. This method produced models that passed the rigorous validation procedures undertaken in this study. For example, the RMSD between LacY and OCT1 was 0.84 Å. Considering the RMSD value for proteins with 50% sequence identity is expected to 1 Å, a value of <0.84 Å is a highly acceptable given the OCT proteins share <15.25% sequence similarity with LacY. The RMSD value for the OCT2 model was 3.51 Å; although higher, given the low sequence homology, this is still regarded as an acceptable value.

Interesting all crystal structures identified as possible templates for OCTs (Table 3.1) share common structural features. Each protein has 12 TMDs which form a barrel containing a substrate binding core. More specifically TMDs 3, 6, 9 and 12 do not contribute to the substrate binding core of the transporters but in

fact are located in the peripheries of the protein, embedded within the plasma membrane. Although there is low sequence similarity between the template and OCTs the structural features, number of TMDs, alpha-helices etc, are more important to base a predictive structure than absolute sequence percentage similarity. Conversely the sequence similarity between Lac Y permease and OCT is regarded as more than acceptable to model a predictive structure based on the crystal. The helical wheel plots revealed that these TMDs are mainly composed of hydrophobic residues and do not possess a hydrophilic face. Therefore helical wheel plots were produced from the predicted TMDs of the OCTs to see if this correlated with known crystal structures. With regards to the OCTs specificity for organic cations, one would expect a high number of polar hydrophilic amino residues in TMDs, particularly orientated towards the substrate binding cleft with the hydrophobic residues facing and buried within the plasma membrane. Further analysis revealed that all 3, 6, 9 and 12 TMDs from OCT1 and 2 are >78% composed of hydrophobic residues suggesting these TMDs are not directly involved in the binding cleft and most probably embedded in the plasma membrane. Conversely, TMDs 1, 2, 4, 5, 7, 8, 10 and 11 all contained a hydrophilic face suggesting these TMDs contribute to a binding cleft core.

Two templates were initially used in this study for predictive OCT modelling. LacY and GlpT templates successfully produced acceptable models in accordance with Ramachandran plots. These transporters share >15.4% sequence identity, >29.6% sequence similarity and display similar structures containing 12 TMDs forming large clefts orientated towards the cytosol. Further analysis was implemented to determine if the TMDs of OCTs were correctly orientated by studying if hydrophilic residues orientated and exposed towards the binding cleft. This revealed that models using the GlpT template exhibited TMDs that were not all correctly orientated, unlike the LacY template. Therefore the best scoring OCT model using the LacY template was chosen for subsequent docking analysis.

Predicted metformin docking experiments were restricted to the binding cleft of the OCT models, rather than the entire protein including helices embedded in the plasma membrane. Over 400 hits per model were produced and ranked accordingly; top scoring hits were used for binding affinity predictions. The majority of docking hits predicted that aspartic acid residues were important in the binding of metformin. Additionally polar residues such as serine, asparagine and tyrosine residues were identified as important contributors to metformin binding. This finding conforms to metformin's polar properties exerted through its guanide, amide rich backbone. Conversely, some hydrophobic residues were found to interact with the two CH<sub>3</sub> groups of metformin.

Top binding affinities of metformin ranged from -11 to -16 kJ/mol. In respect to the size of the metformin molecule, this affinity is considered to be rather strong. Computational docking experiments often use the phrase 'ligand efficiency (LE)' which refers to the size of the molecule and number of atoms with the overall affinity of the ligand binding to the protein. Metformin's LE was calculated to be -1.78 kJ/atom and also revealed the positively charged amide group contributed to a large fraction of the binding affinity. This information provides a useful insight when designing compounds for known protein target structures. For example Huttunen et al., 2009 designed prodrugs based on metformin's structure in order to improve bioavailability. This was achieved by removing or shielding the positive charged tail end of metformin. Though this may increase metformin's bioavailability, the results discovered in this chapter suggest this may produce a compound with decreased OCT transport affinity and thus potentially decrease its pharmacological action.

Polymorphic residues in OCTs, as identified in Chapter 2, were used in docking experiments to assess their impact on metformin binding or affinity (Table 3.2). Firstly, residues were visually examined if they were orientated towards the binding cleft. This could indicate that they are directly involved in substrate recognition for specific substrates, and thus variants could influence transport

activity. Additionally polymorphic residues were identified if they were within close contact (10Å) of residues predicted to be involved in metformin binding.

The L160 residue was the only amino acid in OCT1 within 10 Å of the area predicted to contribute to metformin binding. *In vitro studies* have similar transport activity between both L160F variants (Nies et al., 2009). This may be due to both residues having hydrophobic properties. Additionally this variant was shown in Chapter 2 (Table 2.4) through the algorithms to not exert a negative impact on protein function. Adjacently, the M165 residue in OCT2 was both orientated into the binding cleft and within 10 Å of residues involved in metformin binding. These results support that of Leabman et al., 2009 who observed reduced metformin transport in the variant, I165, in comparison to the M165 residue. This shows our predictive results reflect the results of Leabman's et al., 2009 *in vitro* study. We observed the G465R variant to be orientated into the binding cleft (Figure 3.7), which has been shown to decrease metformin transport *in vitro*. Although this residue was not located near our predicted metformin binding site, it is clear that it structurally impacts the substrate binding cleft. Glycine is a small residue in comparison to the long, charged chain of arginine and thus may interfere with the conformational structure of OCT1.

In summary, we found discrepancies between our *in silico* predictive system to that observed *in vitro*.

We included two known OCT1 inhibitors for docking; quinidine and cimetidine (Tu et al., 2013, Lee et al., 2009b). Interestingly the residues involved in binding these not only overlapped with each other but also with those involved with metformin binding. Predictively, the inhibitors exhibited a higher binding affinity than the substrate, metformin. This may provide the exact binding pocket these inhibitors bind and provide a mechanistic relationship into how they specifically inhibit metformin.

What the structural models fail to account for is amino acid variants affecting the conformation of the protein. Although some residues were predicted to have an impact on metformin transport they could play an important role in the conformational stability of the transporter and thus significantly impact transport activity. Additionally the 3D-models are only produced with an inward facing binding cleft and thus may explain efflux of substrates whereas the *in vitro* transport results relate to metformin influx. Crystal structures of templates including the binding cleft orientated towards the extracellular matrix would prove highly beneficial for understanding the complete transport mechanisms of a particular transporter.

There are numerous limitations to predictive computational modelling. The crystal structures used in this study as a target-template for OCT structures were in one, inward (cytoplasmic) facing orientation only. This only provides possible mechanisms to substrates binding in the cytoplasmic facing binding cleft and substrate efflux. The OCTs are regarded as bi-directional facilitated transporters which may give equilibrative concentrations across the membrane. Furthermore, transporters exist in different structural states under different environment conditions, such as pH. This is particularly important when assessing transporters expressed in the intestinal epithelium where the environmental pH can vary dramatically and thus may contribute to different protein conformations. PMAT is an intestinal metformin transporter which is sensitive to pH changes. Zhou and Wang, 2006, discovered metformin transport through PMAT decreased under acidic conditions.

Unfortunately, low sequence identity between available crystal structures and the large extracellular loops of OCTs resulted in the loop being excluded from predictive models. OCTs contain a large extracellular loop between residues 43 and 149. Therefore we analysed potential N and O-linked glycosylation sites using online servers and examined whether they were near any variants. The results showed no variants were near any predicted glycosylation sites. These

sites could be involved in substrate recognition or protein stability and therefore could be important in its function. For example the OCT1 amino acid variant R61C located in the large extracellular loop has been shown to significantly reduce metformin transport *in vitro* (Nies et al., 2011b).

Similarly intracellular loops of the OCTs were not incorporated into the structural models. Therefore we used an ubiquitination prediction server on OCTs to determine if any variants were expressed near any ubiquitination sites. The results concluded no variants were located near any sites. Other studies have identified several residues that are predicted to be involved in PKC binding and decreased transport activity when mutated (Biermann et al., 2006). Nevertheless, these were not located near any variants identified in chapter 2.

Using docking software to investigate the potential of two substrates binding simultaneously would provide useful information when investigating the effects of an inhibitor or multiple substrate transport mechanisms. Due to the large binding cleft in OCTs, it has been previously hypothesised that these may be able to transport more than one small molecule under, a single transport mechanism (Higashi et al., 2014). Traditionally, studies investigating the effects of substrates or inhibitors on transporters will use a general high-throughput *in vitro* assay to generate a bank of known ligands and inhibitors with corresponding activity values ( $K_m$  and  $V_{max}$ ). Computer models can then offer an insight into the mechanisms, of these substrates and ligands undergo *in vivo*, supporting laboratory findings. This chapter has taken a backward approach using 3D-structural computer models as an starting point. However this approach could offer a rationale for deciding which particular amino acids for further investigation using laboratory techniques.

Other members of the MFS family that are known to transport metformin *in vitro* include OCT3, MATE1, MATE2K and PMAT (Zhou et al., 2007a, Chen et al., 2013). Therefore it would also be beneficial for this chapter to construct

structural models for these proteins. However, unlike OCTs, MATE1 and MATE2K are predicted to have 13 TMDs and PMAT to have 11 TMDs. Therefore using a template containing 12 TMDs would produce inaccurate results. Crystal structures of membrane proteins containing 13 or 11 TMDs would need to be used as templates. Conversely helical wheel plots could predict whether TMDs are involved with substrate binding in the binding cleft or interact with the plasma membrane. Individual TMDs could then be modelled on standard  $\alpha$ -helices and applied to docking experiments using a bank of compounds. However, as discovered in this report, several TMDs in close contact all play a synergistic role in the binding of metformin.

Although predictive structural modelling may not overtake classical ligand-based 'wet' laboratory techniques to assess possible ligand specificity for transporters they provide a visual aid to possible structure mechanistic understanding of transporter mechanisms which are not fully elucidated today. The chapter has used these techniques to provide an illustrative understanding to how some genetic variants may impact substrate transport.

# **Chapter 4**

**Development and validation of a  
Hydrophilic Interaction Liquid  
Chromatography –Tandem Mass  
Spectrometry method for the  
Determination of metformin in human  
plasma in T2DM patients**

## CONTENTS

<b>4.1 INTRODUCTION.....</b>	<b>114</b>
<b>4.2 MATERIALS &amp; METHODS.....</b>	<b>118</b>
4.2.1 CHEMICALS AND REAGENTS .....	118
4.2.2 PREPARATION OF STANDARDS AND QC SAMPLES .....	118
4.2.3 EXTRACTION PROCEDURE.....	118
4.2.4 CHROMATOGRAPHY .....	119
4.2.4.1 <i>UV detection</i> .....	119
4.2.4.2 <i>MS/MS detection</i> .....	119
4.2.5 METHOD VALIDATION .....	120
4.2.5.1 <i>Limit of quantification</i> .....	120
4.2.5.2 <i>Limit of detection</i> .....	120
4.2.5.3 <i>Selectivity</i> .....	122
4.2.5.4 <i>Standard curve and linearity</i> .....	122
4.2.5.5 <i>Recovery</i> .....	123
4.2.5.6 <i>Precision and accuracy</i> .....	123
4.2.5.7 <i>Stability</i> .....	123
4.2.6 APPLICATION TO CLINICAL SAMPLES .....	124
4.2.6.1 <i>Metformin dosing</i> .....	124
4.2.6.2 <i>Plasma time sampling</i> .....	124
4.2.6.3 <i>Sample collection</i> .....	125
4.2.7 EFFECTS OF COMPOUNDS ON METFORMIN DETERMINATION .....	125
<b>4.3 RESULTS.....</b>	<b>126</b>
4.3.1 METHOD DEVELOPMENT .....	126
4.3.1.1 <i>Column selection</i> .....	126
<b>Figure 4.2</b> .....	127
4.3.1.2 <i>Internal standard selection</i> .....	129
4.3.1.3 <i>Extraction procedure</i> .....	129
4.3.2 METHOD VALIDATION .....	130
4.3.2.1 <i>Limits of quantification and detection</i> .....	130
4.3.2.2 <i>Selectivity</i> .....	130
4.3.2.3 <i>Standard curve and linearity</i> .....	130
4.3.2.4 <i>Carry-over</i> .....	133

4.3.2.5 <i>Intra- and inter-day accuracy and precision</i> .....	133
4.3.2.6 <i>Recovery</i> .....	133
4.3.2.7 <i>Stability</i> .....	133
4.3.2.8 <i>Robustness</i> .....	135
4.3.3 APPLICATION TO CLINICAL SAMPLES .....	135
4.3.4 EFFECTS OF COMPOUNDS ON METFORMIN DETERMINATION .....	136
<b>4.4 DISCUSSION .....</b>	<b>137</b>

## 4.1 Introduction

A wide variety of HPLC methods have been developed for the quantification of metformin in biological fluids. They vary considerably in the choice of HPLC columns, detection methods, internal standards and extraction procedures, as demonstrated in Table 4.1, thus generating enormous differences in sensitivity, retention time and reproducibility. The choice of stationary phase for the optimum retention of a compound is known to be important and should be based on its physicochemical properties. Compounds with positive or high LogP values are predicted to be retained on a hydrophobic column (reversed-phase chromatography). Conversely compounds with a negative or low LogP value, such as metformin, are predicted to be retained on a hydrophilic column (HILIC or normal-phase chromatography). Despite this, the majority of published studies have used reversed-phase chromatography (Porta et al., 2008, Chen et al., 2004, Wang et al., 2004, AbuRuz et al., 2003).

Metformin has two acid dissociation constants (pKa) of 2.8 and 11.5 and a partition coefficient logP of -2.64. Consequently, under physiological conditions, metformin exists as a single protonated, highly polar cation and is 0.01% unionized in blood (Brittain, 1998, Craig, 1990). These properties collectively contribute to the poor bioavailability (40-50%) of metformin in comparison to other anti-T2DM drugs such as pioglitazone (pKa, 6.8 and 6.1; logP, 2.4) and glibenclamide (pKa, 5.3; logP, 4.79), which exert high bioavailability of 99% and 80%, respectively (Malinowski and Bolesta, 2000, Campbell et al., 1991). Given its poor bioavailability, metformin is not likely to be absorbed passively from the GI tract. Metformin does not bind to plasma proteins (Scheen, 1996) making extraction from biofluids relatively straightforward.

Our initial studies showed the high polarity of metformin resulted in poor retention times when using reversed-phase chromatography despite using low organic content in the mobile phases. What is not apparent or stated in previous studies is the quality of the reverse phase columns used for separation of

**Table 4.1. Reported HPLC methods for the determination of metformin**

Column	Mobile phase	Flow (m/min)	Detection	Internal Standard	Retention (min)	Extraction	Volume injected (µl) plasma volume %	pH	Recovery (%)	LLOQ (ng/m)	Linearity (ng/ml)	Reference
C <sub>18</sub>	MeCN, MeOH, 10 mM ammonium acetate (20:20:60, v/v/v)	0.65	MS	Phenformin	1.2	OSPP	20 (-)	7.0	-	1	1-2000	(Wang et al., 2004)
C <sub>8</sub>	MeCN, water, formic acid (70:30:1, v/v/v)	0.5	MS	DiPhenhydramine	2.63	OSPP	20 (-)	-	>96.5	2	2-2000	(Chen et al., 2004)
C <sub>18</sub> Ion pair	2mM sodium dodecyl sulphate in MeCN, 20 mM KH <sub>2</sub> PO <sub>4</sub> (37.5:62.5, v/v)	-	UV	Phenformin	4.85	IPSPE	150 (0%)*	7.3	98	5	5 – 1500	(AbuRuz et al., 2003)
Silica	MeCN, 30 mM (NH <sub>4</sub> ) <sub>2</sub> HPO <sub>4</sub> (25:75, v/v)	1.0	UV	Atenolol	6.8	OSPP	-	7	>76	10	10-2000	(Cheng and Chou, 2001)
Silica	MeCN, 40 mM NaH <sub>2</sub> PO <sub>4</sub> (25:75, v/v)	1.0	UV	Ranitidine	5.7	OSPP	50 (20%)	6	>97.5	15.6	15.6-2000	(Amini et al., 2005)
HILIC	Water, MeCN, formic acid (30:70:0.1, v/v/v)	0.65	MS	metformin-D6	0.99	OSPP	1 (20%)		81	0.5	0.5–500	(Liu and Coleman, 2009)

**Table 4.1. (continued) Reported HPLC methods for the determination of metformin**

Column	Mobile phase	Flow (ml/min)	Detection	Internal Standard	Retention (min)	Extraction	Volume injected (μl) plasma volume %	pH	Recovery (%)	LLOQ (ng/ml)	Linearity (ng/ml)	Reference
HILIC	10 mM ammonium acetate, MeCN (40:60, v/v)	1.0	UV	Tetramethyl guanidine	9.5	OSPP	-	5	92	1000	1000-10000	(Huttunen et al., 2009)
Cation exchange	5mM KH <sub>2</sub> PO <sub>4</sub> , MeCN (76:24, v/v)	1.0	UV	Buformin	9.5	OSPP	50 (30%)	5.3	99.4	20	20-4000	(Bonfigli et al., 1999)
Cation exchange	400 mM ammonium acetate	2.0	UV	-	5	UF	98.5 (-)	-	98	50	100-4000	(Vesterqvist et al., 1998)
Meta Sil-Phenyl	20 mM KH <sub>2</sub> PO <sub>4</sub> , MeCN (50:50, v/v)	1.0	UV	Propranolol	7.5	OSPP	25 (20%)	7.0	93.7	30	30-4000	(Porta et al., 2008)
Ciano	10 mM KH <sub>2</sub> PO <sub>4</sub> , MeCN (60:40, v/v)	1.0	UV	-	5.9	APP	50 (96)	3.5	97	60	62.5-4000	(Yuen and Peh, 1998)

0% plasma volume -solid phase extraction. IPSPE, ion pair solid phase extraction; OSPP, organic solvent protein precipitation (liquid-liquid); UF, ultrafiltration; UV, Ultra-violet.

metformin from biological fluids. It is appreciated that prolonged use of reverse phase columns can result in the loss of C<sub>18</sub> groups from the columns polymer, exposing a bare silica surface, transforming the stationary phase from hydrophobic to hydrophilic. This could provide a mechanistic explanation to the retention times exhibited when using reverse phase columns. This theory supports the finding by Van de Merbel et al., 1998 who experienced greater retention of metformin using old C<sub>18</sub> columns over new C<sub>18</sub> columns.

The most common extraction method for metformin is liquid-liquid plasma protein precipitation using organic solvents (Porta et al., 2008, Wang et al., 2004, Zarghi et al., 2003, Marques et al., 2007). This simple, rapid technique exhibits high recovery but sacrifices sensitivity through sample dilution. Moreover, it does not remove endogenous compounds in plasma such as lipids which can interfere with the mass spectrometer instrumentation. Other alternatives such as ion-pair solid-phase (AbuRuz et al., 2003) and ultrafiltration (Vesterqvist et al., 1998) have been utilised to yield pure extracts; however, they are time consuming methods which also have poor sensitivity.

In order to overcome the deficiencies of currently available assays which have not been applied to T2DM clinical samples with high lipid levels, the development of a simple, sensitive and reproducible HPLC method for the quantification of metformin which is transferable with both ultra violet (UV) and mass spectrometric detection is described. This method was validated using an easy to follow work-flow diagram and subsequently applied to the measurement of plasma concentrations of metformin in T2DM patients. The effects of common comedications associated with this patient group were also investigated to elucidate whether these drugs may influence the quantification of metformin *ex vivo*.

## 4.2 Materials & Methods

### 4.2.1 Chemicals and reagents

All chemicals used in this study were purchased from Sigma-Aldrich (Poole, UK). Water was purified using a Milli-Q Gradient system.

### 4.2.2 Preparation of standards and QC samples

All concentrations of metformin and phenformin refer to their hydrochloric salts. Stock solutions of metformin (1 mg/mL) and internal standard (IS) phenformin (1 mg/mL) were prepared by dissolving the hydrochloride salts in mobile phase A which comprised acetonitrile, 5 mM ammonium acetate, formic acid (90:10:0.1, v/v/v; pH 5.1). A series of metformin standard solutions at different concentrations (0.3-10,000 ng/mL) were prepared through serial dilutions of the stock concentration with mobile phase A. A working solution of phenformin (1 µg/mL) was also prepared. High, medium and low and LLOQ QC concentrations of 300, 30, 3 and 0.3 ng/mL, respectively, were chosen and prepared. Metformin concentrations are quoted as their salt (metformin·HCl), free base concentrations were calculated by dividing the salt concentration by 1.28. All working solutions were stored at +4°C and used within 24 hours of preparation.

### 4.2.3 Extraction procedure

To 50 µl of plasma, 2.5 µl of the IS (10 µg/mL) and metformin (appropriate concentrations) working solutions were added and vortexed for 5 sec. Mobile phase A (447.5 µl) was added, vortexed and left for 15 min at room temperature to ensure complete protein precipitation had occurred. The solution was then centrifuged at 14000 rpm (17,500×g) for 10 min at room temperature. The supernatant was transferred to a clean container and centrifuged again under the same conditions to minimise precipitate being transferred prior to analysis by LC-MS/MS.

#### 4.2.4 Chromatography

Chromatography was performed using a Phenomenex Luna HILIC column (250 mm x 4.6 mm, i.d. 5 $\mu$ ) connected to a HILIC guard cartridge (4 mm x 3 mm). A gradient mobile phase was used consisting of gradient mobile phase A (see section 4.2.2) and mobile phase B (5mM ammonium acetate, formic acid (100:0.1, v/v) pH 5.1). Mobile phase A was held at 80% for 2 min, then 50% for 5 min, then returned at 80% for 5 min equilibration. A 10 $\mu$ L sample was used for detection. A solution of mobile phase A was used for needle and valve wash to minimise carry-over in the autosampler. The total run time was 12.0 min. The flow rate was maintained at 0.6 mL/min. The autosampler temperature was set to 4°C and the column remained at room temperature (23°C). To establish possible matrix effects ionisation effects we used post plasma precipitation extracts from blank plasma samples and monitored any differences in electron spray ionisation responses for both metformin and the IS through a post-column infusion. The results revealed that both retention times and response appeared satisfactory.

##### 4.2.4.1 UV detection

HPLC-UV detection was performed using a Dionex P580 pump online with the ASI-100 autosampler and UVD340U detector. Detection of metformin was analysed at 235 nm. Chromatograms were analysed using Chromeleon® software v.6.8.

##### 4.2.4.2 MS/MS detection

Detection was performed on an API 3000 LC-MS/MS (Applied Biosystems). The operating conditions were: ionisation, positive mode; source temperature, 450°C; ion spray, 5000v; Nitrogen gas (99.999%) at 3, 10 and 14 psi as the collision gas, curtain gas and nebuliser gas, respectively. Optimised parameters for metformin and phenformin were: entrance potential (EP), 10v; declustering potential (DP), 31 and 36v; focusing potential (FP), 130v; collision energy (CE), 27 and 29v; collision cell exit potential (CXP), 12 and 10v, respectively. Analytes

were detected using multiple reaction monitoring (MRM) with transitions of  $m/z$  for metformin and phenformin monitored at 130.14→70.9 and 206.15→59.9, respectively (Appendix 2.7.1) with a dwell time of 200 ms per transition. Data acquisition was performed with Analyst™ (v.4.2) on a MS workstation.

#### 4.2.5 Method validation

This method has followed the validation procedures and acceptance criteria laid down in the Guidance for Bioanalytical Method Validation for Human Studies set by the Food and Drug Administration, (FDA, 2001) and Guideline on Validation of Bioanalytical methods set by the European Medicines Agency (EMA, 2010). However, the guidelines differed in which procedures should be carried out sequentially, and therefore a summary of the sequential validation steps has been summarised in Figure 4.1.

##### 4.2.5.1 Limit of quantification

Lower limit of quantification (LLOQ) was defined as the lowest concentration peak response with at least 5 times the response as compared to a blank sample with a precision and accuracy of  $\leq 20\%$  and  $\pm \geq 20\%$  respectively. This was evaluated by spiking plasma (n=6) with metformin before extraction and determined on two different days (inter-day assay).

##### 4.2.5.2 Limit of detection

Limit of detection (LOD) was defined as the lowest concentration of metformin with a signal-to-noise ratio  $\geq 3$ . This was evaluated by spiking plasma (n=6) with metformin before extraction and determined on three different days (inter-day assay).

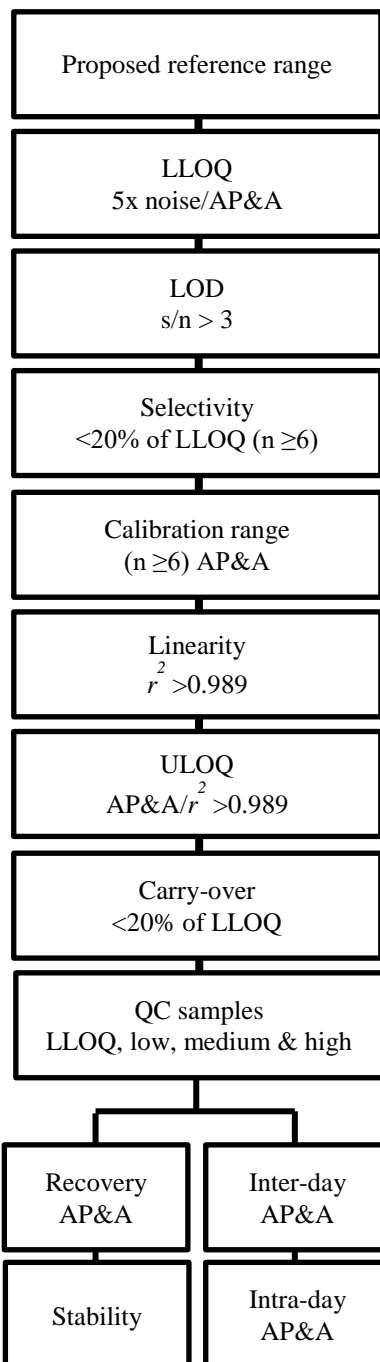


Figure 4.1. Work flow diagram for method validation.

A systematic flow diagram for undertaking sequential validation steps with acceptable criteria based on guidelines and recommendations from the FDA. Reference range was chosen based on previous reports in the literature. AP&A; Acceptable precision & accuracy, defined a CV<20% and  $\pm 20\%$ . QC samples are accordingly; low 2-3 times the LLOQ; medium, middle of the range; high, 80-85% of the ULOQ. After the QC sample concentrations have been established, subsequent validation analyses may be performed.

#### 4.2.5.3 *Selectivity*

Selectivity was defined as the ability of a method to differentiate and quantify the analyte in the presence of other components in the sample. Analyses of blank plasma samples obtained from 6 individuals (3 male, 3 female) were examined to determine if interfering peaks were present at the retention time of metformin and the internal standard, phenformin. Acceptable criteria state that a peak present at the retention time of the analyte and internal standard peak area should be  $\leq 20\%$  and  $< 3\%$  at the LLOQ, respectively.

#### 4.2.5.4 *Standard curve and linearity*

A stock solution was prepared by spiking metformin into human plasma. Calibration standards were then produced by diluting the stock with blank human plasma to give 0.1, 0.3, 1, 3, 10, 30, 100, 300, 1000, 3000 and 10000 ng/mL of metformin. A calibration curve was constructed by plotting peak area ratio of metformin to IS (y) versus metformin concentrations (x). Slope, intercept and correlation coefficients were calculated as regression parameters. Linearity between concentrations were defined as having a correlation coefficient of  $> 0.989$  with coefficient of variation (CV)  $\leq 15\%$  for all concentrations with the exception of that related to the LLOQ for which  $\leq 20\%$  was acceptable.

#### 4.2.5.5 Recovery

Recovery of metformin was determined through comparison of peak areas from spiked human plasma before and after the extraction procedure using the high, middle, low QC and LLOQ (300, 30, 3, 0.3 ng/mL) concentrations (n=3) on one day. Recovery was recorded as absolute and relative recovery. Absolute recovery was defined as the peak area of metformin in extracted plasma with reference to the peak area of metformin in mobile phase A (different matrix). The relative recovery was defined as the peak areas of metformin in extracted plasma with reference to the peak area of metformin in spiked extracted plasma.

#### 4.2.5.6 Precision and accuracy

Assay precision and accuracy was evaluated both intra- and inter-day by determining the four QC samples as described above. Precision was defined by coefficient of variation (CV), and accuracy was defined as bias. A precision of  $\leq 15\%$  for all concentrations analysed with exception of that related to the LLOQ ( $\leq 20\%$ ) were acceptable with a mean accuracy between 85-115% for all concentrations with the exception of the LLOQ (80-120%), as recommended by the FDA (2001).

#### 4.2.5.7 Stability

Stability was assessed in QC samples under various conditions reflecting storage processes encountered in this experimental study. Stability parameters assessed were short term (24 hours), long term (7 days) post preparative storage and following three freeze-thaw cycles at  $-80^{\circ}\text{C}$ . Samples were thawed at room temperature and when appropriate, refrozen for at least 24 hours. Solutions were stored in polypropylene cryovials to minimise evaporation. The acceptance criteria state that samples should have a precision of  $\leq 15\%$  for all concentrations analysed with exception of that related to the LLOQ ( $\leq 20\%$ ).

## 4.2.6 Application to clinical samples

Plasma samples were collected from 75 T2DM patients who had been prescribed metformin therapy as a part of their usual management between 2005 and 2007. Patients were excluded if they consumed alcohol in excess of the recommended weekly safe drinking limits (>21 units in men; >14 units in women), and undertook any form of strenuous exercise (defined as more than typical walking pace) for a period of 8 hours prior to the study. Patients were also excluded receiving any known medications to affect metformin pharmacokinetics in the previous 4 weeks before the start of the study. Known medications are amantidine, cimetidine, clonidine, desipramine, midazolam, procainamide, quinidine, quinine, verapamil. There were no restrictions on caffeine or smoking.

### 4.2.6.1 Metformin dosing

Metformin was administered orally. In order to assess steady-state pharmacokinetics patients established a dose of metformin for at least three months and not missed a dose for a period of 5 days prior to sample collection. Compliance had been assessed through a validated compliance questionnaire. Metformin doses varied in respect of their usual treatment dose of 500, 850 and 1000 mg which were taken once (oid), twice (bid) or three times daily (tid).

### 4.2.6.2 Plasma time sampling

Patients received their usual dose of metformin (500, 850 or 1000 mg) in the morning of the study. A maximum of three blood samples were subsequently collected at random time intervals following the same dose of metformin. The timing of the blood sample collection in relation to dosing was recorded and differed between patients. Dosing of metformin times ranged from 02:00 to 12:50 with a median time of 08:17. The first of the blood samples taken ranged from 08:37 to 15:10 with a median time of 11:19. Time from dose received and blood sample taken ranged from 4 to 545 minutes with a median time of 3

hours. Time between the first sample of blood taken and the last ranged from 45 to 195 minutes with a median time of 80 minutes.

#### *4.2.6.3 Sample collection*

Blood was collected by venipuncture from the antecubital vein using a 21 gauge butterfly needle into vacutainers containing Ethylenediaminetetraacetic acid (EDTA) and centrifuged at 3000 rpm (1610 X *g*) for 10 min. Separated plasma was transferred and aliquoted into a 1 mL polypropylene tubes and stored at approximately -20°C until analysis. The study was approved by Liverpool Local Research Ethics Committee with clinical samples collected from the Royal Liverpool Hospital. All blood donors gave written informed consent before participating. Blank human plasma was obtained internally from healthy volunteers at the University of Liverpool.

#### **4.2.7 Effects of compounds on metformin determination**

For assessing the selectivity of the assay for the detection of metformin, the effect of concomitant medications that are typically co-prescribed in patients with T2DM was tested. Two concomitant groups were categorised for further investigation: those with a logP value of  $\leq 0.5$ , predicted to interact with the hydrophilic-polar stationary phase of the HILIC column, and compounds that were being received by  $\geq 10\%$  patients, Table 4.2. To investigate whether a compound may affect the quantification of metformin, we analysed differences in peak height, AUC, retention time and the accuracy and precision between samples ( $n=3$ ). The compound and metformin concentrations remained constant at 100 ng/mL.

**Table 4.2 Comedications investigated to determine their effect on metformin quantification**

Compound	Drug Class	n (%)
Ipratropium	Anticholinergic	2 (2.7)
Lactulose	Laxative	1 (1.3)
Macrogol	Laxative	1 (1.3)
Levetiracetam	Antiepileptic	1 (1.3)
Theophylline	Antiasthmatic	1 (1.3)
Timolol maleate	Antihypertensive	1 (1.3)
Sotalol	Antiarrhythmic	1 (1.3)
Moxonidine	Antihypertensive	1 (1.3)
Aspirin	Anticoagulant	37 (49.3)
Atorvastatin	Lipid regulator	25 (33.3)
Simvastatin	Lipid regulator	23 (30.7)
Furosemide	Antihypertensive	18 (24)
Rosiglitazone	Antidiabetic	8 (10.7)
Pravastatin	Lipid regulator	8 (10.7)
Paracetamol	Analgesic	4 (5.3)

Two groups of comedications were investigated for possible interference effects, those with a logP value of  $\leq 0.5$  and compounds present in  $\geq 10\%$  of the population group.

## 4.3 Results

### 4.3.1 Method development

#### 4.3.1.1 Column selection

Metformin quantification was initially examined on an RP-C18 column (Phenomenex, UK). Initial experiments confirmed the poor retention of metformin on RP columns, (Figure 4.2). In order to increase retention time using a RP column 2 mM sodium dodecyl sulphate (NaDS) as a ion-pair reagent was included in the mobile phase. The retention time increased from 2.2 min to 3.2 min, (Figure 4.2c). Unfortunately reproducibility between samples was unsatisfactory and for MS/MS detection, the inclusion of NaDS in the assay was not desirable.

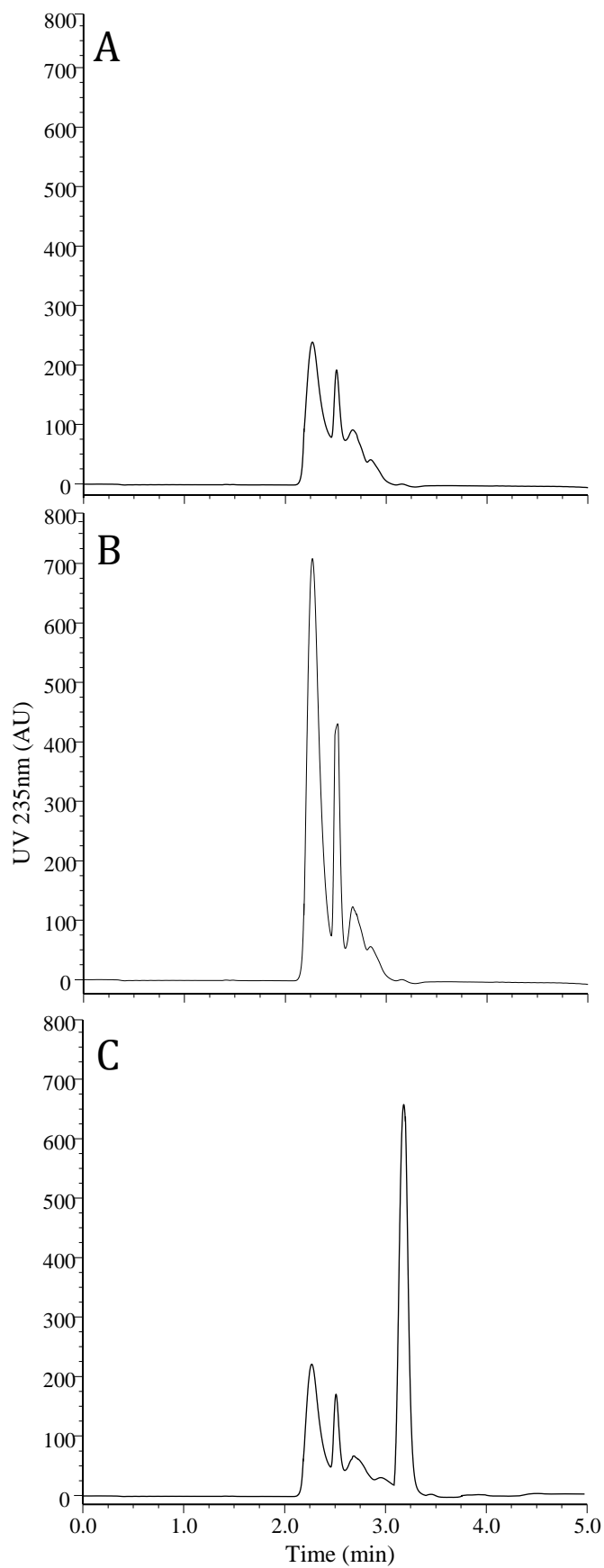


**Figure 4.2. Reverse phase chromatography of metformin from human plasma.**

UV detection at 235 nm.

(A) Blank plasma.

(B) Plasma spiked with 3 µg/mL metformin.

(C) Plasma spiked with 3 µg/mL metformin with addition of NaDS in the mobile phase.

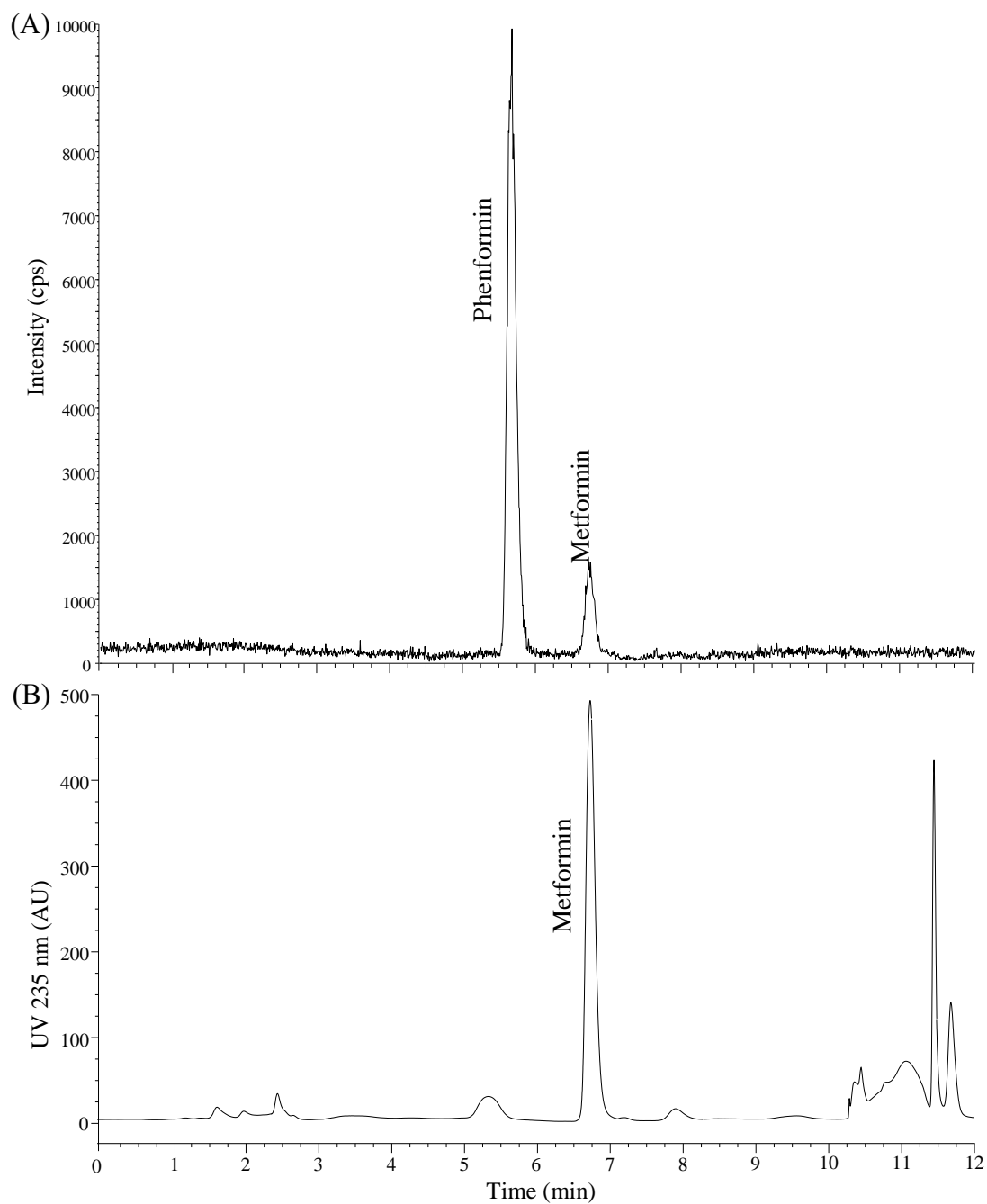


**Figure 4.3 HILIC separation of metformin from human plasma.**

HILIC of metformin spiked plasma. (A) The gradient allows plasma components to elute between 2-3 min and 12- 15 min; metformin elutes at 6.8 min. UV detection of 3  $\mu\text{g}/\text{mL}$  at 235 nm. (B) MS/MS Chromatogram representation of a T2DM patient. Chromatogram illustrates the excellent resolution and low noise level. Internal standard phenformin; 50 ng/mL.

A hydrophilic interaction liquid chromatography (HILIC) column was subsequently used for the method increasing their retention time and allowing metformin to be separated from the plasma components. The gradient method successfully retained metformin while allowing good separation from polar plasma components (Figure. 4.3a). The retention time using a HILIC column was 6.6 min.

#### *4.3.1.2 Internal standard selection*

To eliminate different responses and increase assay accuracy and precision between batches, an internal standard of known concentration was included in the matrix. Two internal standards with similar chemical structural properties to metformin were investigated, phenformin and tetramethyl guanidine (TMG). These molecules all exhibit a guanidine backbone.

Under optimal MS/MS operating conditions, phenformin but not TMG significantly decreased noise (response with no analyte present in sample) when no analyte was present in the sample thus increasing sensitivity. Additionally, TMG produced an undesirable tailing effect; therefore phenformin was selected as the most appropriate IS. Metformin and phenformin exhibited peak elution times of 6.6 and 5.6 min  $\pm$  3.8 sec respectively.

#### *4.3.1.3 Extraction procedure*

A liquid-liquid extraction procedure was evaluated and developed. A series of plasma:acetonitrile extraction ratios were used to determine an optimal ratio for complete protein precipitation. Although a 1:1 ratio was sufficient for complete precipitation in healthy plasma samples, this could not be applied to T2DM clinical samples as high plasma lipid levels interfered with the mass spectrometric instrumentation, preventing consecutive quantitative analyses. After exploring different extractant ratios, it was found that a ratio of 1:10 averted the problem without significantly compromising assay sensitivity.

### 4.3.2 Method validation

This study used validation procedures and acceptance criteria as laid down by the FDA and EMEA. A sequential summary is displayed in the flow diagram described in Figure 4.1.

#### 4.3.2.1 Limits of quantification and detection

The LLOQ and LOD was determined as 300 pg/mL (0.3 pg on-column) with a precision of <15% (n=5) for both intra- and inter-day with a signal-to-noise ratio (s/n) of 5. The described method has a similar sensitivity to previously published methods (Liu and Coleman, 2009). The LLOQ was more than adequate for this study given the high metformin plasma concentrations observed in the T2DM patients. The ULOQ was found to be 300 ng/mL - concentrations exceeding this gave undesirable linearity and precision. Subsequently clinical plasma samples exhibiting a concentration >300 ng/mL were diluted.

#### 4.3.2.2 Selectivity

Acceptable criteria state that a peak present at the retention time of the analyte and internal standard should be  $\leq 20\%$  and <3% at the LLOQ respectively. In relation to the developed method, the relevant peaks were <3% for both metformin and phenformin with no interfering peaks present at their retention times.

#### 4.3.2.3 Standard curve and linearity

Standard curves were produced from extracted plasma samples, with concentrations ranging from 100 pg to 10  $\mu\text{g/mL}$  using HILIC with MS/MS detection (Table 4.3). Concentrations between 300 pg – 300 ng/mL produced a coefficient of correlation ( $r^2$ ) value of 0.999 (n=10). All concentrations produced CV% values of <15. The equation of the final calibration curve was  $y = 0.1884x + 0.0096$  with an  $r^2$  value of 0.999 (Figure 4.4). Concentrations between 300 pg – 3000 ng/mL produced acceptable precision and linearity, while concentrations above 300 ng/mL resulted in carryover. Therefore linearity in this method was evaluated to be 300 pg/mL – 300 ng/mL (Figure 4.4).

**Table 4.3 Linearity of extracted plasma samples.**

Concentration range	Day 1 (n = 2)		Day 2 (n = 2)		Day 3 (n = 3)	
	<i>r</i> <sup>2</sup>	CV%	<i>r</i> <sup>2</sup>	CV%	<i>r</i> <sup>2</sup>	CV%
300pg-3µg/mL	0.99675	0.0780	0.9991	0.0849	0.997633	0.0759
300pg-300ng/mL	0.99935	0.00708	0.99955	0.0637	0.9995	0.0265

Acceptable concentration range is between 300 pg/mL and 3µg/mL. As the ULOQ was evaluated to be 300 ng/mL two concentration ranges are shown.

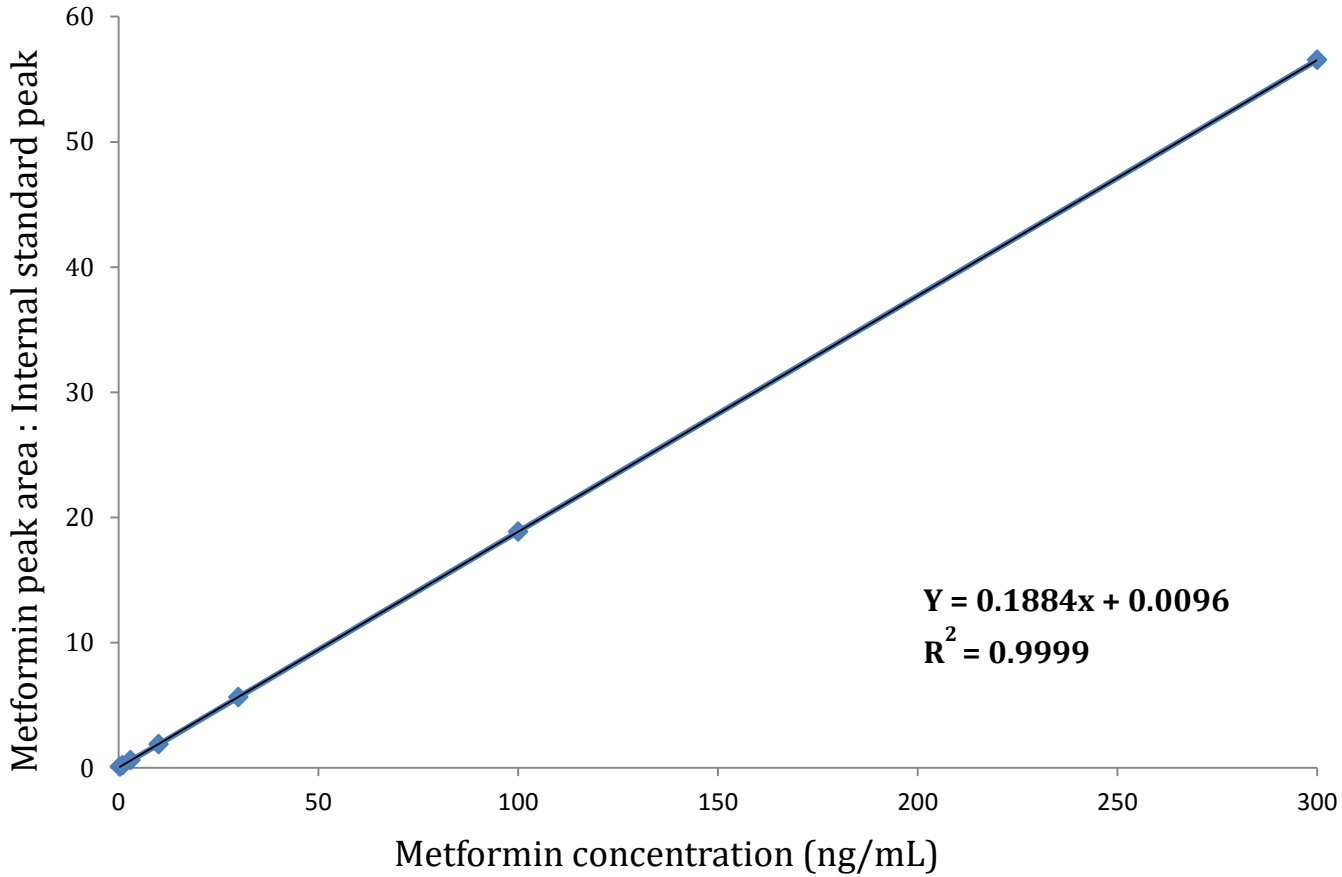


**Figure 4.4. Metformin standard curve.**  
Concentrations shown ranged between 300 pg – 3000 ng/mL, see 4.3.2.3.

#### 4.3.2.4 Carry-over

Carry-over was assessed by analysing calibration standards immediately followed by analysis a blank matrix sample. The responses in the blank samples were expressed as a percentage of the mean LLOQ. Although there are no acceptance criteria for carry-over, we wanted to minimise injection carry-over to <20% of the LLOQ to facilitate the quantification of low concentration samples following high concentration samples. The percentage carry-over of LLOQ for 300 ng, 1 µg and 3 µg/mL were 18.63%, 50.37% and 156.31 % respectively. Our results indicate that the absolute amount of drug the column can sustain without carry-over is 3 ng (10 µl of 300 ng/mL).

#### 4.3.2.5 Intra- and inter-day accuracy and precision

Intra- and inter-day accuracy and precision were assessed by analysing QC samples within and between batches (Table 4.4). Throughout the development, validation and quantitative procedures, the column had passed 7.835 L of solution over >200 hours of run time, with peak elution times of metformin and phenformin on average 6.6 and 5.6 min, respectively, which differed  $\pm 3.8$  sec over the course of the study. Throughout the length of the study, QC samples consistently produced acceptable accuracies and precision estimates.

#### 4.3.2.6 Recovery

The liquid-liquid protein precipitation extraction method described produced absolute and relative recoveries with metformin ranges of 78.3-89.3% and 80.5-100.6 % respectively. All concentrations tested had consistent and acceptable recoveries (Table 4.4).

#### 4.3.2.7 Stability

Stability was assessed in QC samples under various conditions reflecting storage processes encountered in this experimental study, as listed in Table 4.5. All concentrations were acceptable with an accuracy of between 80-120%. All determinations of stability were satisfactory according to the acceptance criteria.

**Table 4.4 Intra- & inter-day and absolute and relative recovery of metformin extraction precision and accuracy of metformin**

Standard (ng/mL)	Inter-day (n=3)			Intra-day (n=8)			Absolute recovery (n=6)		Relative recovery (n=6)	
	Mean	Precision (CV%)	Accuracy (%)	Mean	Precision (CV%)	Accuracy (%)	%	Precision (CV %)	%	Precision (CV %)
LLOQ (0.3)	0.33	3.8	9.63	0.29	17.42	-3.06	78.3	16.2	80.5	19.2
QC-Low (3)	2.92	7.29	-2.65	2.85	5.45	-4.86	98.2	11.5	98.7	15.1
QC-Middle (30)	31.10	11.41	3.67	30.54	7.95	1.79	87.8	14.2	108.8	7.6
QC-High (300)	327.14	2.56	9.05	343.26	6.12	14.42	89.3	13.1	100.6	14.1

Precision is defined as coefficient of variance; CV(%) = (standard deviation/mean value) x 100. Accuracy is defined as Bias (%) = ((determined value – nominal value)/nominal value) x 100.. Absolute recovery was defined as the AUC of metformin in extracted plasma with reference to the AUC of metformin in buffer A (different matrix). The relative recovery was defined as the AUC of metformin in extracted plasma with reference to the AUC of metformin in spiked extracted plasma.

**Table 4.5 Metformin stability under different conditions**

Condition	Temperature	Duration	Sample	Accuracy Bias (%)	Precision CV (%)
Short term	4°C	24 hr	Low QC	-6.95	2.22
			High QC	-8.36	1.99
			Stock	-2.21	1.91
Long term	-80°C	7 days	Low QC	7.54	9.51
			High QC	4.96	2.64
			Stock	2.19	5.46
Freeze-thaw	-80°C	3 cycles	Low QC	-6.71	12.59
			High QC	6.58	4.46
			Stock	2.46	1.44
Extract	4°C	24 hr	Low QC	5.33	8.34
			High QC	6.48	4.61

#### 4.3.2.8 Robustness

The HPLC-MS/MS method conditions were repeated at two separate sites, different HPLC and MS instruments and applied to two different HILIC columns. The chromatographic results and analyses were consistent, which could be attributed to the robustness and versatility of the method.

#### 4.3.3 Application to clinical samples

The method was used to quantify metformin from 218 plasma samples from 75 T2DM patients who had been prescribed metformin therapy as a part of their usual management. Three blood samples were collected at random time intervals following the last oral dose of metformin which ranged from 2 min to 9 hours. Average intraindividual metformin plasma concentrations (steady-state) ranged from 49 to 4908 ng/mL with an mean of 1879 ng/mL (Figure 4.5).

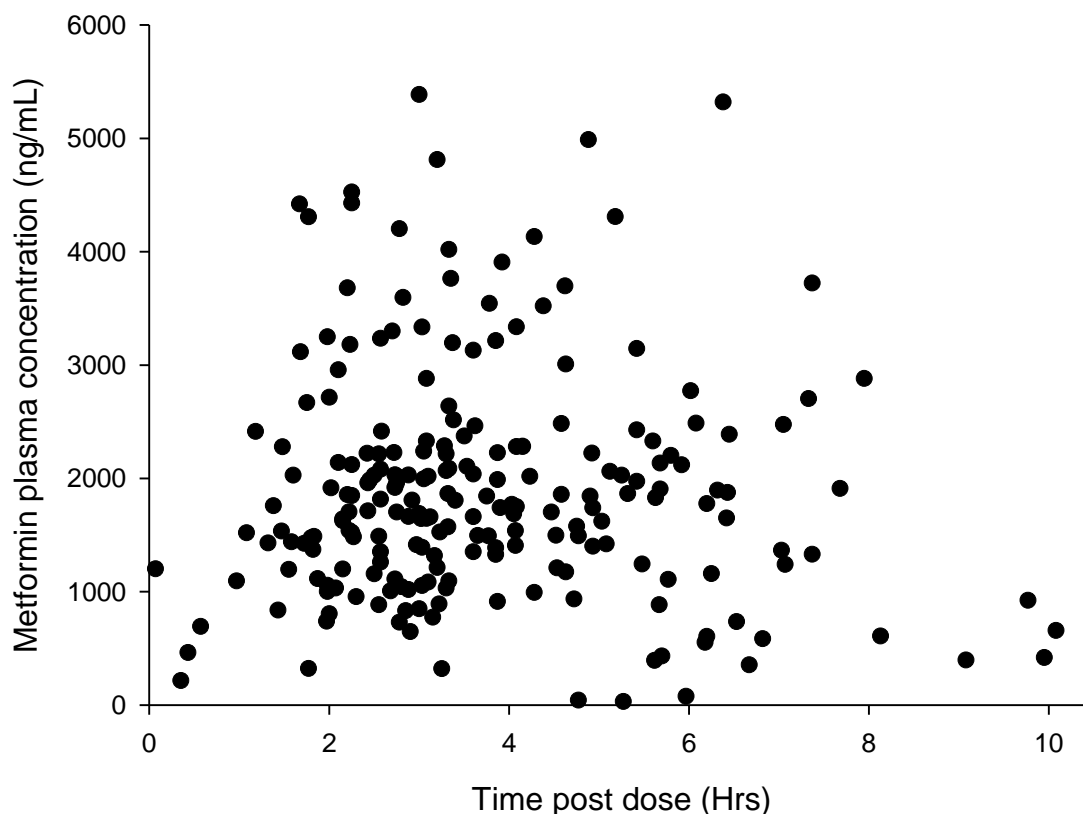


**Figure 4.5. Metformin plasma concentrations post metformin dose.**

Black dots represent all 218 metformin plasma concentrations from 75 patients. The coefficient of variation (CV%) between multiple plasma levels of one individual were small (mean <20%) suggesting steady-state PK was achieved

#### 4.3.4 Effects of compounds on metformin determination

In total, 104 comedications were being used by the patients in this study with an average of 5.96 prescription drugs per patient. We investigated two categorised comedication groups, those associated with >10% of patients and those with low logP values (Table. 4.6). There was no significant effect observed on the determination of metformin from plasma samples spiked with compounds investigated based on precision, accuracy, retention time and peak height

**Table 4.6 Effects of other comedications on metformin quantification**

Compound	LogP	Precision (%)	Accuracy (%)
Ipratropium	-3.712	2.57	2.89
Lactulose	-2.885	4.45	-1.41
Macrogol	-1.4	2.93	7.24
Levetiracetam	-0.67	4.83	9.54
Theophylline	-0.025	4.52	7.47
Timolol maleate	0.189	5.97	5.80
Sotalol	0.24	3.82	10.96
Moxonidine	0.325	2.74	11.12
Aspirin	1.399	2.11	9.52
Atorvastatin	3.846	4.29	6.45
Simvastatin	4.723	3.54	8.71
Furosemide	2.304	4.38	5.34
Rosiglitazone	3.023	2.84	4.66
Pravastatin	2.21	2.56	8.64
Paracetamol	0.475	2.66	5.12

Metformin and comedications remained constant at 100 ng/mL. LogP values were obtained from ChemSpider database. All comedications were measured in triplicate and accuracies were calculated from the nominal metformin concentrations.

## 4.4 Discussion

Initially this project aimed to quantify metformin from human plasma using reverse phase chromatography. Although, as Table 4.1 shows, reverse phase chromatography has been extensively used, initial experiments confirmed the poor retention of metformin on reversed-phase columns, as reported by other groups (Chen et al., 2004, AbuRuz et al., 2003). What is not apparent or stated by these studies is the quality of the reverse phase columns used for metformin retention. Van de Merbel et al., 1998 showed prolonged use of reverse phase columns can result in the loss of C<sub>18</sub> groups from the polymer used exposing a bare silica surface, transforming the stationary phase from hydrophobic to hydrophilic (van de Merbel et al., 1998). They suggested that the quality of the

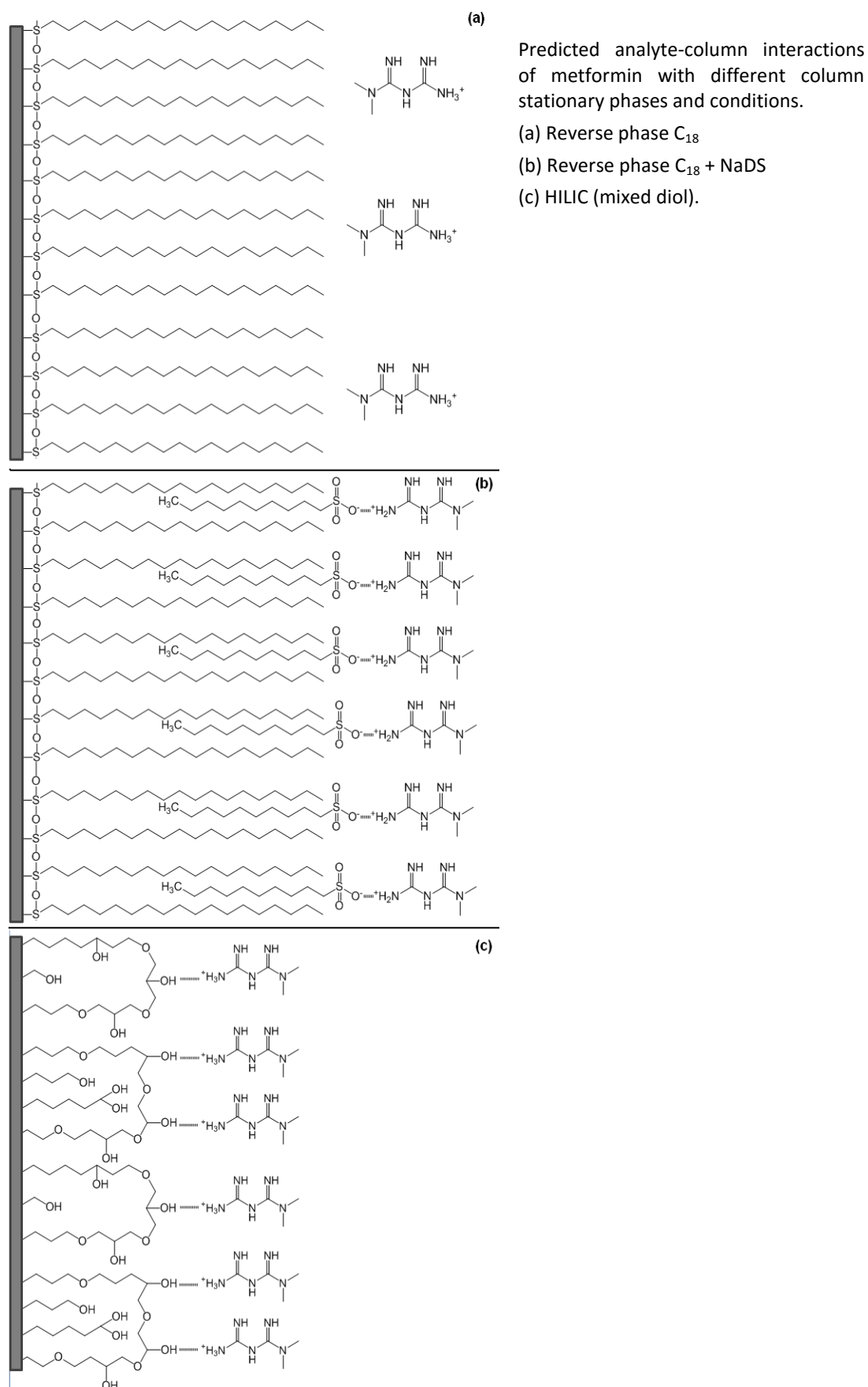
available reverse phase columns today are better than the columns available in the early 1990s. It is extremely rare that a study will state or record the history of the column including number of runs and changes in retention times of the analyte over an extended period of time. Therefore we have to assume the equipment used in retrospective studies are reliable and in the condition as it was originally. This might not be the case, however.

Consistent with other reports (AbuRuz et al., 2003), we found that the addition of sodium dodecyl sulphate (NaDS) as a ion-pair reagent in the mobile phase increased the retention time of metformin by 1 min. We propose that the negatively charged head group of NaDS molecules interacts with the positively charged metformin molecules while its hydrophobic tail interacts with the hydrophobic C<sub>18</sub> groups of the column's stationary phase as depicted in Figure. 4.6b. Unfortunately, reproducibility between samples was unsatisfactory and for MS/MS detection, the inclusion of NaDS in the assay was not desirable.

A HILIC column was subsequently used for the method. The HILIC column's mixed-diol polar groups allowed strong dipole-dipole interactions between polar molecules, metformin, and the stationary phase (Figure. 4.6c), increasing metformin's retention time and allowing exceptional separation from plasma components. The buffers were maintained at an acidic pH (5.1) in order to fully protonate metformin. The gradient mobile phase is essential for UV detection in allowing metformin retention while eluting polar plasma components between 1-3 minutes and 10-12 minutes (Fig. 4.3b). This is additionally advantageous in removing all retained plasma contaminants from the stationary phase which may interfere with subsequent high-throughput sample analysis and decrease column lifetime.

The HILIC chromatography method unlike others previously reported is transferable to either UV or MS detection. The use of UV detection for the method was investigated, but as metformin exists as a small molecule with no aromatic groups (Appendix 4.7.1), a selective wavelength could not be used exclusively to detect metformin. This resulted in high background noise and contributed to an unacceptable LLOQ of ~1 µg/mL. Although the described

Figure 4.6 Predicted analyte-column interactions of metformin



HPLC method does allow for both UV and MS/MS detection, due to the poor LLOQ of the UV detection, MS/MS detection was subsequently used to validate the method and its application to clinical samples.

Two compounds were evaluated as internal standards; phenformin and tetramethyl-guanidine (TMG). Under optimal MS/MS operating conditions, phenformin but not TMG significantly decreased noise when no analyte was present in the sample. Additionally, TMG produced an undesirable tailing effect; therefore phenformin was selected as the most appropriate IS.

The liquid-liquid extraction procedure was simple, quick and required no drying or concentration of samples which could compromise sensitivity. A series of plasma:acetonitrile extraction ratios were used to determine an optimal ratio for complete protein precipitation with minimal plasma dilution to increase assay sensitivity. Although a 1:1 ratio was sufficient for complete protein precipitation in healthy plasma samples, this could not be applied to T2DM clinical samples. Approximately 75% of the T2DM patients receiving metformin were diagnosed with dyslipidaemia and their high plasma lipid levels interfered with the mass spectrometric instrumentation, preventing consecutive quantitative analyses. The interference did not involve the ionisation or quantification but physically with the instrumentation. Although a higher ratio of organic solvent to sample could increase lipid solubilisation we found that a ratio of 1:10 averted the problem without significantly compromising assay sensitivity. Lui and Coleman (Liu and Coleman, 2009) also used protein precipitation to extract metformin from human plasma. However, it is likely that their plasma:extractant precipitation ratio of 1:5 could not be applied to T2DM plasma samples since extractant ratios less than 1:8 were found to incur problems with the mass spectrometric apparatus due to the high lipid levels observed in T2DM patients. Furthermore, we found that their isocratic mobile phase did not elute plasma components quickly or efficiently which could remain retained on the column. To our knowledge, this is the first study reporting the effects of lipid levels in serum of T2DM patients impeding mass spectrometric detection.

The assay as described in this report has acceptable linearity between 300 pg – 3 µg/ml with excellent linearity between 300 pg – 1 µg/mL. This 1000 fold linearity is consistent with Liu (Liu and Coleman, 2009) who also used HILIC and reported a linearity range of 500 pg/mL – 500 ng/mL. However, the precision decreases above concentrations of 1 µg/ml as the HILIC column was becoming fully saturated and contributing to carryover. This could account for the fall in  $r^2$  values at concentrations >1 µg/ml. Therefore the upper limit of quantification was investigated and evaluated to be 300 ng/mL. At this concentration, the carry-over of metformin was <20%. When analyzing a high metformin plasma concentration from a clinical sample, a blank matrix sample was used following the reanalyzed sample.

The method was used to quantify metformin from 218 plasma samples from 75 T2DM patients who had been prescribed metformin therapy as a part of their usual management. The metformin plasma concentrations ranged from 49 to 4908 ng/mL with an average of 1879 ng/mL, equating to a 100-fold difference in metformin plasma concentrations between patients receiving 0.5-3 g per day. This finding is consistent with Christensen et al., 2011 who report an 80 fold variability when using 2.0 g a day. All patients achieved steady-state metformin plasma concentrations which were independent of the time the blood samples were taken following metformin administration.

This study demonstrated there was no significant effect observed on the determination of metformin from plasma samples spiked with compounds investigated based on their precision, accuracy, retention time and peak height. Medications analysed were those associated with treating comorbidities associated with T2DM, including dyslipidaemia (atorvastatin, simvastatin, pravastatin) and hypertension (furosemide). The logP values were acquired from the chemical database, ChemSpider. LogP values ranged from -3.712 to 8.945 with an average of 2.56. In total 15 compounds were selected for investigation. We predicted that compounds with low logP values would be most likely to be retained on the HILIC column; however none of these compounds investigated exhibited an effect on metformin quantification, demonstrating the high selectivity of the developed method. Only parent

compounds were investigated and no assessment was made of their potential metabolites, which could exhibit different logP values. Given the range of compounds investigated and the fact that even low logP compounds were not retained on the HILIC column, it is likely that other comedications present in the patient samples had no effect on metformin quantitation using this assay.

A systematic and thorough validation procedure was performed and applied to a developed HILIC analytical method for the determination of metformin in plasma samples from T2DM patients. The HPLC method can be used for both UV and MS/MS detection and not influenced by concomitant medications or by the presence of high lipid levels in the plasma samples, which were removed using an improved sample extraction technique. HILIC-tandem MS/MS proved to be a reproducible, precise and robust method for application to pharmacokinetic studies. The metformin plasma levels obtained in this chapter will be used for PopPK modelling in chapter 5.

# **Chapter 5**

## **Population pharmacokinetic modelling of metformin in type II diabetes patients**

**CONTENTS**

<b>5.1 INTRODUCTION.....</b>	<b>145</b>
<b>5.2 MATERIALS &amp; METHODS.....</b>	<b>147</b>
5.2.1 STUDY SUBJECTS .....	147
5.2.2 POPULATION PHARMACOKINETIC ANALYSIS .....	147
5.2.2.1 <i>Software</i> .....	147
5.2.2.2 <i>Normal distribution analysis</i> .....	147
5.2.2.3 <i>Multiple Imputation</i> .....	148
5.2.2.4 <i>Base Model</i> .....	148
5.2.2.5 <i>Univariate analysis</i> .....	150
5.2.2.6 <i>Genetic covariates</i> .....	152
5.2.2.7 <i>Haplotypes</i> .....	153
5.2.2.8 <i>Multicovariate analysis</i> .....	154
5.2.3 MODEL SELECTION & EVALUATION .....	154
<b>5.3 RESULTS.....</b>	<b>155</b>
5.3.1 BASE MODEL .....	155
5.3.2 UNI-COVARIATE MODELLING .....	158
5.3.3 MULTIVARIATE ANALYSIS.....	161
5.3.4 MODEL EVALUATION .....	162
<b>5.4 DISCUSSION .....</b>	<b>164</b>

## 5.1 Introduction

Pharmacometrics is defined as the science of developing and applying mathematical and statistical models to understand and predict a drug's pharmacokinetics and pharmacodynamics (drug models) and biomarker-outcomes behaviour (disease models). In addition, these models can be linked and applied to support clinical study design (Powell and Gobburu, 2007). It is widely accepted that subjects receiving the same dose of a drug exhibit high variability in PK, drug efficacies and toxicities risk. The population approach attempts to understand such PK/PD differences among a sub-population and determine and classify sources of variability. Population pharmacokinetics (PopPK) is defined as the study of the sources of variability in drug bioavailability among individuals who are the target patient population receiving clinically relevant doses of a drug of interest. This knowledge is applied to develop rational guidelines for individualised drug dosage regimens, which can significantly increase drug efficacy and safety. PopPK has been widely used in a number of drug studies over a wide range of drug classes during drug development including, anticoagulants, antibacterial and anti-cancer drugs (Lee et al., 2012, Zhao et al., 2012, Menon et al., 2006).

PopPK modelling aims to understand the mean population response and identify, and explain, the variability using demographic and biological data to derive information about an individual, which may not be obtained from each individual directly.

Despite PopPK methodology being used since the 1970s the first report of its use with metformin was published in 2006 and investigated the pharmacokinetic disposition of metformin in late pregnancy and in fetal exposure at birth (Charles et al., 2006). Since then several PopPK and PD studies of metformin have been undertaken in both healthy volunteers and with T2DM patients (Table 5.1).

The overall objectives of the studies described in this chapter are to investigate the pharmacokinetic properties of metformin in T2DM patients using a

**Table 5.1 Previous metformin PopPK studies**

Reference	Hong et al., 2008		Bardin et al., 2012		Chae et al., 2012		Yoon et al., 2013		Gruen et al., 2013		de Oliveira Baraldi et al., 2011		Duong et al., 2013	
Recruitment area	New York, USA		Paris, France		South Korea		South Korea		Germany		Brazil		Malaysia	
T2DM	Yes		Yes		No		No		No		No		120 T2DM, 185 Healthy	
n	12		105		42		96		23		8		305	
Male %	25%		63%		100%		100%		-		0%		-	
Age (years)	56		62 (34-87)		26		22.41 (19-31)		31 (18-60)		26 (18-40)		28 (18-86)	
Weight (kg)	89		90 (49-149)		69		68 (53-96)		52		95 (80-126)		65 (41-165)	
CL <sub>CR</sub> (ml/min)	83		103 (33-227)		107		-		110±24		-		65 (41-165)	
Dose (mg)	500 - 850 bd (5d)		500-3000 od		500 od		500 od		500 tid		850 bd		250-3000 od	
Sample collection time post dose (n)	Trough d7-9 (15)		Trough 0- 6hr (3)		0-12hr (11)		0-24hr (12)		0-8hr (12)		0-12hr (17)		-	
Compartment	1		1		1		1		Non compartmental		Non compartmental		2	
Order	1st		-		1st		1st		-		-		Zero & 1st	
	Estimates	ISV	Estimates	ISV	Estimates	ISV	Estimates	ISV	Estimates	Estimates	Estimates	Estimates	ISV	
Ka (h <sup>-1</sup> )	2.15 (20.8)	58 (50)	0.51 (36)	0.39(4)	0.41 (2.4)	29.7	0.25 (3.0)	0.06 (10)	-	-	0.35 (2.5)	-	-	
CL/F (L.h <sup>-1</sup> )	79 (6.8)	23 (60)	56 (6)	0.71(5)	52.6 (4.2)	22.1	136 (18.4)	0.08 (13)	74 (65-84)	105 (60-274)	73 (2.3)	34 (12)		
V/F (L)	648 (13.8)	43 (47)	558 (22)	-	113 (57)	-	112 (6.9)	0.30 (15)	286 (245-333)	551 (385-1173)	149 (4.2)	54 (12)		

Summary of previous PopPK studies with metformin. ISV; inter subject variability, od; once daily, bd; twice daily, tid; thrice daily. Values represented are means (range). Estimate and ISV values in brackets are Relative standard error (RSE).

nonlinear mixed-effect modelling approach and to evaluate the effect of clinical covariates and transporter genetics on the pharmacokinetics of metformin and vitamin B<sub>12</sub> levels. With the additional data described in chapter 2, we also aimed to characterise the relationship between plasma metformin pharmacokinetics and the presence of polymorphisms in human organic cation transporter genes in T2DM patients on chronic metformin therapy.

## **5.2 Materials & Methods**

### **5.2.1 Study Subjects**

T2DM patients, as described in chapter 2, were recruited at the Royal Liverpool and Broadgreen University hospitals between 2005 and 2007.. In total 75 (45 (59%) male; 31 (41%) women) individuals were enrolled for the study.

### **5.2.2 Population pharmacokinetic analysis**

#### *5.2.2.1 Software*

Development and analyses of population PK/PD models, were performed using the software NONMEM version 7.2 (NONMEM Project Group, University of California at San Francisco, 1998)(Beal and Sheiner, 1980) using an open-source Fortran 2003 complier on Microsoft Windows. Graphical model diagnostics were produced and explored using, SPSS Statistics package version 20.0.0.1 (IBM) and Microsoft Excel 2007. Multiple imputations runs were performed using NORM version 2.03 (Schafer, 1999).

#### *5.2.2.2 Normal distribution analysis*

To assess if the data variables fell within the normal distribution, normality curves and normality tests were produced using SPSS. The Kolmogorov-Smirnov and the Shapiro-Wilk's tests were both used to assess normality. For both tests a significance level of 0.05 was used. Variables not within a normal distribution were transformed in a sequential order and reassessed using Log<sub>10</sub>,

SQRT, or SQRT(SQRT). Data outliers were identified through analyzing histograms.

#### *5.2.2.3 Multiple Imputation*

Any associations between covariates and each gender were revealed through graphical plot (covariate vs sex blox plots). Any associations between covariates were used in the NORM software package for imputation data (<http://sites.stat.psu.edu/~jls/misoftwa.html>). Six separate data sets were generated for both male and female populations and the mean of each imputed variable as the final model estimate. Each imputed data value was assessed graphically to determine if they fell within the normality plots and were not themselves an outlier. Models using imputed data were re-run and compared with models using median values to see if they significantly influenced the objective function. Although small differences, of no less than 1.6 were observed, these were not significantly different and demonstrate the MI data could be utilised in the input data.

#### *5.2.2.4 Base Model*

The population PK analysis for the data set was performed by using NONMEM with the subroutine ADVAN2, TRANS2. The first order conditional estimation with interaction (FOCEI) method was used to estimate parameters.

The models were parameterised using clearances and volume of distribution and absorption constants using the PREDPP subroutine supplied in NONMEM. Inter-subject variability (ISV) of the pharmacokinetic parameters was modelled assuming a log-normal distribution, as follows:

$$\theta_i = \theta_{TV} \cdot \text{EXP}(\eta_i)$$

Where  $\theta_i$  is the estimated parameter value for individual  $i$ ,  $\theta_{TV}$  represents the population's typical value for the corresponding parameter. Initial values for parameters were chosen based on previous studies, as displayed in table 1.  $\eta_i$  is the deviation of  $\theta_i$  from  $\theta_{TV}$  known as the between subject variability (BSV). The  $\eta$  random effects were assumed to be independent and symmetrically distributed with zero mean and variance  $\omega^2$ , which represents the ISV of the parameter. The magnitude of ISV was expressed as coefficient of variation (%CV). A combined proportional-additive error model was tested to explain the residual variability (RV) of untransformed data. The error model is as follows:

$$Y = F + F * \text{ERR}(1) + \text{ERR}(2)$$

$$(1) 0.09 (30\%)$$

$$(2) 100 (\text{ng/ml})$$

$$\ln C_{ij} = \ln C_{\text{pred},ij} + \epsilon_{ij}$$

where  $C_{ij}$  and  $C_{\text{pred},ij}$  represent the  $j$ th observed and model predicted concentrations, respectively, for individual  $i$  and  $\epsilon_{ij}$  denotes the additive residual random error for individual  $i$  and observation  $j$ . The  $\epsilon$  random effects were assumed to be independent and symmetrically distributed with mean of zero and variance  $\sigma^2$ . Model selection decisions were based on a number of different criteria, including objective function value (OFV), condition number, visual examination of index plots, the precision of the parameter estimates (%RSE) and the reductions in both ISV and RV.

NONMEM minimizes  $-2\log$  likelihood as the OFV which maximises the likelihood value (Beal and Sheiner, 1980). With regard to NONMEM, the likelihood is a statistical answer to the question: If the model was true given the present values parameters, how likely would the predicted values have been observed? Therefore a useful model has predicted observations that are quite likely. Conversely a poor model would produce observations that are not likely and is not adequate to describe the data. The distribution of  $-2 \log$  follows a  $\chi^2$  distribution with the degrees of freedom being the difference in the number of

parameters. Once a base model was defined, its robustness was assessed before implementing covariates into the model. This was achieved through changing the model parameters.

#### 5.2.2.5 Univariate analysis

Once a base model can be identified, the possible influence of covariates on the estimated pharmacokinetic parameters and inter-individual variability can be assessed. There were many covariates available for analysis; however, we chose to examine covariates, which were predicted to have an impact on the estimated parameters based on the available data in the literature and the physiochemical properties of metformin. Graphical analysis of the individual parameter estimate (CL) versus covariates was evaluated to help identify possible covariate relationships.

Categorical covariates included in the analysis were sex (female or male). The continuous covariates to be analysed were age, body weight (WT), height (HT), body mass index (BMI), serum urea (UREA), serum creatinine (CREAT), estimated creatinine clearance (CL<sub>CR</sub>), and glomerular filtration rate (GFR). BMI, GFR and CL<sub>CR</sub> were calculated as follows:

$$\text{BMI} = \text{WT} / \text{HT}^2$$

$$\text{GFR} = 186 * ((\text{CREAT} / 88.4)^{-1.154}) * (\text{AGE}^{-0.203}) * \text{SEX}$$

(If female then SEX=0.742, if male then SEX=1)

$$\text{CLCR was calculated using the Cockcroft-Gault equation} = (((140 - \text{AGE}) * \text{WT}) / \text{CREAT}) * \text{SEX}$$

(If female then SEX=1, if male then SEX=1.2)

The covariates were included in the model building process through the forward addition procedure. All continuous covariates were centred around the median meaning the population estimates represent those of an average patient.

Centring the covariate around the mean assumes the data is within normal distribution. Each covariate model was tested using linear, power and exponential functions using the following equations:

$$\theta_i = TVCL \cdot EXP(\eta_i) \text{ where,}$$

$$\text{Linear:} \quad TVCL = \theta_{TV} + \theta_{COV} \cdot (TV_{COV} - \bar{x}_{COV})$$

$$\text{Power:} \quad TVCL = \theta_{TV} \cdot \theta_{COV} \cdot (TV_{COV} - \bar{x}_{COV})$$

$$\text{Exponential:} \quad TVCL = \theta_{TV} \cdot (TV_{COV} / \bar{x}_{COV})^{\theta_{COV}}$$

Where  $\theta_i$  is the estimated parameter value for individual  $i$ ,  $\theta_{TV}$  is the typical value for clearance of an individual with the typical value of the covariate value ( $TV_{COV}$ ) centred around the mean ( $\bar{x}_{COV}$ ) and  $\theta_{COV}$  represents a factor describing the influence of the covariate. Initial  $\theta_{COV}$  values were obtained from corresponding regression line equations through plotting the estimated parameter values vs the covariate.

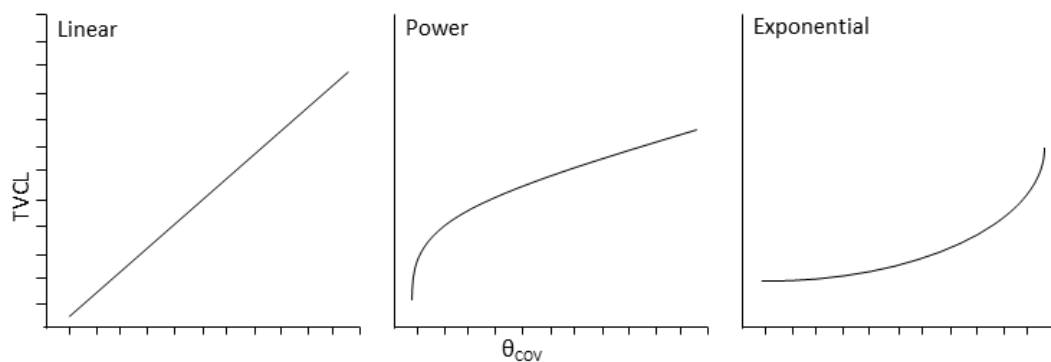


**Figure 5.1. Schematic representation of effect models**

Schematic representation of the three models for continuous covariates with the typical value of the parameter, clearance, vs the covariate  $\theta_{COV}$ .

The binary covariate, gender, was modelled using the following relationship:

$$\theta_i = \text{TVCL} \cdot \text{EXP where:}$$

if sex is equal to 0, TVCL =  $x$

if sex is equal to 1, TVCL =  $y$

where subjects coded with 0 (female) TVCL is equal to the predefined typical value of  $x$  and with 1 (male) TVCL is equal to the predefined typical value of  $y$ .

#### 5.2.2.6 Genetic covariates

For modelling purposes, *SLC22A1* and *SLC22A2* genetic variants were labelled using two methods. Firstly, variants were labelled to conform to a dominant model (wild-type vs heterozygous + homozygous) as 0 and 1, respectively. Secondly, SNPs were labelled into three groups, based on the genotype, wild-type, heterozygous and homozygous as 0, 1 and 2 respectively (recessive/additive model). We decided not to include a recessive model for all the included variants, as most variants are heterozygous with low number of homozygous patients for comparison in a model. Additionally any significant change in OFV between groups will be observed in the multi-comparison model (WT vs Het vs Hom). The MAF for inclusion of SNPs was 0.05.

The variants were modelled using a template used for modelling gender:

$$\theta_i = \text{TVCL} \cdot \text{EXP where:}$$

if SNP1 is equal to 0, TVCL =  $x$

if SNP2 is equal to 1, TVCL =  $y$

where subjects coded with 0 (wild-type) TVCL is equal to the predefined typical value of  $x$  and with 1 (heterozygous+homozygous) TVCL is equal to the predefined typical value of  $y$ . As we could only estimate individual CL values we firstly included SNPs from *SLC22A2* (OCT2) which is expressed in the kidney impacting on metformin clearance. We however included variants from OCT1 to explore if they would have an impact on the OFV.

Typical values of  $x$  and  $y$  were initially estimated using information cited in the literature to whether a particular variant would increase or decrease transport function and thus influence the estimation of clearance. For example, rs316019 SNP in *SLC22A2* is predicted to decrease transport function and thus would lead to a decrease in metformin clearance. The typical values of  $x$  and  $y$  were modelled in two ways; as a fraction (0.5 =50%, clearance could be decreased by 50%), or as an integer.

#### 5.2.2.7 Haplotypes

A number of SNPs and variants, as described in chapter 3, are in linkage disequilibrium, Figure 3.4. In population genetics, linkage disequilibrium is the non-random association of alleles at two or more loci. Consequently an individual will express the same haplotype for two or more SNPs.

We also ran another model using a haplotype containing the p.R61C SNPs and p.M420del. These two were chosen as these SNPs were in complete LD with other variants expressed in *SLC22A1* (p.R61C is in LD with p.L160F, p.M408V; p.M420del is in LD with p.M408V). This resulted in 4 groups included in the p.M420del/R61C model; WT/WT, V/WT, WT/V and V/V where WT=wild-type and V= variant (either heterozygous or homozygous for the variant respectively).

We also grouped patients into patients carrying an nsSNP (SNP encoding amino acid substitutions) and grouped them vs wild-type.

#### 5.2.2.8 Multivariate analysis

Before employing multiple covariates in to model building, significant covariates pairs were assessed for multicollinearity, (Appendix Table A5.1). Individual scatter plots of covariates pairs were examined. Traditionally the advice for multivariate analysis is not to use covariates that present multicollinearity, but for the purposes of discussion, we used all the covariates for model building with the knowledge of multicollinearity.

Covariates reducing the OFV by >6.63 points were chosen for multivariate analysis which were; urea, age, CL<sub>CR</sub> and creatinine. A forward inclusion step was implemented using the covariate first with the biggest change; urea. Therefore the OFV for base + urea (2937.38) was used as a starting value.

### 5.2.3 Model Selection & Evaluation

The decision for inclusion of a covariate in a model was made based on a combination of statistical significance (change in OFV), biological mechanistic plausibility and the clinical relevance of the relationship. Model discrimination was based as a change in the objective function values (OFV), the statistic proportional to minus twice the log likelihood of the data. In the forward addition step a decrease in the OFV of 6.63 was considered statistically significant (p-value <0.01) for the addition of one covariate.

The accuracy and robustness of the final population model were evaluated using visual predictive checks. The predicted metformin estimates for 250 data sets at time points at hourly intervals (from 0.5 to 9.5 hour) were generated from the parameters and variances for both the base model and the final model for comparative analysis. The 90% prediction intervals (5<sup>th</sup> percentile, median and 95<sup>th</sup> percentile) of simulated metformin concentrations corresponding to the observed values were calculated and plotted for comparison with observed values.

## 5.3 Results

### 5.3.1 Base model

The data were best represented using a 1-compartment model with first-order absorption and elimination from a central compartment as implemented in NONMEM using its ADVAN2 TRAN2 subroutine. The estimated structural model parameters included absorption rate constant ( $K_a$ ), volume of distribution ( $V/F$ ) and clearance ( $CL/F$ ) where  $F$  is oral bioavailability. The data did not support ISV on  $K_a$  and  $V$  as characterised by poor precision of the parameter estimates and inability to converge successfully. Furthermore, the model fixing these parameters did not significantly increase either the OFV. The normality tests suggested that the raw metformin concentrations were normally distributed. Transforming the data (SQRT) depicts the data is within the normal distribution. However transforming the data did not influence the base model estimated parameters or OFV. Therefore data was left untransformed for analysis. Initial estimates were obtained from previous models in the literature with similar population characteristics. The control stream for the base model can be viewed in the appendix.

The population base model  $CL/F$  was 57.2 (L/h), RSE 6.8%,  $V/F$  was 391 (L), RSE 23% and  $K_a$  0.605 ( $h^{-1}$ ), RSE 26.7%. The OFV for the base model was 2971.879. Relative standard error for  $CL$  and  $K_a$  was 26.4% and 4.31% respectively whereas  $V$  was associated with a higher degree of uncertainty with 2061.4%. The ISV estimate for  $CL$  was 52%.

All base model parameters were changed in order to determine if the model was stable. The OFV did not change significantly ( $\Delta=0.001$ ) and parameter estimates remained unchanged indicative of a stable base model. In general, the diagnostic plots, (Figure 5.2), showed an acceptable model fit to the observed data. The individual-predicted concentrations (IPRED) versus observed metformin concentrations exhibited a good correlation ( $r^2=0.8954$ ) but the population-predicted (PRED) showed poor fitness ( $r^2=0.221$ ) indicating that covariates may increase the fitness. As illustrated, the predicted metformin concentrations did not exceed 2700 ng/mL despite a number of observed concentrations

exceeding this level. The distribution of the weighted residual plot values (Figure 5.2 C) were around zero and relatively symmetric across the range for the predicted concentrations although peak WRES values were overestimated in a few individuals with low predicted metformin concentrations. Examples of individual patient plots for comparison of observed, IPRED and PRED illustrating good fit and poor fit are displayed in Figure 5.3. Once a base model was defined robustness was tested before implementing covariates into the model.

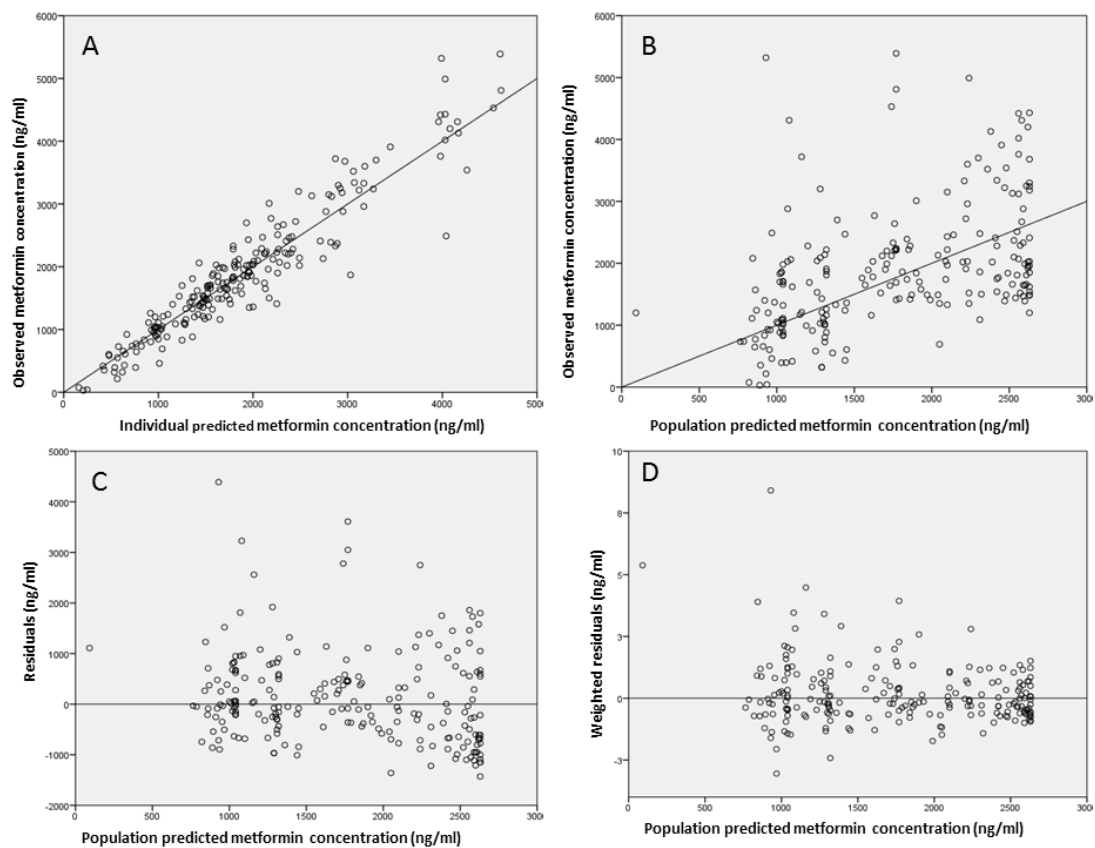


**Figure 5.2. Goodness of fit plots for base model**

[A] Individual predicted concentration versus observed concentration,  $R^2 = 0.8954$  [B] Population predicted concentration versus observed concentration.  $R^2 = 0.221$ . The solid lines are lines of identity; a model which is representative of the data will show points as close to the line as possible. Population predicted shows poor goodness of fit due to variability in the population, which may be resolved by including covariates into the model. [C] and [D] Conditional residual plot and weighted residual (respectively) plot for the base model, these display any unaccounted heterogeneity within the data.

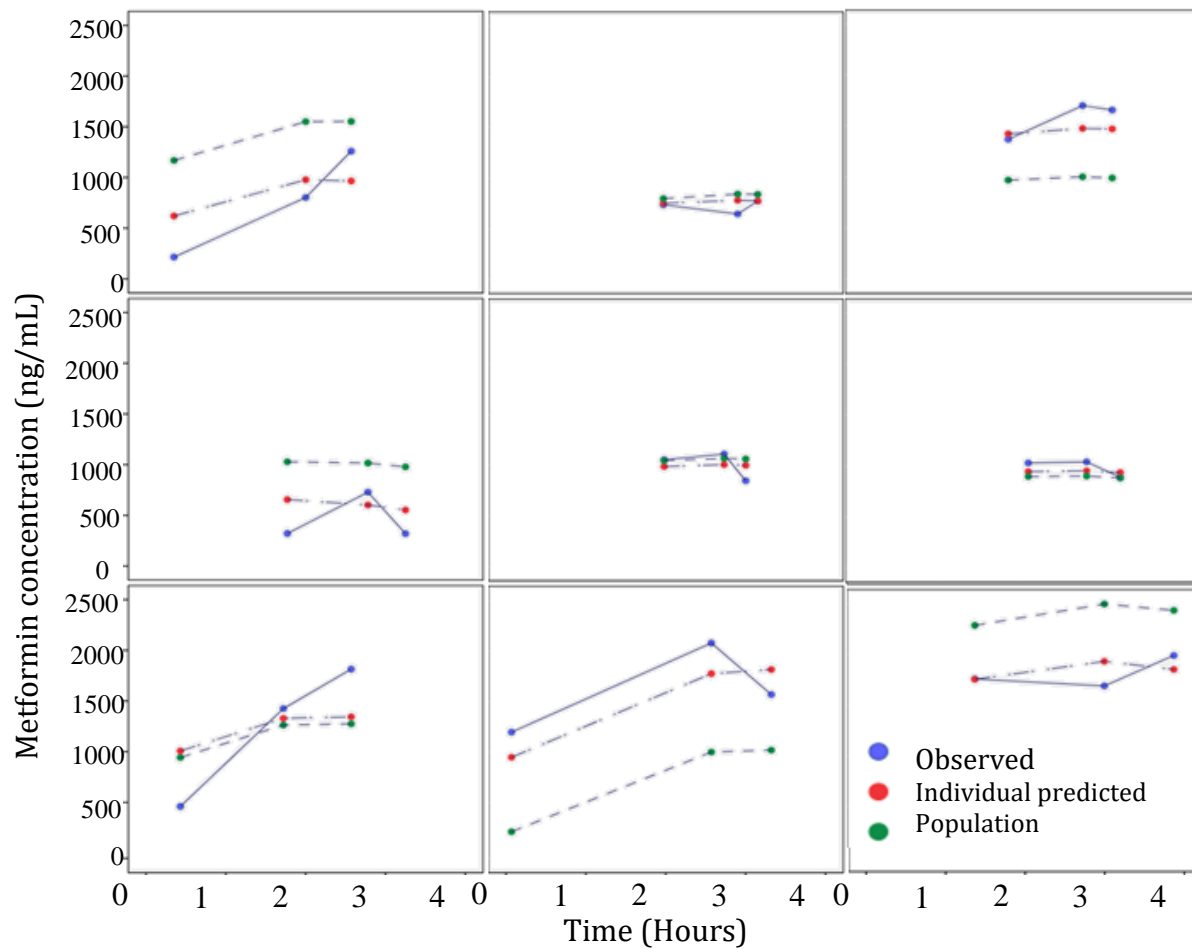


**Figure 5.3. Individual PK patient estimations examples**

This illustrates the individual predicted model gives better estimates than the population predicted. Both individual and population predicted have parallel values.

### 5.3.2 Uni-covariate modelling

As metformin CL was the only population PK parameter that could be estimated, covariates were included in the model which could potentially impact kidney function or are related to metformin pharmacokinetics. The univariate analysis used a forward addition stepwise inclusion procedure. A decrease of 6.63 points in the OFV was considered statistically significant (p-value <0.01).

Each covariate using the three model relationships produced very similar OFVs. Model relationships were chosen based on the parameter estimates, standard error and model error, table 5.3.

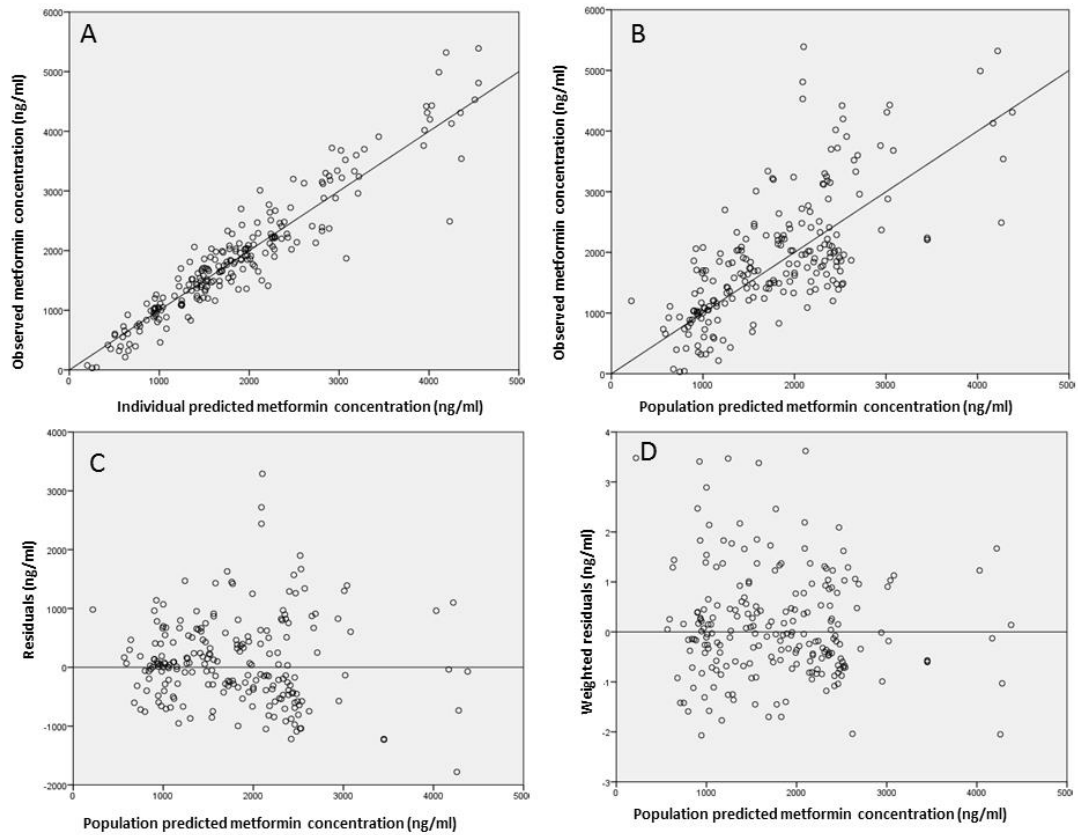
**Table 5.3. Univariate covariate impact on OFV.**

Model	Relationship	OFV	OFV $\Delta$	p value
Base	-	2971.879	-	-
Base + Urea	Linear	2937.38	34.50	<0.00001
Base + CL <sub>CR</sub>	Exponential	2951.66	20.22	<0.0001
Base + Age	Exponential	2957.536	14.34	<0.0002
Base + Creatinine	Linear	2961.546	10.33	<0.0020
Base + rs113569197	Categorical	2963.293	8.59	<0.004
Base + GFR	Exponential	2965.983	5.90	<0.020
Base + Albumin	Exponential	2966.22	5.66	<0.020
Base + BMI	Linear	2971.182	0.70	<0.45
Base + Lactate	Linear	2971.182	0.70	<0.45
Base + LBW	Linear	2971.410	0.47	<0.65
Base + Weight	Exponential	2971.639	0.24	<0.65
Base + Sex	Categorical	2971.811	0.07	<0.80
Base + Height	Linear	2971.832	0.05	<0.85
Base + IBW	Linear	2971.861	0.02	<0.90
Base + Length of treatment	Linear	2991.583	19.7 <sup>a</sup>	-

Covariates above the dotted line displayed reduced the OFV by >6.63 points (p-value <0.01) and are considered significant descriptors of metformin clearance. <sup>a</sup> This covariate increased the OFV, thus is not significant.

Urea was shown to be the best descriptor for clearance. The ISV estimate for CL in the base model with the inclusion of urea as a covariate (base+urea) was 39.5%. A more detailed summary of the base+urea model is presented in Table 5.4. The goodness of fit plots for the base model show a good correlation suggesting that the resulting model fits the observed data well, (Figure 5.4).

Figure 5.4. Goodness of fit plots for urea model.



[A] Individual predicted concentration versus observed concentration,  $R^2 = 0.8927$  [B] Population predicted concentration versus observed concentration.  $R^2 = 0.4903$ . Population predicted shows improved goodness of fit as serum urea levels have explained some variability in the population. [C] and [D] Conditional residual plot and weighted residual (respectively) plot for the base model, these display any unaccounted heterogeneity within the data.

Only one genetic variant, rs113569197 in *SLC22A1*, significantly reduced the OFV. All other genetic variants, haplotypes and grouped variants did not significantly impact the OFV, (Table 5.5). rs113569197 reduced the OFV by 8.59 points equivalent to a p value of <0.004. Further analysis revealed the recessive model, but not the dominant model significantly reduced the OFV ( $\Delta$  OFV 8.22).

**Table 5.5. Genetic variants impact on OFV in univariate modelling**

	Variant included in base model	$\Delta$ OFV (+/+, +/-, -/-)	$\Delta$ OFV (Dominant)	$\Delta$ OFV (Recessive)
SLC22A1 (OCT1)	rs12208357	N/A	0.730	-
	rs683369	1.562	0.598	0.553
	rs45584532 <sup>a</sup>	0.319	0.224	-
	rs628031	0.970	0.620	0.964
	rs72552763	3.896	2.626	-
	rs113569197	8.588	1.684	8.220
	rs9457843	1.762	0.463	-
	rs622591	2.036	0.064	1.997
SLC22A2 (OCT12)	rs3127573	2.029	1.708	-
	rs316023	0.229	0.286	0.155
	rs34129302	2.088	1.746	-
	rs624249	1.358	1.166	0.556
	rs2774230	1.843	1.725	0.001
	rs316019	0.417	0.417	-
	rs2279463	0.639	0.068	-
	rs316003	0.846	0.039	0.848
	rs3127594 <sup>b</sup>	2.610	2.294	-
	rs2450975	0.850	0.102	0.842
	rs694812	0.900	0.900	-

Summary of genetic variants as covariates on the OFV. MAF >5%. SNPs which are in linkage disequilibrium; <sup>a</sup> in LD with rs7762846, <sup>b</sup> in LD rs3103353, rs3127593 and rs3127592. Dominant model, homozygous variant (-/-) + heterozygous (+/-) vs wild-type (+/+). Recessive model, wild-type (+/+) + heterozygous (+/-) vs homozygous (-/-).

To elucidate the effect of the rs113569197 on metformin clearance a plot was produced revealing the patients with the WT genotype had a significantly increased metformin clearance when compared with the other genotypes, figure 5.5. The WT genotype exhibited a significant increase when compared to heterozygous and homozygous insertion genotypes (p<0.03). There was no significant difference in metformin clearance between homozygous insertion and the heterozygote group (p=0.929).

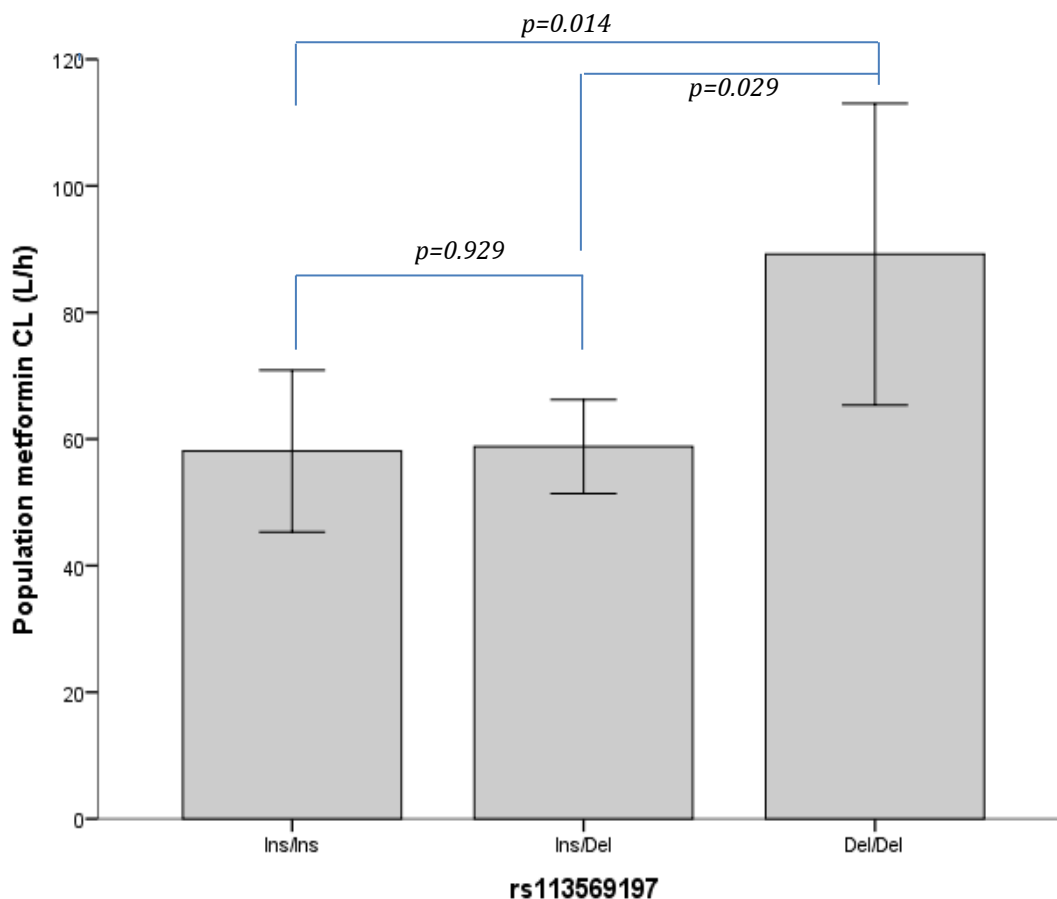


**Figure 5.5. rs113569197 variant effect on metformin clearance.**

Estimated population metformin clearance between rs113569197 genotypes. Homozygous deletion exhibited a significant increase in metformin clearance. Non-parametric tests were used; Kruskal-Wallis  $p = 0.038$  between the three groups and Mann-Whitney for analysis between two groups.

### 5.3.3 Multivariate analysis

Covariates reducing the OFV by  $>6.63$  points were chosen for multivariate analysis, which were; urea, age,  $CL_{CR}$  and creatinine. A forward inclusion step was implemented using the covariate first with the biggest change; urea. Therefore the OFV for base + urea (2937.38) was used as a starting value. However, we also used base +  $CL_{CR}$  as a second univariate model for model building.

In the forward addition step, a more stringent criterion was used to avoid any possible false-positives or artefacts; with a decrease in the MOFV of 10.60 was

considered statistically significant ( $p$ -value  $< 0.005$ ) for addition of two parameters to the model.

**Table 5.6. Multivariate impact on the base+urea/ $CL_{CR}$  models OFV.**

Model	Relationship	OFV	OFV $\Delta$	p value
Base + urea	Linear	2937.38	-	-
Base + urea + age	Linear	2931.188	6.19	$<0.05$
Base + urea + rs113569197	Power	2932.522	4.856	$<0.09$
Base + urea + $CL_{CR}$	Power	2934.934	2.444	$<0.3$
Base + urea + creatinine	Power	2935.917	1.461	$<0.5$
Base + $CL_{CR}$	Power	2952.73	-	-
Base + $CL_{CR}$ + rs113569197	Power	2946.11	6.621	$<0.04$
Base + $CL_{CR}$ + age	Power	2951.66	1.069	$<0.6$
Base + $CL_{CR}$ + creatinine	Power	2950.46	2.269	$<0.35$

Two models (urea and  $CL_{CR}$ ) were used for multivariate analysis. In comparison to the two univariate models the addition of other covariates did not significantly change the OFV.

The multivariate analysis showed the addition of other covariates to the models did not significantly decrease the OFV by 10.6 points and therefore did not explain more variability than the univariate models. The inclusion of age in the base + urea model decreased the OFV more than other covariates but was not significant. Similarly, the addition of the rs113569197 variant in the base + urea +  $CL_{CR}$  model reduced the OFV the most, but was not significant. Table 5.4 displays a detailed summary of base+urea and base+ $CL_{CR}$  models.

### 5.3.4 Model evaluation

Two hundred and fifty simulations for each time point were acquired. The mean parameter estimates resulting from the simulation analysis were very similar to the population estimates of the final model and were within the 95% confidence intervals. These results indicate that the model was stable and robust. Figure 5.6 shows the results of the visual predictive check for metformin plasma concentrations vs time. The final model adequately described the observed concentrations.

**Table 5.4. Detailed summary of the two top models**

Model	OFV	Relationship	OFV Δ	Random effects			BSV		Error model			Condition number	Shrinkage
				Parameter	Estimate	RSE (%)	%	RSE		RSE			
Base	2971.879	-	-	CL	57.2	6.79	51.96	1.24	Prop	16.82	23.57	-	<17%
				V	391	22.96	-	Add	169.12	47.55			
				Ka	0.605	26.70	-						
Base + CL <sub>CR</sub>	2951.66	Exponential	20.219	CL	55.8	3.41	43.82	23.49	Prop	16.40	24.39	18.89	<17%
				V	416	2.44	-	Add	182.48	44.14			
				Ka	0.615	68.99	-						
Base + Urea	2965.983	Linear	34.501	CL	62	5.73	39.50	22.05	Prop	16.43	23.33	15.85	<17%
				V	396	22.80	-	Add	182.76	42.81			
				Ka	0.645	26.20	-						

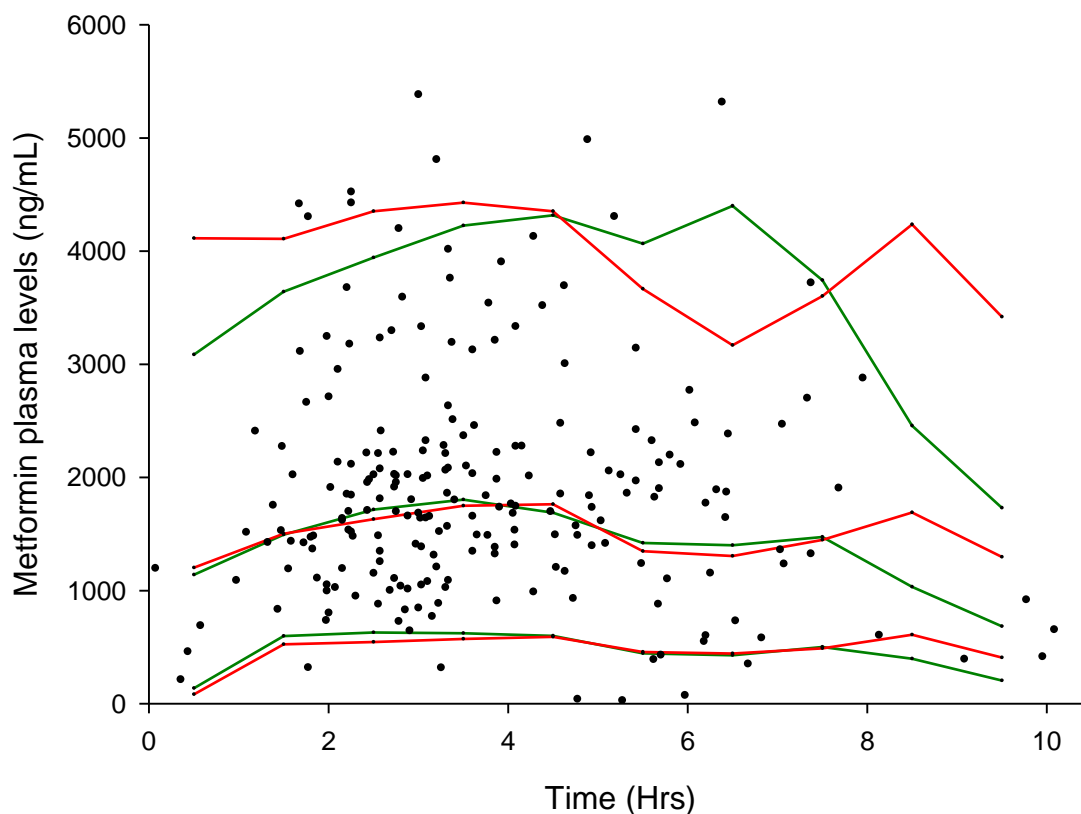


**Figure 5.6. Simulated concentration-time profile from the final base+urea model.**

Black circles are the observed metformin time profiles of the 75 T2DM patients. The middle green line represents the median values of the 250 simulated values. The top and bottom green line represents the 95th and 5th percentile respectively. The top, middle and bottom red lines represent the 90th, median and 5th percentile for the base model respectively.

## 5.4 Discussion

The quantified metformin plasma levels from Chapter 2 was used successfully used in a PopPK model for estimating the metformin clearance in T2DM patients. The 100-fold difference observed in metformin plasma concentrations between patients receiving 0.5-3 g/day is consistent with Christensen et al who reported 80-fold variability in those using 2.0 g a day (Christensen et al., 2011). They suggest that the activity and genotype of the organic cation transporter; OCT1, affects the pharmacokinetics of metformin and thus the observed variability. In this population, the metformin plasma concentration-time profile

does not exhibit a usual form, where a clear  $T_{\max}$  or  $C_{\max}$  is observed. This is primarily due to the sparse number of samples per patient, whereas the majority of PK studies use a large number of samples ( $n > 3/\text{patient}$ ) over a wide time period as shown in table 5.1. Unfortunately, the majority of the metformin samples acquired per patient were collected within a relatively narrow time-frame, (see Appendix Figure A5.1). This may reflect why metformin plasma levels did not dramatically change within a subject and thus a clear population  $T_{\max}$  or  $C_{\max}$  could not be observed. However, we assume patients are at steady-state in having received metformin for at least 3 months with a mean duration of metformin treatment of 8.05 years and no 'wash-out' period was employed before sample collection. This population are all T2DM patients receiving a number of medications for comorbidities associated with T2DM such as hypertension and dyslipidaemia. Concomitant medications are well known to influence the PK profile of drugs (Ding et al., 2014). This with a number of other cofounding factors can affect the PK of metformin, which may influence the concentration-time profile of metformin.

A major limitation to the PK modelling reported here is the data itself. Although population PK modelling can use sparse data the manner in which the samples were collected and trial designed were not desirable for PopPK modelling. Traditionally PK modelling is performed in order to plan clinical trials and inform which patients to recruit and fundamentally inform and steer how a clinical trial is designed, particularly when in sample collection. This trial was firstly designed in 2005 when statistical methodology for the field of investigating the effect of genetic associations on pharmacokinetics was a developing and emerging practise. There was no gold standard or consensus as to which was the most effective method. The available methodologies available were not sufficient to deal with the nature and biological complexities of genetic influences on drug's PK properties. Therefore, strict guidelines on patient recruitment time sampling and trial design were not implemented in order to gain the most valuable information that can be acquired from PopPK studies using the data.

Due to the small sample size and available data, clearance (CL) estimates for population and individual parameters were acquired, whereas the population V and  $K_a$  parameters could only be estimated. The main covariates that reduced the OFV for CL, as expected, were all related to kidney function. Surprisingly although related to renal function, GFR did not significantly decrease the OFV (OFV  $\Delta = 5.90$ ,  $P < 0.02$ ). As GFR takes into account gender differences, which did not significantly reduce the OFV, this may explain why GFR did not significantly reduce OFV.

The results show serum urea levels to be the best descriptor for clearance. In comparison to the base model, base + urea decreased the ISV for CL from 52% to 39.5%. Therefore, urea, as a covariate, explains 12.5% of the CL variability in this population. In comparison,  $CL_{CR}$  ISV for CL was 43.8%, therefore explaining only 7.18% of the variability. The population base model showed a poor fit to the observed data, in contrast to base + urea model. This illustrates why serum urea levels are explaining some of the variability observed in the data.

The population PK parameter estimates obtained from modelling for CL, V and  $K_a$  are comparable to previous results reported in the literature as summarised in table 5.1. These studies used similar population demographic characteristics, Bardin et al., 2012 used 105 T2DM Caucasian patients and obtained similar results with serum creatinine and age being descriptors of metformin CL. Conversely, they also reported lean body weight as a significant descriptor whereas our study did not find body weight explained the variability in CL. Weight in our study was a poor size descriptor because it included a great proportion of fat mass, in which metformin is not expected to distribute. Therefore, lean body weight should have been a better descriptor, but was marginally better than total body weight.

The inclusion of genetic variants as covariates in the modelling, only presented one variant as a significant descriptor of metformin CL. The variant,

rs113569197, as described in chapter 2, is a TGGTAAGT insertion located across a splice donor site SDS in *SLC22A1*. The variant has previously been associated with the presence of metformin-induced gastrointestinal side effects, and found to promote a premature stop codon in OCT1 possibly leading to decreased transporter expression and thus decreased activity (Grinfeld et al., 2013, Tarasova et al., 2012).

As rs113569197 is located in *SLC22A1* (OCT1), which is primarily expressed in the liver, one would assume the variant would not impact the clearance of metformin, in the kidneys. However, variants in *SLC22A2* (OCT2) which are expressed in the kidney could directly impact and have a greater influence on metformin clearance (Leabman et al., 2002).

Conversely, one can hypothesise that individuals with genetic variants reducing OCT1 transport function and or expression, could decrease hepatocellular uptake, which may lead to greater metformin plasma concentrations and increased metformin renal clearance. The literature seems to support the latter hypothesis where a relationship between OCT1 reduced-function genotypes and metformin renal clearance has been shown (Tzvetkov et al., 2009). Additionally Shu et al observed higher metformin AUC and  $C_{max}$  in subjects who expressed reduced-function OCT1 alleles (Shu et al., 2007).

Therefore, the relationship between the rs113569197 variant and predicted metformin clearance is biologically plausible. However, further analysis between predicted metformin clearance and rs113569197 genotypes revealed the reduced-function allele, the TGGTAAGT insertion, was associated with decreased metformin clearance, contradicting the hypothesis that reduced-function alleles in OCT1 lead to increased metformin clearance. Additionally the dominant model for rs113569197 did not significantly change the OFV and its inclusion in the multivariate model (Table 5.6) did not significantly change the

OFV. This collectively suggests the significance of rs113569197 on the OFV is most likely an artefact.

Although there are racial differences in the frequency of mutant alleles, no exclusion of subjects was made on the basis of their ethnicity. Furthermore, since the outcome measures are primarily pharmacokinetic and related to a specific set of genotypes, the effect of ethnicity is negligible. Haplotypeanalysis based in LD observations did not result in a significant decrease in the OFV.

We included covariates into the multivariate model knowing they exhibited a high correlation, e.g. urea and creatinine ( $r^2 = 0.453$ ), and therefore the inclusion of just one parameter in the model would be justified as the decrease in OFV may be driven and explained by the inclusion of one parameter. It has been demonstrated that the inclusion of covariates exhibiting multi-collinearity ( $r^2 > 0.5$ ) in NONMEM may reduce the accuracy of the parameter estimates themselves and estimates may be inflated due to ill-conditioning (Bonate, 1999). However, we conducted multi-variate modelling with variates exhibiting high collinearity as we had few covariates to implement in the model. The univariate model with the biggest decrease in OFV was used as a starting point. However, we used two; urea and  $CL_{CR}$ . The latter is regarded as the gold standard covariate as a predictor for renal function and is often used in PopPK clearance models (Hong et al., 2008, Chae et al., 2012). The British National Formulary (Joint Formulary Committee, 2014) states clinicians should use metformin with caution with patients displaying a GFR of  $<30$  mL/min. In contrary, our results suggest in this population, urea is a greater descriptor of metformin clearance over  $CL_{CR}$ .

Once a stable and robust PK model has been established, the next stage would be to use the PK model for developing a PD model. PD modelling would be used to determine any associations between serum vitamin B<sub>12</sub> levels and any covariates.

Two models would be suitable for PD modelling; urea and  $CL_{CR}$ . Urea as the best descriptor of metformin CL variability and  $CL_{CR}$  as it is commonly used as the gold standard in PKPD modelling for describing drug clearance variability. The two models are summarised below;

$$\theta_i = TVCL \cdot \text{EXP}(\eta_i) \text{ where,}$$

$$\text{Urea: } TVCL = \theta_{TV} \cdot \theta_{COV} \cdot (TV_{COV} - \bar{x}_{COV})$$

$$CL_{CR}: TVCL = \theta_{TV} \cdot (TV_{COV} / \bar{x}_{COV})^{\theta_{COV}}$$

Where  $\theta_i$  is the estimated parameter value for individual  $i$ ,  $\theta_{TV}$  is the typical value for clearance of an individual with the typical value of the covariate value ( $TV_{COV}$ ) centred around the mean ( $\bar{x}_{COV}$ ) and  $\theta_{COV}$  represents a factor describing the influence of the covariate. Initial  $\theta_{COV}$  values were obtained from corresponding regression line equations through plotting the estimated parameter values vs the covariate.

As a part of this work, the original aim was to characterise the relationship between the plasma pharmacokinetics of metformin and the levels of vitamin B<sub>12</sub>. Unfortunately, the data is unsuitable for PD modelling. We have one vitamin B<sub>12</sub> level per patient, post metformin dosage, and therefore are lacking a baseline (pre metformin) vitamin B<sub>12</sub> level. Vitamin B<sub>12</sub> levels do not dramatically change over a short period of time the shortest length of metformin treatment in this cohort, 3 months, was ample time for vitamin B<sub>12</sub> levels to change (de Jager et al., 2010). Therefore, we could assume the effect metformin has on vitamin B<sub>12</sub> levels would of reached a plateau. However, baseline vitamin B<sub>12</sub> level is essential in order to build a robust and stable PKPD model to draw to conclusions. Therefore, we could not produce a PKPD model using these data. One alternative to this problem is to use baseline vitamin B<sub>12</sub> levels from a T2DM population who are not on metformin therapy. However,

this data would be hard to acquire and the two populations would need to be similar in other demographic parameters.

In comparison to some published studies as summarised in table 5.1, this study reveals several strengths for PopPK modelling. This includes the inclusion of T2DM patients rather than healthy controls. Additionally these patients were prescribed multiple doses rather than a single dose. Traditionally for well-controlled PK studies the dose would preferably be uniform throughout the population. However, multiple doses are advantageous in PopPK modelling where a range of doses and plasma levels can be incorporated into a model to reflect a population receiving different doses. Urine samples from the patients used in this study would be beneficial to obtain renal metformin clearance data. This would clarify the impact of OCTs genetic polymorphisms on metformin clearance and disposition.

In summary, the data from this population was applied successfully to a population PK model, which showed urea as the best descriptor for estimated metformin clearance. Only one genetic variant in *SLC22A1*, rs113569197, was associated with metformin clearance in the univariate model but dropped out the multivariate model. This is therefore most likely to be an artefact. Other genetic variants in *SLC22A1* and *SLC22A2* did not significantly impact metformin clearance. Despite producing an acceptable PK model to take forward for PD modelling, the data available was not optimal and therefore could not be utilised effectively in a PD model to establish a link between metformin and vitamin B<sub>12</sub> levels. Chapter 6 will investigate the association between metformin dose/concentration and vitamin B<sub>12</sub> levels.

## **Chapter 6**

### **Investigation of factors influencing metformin induced vitamin B<sub>12</sub> deficiency**

## CONTENTS

<b>6.1 INTRODUCTION.....</b>	<b>173</b>
<b>6.2 MATERIALS &amp; METHODS.....</b>	<b>175</b>
6.2.1 STUDY SUBJECTS .....	175
6.2.2 METFORMIN PARAMETERS.....	175
6.2.4 ANALYTIC METHODS.....	175
6.2.4.1 <i>Determination of metformin plasma concentrations.....</i>	<i>175</i>
6.2.4.2 <i>Biochemistry Analytes.....</i>	<i>175</i>
6.2.4.3 <i>SLC22A1 &amp; SLC22A2 Gene sequencing.....</i>	<i>176</i>
6.2.5 STATISTICAL ANALYSIS .....	176
6.2.5.1 <i>Linear regression.....</i>	<i>176</i>
6.2.5.2 <i>Analysis of genetic covariates.....</i>	<i>177</i>
6.2.5.3 <i>Anthropometric estimations .....</i>	<i>177</i>
<b>6.3 RESULTS.....</b>	<b>178</b>
6.3.2 VITAMIN B <sub>12</sub> CONCENTRATIONS.....	178
6.3.3 EFFECT ON HAEMATOLOGICAL PARAMETERS.....	183
6.3.4 SERUM LACTATE.....	183
6.3.5 GENETIC VARIANTS.....	184
6.3.6 COMORBIDITIES & CONCOMITANT DRUG CLASSES.....	187
<b>6.4 DISCUSSION .....</b>	<b>187</b>

## 6.1 Introduction

Metformin is generally well-tolerated, with gastrointestinal intolerance being the commonest adverse effect. However, a common, potentially damaging and well documented complication of metformin therapy is vitamin B<sub>12</sub> deficiency (Anfossi et al., 2010). This is poorly recognised and not currently screened for or treated by the majority of physicians who prescribe metformin. Approximately 10-30% of patients with prolonged use of metformin develop vitamin B<sub>12</sub> deficiency (<200 pmol/L) (de Jager et al., 2010, Ting et al., 2006). Vitamin B<sub>12</sub> deficiency can cause a megaloblastic anaemia with associated symptoms of fatigue, shortness of breath and light-headedness. A more serious and irreversible effect of vitamin B<sub>12</sub> deficiency is peripheral neuropathy, a result of demyelination of axons in the peripheral nervous system. In the central nervous system, vitamin B<sub>12</sub> deficiency can cause sub-acute combined degeneration of the spinal cord (Bell, 2010). Low serum vitamin B<sub>12</sub> levels have also been associated with cognitive impairment (Moore et al., 2012) . This may be particularly important in patients with T2DM who have a higher incidence of dementia than the general population (Butterfield et al., 2014, Li et al., 2014). With the prevalence of vitamin B<sub>12</sub> deficiency and T2DM increasing with age (Guariguata et al., 2014, Food and Nutrition Board, 1998), it is therefore important to characterise vitamin B<sub>12</sub> levels in an aging population receiving metformin for the treatment of T2DM.

As data presented in Chapter 1 suggests, metformin dose and treatment duration are the most consistent risk factors for vitamin B<sub>12</sub> deficiency in patients with T2DM (de Jager et al., 2010, Ting et al., 2006). Early studies, which used the Schilling test to investigate how metformin causes B<sub>12</sub> deficiency (Berger et al., 1972, Tomkin, 1973), suggested that it was a result of vitamin B<sub>12</sub> malabsorption. Previous studies have demonstrated that metformin induces a positive charge to the surface of the ileal membrane, which would act to displace divalent cations such as calcium (Schafer, 1976). Therefore, metformin, by impairing calcium availability, interferes with the calcium-dependent

process of vitamin B<sub>12</sub> absorption. Although a complementary clinical study illustrated that metformin induced vitamin B<sub>12</sub> deficiency was reversed by dietary supplements of calcium carbonate (Bauman et al., 2000), there are no experimental reports to support this hypothesis. Interestingly, metformin's major site of distribution, the liver, stores 50% of the total body content of vitamin B<sub>12</sub> (Food and Nutrition Board, 1998). Additionally metformin's primary route of elimination, the kidneys, play a role in vitamin B<sub>12</sub> homeostasis (Birn, 2006). Thus, there is a possibility that systemic effects of metformin may also contribute to vitamin B<sub>12</sub> deficiency.

We also studied other parameters related to vitamin B<sub>12</sub>, such as folate, haemoglobin (Hb), haematocrit (HCT) and mean corpuscular volume (MCV). As described earlier in section 1.10.2, folate acts as an intermediate in the methionine synthase reaction where vitamin B<sub>12</sub> deficiency, can trap folate; known as the methyl-folate trap (Sauer and Wilmanns, 1977). Additionally folate supplementation can mask the underlying vitamin B<sub>12</sub> deficiency and its clinical consequences (Johnson, 2007). Both folate and vitamin B<sub>12</sub> deficiency can lead to anaemia. This can be through analysing such haematological parameters, such as Hb, HCT and MCV. More specifically macrocytic anaemia, characterised by increase in MCV and decrease in Hb and HCT are primarily caused by vitamin B<sub>12</sub> deficiency rather than iron deficiency (Aaron et al., 2005, Fishman et al., 2000).

This chapter, the relationship between metformin and vitamin B<sub>12</sub> is explored. It was hypothesised that, if the major mechanism by which metformin induces vitamin B<sub>12</sub> deficiency is through intestinal malabsorption rather than systemically, the dose may be a better predictor than serum metformin concentrations.

## 6.2 Materials & Methods

### 6.2.1 Study Subjects

Seventy-five T2DM patients, as described in Chapter 2 were recruited at the Royal Liverpool and Broadgreen University hospitals between 2005 and 2007. The protocol was reviewed and approved by the NHS Research Ethics Committee. Written consent was obtained from all subjects prior to their participation in the study.

### 6.2.2 Metformin parameters

Metformin was administered as described in Chapter 2, section 2.2.1.

### 6.2.4 Analytic methods

#### *6.2.4.1 Determination of metformin plasma concentrations*

Metformin was quantified using the HPLC-MS/MS method described earlier in chapter 4.

#### *6.2.4.2 Biochemistry Analytes*

Biochemistry and haematology analytes were quantified at the Royal Liverpool University hospital. For vitamin B<sub>12</sub> and folate quantification, serum was collected into plain tubes for clotting and transported immediately to the laboratory. Analysis was performed on an Access 2 immunoassay analyser using manufacturer's reagents and protocols (Beckman-Coulter Inc., Fullerton, CA). Based on previous literature vitamin B<sub>12</sub> deficiency was defined as vitamin B<sub>12</sub> serum levels <150 pmol/L (203 ng/L), with borderline deficiency defined as 150-220 pmol/L (203-298 ng/L) (Lindenbaum et al., 1990, de Jager et al., 2010).

Haematology and other biochemistry analytes were collected at the first time sample and analysed within 48 hours. Reference ranges for Hb for male and female were 133-167 and 118-148 g/L respectively; HCT were 39-50% and 36-44% respectively; MCV were 80-100 fL and lactate were 0.5-2.2 mmol/L.

#### 6.2.4.3 *SLC22A1 & SLC22A2 Gene sequencing*

*SLC22A1* and *SLC22A2* genes were sequenced as described in chapter 3. In brief, primers were designed manually to amplify and sequence all exons, including intron-exon boundaries plus up to 2 kb of 5' sequence to capture variants in nearby regulatory elements.

### 6.2.5 Statistical analysis

#### 6.2.5.1 *Linear regression*

In order to identify variables associated with vitamin B<sub>12</sub> levels linear regression analyses were applied using a two-step procedure. Firstly, each clinical covariate was tested for a significant association with vitamin B<sub>12</sub> in univariate analyses. To identify all potential covariates for inclusion in a multivariate model, variables with  $P < 0.1$  were considered to be sufficiently associated with the outcome variables and were retained for further model building. Secondly, a stepwise multivariate model was built using the enter method. Covariates deemed appropriate based on prior published work and biological plausibility with  $P < 0.1$  were included in the analyses. Associations with  $P < 0.05$  in multivariate analyses were considered significant. The same procedures were performed to estimate the impact of covariates influencing Hb, HCT, MCV, lactate and metformin plasma concentrations. All calculations were performed using SPSS 20.0 software (SPSS Inc., Chicago, IL, USA). Both untransformed and transformed ( $\log_{10}$ ) data for metformin plasma levels were used and compared for analysis. Transforming the data did not make an impact on significance between metformin plasma levels and outcome variables. See appendix Table A6.1.

Non-parametric Kruskal-Wallis tests were used to further investigate the association between grouped metformin daily doses and vitamin B<sub>12</sub> levels. Grouped metformin daily doses were defined as  $\leq 1000$  mg, low; 1500-2000 mg, medium and  $\geq 2500$ , high. Associations between paired categorical variables, including vitamin B<sub>12</sub> deficiency, metformin daily dose and anaemia status were determined with Fisher's exact test.  $P < 0.05$  was accepted as statistically

significant. Additionally grouped variables including comorbidities and concomitant drug classes were analysed using non-parametric tests as described above. Groups representing >10% of the population were used for analysis. Appendix Figure A6.1, and A6.2 display comorbidities and concomitant medications prevalence for this patient group.

#### *6.2.5.2 Analysis of genetic covariates*

*SLC22A1* and *SLC22A2* genes were sequenced as described in chapter 3. Due to the small sample size and additionally low frequency of variants expressed, only genetic variants with a MAF of >0.05, (see table 3.2 and 3.3) were included in the analysis. Although considered low, a MAF of >0.05 was chosen to increase the number of genetic variants in the analysis to determine if rare variants exhibit an effect on outcome variables.

Non-parametric tests were used to investigate associations between genotypes and continuous variables. For statistical purposes, genetic variants with three genotypes (wild-type, heterozygous and homozygous), were analysed using Kruskal-Wallis tests and those with two groups; (wild-type and heterozygous), were analysed using Mann-Whitney U tests. However, if one variant had a small group number ( $n \leq 5$ ), these were included in a dominant model (wild-type vs heterozygous + homozygous) and analysed using the Mann-Whitney U tests.

Probability *P* values were adjusted using multiple testing corrections in order to correct for the occurrence of false-positive results. The Bonferroni correction method was used for small numbers of comparisons in which the *p* value is divided by the number of statistical tests performed, ( $n=3$  groups,  $0.05/3 = 0.0167$ ).

#### *6.2.5.3 Anthropometric estimations*

In addition to body mass index, we explored related anthropometric variables. Ideal body weight (IBW) was estimated using the Devine formula (Pai and Paloucek, 2000); for males,  $IBW = 45.4 + 0.089 \times (\text{height (cm)} - 152.4) + 4.5$ , for females,  $45.4 + 0.089 \times (\text{height(cm)} - 152.4)$ . Lean body weight (LBW) was estimated using the following formulae (Hume, 1966); for men,  $LBW = (0.32810$

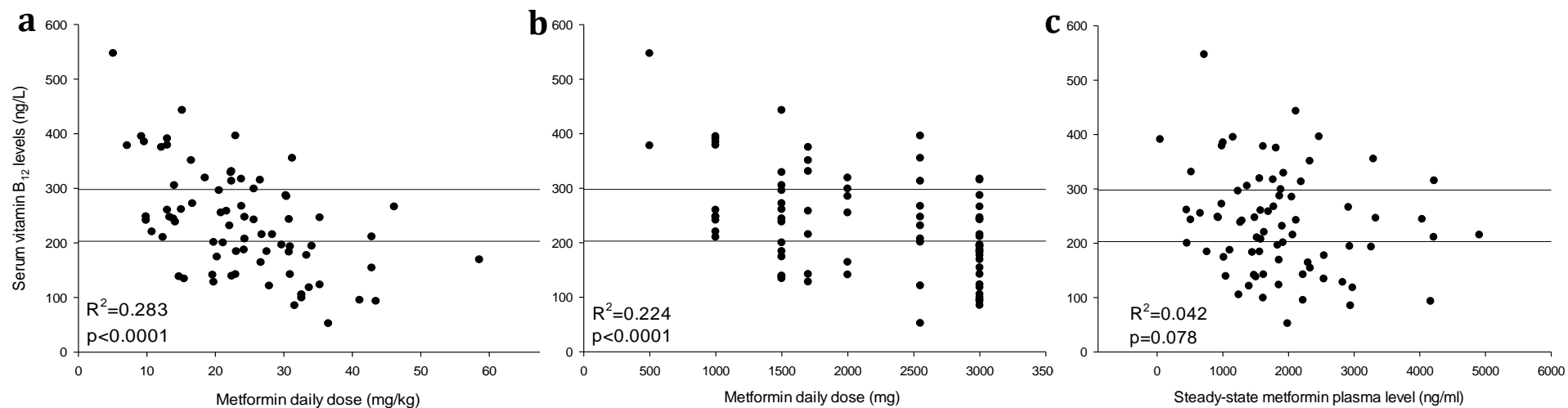
$\times \text{weight (kg)} + (0.33929 \times \text{height (cm)}) - 29.5336$ , for women,  $\text{LBW} = (0.29569 \times \text{weight (kg)} + (0.41813 \times \text{height (cm)}) - 43.2933$ . Body surface area (BSA) was calculated using the Dubois formula (Du Bois and Du Bois, 1916); surface area =  $\text{weight}^{0.425} \times \text{height}^{0.725} \times 0.007184$ , where height is in cm and surface area is in  $\text{m}^2$ .

## 6.3 Results

### 6.3.2 Vitamin B<sub>12</sub> concentrations

Thirty (40%) out of the 75 patients were classified as vitamin B<sub>12</sub> deficient, 26 (34.7%) were borderline deficient and 19 (25.3%) exhibited normal vitamin B<sub>12</sub> levels. Demographic and clinical variables were used in a linear regression analysis to estimate serum vitamin B<sub>12</sub> levels in T2DM patients. Univariate analysis identified that metformin related covariates and anthropometric measurements (with the exception of BMI and LBW) were all significantly associated with vitamin B<sub>12</sub> levels ( $P < 0.05$ ) (Table 6.1). The main predictors were metformin dose expressed as either daily dose or mg/kg of body weight ( $P < 0.001$ ) (Figure 6.1a,b). The final prediction model accounted for >34% of the variance in vitamin B<sub>12</sub> levels ( $R^2 = 0.345$ , Adjusted  $R^2 = 0.327$ ). Vitamin B<sub>12</sub> levels were primarily predicted by metformin dose expressed mg/kg of body weight and to a lesser extent by serum folate levels. The final regression model to estimate vitamin B<sub>12</sub> levels was  $317.992 + (5.02 \times \text{serum folate } (\mu\text{g/ml})) - (5.20 \times \text{mg/kg metformin})$  ( $p < 0.001$ ). The  $R^2$  value for this equation was higher than the  $R^2$  value for each individual covariate. Therefore, the combination of serum folate levels and metformin mg/kg of body weight produced a more reliable prediction of the individual covariates. Results of the multivariate linear regression analysis are shown in Table 6.2.

Figure 6.1. Associations between serum vitamin B12 levels and metformin parameters



Serum vitamin B<sub>12</sub> levels vs (a) daily dose metformin daily dose mg/kg of body weight; (b) daily dose metformin; and (c) steady-state metformin plasma levels. Normal vitamin B<sub>12</sub> levels (>298 ng/mL) are defined as values above the top horizontal line, vitamin B<sub>12</sub> deficient values (<203 ng/mL) are below the bottom horizontal line. Values between the two lines are defined as borderline vitamin B<sub>12</sub> deficiency (203-298 ng/mL).

**Table 6.1. Univariate linear regression analysis.**

Independent variables	Dependent variables													
	Vitamin B <sub>12</sub>		Folate		Haemoglobin		Haematocrit		Mean Corpuscular volume		Lactate		metformin plasma levels	
	R <sup>2</sup>	P value	R <sup>2</sup>	P value	R <sup>2</sup>	P value	R <sup>2</sup>	P value	R <sup>2</sup>	P value	R <sup>2</sup>	P value	R <sup>2</sup>	P value
<b>Demography</b>														
Age	0.001	0.772	0.005	0.55	<b>0.095</b>	<b>0.007</b>	<b>0.076</b>	<b>0.016</b>	-0.003	0.631	0.01	0.399	<b>0.091</b>	<b>0.009</b>
Height	<b>0.114</b>	<b>0.003</b>	-0.002	0.704	0.029	0.147	0.019	0.24	<b>0.117</b>	<b>0.003</b>	<0.001	0.965	-0.011	0.378
Weight	<b>0.058</b>	<b>0.038</b>	-0.008	0.446	<b>0.06</b>	<b>0.034</b>	0.049	0.057	<b>0.101</b>	<b>0.005</b>	0.01	0.406	-0.005	0.541
BMI	0.002	0.713	-0.009	0.425	0.034	0.113	0.032	0.127	0.018	0.257	0.013	0.342	<0.0001	0.859
IBW	<b>0.107</b>	<b>0.004</b>	-0.003	0.652	0.036	0.101	0.026	0.169	<b>0.109</b>	<b>0.004</b>	<0.0001	0.955	-0.006	0.5
LBW	0.043	0.076	-0.002	0.727	0.012	0.346	0.008	0.458	<b>0.09</b>	<b>0.009</b>	0.001	0.745	-0.024	0.18
BSA	<b>0.087</b>	<b>0.01</b>	-0.007	0.482	<b>0.057</b>	<b>0.04</b>	0.043	0.073	<b>0.128</b>	<b>0.002</b>	0.004	0.574	-0.009	0.419
<b>Biochemistry &amp; Haematology</b>														
Vitamin B <sub>12</sub>	-	-	0.041	0.082	0.006	0.494	0.003	0.626	0.018	0.254	-0.043	0.077	-0.042	0.078
Folate	0.041	0.082	-	-	-0.004	0.581	-0.005	0.529	-0.006	0.505	<0.0001	0.99	0.034	0.115
Lactate	-0.043	0.077	<0.0001	0.99	0.011	0.371	0.018	0.26	<0.001	0.943	-	-	<b>0.097</b>	<b>0.007</b>
Hb	0.006	0.494	-0.004	0.581	-	-	<b>0.978</b>	<b>&lt;0.0005</b>	<b>0.199</b>	<b>&lt;0.0005</b>	0.011	0.371	0.008	0.451
HCT	0.003	0.626	-0.005	0.529	<b>0.978</b>	<b>&lt;0.0005</b>	-	-	<b>0.168</b>	<b>&lt;0.0005</b>	0.018	0.26	0.003	0.636
MCV	0.018	0.254	-0.006	0.505	<b>0.199</b>	<b>&lt;0.0005</b>	<b>0.168</b>	<b>&lt;0.0005</b>	-	-	<0.001	0.943	-0.016	0.281
<b>Kidney function</b>														
Creatinine	0.041	0.08	0.005	0.534	-0.032	0.127	0.023	0.193	0.004	0.582	0.028	0.158	<b>0.08</b>	<b>0.014</b>
Urea	0.007	0.49	0.036	0.101	<b>0.073</b>	<b>0.019</b>	<b>0.051</b>	<b>0.05</b>	-0.004	0.579	0.017	0.271	<b>0.167</b>	<b>&lt;0.0005</b>
CL <sub>CR</sub>	<0.001	0.913	-0.023	0.194	<b>0.152</b>	<b>0.001</b>	<b>0.119</b>	<b>0.002</b>	0.041	0.08	-0.003	0.622	<b>-0.079</b>	<b>0.015</b>
GFR	-0.012	0.355	-0.021	0.218	<b>0.102</b>	<b>0.005</b>	<b>0.078</b>	<b>0.016</b>	0.004	0.597	-0.008	0.444	<b>0.065</b>	<b>0.027</b>

Significant values are shown in bold.

**Table 6.1. (continued) Univariate linear regression analysis.**

Independent variables	Dependent variables													
	Vitamin B <sub>12</sub>		Folate		Haemoglobin		Haematocrit		Mean Corpuscular volume		Lactate		metformin plasma levels	
	R <sup>2</sup>	P value	R <sup>2</sup>	P value	R <sup>2</sup>	P value	R <sup>2</sup>	P value	R <sup>2</sup>	P value	R <sup>2</sup>	P value	R <sup>2</sup>	P value
Liver function														
Albumin	<0.0001	0.961	0.01	0.384	<b>0.235</b>	<b>&lt;0.0005</b>	<b>0.235</b>	<b>&lt;0.0005</b>	<b>0.083</b>	<b>0.012</b>	-0.001	0.781	-0.001	0.845
AP	<0.0001	0.968	0.002	0.729	-0.015	0.289	-0.013	0.328	-0.046	0.065	0.036	0.104	0.001	0.743
GammaGT	0.023	0.196	-0.006	0.519	<0.0001	0.964	-0.001	0.788	0.009	0.413	0.028	0.155	-0.006	0.522
ALT	<0.0001	0.905	-0.023	0.196	<b>0.089</b>	<b>0.02</b>	<b>0.086</b>	<b>0.011</b>	0.009	0.43	0.023	0.194	-0.003	0.653
Bilirubin	0.009	0.413	0.028	0.152	0.003	0.647	0.002	0.682	<0.001	0.946	0.002	0.687	-0.031	0.131
Metformin variables														
Daily dose	<b>-0.224</b>	<b>&lt;0.001</b>	<0.0001	0.954	0.004	0.585	0.005	0.56	0.001	0.823	0.025	0.175	<b>0.18</b>	<b>0.001</b>
Trial dose	<b>-0.135</b>	<b>0.001</b>	0.004	0.571	0.003	0.638	0.003	0.643	-0.001	0.82	0.021	0.222	<b>0.178</b>	<b>0.001</b>
Cumulative dose	<b>-0.127</b>	<b>0.002</b>	-0.009	0.413	<0.0001	0.916	<0.0001	0.976	0.002	0.681	0.044	0.073	<b>0.118</b>	<b>0.003</b>
Dose (mg/kg)	<b>-0.283</b>	<b>&lt;0.001</b>	0.008	0.448	-0.004	0.577	-0.002	0.674	-0.023	0.198	0.016	0.275	<b>0.212</b>	<b>&lt;0.0005</b>
Plasma concentration	-0.042	0.078	0.034	0.115	0.008	0.451	0.003	0.636	-0.016	0.281	<b>0.097</b>	<b>0.007</b>	-	-
Length of T2DM	-0.003	0.644	-0.03	0.142	-0.049	0.057	-0.037	0.1	-0.004	0.611	0.021	0.213	0.051	0.052
Length of treatment	<b>-0.079</b>	<b>0.015</b>	-0.01	0.393	<0.0001	0.315	-0.009	0.41	-0.006	0.529	0.034	0.119	<b>0.107</b>	<b>0.004</b>

Significant values are shown in bold.

Increases in grouped metformin doses were negatively associated with vitamin B<sub>12</sub> concentrations ( $P<0.001$ ) (Figure 6.2). Additionally there was a significant association between low ( $\leq 1000$  mg) and medium (1500-2000 mg) metformin doses and vitamin B<sub>12</sub> levels ( $p<0.03$ ) and between low and high ( $\geq 2550$  mg) metformin daily doses ( $P<0.001$ ). Although there was a decrease in vitamin B<sub>12</sub> levels between medium and high metformin doses it was not significant ( $P<0.069$ ). No other associations were observed between grouped metformin doses with clinical variables in this study. Furthermore no genetic variants were associated with vitamin B<sub>12</sub> levels.

There was a slight negative relationship observed between vitamin B<sub>12</sub> levels and steady-state metformin plasma concentrations (Figure 6.1c) ( $R^2=0.042$ ), but this was not significant ( $P=0.08$ ).

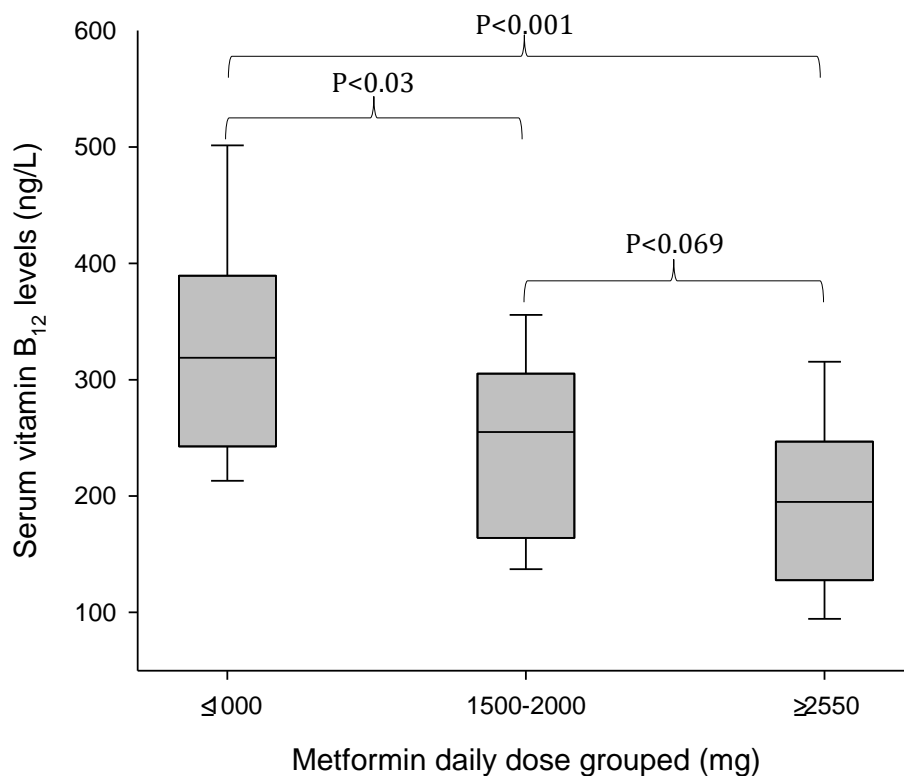


**Figure 6.2.** Serum vitamin B<sub>12</sub> levels vs grouped metformin doses.

### 6.3.3 Effect on haematological parameters

Twenty-nine (39%) patients exhibited low haemoglobin (Hb) levels (male <133 g/L, female <118 g/L) with 30 (40%) having low haematocrit (HCT) levels (male <39%, female <36%). As expected Hb and HCT levels were positively correlated ( $R^2 = 0.978$ ). Of the 30 patients with vitamin B<sub>12</sub> deficiency, 10 (33.3%) were anaemic (defined as both exhibiting low haemoglobin and haematocrit levels). In the 45 patients who exhibited borderline deficiency or normal levels, nineteen (42%) patients were anaemic. Overall anaemic patients had mean vitamin B<sub>12</sub> levels of 252.7 ng/L compared with 226.6 ng/L in patients without anaemia ( $P = 0.4$ ). Metformin daily dose did not influence anaemia ( $P = 0.6$ ).

Serum albumin levels were the biggest predictors of both Hb and HCT levels accounting for 23.5% of the variability. The final multivariate model included albumin and CL<sub>CR</sub> as the best predictors for Hb levels. Four (5%) patients exhibited high MCV levels (>100 fL) with low Hb and HCT levels indicative of macrocytic anaemia. All anthropometric measurements with the exception of BMI were positively associated with MCV ( $P < 0.01$ ) with BSA as the greatest predictor. The final model included albumin and BSA ( $R^2 = 0.019$ ,  $P < 0.005$ ).

### 6.3.4 Serum lactate

Metformin plasma concentrations were the only predictor for serum lactate levels ( $P = 0.007$ ). 33% of patients exhibited high lactate levels above the reference range; exceeding 2.2 mmol/L. The average metformin plasma concentrations for patients with lactate levels below and above 2.2 mmol/L were 1700 and 2262 ng/mL respectively.

**Table 6.2. Multivariate linear regression analysis.**

Dependent variable	Explanatory variable	Model $R^2$	$P/P$ value	Parameter estimate	SE
Vitamin B <sub>12</sub> (ng/L)		0.345	<0.0001	317.99	27.48
	metformin daily dose (mg/kg)		<0.0001	-5.20	0.899
	Folate ( $\mu$ g/L)		0.011	5.02	1.91
Haemoglobin (g/dL)		0.303	<0.0001	4.14	1.929
	Albumin (g/L)		<0.0001	0.19	0.048
	CL <sub>CR</sub>		0.01	0.013	0.005
Hematocrit (%)		0.281	<0.0001	12.836	5.59
	Albumin (g/L)		<0.0001	0.554	0.14
	CL <sub>CR</sub>		0.036	0.031	0.014
Mean Corpuscular Volume (fL)		0.202	<0.0005	59.20	7.162
	Albumin (g/L)		0.012	0.366	0.142
	Body surface area (m <sup>2</sup> )		0.002	6.89	2.103
Steady state metformin plasma concentration (ng/mL)		0.495	<0.0001	-1023.97	357.99
	metformin daily dose (mg/kg)		<0.0001	53.42	8.10
	Urea (mmol/L)		<0.0001	238.26	37.50

### 6.3.5 Genetic variants

Genetic variants did not have a significant effect on metformin plasma levels, vitamin B<sub>12</sub>, serum lactate, haemoglobin or haematocrit levels, Table 6.3. Several genetic variants in both *SLC22A1* (rs12208357, rs683369) and *SLC22A2* (rs3127573, rs34129302, rs2774230, rs2279463, rs3127594) were associated with serum folate levels, with the minor allele being associated with decreased serum folate levels.

Two variants were associated with MCV; rs202220802 in *SLC22A1* and rs624249 in *SLC22A2*. Paradoxically, the minor allele of rs202220802 was associated with decreased MCV whereas rs624249 was associated with increased MCV. However, after correction for multiple testing, only rs202220802 remained significantly associated with MCV.

Two variants, all expressed in *SLC22A2*, were associated with variables related with kidney function. The rs316003 and rs3127594 minor allele variants were initially associated with increased CL<sub>CR</sub>. Additionally, rs31275944, was

Table 6.3. *SLC22A1* & *SLC22A2* effect on outcome variables

	Genetic variant	Vitamin B <sub>12</sub>	Folate	Hb	HCT	MCV	Lactate	Urea	Creatinine	CL <sub>CR</sub>	GFR	Metformin plasma levels
<i>SLC22A1</i> (OCT1)	rs12208357	0.791	<b>0.024</b>	0.729	0.683	0.348	0.814	0.391	0.458	0.559	0.605	0.913
	rs683369	0.171	<b>0.015</b>	0.609	0.617	0.392	0.866	0.502	0.983	0.710	0.799	0.395
	rs45584532	0.453	0.663	0.816	0.954	0.894	0.279	0.701	0.259	0.376	0.872	0.907
	rs628031	0.298	0.547	0.268	0.299	0.423	0.813	0.369	0.606	0.904	0.838	0.261
	rs202220802	0.869	0.609	0.893	0.970	<b>0.036</b>	0.365	0.638	0.803	0.330	0.557	0.223
	rs113569197	0.291	0.825	0.386	0.552	0.214	0.364	0.089	0.125	0.545	0.535	0.213
	rs9457843	0.447	0.260	0.976	0.829	0.839	0.309	0.806	0.202	0.375	0.950	0.429
	rs622591	0.105	0.983	0.663	0.910	0.082	0.564	0.828	0.296	0.389	0.489	0.110
<i>SLC22A2</i> (OCT2)	rs3127573	0.306	<b>0.007</b>	0.487	0.369	0.657	0.764	0.367	0.089	0.218	0.183	0.124
	rs316023	0.321	0.089	0.230	0.184	0.790	0.599	0.615	0.136	0.472	0.099	0.224
	rs34129302	0.426	<b>0.005</b>	0.618	0.535	0.862	0.782	0.341	0.111	0.129	0.133	0.099
	rs624249	0.440	0.504	0.829	0.672	<b>0.024</b>	0.964	0.771	0.237	0.110	0.053	0.549
	rs2774230	0.422	<b>0.034</b>	0.558	0.437	0.496	0.617	0.674	0.137	0.072	0.143	0.338
	rs316019	0.933	0.533	0.922	0.737	0.450	0.442	0.624	0.726	0.229	0.363	0.900
	rs2279463	0.280	<b>0.003</b>	0.577	0.621	0.739	0.935	0.243	0.087	0.081	0.095	0.550
	rs316003	0.613	0.077	0.576	0.513	0.907	0.339	0.527	0.119	<b>0.041</b>	0.071	0.166
rs3127594	0.494	<b>0.004</b>	0.931	0.918	0.462	0.721	0.248	0.053	<b>0.049</b>	<b>0.042</b>	0.210	
rs694812	0.786	0.473	0.556	0.526	0.578	0.343	0.703	0.786	0.179	0.250	0.386	

Number displayed correspond to P value from non-parametric analysis. Significant P values ( $p < 0.05$ ) are shown in bold. All genetic variants were analysed with Mann-Whitney U test unless marked with a \* which corresponds with Kruskal-Wallis ( $n = 3$  groups). Hb, haemoglobin; HCT, haematocrit; MCV, mean Corpuscular volume; CL<sub>CR</sub>, creatinine clearance; GFR, glomerular filtration rate.

**Table 6.4. Comorbidities and Concomitant drug classes effect on outcome variables**

	Vitamin B <sub>12</sub>	Folate	Hb	HCT	MCV	Lactate	Urea	Creatinine	CL <sub>CR</sub>	GFR	Metformin plasma levels
Comorbidity											
Dyslipidemia	0.422	0.140	0.909	0.790	0.573	0.832	0.327	0.130	0.311	0.739	0.714
Ischaemic heart disease	0.681	0.438	0.615	0.701	0.905	0.373	0.063	0.203	0.361	0.287	0.283
Osteoarthritis	0.337	0.910	0.994	0.902	0.366	0.708	0.068	0.488	0.573	0.917	0.418
Neuropathy & Retinopathy	0.828	0.281	0.140	0.140	0.894	0.648	0.756	0.524	0.706	0.762	0.889
Concomitant medication											
Atenolol	0.659	0.583	0.628	0.568	0.994	0.418	0.970	0.795	0.085	0.102	0.534
Aspirin	0.894	0.766	0.318	0.448	0.844	0.711	0.623	0.636	0.510	0.466	0.941
Anti-diabetic drugs	0.179	0.120	0.247	0.247	0.176	0.739	0.057	0.077	0.185	0.285	0.351
PPIs	0.760	0.448	0.256	0.191	0.492	0.124	0.371	0.795	0.452	0.770	0.775
OCT inhibitors	0.121	0.652	0.166	0.116	0.969	0.188	0.116	0.382	0.316	0.771	0.576

Number displayed correspond to P value from non-parametric analysis. There are no significant P values ( $p < 0.05$ ). All grouped variables were analysed with Mann-Whitney U test. Hb, haemoglobin; HCT, haematocrit; MCV, mean Corpuscular volume; CLCR, creatinine clearance; GFR, glomerular filtration rate; PPIs, Proton-pump inhibitors.

associated with increased eGFR. However, after correction for multiple testing, none of these associations with kidney function remained significant.

### **6.3.6 Comorbidities & Concomitant drug classes**

There was no significant association of grouped comorbidities on the outcome variables, Table 6.4. Additionally grouped concomitant drug classes were investigated. Known OCT inhibitors included the PPIs (lansoprazole and omeprazole), quinine, rantidine and atenolol. Grouped additional anti-diabetic drug medications included gliclazide, rosiglitazone, pioglitazone and glimepiride. There was no significant effect concomitant drug classes had on the outcome variables. See appendix Figures A6.1 and A6.2 for summary of all comorbidities and concomitant medications.

## **6.4 Discussion**

In this chapter we observed a prevalence of vitamin B<sub>12</sub> deficiency in metformin treated T2DM patients of 40%, which is greater than other recent reported prevalence's ranging from 14-28.1% (Beulens et al., 2014, de Groot-Kamphuis et al., 2013). The differences may be accountable for the duration of metformin treatment which is higher in our study (8.05 years) compared with their mean duration ranged from 4-5.3.

The negative relationship between metformin and vitamin B<sub>12</sub> has been widely reported in a number of populations (Tal et al., 2010, Ting et al., 2006, de Groot-Kamphuis et al., 2013) and a recent meta-analysis showed metformin had a significant effect on vitamin B<sub>12</sub> concentrations in a dose-dependent manner in comparison to other interventions (mean difference, 253.93 pmol/L; 95% CI, 281.44 to 226.42 pmol/L,  $P=0.0001$ ) (Liu et al., 2014). See Chapter 1, section Our study lacked a placebo group for comparative analysis, but due to the plethora of evidence showing metformin induces vitamin B<sub>12</sub> deficiency we feel , Table 1.4 for previous studies on metformin and vitamin B<sub>12</sub> levels. This is not a

limitation. To our knowledge, this is the first study to illustrate that the effect of metformin on vitamin B<sub>12</sub> deficiency in T2DM is driven by metformin dose and not systemic exposure. This suggests metformin induces malabsorption of vitamin B<sub>12</sub> at the intestinal level.

Metformin's major route of absorption is not through cellular transport but through tight junctions of ileal cells (Proctor et al., 2008). Furthermore metformin is absorbed by cells through the apical membrane but not transported through the basolateral membrane resulting in metformin being sequestered in the cells leading to high cellular concentrations. Previous reports have suggested, but not provided evidence, that the metformin transporter *SLC22A1* (OCT1) is expressed in the basolateral membrane of enterocytes and thus aids in the cellular transport of metformin from the cell to the blood (Mulgaonkar et al., 2013). In contrary Han et al., 2013, discovered that OCT1 was not expressed on the basolateral membrane of human and mouse enterocytes and inhibition of the transporter did not influence basolateral transport of known OCT1 substrates. Together these data collectively suggest that metformin is transported in enterocytes through the apical membrane only. This is also supported by studies demonstrating OCT3 and Plasma membrane monoamine transporter (PMAT) are apically expressed enterocyte metformin transporters (Zhou et al., 2007a, Muller et al., 2005).

Under normal conditions vitamin B<sub>12</sub> is bound to intrinsic factor (IF) in the duodenum. The vitamin B<sub>12</sub>-IF complex is recognised by the multi-ligand apically expressed membrane protein, Cubam, which endocytoses the complex into the epithelium of the terminal ileum (Fyfe et al., 2004, He et al., 2005). Following Cubam internalisation the IF-Cbl complex is sorted through lysosomes (Fyfe et al., 2004), degrading the IF allowing free B<sub>12</sub> to be trafficked to and transported out of the basolateral membrane through transcobalamin receptor II into the bloodstream (Seetharam, 1999). As metformin is prescribed in large doses, commonly 3000 mg/day, enterocyte accumulation of metformin may be high. This may induce enterocyte dysfunction through cellular glucose depletion and directly or indirectly impacting on intracellular trafficking of

vitamin B<sub>12</sub> from the apical to the basolateral membrane and transfer into the blood contributing to vitamin B<sub>12</sub> malabsorption. Interestingly the most common side effect of metformin is gastrointestinal irritability (Bolen et al., 2007) and although not reported, may be linked to vitamin B<sub>12</sub> deficiency.

The univariate analysis revealed several anthropometric measurements, including height, weight, LBW, and IBW, to be positively associated with vitamin B<sub>12</sub> levels ( $P < 0.05$ ). Anthropometric measurements are known predictors of liver weight and size (Chan et al., 2006, Deland and North, 1968). Given that 50% of the body's total vitamin B<sub>12</sub> store is located in the liver, these measurements may mirror the size of the liver and thus its vitamin B<sub>12</sub> storage capacity. Increased liver size may slow down the progression of vitamin B<sub>12</sub> deficiency in metformin treated T2DM patients. Although both male and female groups in our study showed a significant association between metformin dose and vitamin B<sub>12</sub> levels, it was more pronounced in females (males;  $P < 0.05$ , females;  $P > 0.0001$ ) which may reflect the differences in anthropometric measurements and therefore liver size. There was no significant difference in observed metformin daily dose and treatment duration between male and female subjects. Our data shows that no *SLC22A2* or *SLC22A2* variants were associated with vitamin B<sub>12</sub> levels.

Interestingly, two variants in *SLC22A1* and five variants in *SLC22A2* showed an association with serum folate level, with the minor allele being associated with decreased folate levels. Upon first observation it appears that a number of SNPs are independently associated with folate, however as the linkage disequilibrium plot in chapter 3 illustrates (Figure 3.4), these SNPs are in high LD with one another. Additionally, the SNPs in *SLC22A1* (rs12208357, p.R61C; rs683369, p.L160F) associated with folate levels exhibit LD ( $> 0.6$ ) with rs34129302 (p.GAA/-) in *SLC22A2*. Additionally this variant has a smaller  $P$  value than the other variants associated with folate levels. Therefore it is likely that rs34129302 represents the casual variant associated with decreased folate levels. There is no available evidence to support this OCT1-folate relationship which suggests this is an artefact. However, both folate and vitamin B<sub>12</sub>

deficiency can arise from the induction of a functional folate deficiency, which in turn is induced by vitamin B<sub>12</sub> deficiency. The interrelationship between these two vitamins has been explained by the methyl trap hypothesis (see Chapter 1, section 1.10.2) which states that vitamin B<sub>12</sub> deficiency can lead to lowered levels of methionine synthase, which results in folate deficiency by trapping an increased proportion of folate as the 5-methyl derivative. If our data is under powered to find a significant association between vitamin B<sub>12</sub> levels and OCT1 variants we may of found an association with folate levels through the interrelationship vitamin B<sub>12</sub> and folate have in the folate trap. However, we found no significant relationship between vitamin B<sub>12</sub> and folate levels in our population again suggesting the OCT1-folate association is an artefact.

All metformin parameters were negatively associated with vitamin B<sub>12</sub> levels. The final regression model revealed metformin dose (mg/kg) and folate levels to be the greatest explanatory variables for vitamin B<sub>12</sub> levels in T2DM patients ( $P < 0.0005$ ). Patients with a slightly lower folate level and higher metformin dose were more likely to have diminished vitamin B<sub>12</sub> levels. The mean duration of metformin treatment in this study was 8.05 years and was negatively associated with vitamin B<sub>12</sub> levels ( $P=0.015$ ,  $R^2=0.08$ ). The rate of vitamin B<sub>12</sub> depletion from the body stores is reliant on the efficiency of absorption, the initial amount stored, re-absorption from the bile and clearance through the kidney. It has been estimated that a normal person's body store of 1-3 mg would be sufficient to meet the body's needs for 3-6 years, respectively under normal conditions (Allen, 2008). Consequently malabsorption of vitamin B<sub>12</sub> driven by metformin may not be apparent for years of following treatment due to the large internal vitamin B<sub>12</sub> store. This may reflect why systemic levels of metformin were not associated with vitamin B<sub>12</sub>. Our study lacks baseline vitamin B<sub>12</sub> levels, quantifying one measurement per patient; however, given the lengthy time scale needed for B<sub>12</sub> deficiency to present itself versus the lengthy mean duration of metformin treatment in this study; we believe the sample timings are sufficient to draw conclusions of metformin's effect on

serum vitamin B<sub>12</sub> levels. The final linear regression model explains 34% of vitamin B<sub>12</sub> variability observed in this patient group. The remaining variability could be explained by other covariates not incorporated in our study. Interestingly, vitamin B<sub>12</sub> is absorbed in the small intestine, stored in the liver and levels regulated by the kidneys (Birn, 2006); sites of metformin transporter expression and high metformin disposition (Chen et al., 2013). Apically expressed enterocyte metformin transporters *SLC22A3* (OCT3) and *SLC29A4* (PMAT) are known metformin transporters and their genetic variants have been investigated to elucidate their effects on metformin pharmacokinetics (Christensen et al., 2011). Although they report no effects of these polymorphic variants on metformin pharmacokinetics, given their site of expression, further work to investigate the effect of polymorphic variants in these transporters on serum vitamin B<sub>12</sub> levels may be useful.

The importance of vitamin B<sub>12</sub> in haematopoiesis is well known, and can be linked to a number of clinical haematological manifestations including anaemia (Fishman et al., 2000). Therefore we investigated if vitamin B<sub>12</sub> levels influenced reductions in Hb and HCT levels and increases in MCV. We found neither vitamin B<sub>12</sub> levels nor any metformin parameters were associated with decrease in Hb levels. Even though it is not widely reported, there have been reports indicating metformin does slightly decrease haemoglobin and haematocrit levels (Belcher et al., 2005, Bray et al., 2012). However, despite metformin dose decreasing vitamin B<sub>12</sub> levels, it did not affect anaemic status in our cohort. Furthermore, there was no significant difference in vitamin B<sub>12</sub> levels in patients with or without anaemia, 252.7 vs 226.6 ng/L respectively. We may not have observed a vitamin B<sub>12</sub>-anaemia relationship as we exclusively used serum vitamin B<sub>12</sub> as a marker. Others have suggested holotranscobalamin and methylmalonic acid as more sensitive biomarkers for anaemia, as they reflect B<sub>12</sub> status and B<sub>12</sub> internal stores more specifically than vitamin B<sub>12</sub> alone (Chatthanawaree, 2011, Oberley and Yang, 2013). Our results mirror that of de Groot-Kamphuis et al., 2013 who observed that metformin dose decreases vitamin B<sub>12</sub> levels but does not lead to anaemia or in T2DM patients (de Groot-Kamphuis et al., 2013). The most likely explanation therefore is that studies to

date have lacked power to show the association between metformin and megaloblastic anaemia despite the association with decreased vitamin B<sub>12</sub> levels. Such a study would have to be done in patients who have been taking metformin for more than a decade which may prove difficult by conventional means, but may become possible as electronic health records become more widely available.

We did not observe any clinically relevant haematological consequences of vitamin B<sub>12</sub> deficiency in our cohort. However there is documented evidence demonstrating low vitamin B<sub>12</sub> levels or B<sub>12</sub> deficiency to be associated with neurodegenerative diseases and cognitive impairment with vitamin B<sub>12</sub> therapy improving cognitive function (Moore et al., 2012, Aaron et al., 2005). Conversely several contradictory reviews observed no association between serum vitamin B<sub>12</sub> levels and cognitive function but found specific methylmalonic acid, homocysteine and holotranscobalamin to be associated with dementia and decline in cognitive function (O'Leary et al., 2012, Health Quality, 2013, de Jager, 2014), again highlighting that serum vitamin B<sub>12</sub> levels may not reflect true B<sub>12</sub> status.

Factors significantly related to haemoglobin and haematocrit levels in this study were age, albumin, ALT, urea, CL<sub>CR</sub> and GFR ( $P < 0.005$ ). This is consistent with previous reports which observed relationships between haemoglobin with albumin (Feng et al., 2011, Madore et al., 1997, Eliana et al., 2005), creatinine (Feng et al., 2011) and age (Madore et al., 1997, Feng et al., 2011, Carpenter et al., 1992). Our multivariate model revealed both albumin and CL<sub>CR</sub> were the best explanatory variables for Hb and HCT. Albumin and Hb levels are known to increase in dehydrated patients. Furthermore, Feng et al., 2011 suggested diminished albumin levels are a result of poor nutrition which may reflect haemoglobin levels.

Metformin plasma levels were quantified in 218 plasma samples from 75 T2DM patients. The concentrations ranged from 49 to 4908 ng/mL with an average of 1879 ng/mL. This equates to a 100-fold difference observed in metformin

plasma concentrations between patients receiving 0.5-3 g of a day. This finding is consistent with Christensen et al who report an 80 fold variability when using a single dose of 2.0 g/day (Christensen et al., 2011).

The biggest predictor for metformin plasma levels was metformin dose (mg/kg body weight) followed by serum urea levels. Serum urea was positively correlated with serum creatinine and negatively correlated with  $CL_{CR}$  and GFR, all of which were statistically significantly associated with metformin plasma levels. This complements our PopPK results in chapter 5 where serum urea levels were the biggest explanatory variable for predicted metformin clearance; which is directly related to metformin plasma levels. Metformin is primarily eliminated from the body through the kidneys (Robert et al., 2003). Our results show that decreased kidney function is associated with increased metformin plasma concentration due to decreased metformin elimination from the body therefore. This reflects the importance of metformin use in T2DM with kidney disease with current guidelines not recommending its use in patients with a GFR of <30 mL/min and use with caution with <60 mL/min (Lipska et al., 2011).

Metformin plasma concentrations were the only predictor for serum lactate levels ( $P = 0.007$ ). Metformin's primary pharmacological site of action is the liver where metformin acts to inhibit hepatic gluconeogenesis (Wiernsperger and Bailey, 1999). This inhibition not only decreases serum glucose levels but diminishes lactate hepatocyte uptake thus increasing serum lactate levels. Lactic acidosis, although a rare side effect, is a recognised adverse reaction of increased metformin levels (Graham et al., 2011).

Two variants, in *SLC22A2* were initially significantly associated with kidney function, though this was negated by correction for multiple testing. Interestingly, genome-wide association studies reported *SLC22A2* variants to be associated with serum creatinine (Koettgen et al., 2009). However, they report rs2279463 is associated with creatinine production whereas we found this variant had no association with  $CL_{CR}$ . Additionally, another study has found the minor allele rs316003 to be associated with increased GFR which complements

our initial finding of rs316003 being weakly related to increased  $CL_{CR}$  (Reznichenko et al., 2013).

Several conclusions can be drawn from this chapter. First, there is a clear association between metformin dose and serum vitamin B<sub>12</sub> levels. On the contrary steady-state metformin plasma levels were not significantly associated with vitamin B<sub>12</sub> levels. This suggests metformin exerts its effect at the intestinal level inducing vitamin B<sub>12</sub> malabsorption. Consequently the data may shed some light on the mechanism responsible for metformin induced B<sub>12</sub> deficiency which is currently unclear. The study did not identify any association between *SLC22A1* or *SLC22A2* genetic variants and vitamin B<sub>12</sub> deficiency. The inclusion of genetic variants in metformin drug transporters expressed in the gut, such as PMAT or OCT3, may provide a mechanism to how metformin induces vitamin B<sub>12</sub> deficiency. Finally vitamin B<sub>12</sub> deficiency does not influence any clinical hematological manifestations where either more specific biomarkers of B<sub>12</sub> status such as holotranscobalamin and methymalonic acid need to be employed and this needs to be accompanied by much larger sample sizes.

## **Chapter 7**

**Final discussion**

Despite metformin being used for decades and being the most commonly prescribed anti-diabetic medication in the world today, there is a considerable amount unknown about how it leads to vitamin B<sub>12</sub> deficiency. OCT1 (*SLC22A1*) and OCT2 (*SLC22A2*) are highly polymorphic drug transporters responsible for the hepatic and renal uptake of metformin, respectively (Kimura et al., 2005a, Mulgaonkar et al., 2013). We therefore investigated the effect of genetic variants in these genes on metformin parameters and vitamin B<sub>12</sub> levels.

In chapter 4, we developed a HPLC-MS/MS method for the quantification of metformin in human plasma. We found the average intra-individual metformin plasma concentrations (steady-state) ranged from 49 to 4908 ng/mL with an average of 1879 ng/mL. We hypothesised this high variability between individuals on similar metformin doses could possibly be explained by genetic polymorphisms in *SLC22A1* and *SLC22A2*.

Due to the polymorphic nature of OCT genes, we decided to sequence rather than genotype patients for specific known variants. In chapter 6, we showed decreased serum vitamin B<sub>12</sub> concentrations are driven more by metformin dose suggesting that metformin causes vitamin B<sub>12</sub> deficiency as a result of local action in the gut rather than systemically. Therefore, retrospectively we should have considered sequencing other known metformin transporters, particularly those that are expressed in the intestine, such as OCT3 and PMAT (Duan and Wang, 2010, Duong et al., 2013). Christensen et al (Christensen et al., 2011) found a cluster of five intronic SNPs in PMAT associated with decreased metformin absorption. These SNPs were barely significantly associated with trough steady-state metformin concentration, and correction for multiple testing meant they were no longer significant. Conversely Duong et al., 2013 found no SNPs in PMAT or OCT3 that were significant covariates in metformin clearance or volume of distribution. Chen et al., 2015 observed lower metformin bioavailability in knockout OCT3 mice compared with wild-type mice. Other groups have also shown that genetic variants in OCT3 may modulate metformin action (Chen et al., 2010a). Therefore further work is warranted and needed to define the role of OCT3 and PMAT on metformin-induced vitamin B<sub>12</sub> deficiency.

The majority of the clinical studies demonstrating that the administration of metformin leads to vitamin B<sub>12</sub> deficiency refer to the work of *Schafer* (Schafer, 1976) as an explanation for the mechanism behind the association. These reports collectively suggest that the binding of biguanides causes a positive shift to the surface of the ileal membrane, which would displace divalent cations such as calcium. This would then interfere with the calcium-dependent process of vitamin B<sub>12</sub> absorption. However the work focused on phenformin and buformin using murine liver and kidney mitochondrial membranes, and not the effect of metformin on the plasma membrane of ileal cells. Therefore these assumptions cannot be validated based on the work of Schafer (1976). The only evidence to support the theory that metformin impairs calcium availability is from a clinical study which illustrated that metformin induced vitamin B<sub>12</sub> deficiency was reversed with dietary supplements of calcium carbonate (Bauman et al., 2000). They suggested that the hydrophobic tail of metformin could extend into the hydrocarbon core of membranes, thereby displacing divalent cations and leading to vitamin B<sub>12</sub> malabsorption. However, our results in chapter 4 suggest that metformin's high polarity would prevent metformin from interacting with the plasma membranes hydrophobic core from phospholipid tails. We found that reverse phase HPLC columns, which have a non-polar, hydrophobic stationary phase, were poor at retaining metformin, due to its high polarity. Additionally the incorporation of a hydrophilic interaction liquid chromatography (HILIC) column showed that a hydrophilic stationary phase was more than adequate at retaining metformin. Schafer's work used phenformin and buformin, which are compounds with exhibit greater hydrophobicity compared with metformin. Phenformin and buformin are larger compounds which have a benzene and hydrophobic hydrocarbon tail (Figure 1.1). Thus, we conclude this chemical and biological theory is not plausible based on our results.

A plausible molecular explanation may be as follows: the absorption of vitamin B<sub>12</sub> is dependent on binding to Intrinsic factor (IF) produced by parietal cells in the stomach. This vitamin B<sub>12</sub>-IF complex is recognised by the multi ligand apical membrane protein, cubam, which endocytoses the complex into the

epithelium of the terminal ileum (Fyfe et al., 2004, He et al., 2005). Cubam is composed of the extracellular protein cubilin and the transmembrane protein amnionless (Andersen et al., 2010). Cubilin contributes to the recognition and binding of the vitamin B<sub>12</sub>-IF complex. More specifically the CUB<sub>5-8</sub> domains of cubilin bind with high affinity to the vitamin B<sub>12</sub>-IF complex in a Ca<sup>2+</sup> dependent manner (Andersen et al., 2010). Therefore, metformin could induce a positive charge on the membranes of the ileum epithelium, displacing the Ca<sup>2+</sup> from the CUB domains and preventing vitamin B<sub>12</sub>-IF complex binding to cubam receptor for absorption, Figure 7.1. However, additional work is required to investigate this hypothesis. What is evident is that metformin causes vitamin B<sub>12</sub> malabsorption (Mollin et al., 1957, Tomkin, 1973, Callaghan and Hadden, 1980, Mourits-Andersen and Ditzel, 1983, Shaw et al., 1993, Andres et al., 2003).

Metformin is prescribed in large doses; consistent with this, we observed high metformin plasma concentrations (average steady-state, 1879 ng/mL; chapter 4). Therefore we could hypothesise that enterocyte accumulation of metformin in the GI tract may be high. This may induce enterocyte dysfunction through cellular glucose depletion which may either directly or indirectly impact on the intracellular trafficking of vitamin B<sub>12</sub> from the apical to the basolateral membrane and transfer into the blood leading to vitamin B<sub>12</sub> malabsorption. The receptor-mediated endocytosis of vitamin B<sub>12</sub> from the intestinal lumen and subsequent translocation across the cell is a complex and energy dependent process (He et al., 2005, Fyfe et al., 2004). Given metformin induces cellular ATP depletion possibly through mitochondrial dysfunction, this could result in decreased vitamin B<sub>12</sub> absorption (Sanchez-Alvarez et al., 2013). AMPK agonists, such as metformin, can act as stress-energy inducers. This characteristic of metformin has led to its use alongside anti-cancer treatments to promote severe oxygen and glucose deprivation in certain areas of tumour tissues (Sanchez-Alvarez et al., 2013, Menendez et al., 2012, Evans et al., 2005). Figure 7.1 provides a summary of possible sites where metformin could impact on the absorption of vitamin B<sub>12</sub>.

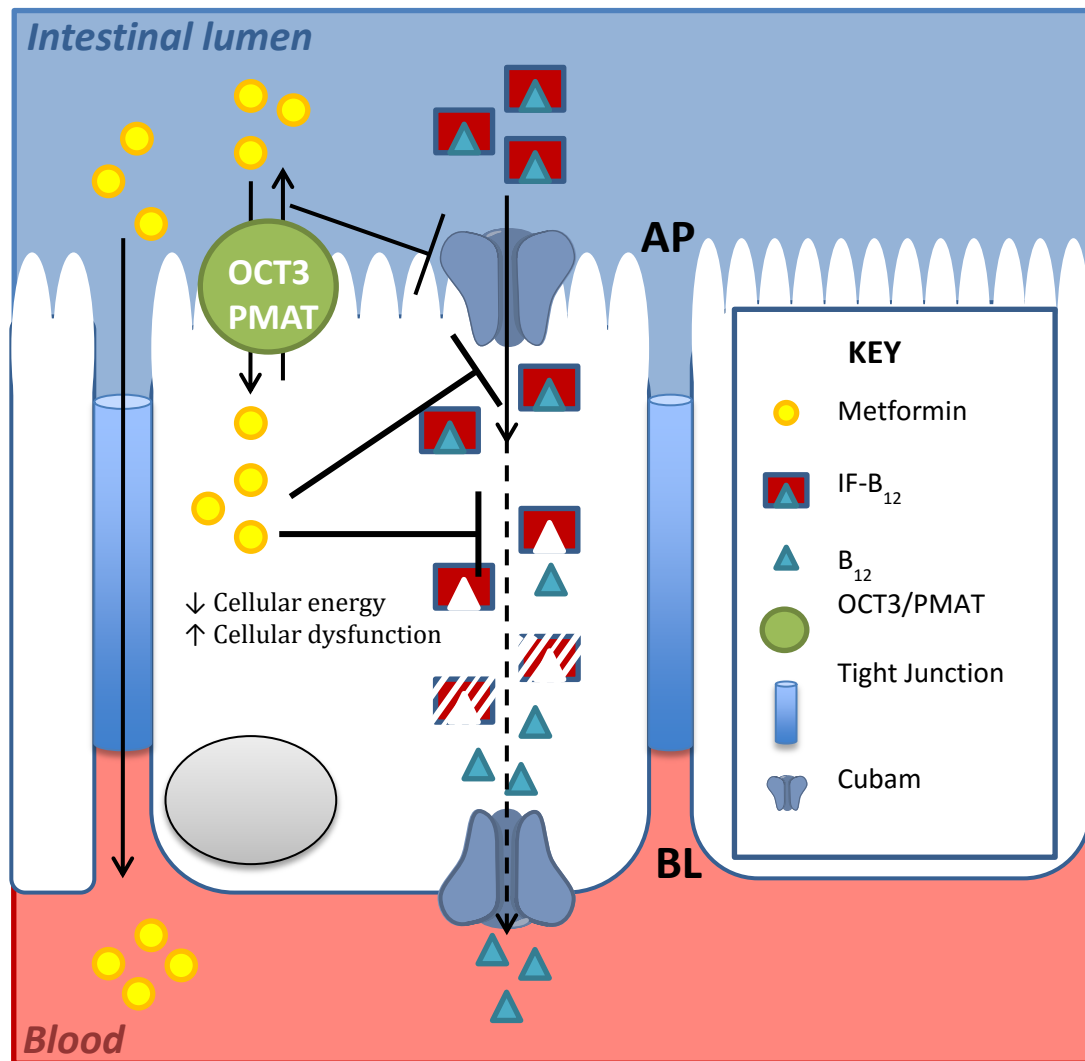


Figure 7.1. Proposed hypotheses to metformin induced vitamin B<sub>12</sub> malabsorption. Under normal conditions vitamin B<sub>12</sub> bound to intrinsic factor in the intestine. Upon binding to the cubam receptor the complex, it is internalised and the IF is degraded allowing free vitamin B<sub>12</sub> to be transported to the basolateral membrane. It has been previously hypothesised that metformin sequesters in enterocytes as there is no known basolateral metformin drug transporters. Metformin may undergo transport via tight junctions using proteins called claudins. We hypothesise that the increased concentration of metformin in the enterocyte cytoplasm may accumulate in enterocytes and impair vitamin B<sub>12</sub> translocation from the intestinal lumen to the blood. The T-bars show possible sites where metformin may interact or bind to reduce vitamin B<sub>12</sub> absorption or how it leads to depleted cellular energy required for vitamin B<sub>12</sub> translocation. AP, apical; BL:basolateral.

The most common side effect of metformin is gastrointestinal irritability (Bolen et al., 2007). Tarasova et al., 2012, described a 8 bp insertion, rs36056065, which may predispose toward an increased prevalence of GI side effects of metformin. As discovered in chapter 2, the GTAAGTTG insertion is in fact the rs113569197 TGGTAAGT variant (refer to Figure 2.5). The possible effect of the 8 bp insertion on OCT1 expression levels has previously been determined by Grinfeld et al., 2013, who found that the 8 bp insertion was included in the transcript, prompting a new splicing donor site. Both this study and our analysis in chapter 2 predicted that the 8 bp insertion would produce a premature stop codon resulting in a truncated OCT1 protein. Thus one could hypothesise that the 8 bp insertion may lead to metformin induced gastrointestinal side effects through the lack of OCT1 protein expression or reduced level of function from a truncated OCT1 transcript.

In chapter 6 we found no association between serum vitamin B<sub>12</sub> levels and rs113569197 in OCT1. Additionally we found no association with other OCT1 or OCT2 genetic variants and outcome variables. However, the rs113569197 8 bp insertion described in chapter 5 was found to be initially associated with predicted metformin clearance in our PopPK model. But this association was dropped when multivariate analysis was performed and serum urea levels were found to be the major explanatory variable of metformin clearance. One possible limitation of our cohort is the low study sample size which may not have sufficient statistical power to detect associations between genetic variants and vitamin B<sub>12</sub> levels.

A more specific measure of metformin clearance would have involved collecting urine samples from the patients, which we could have applied our HPLC-MS method described in chapter 4. The quantification of metformin from urine has previously been done using HILIC (Nielsen et al., 2014). More crucially, we may have been able to use the genetic variant data from OCT2, as it is expressed in the kidney, to determine whether there is an association between metformin clearance and OCT variants. OCT2 has been previously described as the rate limiting step in metformin clearance. Furthermore, OCT2 genetic variants have

been linked to impaired metformin elimination (Christensen et al., 2013, Duong et al., 2013, Aoki et al., 2008, Zolk, 2012). Christensen et al., 2013 also reported that the OCT2 rs316019 variant (p.A270S) increased the renal elimination of metformin. However, other metformin drug transporters are expressed in the kidney, MATE1 and MATE2K (Nies et al., 2011b, Chen et al., 2013, He et al., 2010), and again, their genetic variants have been suggested to impact on metformin clearance. Thus, there is a need to simultaneously consider the effect of several different transporters on metformin clearance – this would need a much larger sample size.

In our population, the metformin plasma concentration-time profile does not exhibit a usual PK curve, where clear  $T_{max}$  or  $C_{max}$  parameter values can be obtained. A major limitation to the PK modelling reported here is the data itself. Due to the small sample size and available data, clearance (CL) estimates for population and individual parameters were acquired, whereas the population  $V$  and  $K_a$  parameters could only be estimated. Usually the next step after producing a PK model is to use it in building and producing a PD model. Unfortunately, our data is unsuitable for PD modelling as we have one vitamin B<sub>12</sub> level per patient, post metformin dosage, and therefore are lacking a baseline (pre metformin) vitamin B<sub>12</sub> level.

This study only used serum vitamin B<sub>12</sub> levels as a marker for vitamin B<sub>12</sub> deficiency. However, there is no precise or gold standard test for the diagnosis of vitamin B<sub>12</sub> deficiency. The diagnosis is usually based on identifying a low level of serum vitamin B<sub>12</sub> with clinical evidence of deficiency, such as anaemia (Wong, 2015). However we found no association between vitamin B<sub>12</sub> levels and Hb or anaemia in this cohort. The quantification of other markers of vitamin B<sub>12</sub> deficiency such as those described in Chapter 1, section 1.10.5, might of provided better evidence for polymorphic metformin drug transporters as predictors of metformin-induced vitamin B<sub>12</sub> deficiency. For example, both the short term and long-term effects of metformin on homocysteine levels have been assessed in T2DM. Following 16 weeks of metformin treatment (850 mg/tds) Wulffele et al (2003) observed a modest, but significant 4% increase in homocysteine levels (Wulffele et al., 2003). Using the same treatment dose De

Jager et al., 2010 found metformin decreased both vitamin B<sub>12</sub> and increased homocysteine levels after 4 years treatment duration. Additionally Carlsen et al., 1997 found that greater than 6 months exposure of metformin decreased vitamin B<sub>12</sub> and increased serum homocysteine and MMA, which led to clinically severe peripheral neuropathy compared with similar patients with no metformin exposure (Carlsen et al., 1997). However, there is an unresolved issue to whether increases in homocysteine is secondary to reduced vitamin B<sub>12</sub> or a combination of both (Buysschaert et al., 2000, Hoogeveen et al., 1997). Nevertheless other markers of vitamin B<sub>12</sub> deficiency may have been beneficial in this small sample cohort.

To gain an understanding to the effects of genetic variants in OCTs we used *in silico* structural modelling techniques to create OCT protein structures. These techniques are routinely and successfully used to screen large databases and identify possible transporter ligands through docking experiments and for enabling rational drug design. However, we wanted to use these to predict whether an nsSNP can elucidate whether it impacts transporter function. The 3D models were solely based on the TMDs of OCT as the templates used did not have the large extracellular or intracellular loops. However, the major substrate specificity site of most membrane transporters is the TMDs (Friedman et al., 1999, Ito et al., 2001). We showed the models were structural accurate using the validation procedures used and through using the helical wheel analysis. The models were therefore useful in assessing how amino acid changing variants influence the substrate binding cleft. We did, however, find discrepancies between our *in silico* predictive system to that observed *in vitro* (Leabman et al., 2002, Nies et al., 2011). One major limitation of our models that may answer this is the protein structures were in one conformation, whereas biologically these transporters change shape conformationally in order to transport substrates. Despite this the structural models provided an illustrative insight into what the genetic variants may do to the protein structure.

The patients in this cohort were receiving metformin for more than 3 months. This was to ensure patients had steady-state metformin plasma levels. However, some patients may not have been able to tolerate metformin for that length of

time and thus were not included in the cohort. It is known that GI intolerance leads to premature discontinuation of therapy in 4% of cases (Tarasova et al., 2012, Scheen, 1996, Bray et al., 2012, Haupt et al., 1991). Additionally, as discussed earlier, GI side effects were shown by Tarasova et al (Tarasova et al., 2012) to be associated with the rs113569197 variant. Our cross-sectional analysis therefore does not represent a true representation of a T2DM patient population on metformin as some participants who were likely to have stopped metformin were not included. Thus a prospective cohort study is required.

PMAT and OCT3 are known metformin transporters located on the apical membrane of ileal cells, which are responsible for metformin uptake into the cell (Han et al., 2015, Proctor et al., 2008). However, with regards to the basolateral membrane, there is conflicting evidence concerning the expression of drug transporters enterocyte basolateral membranes (Han et al., 2015, Mulgaonkar et al., 2013). The only reported metformin drug transporter located on ileal cell basolateral membranes is OCT1. Previous reports have suggested, but not provided evidence, that OCT1 is expressed on the basolateral membrane of enterocytes and thus aids the cellular transport of metformin from the cell to the blood (Mulgaonkar et al., 2013, Muller et al., 2005, Martel et al., 2001). However, Muller et al., 2005 observed strong OCT3 expression whereas they found weak expression of OCT1 on basolateral Caco-2 cell membranes. The Caco-2 cell line is derived from human epithelial adenoma cells which resemble small intestine polarised enterocytes. As Caco-2 cells are of tumorous origin, certain proteins might be over or under expressed compared to normal tissue. Therefore the use of primary human intestinal cells will be of greater use. Furthermore, OCT1 immunolabelling was observed mainly in the cytoplasm and to a lesser extent on the basolateral membrane, while OCT3 was strongly expressed at the apical membrane, in contrast to studies showing enterocyte basolateral OCT1 expression. Han et al., 2013 discovered OCT1 was not expressed on the basolateral membrane of human and mouse enterocytes and inhibition of the transporter did not influence basolateral transport of known OCT1 substrates. In summary, there is conflicting evidence to the expression of OCT1 in enterocytes, but the literature is suggesting that the

expression is minimal. Therefore the major drug transporters that may play a vital role in metformin absorption are most probably PMAT and OCT3.

An *in vitro* model system to characterise the effect of metformin-induced vitamin B<sub>12</sub> malabsorption may be beneficial. Such an intestinal cell line would require over expression of the vitamin B<sub>12</sub> receptor, Cubam, GI metformin drug transporters, OCT3 and PMAT and their amino acid variants. As described by Proctor et al., 2008, a trans-well assay using a primary human intestinal cells, rather than the Caco-2 cell line, could be constructed to provide insight to whether metformin may impair or inhibit vitamin B<sub>12</sub> absorption, translocation, or deplete energy status of the cells. Genetic variants in GI metformin drug transporters could then be included to determine their impact. Determining vitamin B<sub>12</sub> levels can be achieved using enzyme-linked immunosorbent assay ELISA or radiolabelled vitamin B<sub>12</sub> using the commonly used isotope <sup>57</sup>Co.

To summarise, this project has not found any association between OCT1 and OCT2 polymorphisms and vitamin B<sub>12</sub> deficiency. We have, however, observed that metformin induced vitamin B<sub>12</sub> deficiency is dose dependent, suggesting it exerts this adverse effect at the site of the intestine, leading to vitamin B<sub>12</sub> malabsorption. This observation complements those results and hypotheses from the literature, suggest that metformin could accumulate in the GI tract and lead to malabsorption. A number of questions however remain to be answered in order to fully understand the molecular mechanistic explanation of metformin-induced vitamin B<sub>12</sub> deficiency. Future research efforts aimed at defining the mechanism of vitamin B<sub>12</sub> malabsorption would provide insight into the complex mode of action of metformin (in terms of both efficacy and safety) which is still not clear despite its widespread use.

# **Appendices**

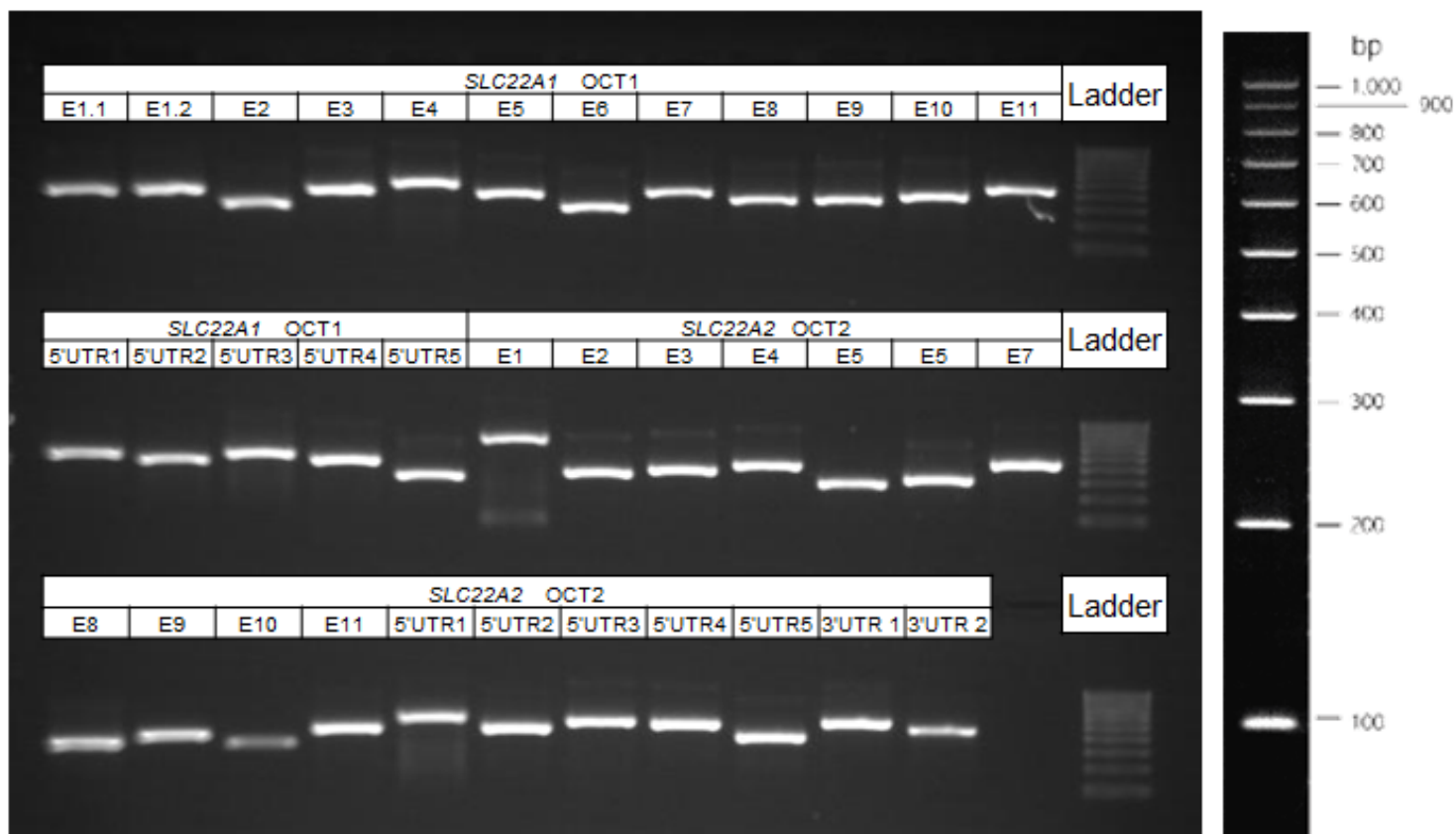


**Figure A2.1. Testing of *SLC22A1* and *SLC22A2* primers on reference DNA.**

Primers were designed to sequence all exons, including intron-exon boundaries plus up to 2 kb of 5'UTR sequence to capture variants in nearby regulatory elements. Product sizes ranged from 254 to 747 bp in length. Ladder inset shows molecular weights of DNA markers.

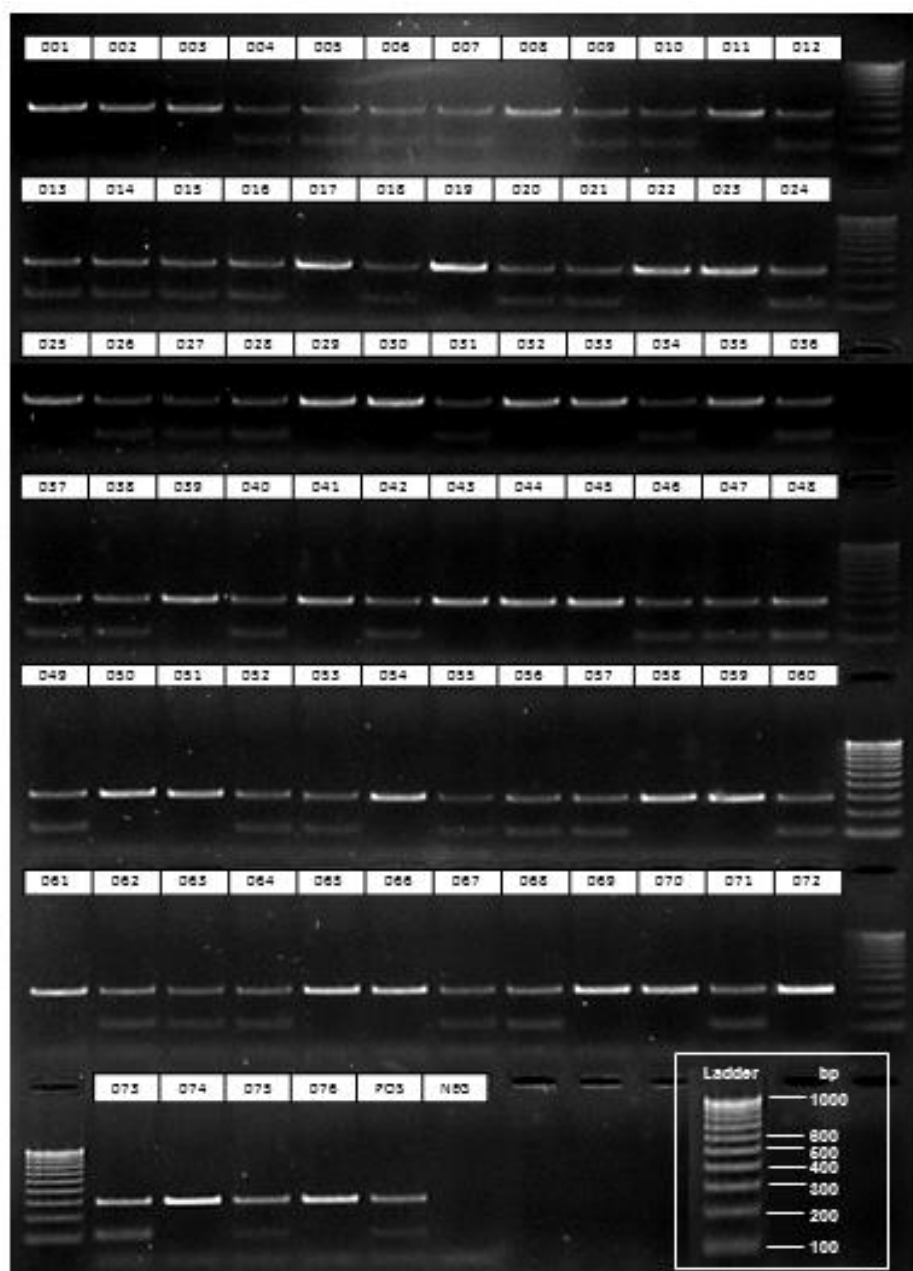


**Figure A2.2 Gender determination for the T2DM patient cohort.**

The amelogenin gene in the X chromosome expresses a 6 bp deletion in intron 1 relative to the Y chromosome. Gel electrophoresis resolves two bands (112 and 106 bp) for male gDNA whereas one is resolved for female gDNA

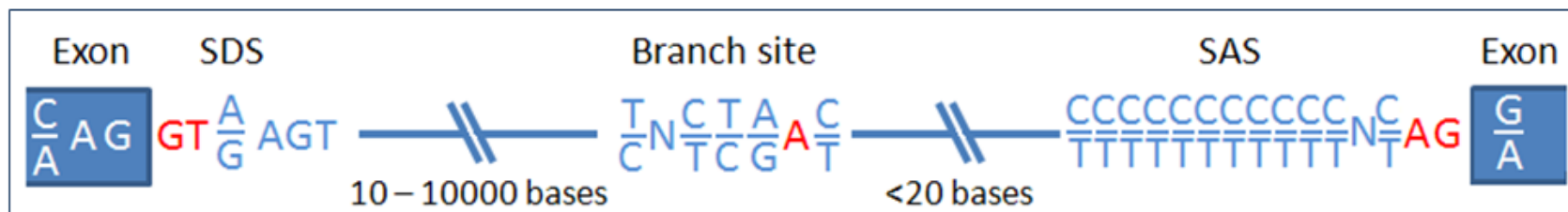
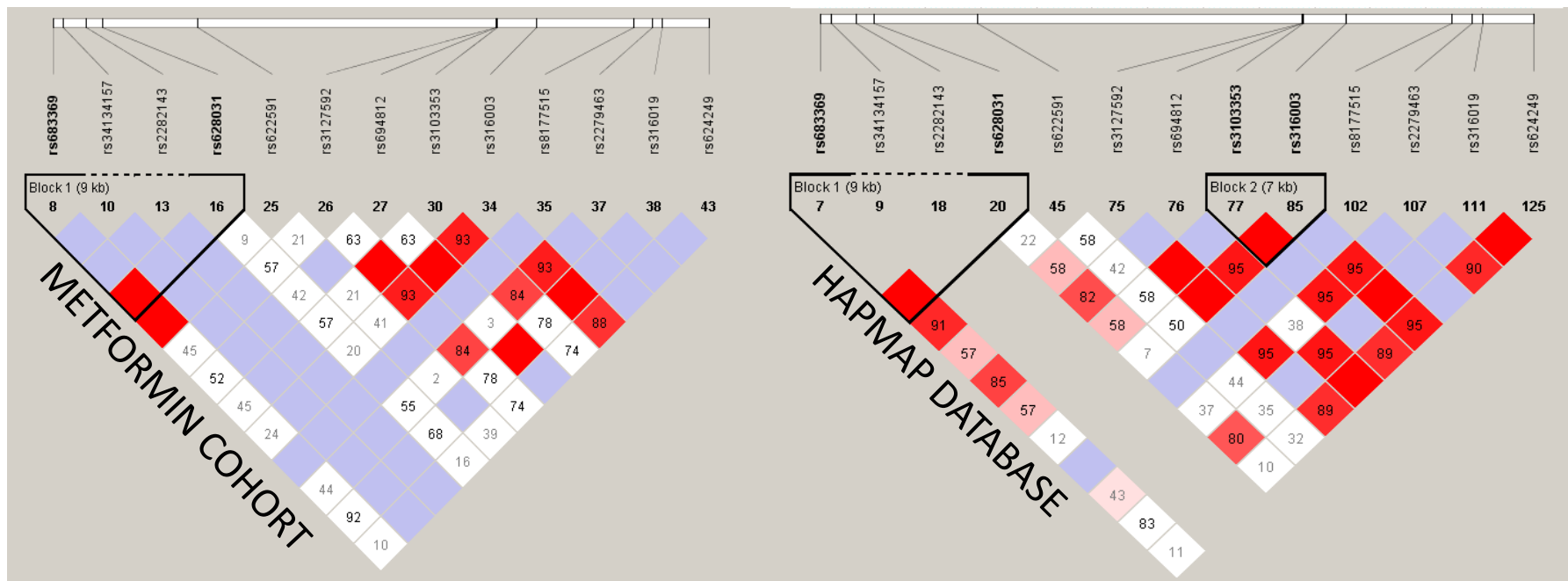


**Figure A2.3. Consensus sequences for intronic splice sites.**

The figure displays the nucleotide sequences required for alternative splicing. The blue boxes depict the ends of exons. Bases in red illustrate nucleotides that are almost invariant in eukaryotes. Other nucleotides represent the major nucleotides found at this site. SDS, splice donor site; SAS, splice acceptor site.



#### Appendix A2.4. Hardy-Weinberg analysis

Frequencies from our study, left, were compared with those available on the International HapMap project, right (release #28, Aug 2010). Allele frequencies for thirteen SNPs were available from the HapMap database for comparing MAF frequencies, including *SLC22A1* (rs683369, rs34134157, rs2282143, rs628031, rs622591) and *SLC22A2* (rs3127592, rs694812, rs3103353, rs316003, rs8177515, rs2279463, rs316019, rs624249). The comparison showed there were no significant deviations from Hardy-Weinberg equilibrium either in the metformin group or the HapMap data (Chi-squared test ( $X^2$ )  $P > 0.05$ ).



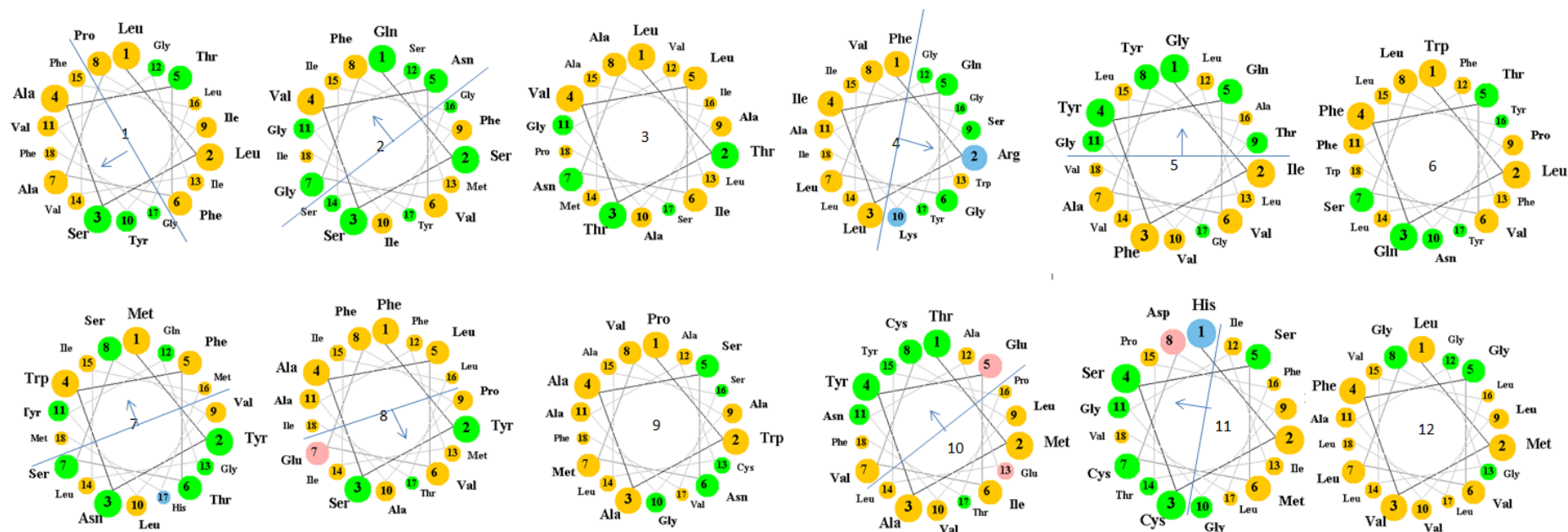


**Figure A3.2. Helical Wheel plots for OCT2**

The blue arrows show the predicted direction of the binding cleft where polar and/or charged residues interact with substrate binding. For TMDs 3 and 12 the  $\alpha$ -helices is composed of mainly hydrophobic residues and therefore predicted not to contribute to the binding cleft and substrate recognition. All TMDs correlated with helical wheel analysis suggesting TMDs are correctly aligned.

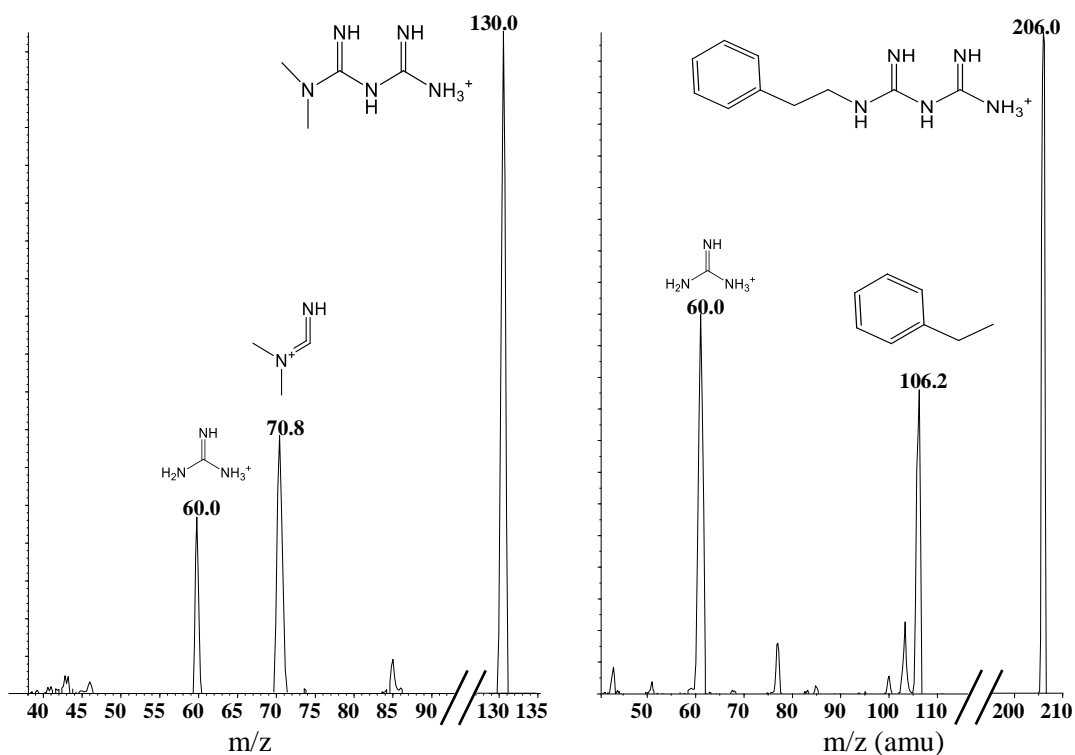


**Figure A4.1 Breakdown products of metformin and phenformin.**

Breakdown products of the analytes with predicted structures. Metformin parent peak at  $m/z$  130.0 and phenformin at  $m/z$  206.0. Chemical structures were drawn using ChemBioDraw Ultra.

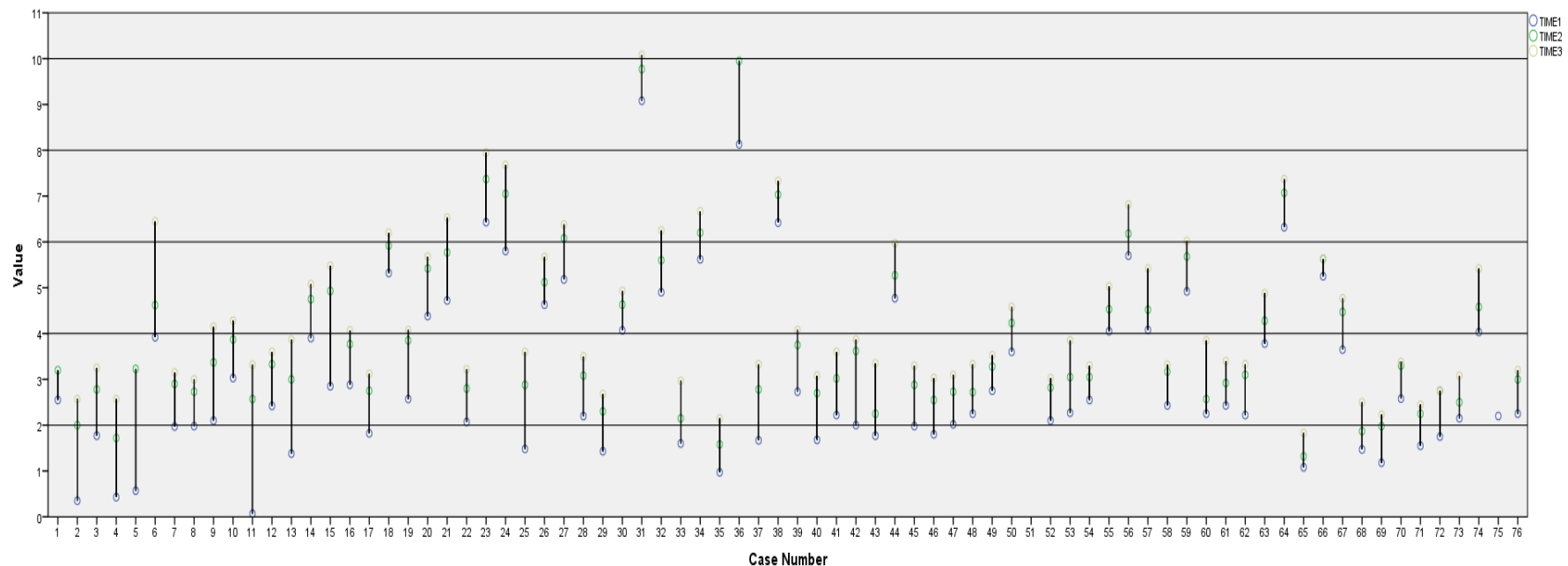


**Figure A5.1. Plasma sampling times.**

Time post metformin dose ordered in mean time sampling post dose. Metformin  $T_{max}$  ranges are reported from 1-3 hours (blue shaded box) with an average of 2.5 hours. The majority of samples were obtained within this range (42%), thereby capturing  $T_{max}$  values.

**Table A5.1. Multicollinearity between covariates.**

Covariates	$r^2$ correlation coefficient
Urea vs $CL_{CR}$	0.378
Urea vs creatinine	0.453
Urea vs age	0.1873
$CL_{CR}$ vs creatinine	0.2813
$CL_{CR}$ vs age	0.449
Age vs creatinine	0.089

All covariate pairs exhibited high multicollinearity with the exception age vs creatinine.

**Appendix 5.3 NONMEM Control File for base model**

```

$PROBLEM S_METFORMIN study
$DATA METFORMIN_2012.CSV IGNORE=C
$INPUT C ID TIME AMT EVID ADDL II SS CMT DV MDV
$SUBROUTINE ADVAN2 TRANS2
$PK
  BSVCL = ETA(1)
  BSVV = ETA(2)
  BSVKA = ETA(3)
  CL = THETA(1)*EXP(BSVCL)
  V = THETA(2)*EXP(BSVV)
  KA = THETA(3)*EXP(BSVKA)
  S2 = V/1000
$ERROR
  IPRED = F
  Y=F+F*ERR(1)+ERR(2)
$THETA
  (55) ;CL
  (550) ;V
  (0.51 FIX) ;KA
$OMEGA
  0.16 ;BSVCL
  0 FIX ;BSVV
  0 FIX ;BSVKA
$SIGMA
  0.09 ;PROP
  100 ;ADD
$ESTIMATION MAXEVAL=9999 SIGDIGITS=3 POSTHOC NOABORT METHOD=COND INTER
$COVARIANCE = E
  $TABLE ID TIME CL V CMT EVID ADDL II SS CMT DV MDV IPRED CWRES NPDE=PDERR BSVCL
  BSVV NOPRINT FILE=MET.fit ONEHEADER ESAMPLE=1000 SEED=1233344

```

**Appendix 5.4 NONMEM Control File for urea model**

```

$PROBLEM S_METFORMIN study
$DATA METFORMIN_2012.CSV IGNORE=C
$INPUT C ID TIME AMT EVID ADDL II SS CMT DV MDV UREA
$SUBROUTINE ADVAN2 TRANS2
$PK
  BSVCL = ETA(1)
  BSVV = ETA(2)
  BSVKA = ETA(3)
  TVCL= THETA(1)*((UREA/6.4)**THETA(4))
  CL = TVCL*EXP(BSVCL)
  V = THETA(2)*EXP(BSVV)
  KA = THETA(3)*EXP(BSVKA)
  S2 = V/1000
$ERROR
  IPRED = F
  Y=F+F*ERR(1)+ERR(2)
$THETA
  (59.44) ;CL
  (550) ;V
  (0.5) ;KA
  (-0.006);UREA
$OMEGA
  0.16 ;BSVCL
  0 FIX ;BSVV
  0 FIX ;BSVKA
$SIGMA
  0.09 ;PROP
  100 ;ADD
$ESTIMATION MAXEVAL=9999 SIGDIGITS=3 POSTHOC NOABORT METHOD=COND INTER
$COVARIANCE PRINT=E
$TABLE ID TIME CL V KA CMT EVID ADDL II SS CMT DV MDV UREA IPRED CWRES NPDE=PDERR BSVCL
BSVV NOPRINT FILE=MET40.fit ONEHEADER ESAMPLE=1000 SEED=1233344

```

**Table A6.1. Data transformation of metformin plasma levels; comparison of P values for linear regression analysis**

Demography	Untransformed	Log Transformed
Age	<b>0.009</b>	0.014
Height	0.378	0.635
Weight	0.541	0.847
BMI	0.859	0.97
IBW	0.5	0.701
LBW	0.18	0.615
BSA	0.419	0.721
Biochemistry & Haematology		
Vitamin B <sub>12</sub>	0.078	0.093
Folate	0.115	0.165
Lactate	<b>0.007</b>	0.011
Hb	0.451	0.292
HCT	0.636	0.405
MCV	0.281	0.517
Kidney function		
Creatinine	<b>0.014</b>	<b>0.013</b>
Urea	<b>&lt;0.0005</b>	<b>0.001</b>
CL <sub>CR</sub>	<b>0.015</b>	<b>0.049</b>
GFR	<b>0.027</b>	0.054
Liver function		
Albumin	0.845	0.896
AP	0.743	0.566
GammaGT	0.522	0.81
ALT	0.653	0.958
Bilirubin	0.131	0.074
Metformin variables		
Daily dose	<b>0.001</b>	<b>&lt;0.0005</b>
Trial dose	<b>0.001</b>	<b>&lt;0.0005</b>
Cumulative dose	<b>0.003</b>	<b>0.003</b>
Dose (mg/kg)	<b>&lt;0.0005</b>	<b>&lt;0.0005</b>
Plasma concentration	-	-
Length of T2DM	0.052	0.087
Length of treatment	<b>0.004</b>	0.007

Significant values are shown in bold.

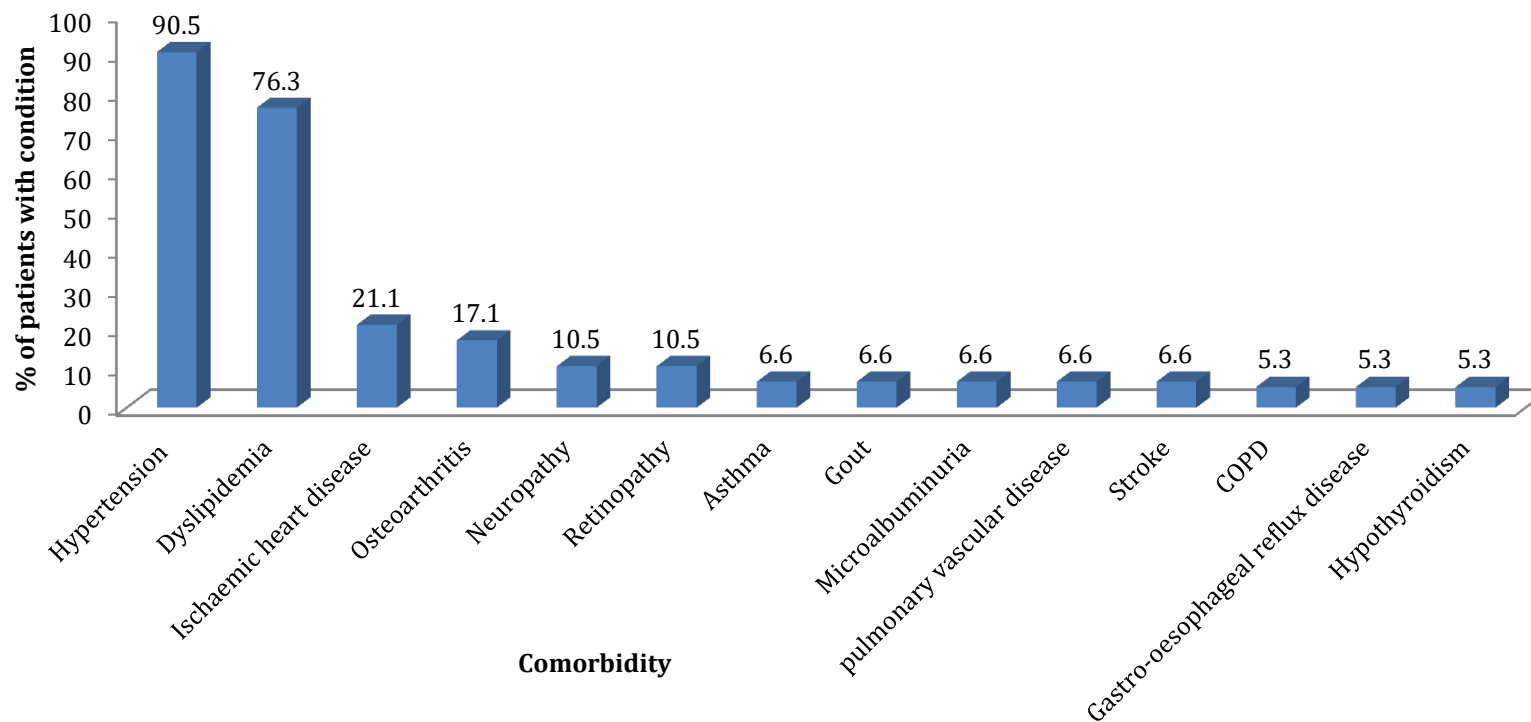


Figure A6.1. Comorbidity prevalence's in the patient group.

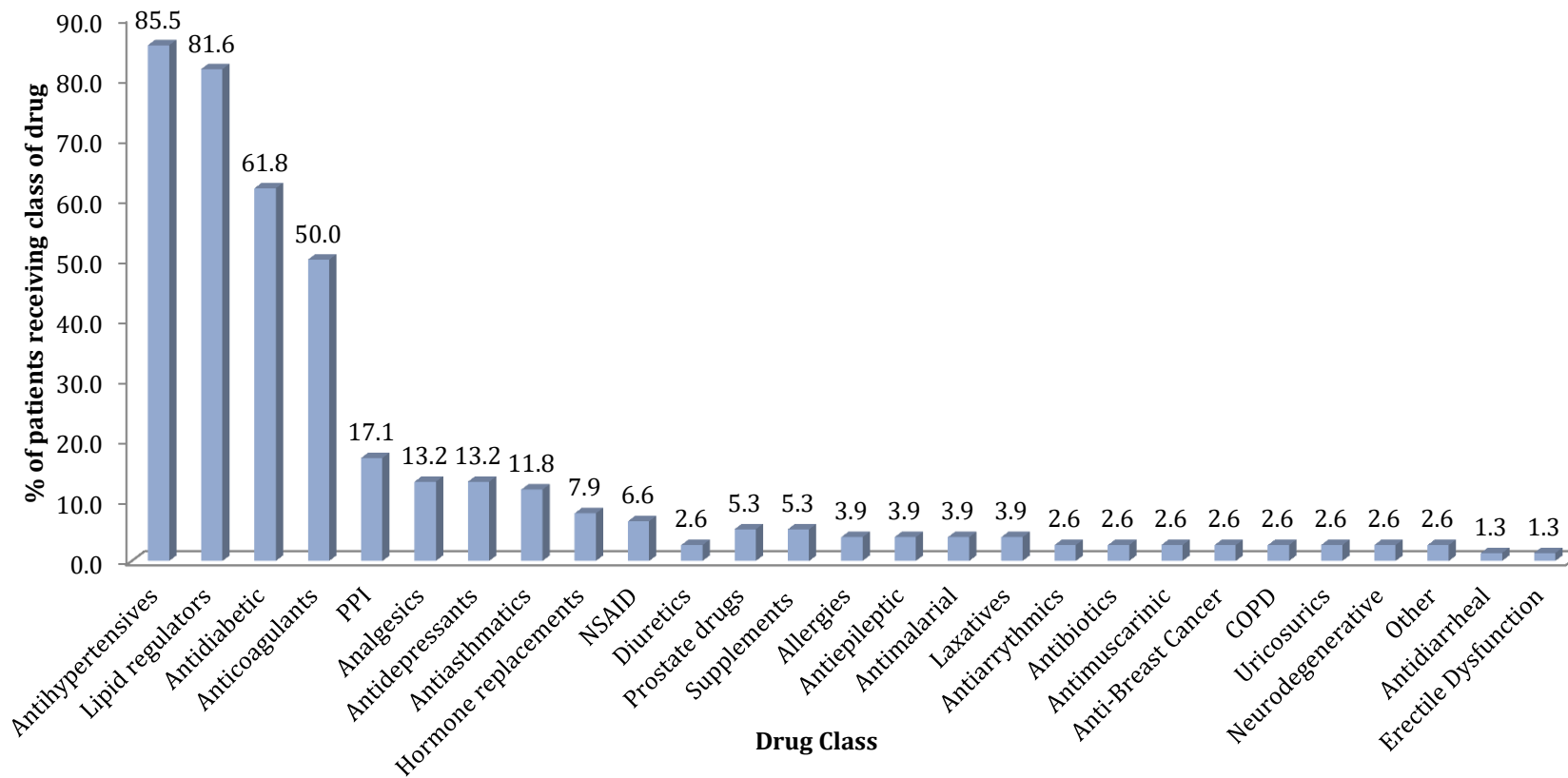


Figure A6.2. Concomitant drug class prevalence in the patient cohort

## Bibliography

- Available from: <http://genetics.bwh.harvard.edu/pph/> [accessed 10/12/10] [Online]. [Accessed 11/10 2010].
- Available from: <http://www.snps3d.org/> [accessed 12/12/10] [Online]. [Accessed].
2001. Food and Drug Administration (FDA) Guidance for Industry: Bioanalytical Method Validation.
- AARON, S., KUMAR, S., VIJAYAN, J., JACOB, J., ALEXANDER, M. & GNANAMUTHU, C. 2005. Clinical and laboratory features and response to treatment in patients presenting with vitamin B-12 deficiency-related neurological syndromes. *Neurology India*, 53, 55-58.
- ABRAMSON, J., SMIRNOVA, I., KASHO, V., VERNER, G., KABACK, H. R. & IWATA, S. 2003. Structure and mechanism of the lactose permease of *Escherichia coli*. *Science*, 301, 610-615.
- ABURUZ, S., MILLERSHIP, J. & MCELNAY, J. 2003. Determination of metformin in plasma using a new ion pair solid phase extraction technique and ion pair liquid chromatography. *Journal of Chromatography B-Analytical Technologies in the Biomedical and Life Sciences*, 798, 203-209.
- AGARWAL, A. A., JADHAV, P. R. & DESHMUKH, Y. A. 2014. Prescribing pattern and efficacy of anti-diabetic drugs in maintaining optimal glycemic levels in diabetic patients. *Journal of basic and clinical pharmacy*, 5, 79-83.
- ALLEN, L. H. 2008. Causes of vitamin B-12 and folate deficiency. *Food and Nutrition Bulletin*, 29, S20-S34.
- ALLEN, R. H., STABLER, S. P. & LINDENBAUM, J. 1998. Relevance of vitamins, homocysteine and other metabolites in neuropsychiatric disorders. *European Journal of Pediatrics*, 15, S122-S126.
- ALLEN, R. H., STABLER, S. P., SAVAGE, D. G. & LINDENBAUM, J. 1993. Metabolic abnormalities in cobalamin (vitamin-b(12) and folate-deficiency. *Faseb Journal*, 7, 1344-1353.
- AMINI, H., AHMADIANI, A. & GAZERANI, P. 2005. Determination of metformin in human plasma by high-performance liquid chromatography. *Journal of Chromatography B-Analytical Technologies in the Biomedical and Life Sciences*, 824, 319-322.
- ANDERSEN, C. B. F., MADSEN, M., STORM, T., MOESTRUP, S. K. & ANDERSEN, G. R. 2010. Structural basis for receptor recognition of vitamin-B-12-intrinsic factor complexes. *Nature*, 464, 445-U147.
- ANDRES, E., NOEL, E., KALTENBACH, G., PERRIN, A. E., VINZIO, S., GOICHOT, B., SCHLIENGER, J. L. & BLICKLE, J. F. 2003. Food-cobalamin malabsorption in elderly patients: A study of 60 patients. *Revue De Medecine Interne*, 24, 218-223.
- ANFOSSI, G., RUSSO, I., BONOMO, K. & TROVATI, M. 2010. The Cardiovascular Effects of Metformin: Further Reasons to Consider An Old Drug as a Cornerstone in the Therapy of Type 2 Diabetes Mellitus. *Current Vascular Pharmacology*, 8, 327-337.
- AOKI, M., TERADA, T., KAJIWARA, M., OGASAWARA, K., IKAI, I., OGAWA, O., KATSURA, T. & INUI, K. I. 2008. Kidney-specific expression of human organic cation transporter 2 (OCT2/SLC22A2) is regulated by DNA methylation. *American Journal of Physiology-Renal Physiology*, 295, F165-F170.
- ATKINSON, M. A. & EISENBARTH, G. S. 2001. Type 1 diabetes: new perspectives on disease pathogenesis and treatment. *Lancet*, 358, 221-229.

- ATWELL, C., LONG, A., YOO, W. & SOLOMON, S. 2012. Metformin And Proton Pump Inhibitors Effect On Vitamin B12 Levels. *Journal of Investigative Medicine*, 60, 435-435.
- BAILEY, R. L., CARMEL, R., GREEN, R., PFEIFFER, C. M., COGSWELL, M. E., OSTERLOH, J. D., SEMPOS, C. T. & YETLEY, E. A. 2011. Monitoring of vitamin B-12 nutritional status in the United States by using plasma methylmalonic acid and serum vitamin B-12. *American Journal of Clinical Nutrition*, 94, 552-561.
- BAKER, H., LEEVY, C. B., DEANGELIS, B., FRANK, O. & BAKER, E. R. 1998. Cobalamin (vitamin B-12) and holotranscobalamin changes in plasma and liver tissue in alcoholics with liver disease. *Journal of the American College of Nutrition*, 17, 235-238.
- BANTING, F. G., CAMPBELL, W. R. & FLETCHER, A. A. 1923. Further Clinical Experience with Insulin (Pancreatic Extracts) in the Treatment of Diabetes Mellitus. *British medical journal*, 1, 8-12.
- BARDIN, C., NOBECOURT, E., LARGER, E., CHAST, F., TRELUYER, J.-M. & URIEN, S. 2012. Population pharmacokinetics of metformin in obese and non-obese patients with type 2 diabetes mellitus. *European Journal of Clinical Pharmacology*, 68.
- BARRETT, J. C., FRY, B., MALLER, J. & DALY, M. J. 2005. Haploview: analysis and visualization of LD and haplotype maps. *Bioinformatics*, 21, 263-265.
- BAUMAN, W. A., SHAW, S., JAYATILLEKE, E., SPUNGEN, A. M. & HERBERT, V. 2000. Increased intake of calcium reverses vitamin B-12 malabsorption induced by metformin. *Diabetes Care*, 23, 1227-1231.
- BEAL, S. & SHEINER, L. 1980. THE NONMEM SYSTEM. *American Statistician*, 34, 118-119.
- BELCHER, G., LAMBERT, C., EDWARDS, G., URQUHART, R. & MATTHEWS, D. R. 2005. Safety and tolerability of pioglitazone, metformin, and gliclazide in the treatment of type 2 diabetes. *Diabetes Research and Clinical Practice*, 70, 53-62.
- BELL, D. S. H. 2010. Metformin-Induced Vitamin B12 Deficiency Presenting as a Peripheral Neuropathy. *Southern Medical Journal*, 103, 265-267.
- BENNETT-LOVSEY, R. M., HERBERT, A. D., STERNBERG, M. J. E. & KELLEY, L. A. 2008. Exploring the extremes of sequence/structure space with ensemble fold recognition in the program Phyre. *Proteins-Structure Function and Bioinformatics*, 70, 611-625.
- BERCHTOLP, BOLLI, P., ARBENZ, U. & KEISER, G. 1969. Disturbance of intestinal absorption following metformin therapy (observations on mode of action of biguanides). *Diabetologia*, 5, 405-&.
- BERGER, W., LAUFFENB.T & DENES, A. 1972. Effect of metformin on absorption of vitamin-B12. *Hormone and Metabolic Research*, 4, 311-&.
- BEULENS, J., HART, H., KUIJS, R., KOOIJMAN-BUITING, A. & RUTTEN, G. 2014. Influence of duration and dose of metformin on cobalamin deficiency in type 2 diabetes patients using metformin. *Acta Diabetologica*, 592-597.
- BIERMANN, J., LANG, D., GORBOULEV, V., KOEPESELL, H., SINDIC, A., SCHROTER, R., ZVIRBLIENE, A., PAVENSTADT, H., SCHLATTER, E. & CIARIMBOLI, G. 2006. Characterization of regulatory mechanisms and states of human organic cation transporter. *American Journal of Physiology-Cell Physiology*, 290, C1521-C1531.
- BIRN, H. 2006. The kidney in vitamin B-12 and folate homeostasis: characterization of receptors for tubular uptake of vitamins and carrier proteins. *American Journal of Physiology-Renal Physiology*, 291, F22-F36.
- BIRN, H., NEXO, E., CHRISTENSEN, E. I. & NIELSEN, R. 2003. Diversity in rat tissue accumulation of vitamin B-12 supports a distinct role for the kidney in vitamin B-12 homeostasis. *Nephrology Dialysis Transplantation*, 18, 1095-1100.
- BIRN, H., WILLNOW, T. E., NIELSEN, R., NORDEN, A. G. W., BONDSCH, C., MOESTRUP, S. K., NEXO, E. & CHRISTENSEN, E. I. 2002. Megalin is essential for renal proximal

- tubule reabsorption and accumulation of transcobalamin-B-12. *American Journal of Physiology-Renal Physiology*, 282, F408-F416.
- BOLEN, S., FELDMAN, L., VASSY, J., WILSON, L., YEH, H.-C., MARINOPOULOS, S., WILEY, C., SELVIN, E., WILSON, R., BASS, E. B. & BRANCATI, F. L. 2007. Systematic review: Comparative effectiveness and safety of oral medications for type 2 diabetes Mellitus. *Annals of Internal Medicine*, 147, 386-399.
- BONATE, P. L. 1999. The effect of collinearity on parameter estimates in nonlinear mixed effect models. *Pharmaceutical Research*, 16, 709-717.
- BONATE, P. L. 2011. Pharmacokinetic-Pharmacodynamic Modeling and Simulation, Second Edition. *Pharmacokinetic-Pharmacodynamic Modeling and Simulation, Second Edition*, 1-618.
- BONFIGLI, A. R., MANFRINI, S., GREGORIO, F., TESTA, R., TESTA, I., DE SIO, G. & COPPA, G. 1999. Determination of plasma metformin by a new cation-exchange HPLC technique. *Therapeutic Drug Monitoring*, 21, 330-334.
- BOR, M. V., NEXO, E. & HVAS, A. M. 2004. Holo-transcobalamin concentration and transcobalamin saturation reflect recent vitamin B-12 absorption better than does serum vitamin B-12. *Clinical Chemistry*, 50, 1043-1049.
- BOULE, N. G., HADDAD, E., KENNY, G. P., WELLS, G. A. & SIGAL, R. J. 2001. Effects of exercise on glycemic control and body mass in type 2 diabetes mellitus - A meta-analysis of controlled clinical trials. *Jama-Journal of the American Medical Association*, 286, 1218-1227.
- BOWER, M. J., COHEN, F. E. & DUNBRACK, R. L. 1997. Prediction of protein side-chain rotamers from a backbone-dependent rotamer library: A new homology modeling tool. *Journal of Molecular Biology*, 267, 1268-1282.
- BOYER, J. L. 2013. Bile Formation and Secretion. *Comprehensive Physiology*, 3, 1035-1078.
- BRAY, G. A., EDELSTEIN, S. L., CRANDALL, J. P., ARODA, V. R., FRANKS, P. W., FUJIMOTO, W., HORTON, E., JEFFRIES, S., MONTEZ, M., MUDALIAR, S., PI-SUNYER, F. X., WHITE, N. H., KNOWLER, W. C. & DIABET PREVENTION PROGRAM RES, G. 2012. Long-Term Safety, Tolerability, and Weight Loss Associated With Metformin in the Diabetes Prevention Program Outcomes Study. *Diabetes Care*, 35, 731-737.
- BRIANI, C., DALLA TORRE, C., CITTON, V., MANARA, R., POMPANIN, S., BINOTTO, G. & ADAMI, F. 2013. Cobalamin Deficiency: Clinical Picture and Radiological Findings. *Nutrients*, 5, 4521-4539.
- BRITISH NATIONAL FORMULARY, B. 2015. The British National Formulary 69.
- BRITAIN, H. G. 1998. Analytical Profiles of Drug Substances and Excipients. *Analytical Profiles of Drug Substances and Excipients*, xi+582p.
- BROWN, J. B., PEDULA, K., BARZILAY, J., HERSON, M. K. & LATARE, P. 1998. Lactic acidosis rates in type 2 diabetes. *Diabetes Care*, 21, 1659-1663.
- BURCKHARDT, G. & WOLFF, N. A. 2000. Structure of renal organic anion and cation transporters. *American Journal of Physiology-Renal Physiology*, 278, F853-F866.
- BUTTERFIELD, D. A., DI DOMENICO, F. & BARONE, E. 2014. Elevated risk of type 2 diabetes for development of Alzheimer disease: A key role for oxidative stress in brain. *Biochim Biophys Acta.*, 1842, 1693-1706. doi: 10.1016/j.bbadis.2014.06.010. Epub 2014 Jun 17.
- BUYSSCHAERT, M., WALLEMACQ, P. E., DRAMAIS, A. S. & HERMANS, M. P. 2000. Hyperhomocysteinemia in type 2 diabetes - Relationship to macroangiopathy, nephropathy, and insulin resistance. *Diabetes Care*, 23, 1816-1822.
- CALLAGHAN, T. S. & HADDEN, D. R. 1980. Megaloblastic-Anemia Due To Vitamin-B12 Malabsorption Associated With Long-Term Metformin Treatment. *British Medical Journal*, 280, 1214-1215.

- CALVO ROMERO, J. M. & RAMIRO LOZANO, J. M. 2012. Vitamin B(12) in type 2 diabetic patients treated with metformin. *Endocrinologia y nutricion : organo de la Sociedad Espanola de Endocrinologia y Nutricion*, 59, 487-90.
- CAMPBELL, D. B., LAVIELLE, R. & NATHAN, C. 1991. The Mode Of Action And Clinical-Pharmacology Of Gliclazide - A Review. *Diabetes Research and Clinical Practice*, 14, S21-S36.
- CANUTESCU, A. A., SHELENKOV, A. A. & DUNBRACK, R. L. 2003. A graph-theory algorithm for rapid protein side-chain prediction. *Protein Science*, 12, 2001-2014.
- CARLSEN, S. M., FOLLING, I., GRILL, V., BJERVE, K. S., SCHNEEDE, J. & REFSUM, H. 1997. Metformin increases total serum homocysteine Levels in non-diabetic male patients with coronary heart disease. *Scandinavian Journal of Clinical & Laboratory Investigation*, 57, 521-527.
- CARMEL, R., GREEN, R., ROSENBLATT, D. S. & WATKINS, D. 2003. Update on cobalamin, folate, and homocysteine. *Hematology / the Education Program of the American Society of Hematology. American Society of Hematology. Education Program*, 62-81.
- CARPENTER, M. A., KENDALL, R. G., OBRIEN, A. E., CHAPMAN, C., SEBASTIAN, J. P., BELFIELD, P. W. & NORFOLK, D. R. 1992. Reduced erythropoietin response to anemia in elderly patients with normocytic anemia. *European Journal of Haematology*, 49, 119-121.
- CARR, D. F., O'MEARA, H., JORGENSEN, A. L., CAMPBELL, J., HOBBS, M., MCCANN, G., VAN STAA, T. & PIRMOHAMED, M. 2013. SLC01B1 Genetic Variant Associated With Statin-Induced Myopathy: A Proof-of-Concept Study Using the Clinical Practice Research Datalink. *Clinical Pharmacology & Therapeutics*, 94, 695-701.
- CHAE, J.-W., BAEK, I.-H., LEE, B.-Y., CHO, S.-K. & KWON, K.-I. 2012. Population PK/PD analysis of metformin using the signal transduction model. *British Journal of Clinical Pharmacology*, 74.
- CHAN, S. C., LIU, C. L., LO, C. M., LAM, B. K., LEE, E. W., WONG, Y. & FAN, S. T. 2006. Estimating liver weight of adults by body weight and gender. *World Journal of Gastroenterology*, 12, 2217-2222.
- CHANG, C., EKINS, S., BAHADDURI, P. & SWAAN, P. W. 2006. Pharmacophore-based discovery of ligands for drug transporters. *Advanced Drug Delivery Reviews*, 58, 1431-1450.
- CHARLES, B., NORRIS, R., XIAO, X. N. & HAGUE, W. 2006. Population pharmacokinetics of metformin in late pregnancy. *Therapeutic Drug Monitoring*, 28, 67-72.
- CHATTHANAWAREE, W. 2011. Biomarkers of cobalamin (vitamin B12) deficiency and its application. *Journal of Nutrition Health & Aging*, 15, 227-231.
- CHEN, E. C., LIANG, X., YEE, S. W., GEIER, E. G., STOCKER, S. L., CHEN, L. & GIACOMINI, K. M. 2015. Targeted Disruption of Organic Cation Transporter 3 Attenuates the Pharmacologic Response to Metformin. *Molecular Pharmacology*, 88, 75-83.
- CHEN, L. G., PAWLIKOWSKI, B., SCHLESSINGER, A., MORE, S. S., STRYKE, D., JOHNS, S. J., PORTMAN, M. A., CHEN, E., FERRIN, T. E., SALI, A. & GIACOMINI, K. M. 2010a. Role of organic cation transporter 3 (SLC22A3) and its missense variants in the pharmacologic action of metformin. *Pharmacogenetics and Genomics*, 20, 687-699.
- CHEN, S., ZHOU, J., XI, M., JIA, Y., WONG, Y., ZHAO, J., DING, L., ZHANG, J. & WEN, A. 2013. Pharmacogenetic Variation and Metformin Response. *Current Drug Metabolism*, 14, 1070-1082.
- CHEN, V. B., ARENDALL, W. B., III, HEADD, J. J., KEEDY, D. A., IMMORMINO, R. M., KAPRAL, G. J., MURRAY, L. W., RICHARDSON, J. S. & RICHARDSON, D. C. 2010b. MolProbity: all-atom structure validation for macromolecular crystallography. *Acta Crystallographica Section D-Biological Crystallography*, 66, 12-21.

- CHEN, X. Y., GU, Q., QIU, F. & ZHONG, D. F. 2004. Rapid determination of metformin in human plasma by liquid chromatography-tandem mass spectrometry method. *Journal of Chromatography B-Analytical Technologies in the Biomedical and Life Sciences*, 802, 377-381.
- CHENG, C. L. & CHOU, C. H. 2001. Determination of metformin in human plasma by high-performance liquid chromatography with spectrophotometric detection. *Journal of Chromatography B*, 762, 51-58.
- CHOI, J. H., YEE, S. W., RAMIREZ, A. H., MORRISSEY, K. M., JANG, G. H., JOSKI, P. J., MEFFORD, J. A., HESSELSON, S. E., SCHLESSINGER, A., JENKINS, G., CASTRO, R. A., JOHNS, S. J., STRYKE, D., SALI, A., FERRIN, T. E., WITTE, J. S., KWOK, P. Y., RODEN, D. M., WILKE, R. A., MCCARTY, C. A., DAVIS, R. L. & GIACOMINI, K. M. 2011. A Common 5'-UTR Variant in MATE2-K Is Associated With Poor Response to Metformin. *Clinical Pharmacology & Therapeutics*, 90.
- CHRAST, R., SAHER, G., NAVE, K.-A. & VERHEIJEN, M. H. G. 2011. Lipid metabolism in myelinating glial cells: lessons from human inherited disorders and mouse models. *Journal of Lipid Research*, 52, 419-434.
- CHRISTENSEN, M. M. H., BRASCH-ANDERSEN, C., GREEN, H., NIELSEN, F., DAMKIER, P., BECK-NIELSEN, H. & BROSEN, K. 2011. The pharmacogenetics of metformin and its impact on plasma metformin steady-state levels and glycosylated hemoglobin A1c. *Pharmacogenetics and Genomics*, 21.
- CHRISTENSEN, M. M. H., PEDERSEN, R. S., STAGE, T. B., BRASCH-ANDERSEN, C., NIELSEN, F., DAMKIER, P., BECK-NIELSEN, H. & BROSEN, K. 2013. A gene-gene interaction between polymorphisms in the OCT2 and MATE1 genes influences the renal clearance of metformin. *Pharmacogenetics and Genomics*, 23, 526-534.
- CHUNG, J.-Y., CHO, S. K., KIM, T. H., KIM, K. H., JANG, G. H., KIM, C. O., PARK, E.-M., CHO, J.-Y., JANG, I.-J. & CHOI, J. H. 2013. Functional characterization of MATE2-K genetic variants and their effects on metformin pharmacokinetics. *Pharmacogenetics and Genomics*, 23, 365-373.
- COLE, C., BARBER, J. D. & BARTON, G. J. 2008. The Jpred 3 secondary structure prediction server. *Nucleic Acids Research*, 36, W197-W201.
- CRAIG, P. N. 1990. DRUG COMPENDIUM. Drayton, C. J. (Ed.). *Comprehensive Medicinal Chemistry: the Rational Design, Mechanistic Study and Therapeutic Application of Chemical Compounds, Vol. 6. Cumulative Subject Index and Drug Compendium. Xv+991p. Pergamon Press Plc: Oxford, England, Uk; New York, New York, USA. Illus, 237-965.*
- CULLEN, E., LIAO, J., LUKACSKO, P., NIECESTRO, R. & FRIEDHOFF, L. 2004. Pharmacokinetics and dose proportionality of extended-release metformin following administration of 1000, 1500, 2000 and 2500 mg in healthy volunteers. *Biopharmaceutics & Drug Disposition*, 25, 261-263.
- DANG, S. Y., SUN, L. F., HUANG, Y. J., LU, F. R., LIU, Y. F., GONG, H. P., WANG, J. W. & YAN, N. E. 2010. Structure of a fucose transporter in an outward-open conformation. *Nature*, 467, 734-U130.
- DE GROOT-KAMPHUIS, D. M., VAN DIJK, P. R., GROENIER, K. H., HOUWELING, S. T., BILO, H. J. G. & KLEEFSTRA, N. 2013. Vitamin B12 deficiency and the lack of its consequences in type 2 diabetes patients using metformin. *The Netherlands journal of medicine*, 71, 386-90.
- DE JAGER, C. A. 2014. Critical levels of brain atrophy associated with homocysteine and cognitive decline. *Neurobiology of aging*, 35 Suppl 2, S35-9.
- DE JAGER, J., KOOY, A., LEHERT, P., WULFFELE, M. G., VAN DER KOLK, J., BETS, D., VERBURG, J., DONKER, A. J. M. & STEHOUWER, C. D. A. 2010. Long term treatment with metformin in patients with type 2 diabetes and risk of vitamin B-12 deficiency: randomised placebo controlled trial. *British Medical Journal*, 340.

- DE OLIVEIRA BARALDI, C., LANCHOTE, V. L., DE JESUS ANTUNES, N., DE JESUS PONTE CARVALHO, T. M., DANTAS MOISES, E. C., DANTES MOISES, E. C., DUARTE, G. & CAVALLI, R. C. 2011. Metformin pharmacokinetics in nondiabetic pregnant women with polycystic ovary syndrome. *European journal of clinical pharmacology*, 67, 1027-33.
- DE ZEEUW, D., REMUZZI, G., PARVING, H. H., KEANE, W. F., ZHANG, Z. X., SHAHINFAR, S., SNAPINN, S., COOPER, M. E., MITCH, W. E. & BRENNER, B. M. 2004. Albuminuria, a therapeutic target for cardiovascular protection in type 2 diabetic patients with nephropathy. *Circulation*, 110, 921-927.
- DELAND, F. H. & NORTH, W. A. 1968. Relationship between liver size and body size. *Radiology*, 91, 1195-&.
- DELL'AGLIO, D. M., PERINO, L. J., KAZZI, Z., ABRAMSON, J., SCHWARTZ, M. D. & MORGAN, B. W. 2009. Acute Metformin Overdose: Examining Serum pH, Lactate Level, and Metformin Concentrations in Survivors Versus Nonsurvivors: A Systematic Review of the Literature. *Annals of Emergency Medicine*, 54, 818-823.
- DIABETES UK 2015. Diabetes: Facts and Statistics. [https://www.diabetes.org.uk/About\\_us/What-we-say/Statistics/](https://www.diabetes.org.uk/About_us/What-we-say/Statistics/)
- DICKENS, D., WEBB, S. D., ANTONYUK, S., GIANNOUDIS, A., OWEN, A., RAEDISCH, S., HASNAIN, S. S. & PIRMOHAMED, M. 2013. Transport of gabapentin by LAT1 (SLC7A5). *Biochemical Pharmacology*, 85, 1672-1683.
- DING, Y., JIA, Y., SONG, Y., LU, C., LI, Y., CHEN, M., WANG, M. & WEN, A. 2014. The effect of lansoprazole, an OCT inhibitor, on metformin pharmacokinetics in healthy subjects. *European Journal of Clinical Pharmacology*, 70, 141-146.
- DU BOIS, D. & DU BOIS, E. F. 1916. A formula to estimate the approximate surface area if height and weight be known. *Archives of Internal Medicine*, 17, 863-871.
- DUAN, H. & WANG, J. 2010. Selective Transport of Monoamine Neurotransmitters by Human Plasma Membrane Monoamine Transporter and Organic Cation Transporter 3. *Journal of Pharmacology and Experimental Therapeutics*, 335, 743-753.
- DUONG, J. K., KUMAR, S. S., KIRKPATRICK, C. M., GREENUP, L. C., ARORA, M., LEE, T. C., TIMMINS, P., GRAHAM, G. G., FURLONG, T. J., GREENFIELD, J. R., WILLIAMS, K. M. & DAY, R. O. 2013. Population Pharmacokinetics of Metformin in Healthy Subjects and Patients with Type 2 Diabetes Mellitus: Simulation of Doses According to Renal Function. *Clinical Pharmacokinetics*, 52, 373-384.
- ELIANA, F., SOEJONO, C. H., WIDJANARKO, A., ALBAR, Z. & BACHTIAR, A. 2005. Iron deposit state and risk factors for anemia in the elderly. *Acta medica Indonesiana*, 37, 118-25.
- EMEA 2010. EMEA release draft guideline on validation of bioanalytical methods. *Bioanalysis*, 2, 171-171.
- ENGEL, K. & WANG, J. 2005. Interaction of organic cations with a newly identified plasma membrane monoamine transporter. *Molecular Pharmacology*, 68, 1397-1407.
- ENGEL, K., ZHOU, M. Y. & WANG, J. 2004. Identification and characterization of a novel monoamine transporter in the human brain. *Journal of Biological Chemistry*, 279, 50042-50049.
- ERMENS, A. A. M., VLASVELD, L. T. & LINDEMANS, J. 2003. Significance of elevated cobalamin (vitamin B12) levels in blood. *Clinical Biochemistry*, 36, 585-590.
- ESPELAND, M., PI-SUNYER, X., BLACKBURN, G., BRANCATI, F. L., BRAY, G. A., BRIGHT, R., CLARK, J. M., CURTIS, J. M., ESPELAND, M. A., FOREYT, J. P., GRAVES, K., HAFFNER, S. M., HARRISON, B., HILL, J. O., HORTON, E. S., JAKICIC, J., JEFFERY, R. W., JOHNSON, K. C., KAHN, S., KELLEY, D. E., KITABCHI, A. E., KNOWLER, W. C., LEWIS, C. E., MASCHAK-CAREY, B. J., MONTGOMERY, B., NATHAN, D. M.,

- PATRICIO, J., PETERS, A., REDMON, J. B., REEVES, R. S., RYAN, D. H., SAFFORD, M., VAN DORSTEN, B., WADDEN, T. A., WAGENKNECHT, L., WESCHETHOBABEN, J., WING, R. R., YANOVSKI, S. Z. & LOOK, A. R. G. 2007. Reduction in weight and cardiovascular disease risk factors in individuals with type 2 diabetes - One-year results of the Look AHEAD trial. *Diabetes Care*, 30, 1374-1383.
- EVANS, J. M. M., DONNELLY, L. A., EMSLIE-SMITH, A. M., ALESSI, D. R. & MORRIS, A. D. 2005. Metformin and reduced risk of cancer in diabetic patients. *British Medical Journal*, 330, 1304-1305.
- EVANS, W. E. & MCLEOD, H. L. 2003. Drug therapy - Pharmacogenomics - Drug disposition, drug targets, and side effects. *New England Journal of Medicine*, 348, 538-549.
- FANKHANEL, S. & GASSMANN, B. 1998. Dietary Reference Intakes, Report 2 - Vitamins B-1, B-2, B-6, B-12, niacin, folic acid, pantothenic acid, biotin, choline. *Ernahrungs-Umschau*, 45, 298-299.
- FDA, U. D. O. H. H. S. 2001. Food and Drug Administration (FDA) Guidance for Industry: Bioanalytical Method Validation.
- FENG, Q.-Z., ZHAO, Y.-S. & LI, Y.-F. 2011. Effect of haemoglobin concentration on the clinical outcomes in patients with acute myocardial infarction and the factors related to haemoglobin. *BMC research notes*, 4, 142-142.
- FISER, A. & SALI, A. 2003. MODELLER: Generation and refinement of homology-based protein structure models. *Macromolecular Crystallography, Pt D*, 374, 461-+.
- FISHMAN, S. M., CHRISTIAN, P. & WEST, K. P. 2000. The role of vitamins in the prevention and control of anaemia. *Public health nutrition*, 3, 125-50.
- FOOD AND NUTRITION BOARD, I. O. M. 1998. Dietary Reference Intakes for Thiamin, Riboflavin, Niacin, Vitamin B6, Folate, Vitamin B12, Pantothenic Acid, Biotin, and Choline. Washington (DC): National Academies Press (US).
- FORETZ, M., HEBRARD, S., LECLERC, J., ZARRINPASHNEH, E., SOTY, M., MITHIEUX, G., SAKAMOTO, K., ANDREELLI, F. & VIOLLET, B. 2010. Metformin inhibits hepatic gluconeogenesis in mice independently of the LKB1/AMPK pathway via a decrease in hepatic energy state. *Journal of Clinical Investigation*, 120, 2355-2369.
- FRIEDMAN, K. J., KOLE, J., COHN, J. A., KNOWLES, M. R., SILVERMAN, L. M. & KOLE, R. 1999. Correction of aberrant splicing of the cystic fibrosis transmembrane conductance regulator (CFTR) gene by antisense oligonucleotides. *Journal of Biological Chemistry*, 274, 36193-36199.
- FYFE, J. C., MADSEN, M., HOJRUP, P., CHRISTENSEN, E. I., TANNER, S. M., DE LA CHAPELLE, A., HE, Q. C. & MOESTRUP, S. K. 2004. The functional cobalamin (vitamin B-12)-intrinsic factor receptor is a novel complex of cubilin and amnionless. *Blood*, 103, 1573-1579.
- GARBER, A. J., DUNCAN, T. G., GOODMAN, A. M., MILLS, D. J. & ROHLF, J. L. 1997. Efficacy of metformin in type II diabetes: Results of a double-blind, placebo-controlled, dose-response trial. *American Journal of Medicine*, 103, 491-497.
- GAUCHAN, D., JOSHI, N., GILL, A. S., PATEL, V., DEBARI, V. A., GURON, G. & MAROULES, M. 2012. Does an Elevated Serum Vitamin B-12 Level Mask Actual Vitamin B-12 Deficiency in Myeloproliferative Disorders? *Clinical Lymphoma Myeloma & Leukemia*, 12, 269-273.
- GAUTIER, J. F., FETITA, S., SOBNGWI, E. & SALAUN-MARTIN, C. 2005. Biological actions of the incretins GIP and GLP-1 and therapeutic perspectives in patients with type 2 diabetes. *Diabetes & Metabolism*, 31, 233-242.
- GIACOMINI, K. M., HUANG, S. M., TWEEDIE, D. J., BENET, L. Z., BROUWER, K. L. R., CHU, X. Y., DAHLIN, A., EVERS, R., FISCHER, V., HILLGREN, K. M., HOFFMASTER, K. A., ISHIKAWA, T., KEPPLER, D., KIM, R. B., LEE, C. A., NIEMI, M., POLLI, J. W.,

- SUGIYAMA, Y., SWAAN, P. W., WARE, J. A., WRIGHT, S. H., YEE, S. W., ZAMEK-GLISZCZYNSKI, M. J., ZHANG, L. & INTERNATIONAL, T. 2010. Membrane transporters in drug development. *Nature Reviews Drug Discovery*, 9, 215-236.
- GIANNOUDIS, A., WANG, L., JORGENSEN, A. L., XINARIANOS, G., DAVIES, A., PUSHPAKOM, S., LILOGLOU, T., ZHANG, J.-E., AUSTIN, G., HOLYOAKE, T. L., FORONI, L., KOTTARIDIS, P. D., MUELLER, M. C., PIRMOHAMED, M. & CLARK, R. E. 2013. The hOCT1 SNPs M420del and M408V alter imatinib uptake and M420del modifies clinical outcome in imatinib-treated chronic myeloid leukemia. *Blood*, 121, 628-637.
- GILLIES, C. L., ABRAMS, K. R., LAMBERT, P. C., COOPER, N. J., SUTTON, A. J., HSU, R. T. & KHUNTI, K. 2007. Pharmacological and lifestyle interventions to prevent or delay type 2 diabetes in people with impaired glucose tolerance: systematic review and meta-analysis. *British Medical Journal*, 334, 299-302B.
- GIRDWOOD, R. H. 1968. Abnormalities of vitamin b12 and folic acid metabolism-their influence on nervous system. *Proceedings of the Nutrition Society*, 27, 101-&.
- GOERGEN, S. K., RUMBOLD, G., COMPTON, G. & HARRIS, C. 2010. Systematic Review of Current Guidelines, and Their Evidence Base, on Risk of Lactic Acidosis after Administration of Contrast Medium for Patients Receiving Metformin. *Radiology*, 254, 261-269.
- GOHLKE, H., HENDLICH, M. & KLEBE, G. 2000. Knowledge-based scoring function to predict protein-ligand interactions. *Journal of Molecular Biology*, 295, 337-356.
- GOLDSTEIN, D. E., LITTLE, R. R., LORENZ, R. A., MALONE, J. I., NATHAN, D., PETERSON, C. M. & SACKS, D. B. 2004. Tests of glycemia in diabetes. *Diabetes Care*, 27, 1761-1773.
- GONG, L., GOSWAMI, S., GIACOMINI, K. M., ALTMAN, R. B. & KLEIN, T. E. 2012. Metformin pathways: pharmacokinetics and pharmacodynamics. *Pharmacogenetics and Genomics*, 22, 820-827.
- GRAHAM, G. G., PUNT, J., ARORA, M., DAY, R. O., DOOGUE, M. P., DUONG, J. K., FURLONG, T. J., GREENFIELD, J. R., GREENUP, L. C., KIRKPATRICK, C. M., RAY, J. E., TIMMINS, P. & WILLIAMS, K. M. 2011. Clinical Pharmacokinetics of Metformin. *Clinical Pharmacokinetics*, 50, 81-98.
- GRANT, M. A. 2009. Protein Structure Prediction in Structure-Based Ligand Design and Virtual Screening. *Combinatorial Chemistry & High Throughput Screening*, 12, 940-960.
- GRANTHAM, R. 1974. AMINO-ACID DIFFERENCE FORMULA TO HELP EXPLAIN PROTEIN EVOLUTION. *Science*, 185, 862-864.
- GREIBE, E., MILLER, J. W., FOUTOUHI, S. H., GREEN, R. & NEXO, E. 2013. Metformin increases liver accumulation of vitamin B12-An experimental study in rats. *Biochimie*, 95, 1062-1065.
- GRINFELD, J., GERRARD, G., ALIKIAN, M., ALONSO-DOMINGUEZ, J., ALE, S., VALGANON, M., NTELIOPOULOS, G., WHITE, D., MARIN, D., HEDGLEY, C., O'BRIEN, S., CLARK, R., GOLDMAN, J. M., MILOJKOVIC, D., APPERLEY, J. F. & FORONI, L. 2013. A common novel splice variant of SLC22A1 (OCT1) is associated with impaired responses to imatinib in patients with chronic myeloid leukaemia. *British Journal of Haematology*, 163, 631-639.
- GROSS, J. L., DE AZEVEDO, M. J., SILVEIRO, S. P., CANANI, L. H., CARAMORI, M. L. & ZELMANOVITZ, T. 2005. Diabetic nephropathy: Diagnosis, prevention, and treatment. *Diabetes Care*, 28, 164-176.
- GRUBER, A. R., FALLMANN, J., KRATOCHVILL, F., KOVARIK, P. & HOFACKER, I. L. 2011. AREsite: a database for the comprehensive investigation of AU-rich elements. *Nucleic Acids Research*, 39, D66-D69.
- GRUEN, B., KIESSLING, M. K., BURHENNE, J., RIEDEL, K.-D., WEISS, J., RAUCH, G., HAEFELI, W. E. & CZOCK, D. 2013. Trimethoprim-metformin interaction and its

- genetic modulation by OCT2 and MATE1 transporters. *British Journal of Clinical Pharmacology*, 76, 787-796.
- GUARIGUATA, L., WHITING, D. R., HAMBLETON, I., BEAGLEY, J., LINNENKAMP, U. & SHAW, J. E. 2014. Global estimates of diabetes prevalence for 2013 and projections for 2035. *Diabetes Research and Clinical Practice*, 103, 137-149.
- HAN, T., EVERETT, R. S., PROCTOR, W. R., NG, C. M., COSTALES, C. L., BROUWER, K. L. R. & THAKKER, D. R. 2013. Organic Cation Transporter 1 (OCT1/mOct1) Is Localized in the Apical Membrane of Caco-2 Cell Monolayers and Enterocytes. *Molecular Pharmacology*, 84, 182-189.
- HAN, T., PROCTOR, W. R., COSTALES, C. L., CAI, H., EVERETT, R. S. & THAKKER, D. R. 2015. Four Cation-Selective Transporters Contribute to Apical Uptake and Accumulation of Metformin in Caco-2 Cell Monolayers. *Journal of Pharmacology and Experimental Therapeutics*, 352, 519-528.
- HARDIE, D. G. 2007. AMP-activated protein kinase as a drug target. *Annual Review of Pharmacology and Toxicology*, 47, 185-210.
- HAUPT, E., KNICK, B., KOSCHINSKY, T., LIEBERMEISTER, H., SCHNEIDER, J. & HIRCHE, H. 1991. Oral Antidiabetic Combination Therapy With Sulfonylureas And Metformin. *Diabetes & Metabolism*, 17, 224-231.
- HE, L., SABET, A., DJEDJOS, S., MILLER, R., SUN, X. J., HUSSAIN, M. A., RADOVICK, S. & WONDISFORD, F. E. 2009. Metformin and Insulin Suppress Hepatic Gluconeogenesis through Phosphorylation of CREB Binding Protein. *Cell*, 137, 635-646.
- HE, Q. C., MADSEN, M., KILKENNEY, A., GREGORY, B., CHRISTENSEN, E. I., VORUM, H., HOJRUP, P., SCHAFFER, A. A., KIRKNESS, E. F., TANNER, S. M., DE LA CHAPELLE, A., GIGER, U., MOESTRUP, S. K. & FYFE, J. C. 2005. Amnionless function is required for cubilin brush-border expression and intrinsic factor-cobalamin (vitamin B-12) absorption in vivo. *Blood*, 106, 1447-1453.
- HE, X. A., SZEWCZYK, P., KARYAKIN, A., EVIN, M., HONG, W. X., ZHANG, Q. H. & CHANG, G. 2010. Structure of a cation-bound multidrug and toxic compound extrusion transporter. *Nature*, 467, 991-U139.
- HEALTH QUALITY, O. 2013. Vitamin B12 and cognitive function: an evidence-based analysis. *Ontario health technology assessment series*, 13, 1-45.
- HEDIGER, M. A., ROMERO, M. F., PENG, J. B., ROLFS, A., TAKANAGA, H. & BRUFORD, E. A. 2004. The ABCs of solute carriers: physiological, pathological and therapeutic implications of human membrane transport proteins - Introduction. *Pflugers Archiv-European Journal of Physiology*, 447, 465-468.
- HEX, N., BARTLETT, C., WRIGHT, D., TAYLOR, M. & VARLEY, D. 2012. Estimating the current and future costs of Type 1 and Type 2 diabetes in the UK, including direct health costs and indirect societal and productivity costs. *Diabetic Medicine*, 29, 855-862.
- HIGASHI, K., IMAMURA, M., FUDO, S., UEMURA, T., SAIKI, R., HOSHINO, T., TOIDA, T., KASHIWAGI, K. & IGARASHI, K. 2014. Identification of Functional Amino Acid Residues Involved in Polyamine and Agmatine Transport by Human Organic Cation Transporter 2. *Plos One*, 9.
- HIRAI, T., HEYMANN, J. A. W., SHI, D., SARKER, R., MALONEY, P. C. & SUBRAMANIAM, S. 2002. Three-dimensional structure of a bacterial oxalate transporter. *Nature Structural Biology*, 9, 597-600.
- HO, H. T. B., XIA, L. & WANG, J. 2012. Residue Ile89 in human plasma membrane monoamine transporter influences its organic cation transport activity and sensitivity to inhibition by dilazep. *Biochemical Pharmacology*, 84, 383-390.
- HOME, P., MANT, J., DIAZ, J., TURNER, C. & GUIDELINE DEV, G. 2008. Guidelines - Management of type 2 diabetes: updated NICE guidance. *British Medical Journal*, 336, 1306-1308.

- HONG, Y., ROHATAGI, S., HABTEMARIAM, B., WALKER, J. R., SCHWARTZ, S. L. & MAGER, D. E. 2008. Population exposure-response modeling of metformin in patients with type 2 diabetes mellitus. *Journal of Clinical Pharmacology*, 48.
- HOOGEVEEN, E. K., KOSTENSE, P. J., JAKOBS, C., BOUTER, L. M., HEINE, R. J. & STEHOUWER, C. D. A. 1997. Does metformin increase the serum total homocysteine level in non-insulin-dependent diabetes mellitus? *Journal of Internal Medicine*, 242, 389-394.
- HUANG, Y. F., LEMIEUX, M. J., SONG, J. M., AUER, M. & WANG, D. N. 2003. Structure and mechanism of the glycerol-3-phosphate transporter from *Escherichia coli*. *Science*, 301, 616-620.
- HULISZ, D. T., BONFIGLIO, M. F. & MURRAY, R. D. 1998. Metformin-associated lactic acidosis. *The Journal of the American Board of Family Practice / American Board of Family Practice*, 11, 233-6.
- HUME, R. 1966. Prediction Of Lean Body Mass From Height And Weight. *Journal of Clinical Pathology*, 19, 389-&.
- HUNDAL, R. S., KRSSAK, M., DUFOUR, S., LAURENT, D., LEBON, V., CHANDRAMOULI, V., INZUCCHI, S. E., SCHUMANN, W. C., PETERSEN, K. F., LANDAU, B. R. & SHULMAN, G. I. 2000. Mechanism by which metformin reduces glucose production in type 2 diabetes. *Diabetes*, 49, 2063-2069.
- HUNT, R., SAUNA, Z. E., AMBUDKAR, S. V., GOTTESMAN, M. M. & KIMCHI-SARFATY, C. 2009. Silent (Synonymous) SNPs: Should We Care About Them? *Single Nucleotide Polymorphisms: Methods and Protocols, Second Edition*, 578, 23-39.
- HUTTUNEN, K. M., RAUTIO, J., LEPPANEN, J., VEPSALAINEN, J. & KESKI-RAHKONEN, P. 2009. Determination of metformin and its prodrugs in human and rat blood by hydrophilic interaction liquid chromatography. *Journal of Pharmaceutical and Biomedical Analysis*, 50, 469-474.
- HVAS, A. M. & NEXO, E. 2003. Holotranscobalamin as a predictor of vitamin B-12 status. *Clinical Chemistry and Laboratory Medicine*, 41, 1489-1492.
- INZUCCHI, S. E. 2002. Oral antihyperglycemic therapy for type 2 diabetes - Scientific review. *Jama-Journal of the American Medical Association*, 287, 360-372.
- IRSIGLER, K., KRITZ, H., REGAL, H. & KASPAR, L. 1979. Biguanide-Induced And Biguanide-Associated Lactic-Acidosis - Serum And Tissue Biguanide Levels In Hyperlactemia And Lactic-Acidosis. *Wiener Klinische Wochenschrift*, 91, 59-65.
- ITO, K., SUZUKI, H. & SUGIYAMA, Y. 2001. Charged amino acids in the transmembrane domains are involved in the determination of the substrate specificity of rat Mrp2. *Molecular Pharmacology*, 59, 1077-1085.
- ITODA, M., SAITO, Y., MAEKAWA, K., HICHIYA, H., KOMAMURA, K., KAMAKURA, S., KITAKAZE, M., TOMOIKE, H., UENO, K., OZAWA, S. & SAWADA, J.-I. 2004. Seven novel single nucleotide polymorphisms in the human SLC22A1 gene encoding organic cation transporter 1 (OCT1). *Drug Metab Pharmacokinet*, 19, 308-12.
- JERMENDY, G. & RUGGENENTI, P. 2007. Preventing microalbuminuria in patients with type 2 diabetes. *Diabetes-Metabolism Research and Reviews*, 23, 100-110.
- JOHNSON, M. A. 2007. If high folic acid aggravates Vitamin B-12 deficiency what should be done about it? *Nutrition Reviews*, 65, 451-458.
- JOINT FORMULARY COMMITTEE 2014. *British National Formulary*. BMJ Group and Pharmaceutical Pres.
- JONES, G. C., MACKLIN, J. P. & ALEXANDER, W. D. 2003. Contraindications to the use of metformin - Evidence suggests that it is time to amend the list. *British Medical Journal*, 326, 4-5.
- JONKER, J. W. & SCHINKEL, A. H. 2004. Pharmacological and physiological functions of the polyspecific organic cation transporters: OCT1, 2, and 3 (SLC22A1-3). *Journal of Pharmacology and Experimental Therapeutics*, 308, 2-9.

- KAHN, S. E. & BUSE, J. B. 2015. Medications for type 2 diabetes: how will we be treating patients in 50 years? *Diabetologia*, 58, 1735-1739.
- KAJBAF, F. D., MARC. LALAU, JEAN-DANIEL. 2015. Therapeutic Concentrations of Metformin: A Systematic Review. *Clinical Pharmacokinetics*, [Epub ahead of print].
- KAJIWARA, M., TERADA, T., ASAKA, J.-I., AOKI, M., KATSURA, T., IKAI, I. & INUI, K.-I. 2008. Regulation of basal core promoter activity of human organic cation transporter 1 (OCT1/SLC22A1). *American Journal of Physiology-Gastrointestinal and Liver Physiology*, 295, G1211-G1216.
- KAJIWARA, M., TERADA, T., OGASAWARA, K., IWANO, J., KATSURA, T., FUKATSU, A., DOI, T. & INUI, K.-I. 2009. Identification of multidrug and toxin extrusion (MATE1 and MATE2-K) variants with complete loss of transport activity. *Journal of Human Genetics*, 54, 40-46.
- KANG, D., YUN, J.-S., KO, S.-H., LIM, T.-S., AHN, Y.-B., PARK, Y.-M. & KO, S.-H. 2014. Higher Prevalence of Metformin-Induced Vitamin B-12 Deficiency in Sulfonylurea Combination Compared with Insulin Combination in Patients with Type 2 Diabetes: A Cross-Sectional Study. *Plos One*, 9.
- KELLEY, L. A. & STERNBERG, M. J. E. 2009. Protein structure prediction on the Web: a case study using the Phyre server. *Nature Protocols*, 4, 363-371.
- KERB, R., BRINKMANN, U., CHATSKAIA, N., GORBUNOV, D., GORBOULEV, V., MORNHINWEG, E., KEIL, A., EICHELBAUM, M. & KOEPESELL, H. 2002. Identification of genetic variations of the human organic cation transporter hOCT1 and their functional consequences. *Pharmacogenetics*, 12, 591-595.
- KIMURA, N., MASUDA, S., TANIHARA, Y., UEO, H., OKUDA, M., KATSURA, T. & INUI, K.-I. 2005a. Metformin is a superior substrate for renal organic cation transporter OCT2 rather than hepatic OCT1. *Drug Metab Pharmacokinet*, 20, 379-86.
- KIMURA, N., OKUDA, M. & INUI, K. 2005b. Metformin transport by renal basolateral organic cation transporter hOCT2. *Pharmaceutical Research*, 22, 255-259.
- KIRPICHNIKOV, D., MCFARLANE, S. I. & SOWERS, J. R. 2002. Metformin: An update. *Annals of Internal Medicine*, 137, 25-33.
- KLEIN, R. 2002. Prevention of visual loss from diabetic retinopathy. *Survey of Ophthalmology*, 47, S246-S252.
- KOEPESELL, H., LIPS, K. & VOLK, C. 2007. Polyspecific organic cation transporters: Structure, function, physiological roles, and biopharmaceutical implications. *Pharmaceutical Research*, 24, 1227-1251.
- KOETTGEN, A., GLAZER, N. L., DEGHAN, A., HWANG, S.-J., KATZ, R., LI, M., YANG, Q., GUDNASON, V., LAUNER, L. J., HARRIS, T. B., SMITH, A. V., ARKING, D. E., ASTOR, B. C., BOERWINKLE, E., EHRET, G. B., RUCZINSKI, I., SCHARPF, R. B., CHEN, Y.-D. I., DE BOER, I. H., HARITUNIANS, T., LUMLEY, T., SARNAK, M., SISCOVICK, D., BENJAMIN, E. J., LEVY, D., UPADHYAY, A., AULCHENKO, Y. S., HOFMAN, A., RIVADENEIRA, F., UITTERLINDEN, A. G., VAN DUIJN, C. M., CHASMAN, D. I., PARE, G., RIDKER, P. M., KAO, W. H. L., WITTEMAN, J. C., CORESH, J., SHLIPAK, M. G. & FOX, C. S. 2009. Multiple loci associated with indices of renal function and chronic kidney disease. *Nature Genetics*, 41, 712-717.
- KOYU, A., OUT, M., LEHERT, P., SCHALKWIJK, C. G. & STEHOUWER, C. D. A. 2013. Metformin treatment is associated with increased serum levels of methylmalonic acid in patients with type 2 diabetes treated with insulin: a placebo-controlled 4-year trial. *Diabetologia*, 56, S386-S386.
- KOS, E., LISZEK, M. J., EMANUELE, M. A., DURAZO-ARVIZU, R. & CAMACHO, P. 2012. effect of metformin therapy on vitamin d and vitamin b-12 levels in patients with type 2 diabetes mellitus. *Endocrine Practice*, 18, 179-184.

- KRISSINEL, E. & HENRICK, K. 2004. Secondary-structure matching (SSM), a new tool for fast protein structure alignment in three dimensions. *Acta Crystallographica Section D-Biological Crystallography*, 60, 2256-2268.
- KROGH, A., LARSSON, B., VON HEIJNE, G. & SONNHAMMER, E. L. L. 2001. Predicting transmembrane protein topology with a hidden Markov model: Application to complete genomes. *Journal of Molecular Biology*, 305, 567-580.
- KRUSE, J. A. 2001. Metformin-associated lactic acidosis. *Journal of Emergency Medicine*, 20, 267-272.
- LALAU, J. D. & RACE, J. M. 1999. Lactic acidosis in metformin-treated patients - Prognostic value of arterial lactate levels and plasma metformin concentrations. *Drug Safety*, 20, 377-384.
- LANDER, E. S., LINTON, L. M., BIRREN, B., NUSBAUM, C., ZODY, M. C., BALDWIN, J., DEVON, K., DEWAR, K., DOYLE, M., FITZHUGH, W., FUNKE, R., GAGE, D., HARRIS, K., HEAFORD, A., HOWLAND, J., KANN, L., LEHOCZKY, J., LEVINE, R., MCEWAN, P., MCKERNAN, K., MELDRIM, J., MESIROV, J. P., MIRANDA, C., MORRIS, W., NAYLOR, J., RAYMOND, C., ROSETTI, M., SANTOS, R., SHERIDAN, A., SOUGNEZ, C., STANGE-THOMANN, N., STOJANOVIC, N., SUBRAMANIAN, A., WYMAN, D., ROGERS, J., SULSTON, J., AINSCOUGH, R., BECK, S., BENTLEY, D., BURTON, J., CLEE, C., CARTER, N., COULSON, A., DEADMAN, R., DELOUKAS, P., DUNHAM, A., DUNHAM, I., DURBIN, R., FRENCH, L., GRAFHAM, D., GREGORY, S., HUBBARD, T., HUMPHRAY, S., HUNT, A., JONES, M., LLOYD, C., MCMURRAY, A., MATTHEWS, L., MERCER, S., MILNE, S., MULLIKIN, J. C., MUNGALL, A., PLUMB, R., ROSS, M., SHOWNKEEN, R., SIMS, S., WATERSTON, R. H., WILSON, R. K., HILLIER, L. W., MCPHERSON, J. D., MARRA, M. A., MARDIS, E. R., FULTON, L. A., CHINWALLA, A. T., PEPIN, K. H., GISH, W. R., CHISSOE, S. L., WENDL, M. C., DELEHAUNTY, K. D., MINER, T. L., DELEHAUNTY, A., KRAMER, J. B., COOK, L. L., FULTON, R. S., JOHNSON, D. L., MINX, P. J., CLIFTON, S. W., HAWKINS, T., BRANSCOMB, E., PREDKI, P., RICHARDSON, P., WENNING, S., SLEZAK, T., DOGGETT, N., CHENG, J. F., OLSEN, A., LUCAS, S., ELKIN, C., UBERBACHER, E., FRAZIER, M., et al. 2001. Initial sequencing and analysis of the human genome. *Nature*, 409, 860-921.
- LEABMAN, M. K. & GIACOMINI, K. M. 2003. Estimating the contribution of genes and environment to variation in renal drug clearance. *Pharmacogenetics*, 13, 581-584.
- LEABMAN, M. K., HUANG, C. C., KAWAMOTO, M., JOHNS, S. J., STRYKE, D., FERRIN, T. E., DEYOUNG, J., TAYLOR, T., CLARK, A. G., HERSKOWITZ, I., GIACOMINI, K. M. & PHARMACOGENETICS MEMBRANE, T. 2002. Polymorphisms in a human kidney xenobiotic transporter, OCT2, exhibit altered function. *Pharmacogenetics*, 12, 395-405.
- LEBOVITZ, H. E. 1998. alpha-glucosidase inhibitors as agents in the treatment of diabetes. *Diabetes Reviews*, 6, 132-145.
- LEE, B., BUCK-KOEHNTOPT, B., MARTINEZ-YAMOUT, M., GOTTESFELD, J., DYSON, H. J. & WRIGHT, P. 2009a. Embryonic Neural Inducing Factor Churchill is not a DNA-Binding Zinc Finger Protein: Solution Structure Reveals a Solvent-Exposed Beta-Sheet and Zinc Binuclear Cluster. *Biological Magnetic Resonance Data Bank*.
- LEE, J., HWANG, Y., KANG, W., SEONG, S. J., LIM, M.-S., LEE, H. W., YIM, D.-S., SOHN, D. R., HAN, S. & YOON, Y.-R. 2012. Population Pharmacokinetic/Pharmacodynamic Modeling of Clopidogrel in Korean Healthy Volunteers and Stroke Patients. *Journal of Clinical Pharmacology*, 52.
- LEE, M. S. Y. 2001. Unalignable sequences and molecular evolution. *Trends in Ecology and Evolution*, 16, 681-685.
- LEE, W.-K., REICHHOLD, M., EDEMIR, B., CIARIMBOLI, G., WARTH, R., KOEPSSELL, H. & THEVENOD, F. 2009b. Organic cation transporters OCT1, 2, and 3 mediate high-

- affinity transport of the mutagenic vital dye ethidium in the kidney proximal tubule. *American Journal of Physiology-Renal Physiology*, 296, F1504-F1513.
- LEUNG, S., MATTMAN, A., SNYDER, F., KASSAM, R., MENEILLY, G. & NEXO, E. 2010. Metformin induces reductions in plasma cobalamin and haptocorrin bound cobalamin levels in elderly diabetic patients. *Clinical Biochemistry*, 43, 759-760.
- LEWIS, L. R., DAVIS, J., AKINOLA, A. & FISHER, J. S. 2009. Inhibition of ataxia telangiectasia mutated (ATM) prevents the prolonged increase in phosphorylation of Akt substrate of 160 kDa (AS160) subsequent to activation of the AMP-activated protein kinase (AMPK). *Faseb Journal*, 23.
- LI, J., SHAO, Y. H., GONG, Y. P., LU, Y. H., LIU, Y. & LI, C. L. 2014. Diabetes mellitus and dementia - a systematic review and meta-analysis. *European review for medical and pharmacological sciences*, 18, 1778-89.
- LIN, J. H. & LU, A. Y. H. 1997. Role of pharmacokinetics and metabolism in drug discovery and development. *Pharmacological Reviews*, 49, 403-449.
- LINDENBAUM, J., HEALTON, E. B., SAVAGE, D. G., BRUST, J. C. M., GARRETT, T. J., PODELL, E. R., MARCELL, P. D., STABLER, S. P. & ALLEN, R. H. 1988. NEUROPSYCHIATRIC DISORDERS CAUSED BY COBALAMIN DEFICIENCY IN THE ABSENCE OF ANEMIA OR MACROCYTOSIS. *New England Journal of Medicine*, 318, 1720-1728.
- LINDENBAUM, J., SAVAGE, D. G., STABLER, S. P. & ALLEN, R. H. 1990. Diagnosis of cobalamin deficiency .2. relative sensitivities of serum cobalamin, methylmalonic acid, and total homocysteine concentrations. *American Journal of Hematology*, 34, 99-107.
- LIPSKA, K. J., BAILEY, C. J. & INZUCCHI, S. E. 2011. Use of Metformin in the Setting of Mild-to-Moderate Renal Insufficiency. *Diabetes Care*, 34, 1431-1437.
- LIU, A. & COLEMAN, S. P. 2009. Determination of metformin in human plasma using hydrophilic interaction liquid chromatography-tandem mass spectrometry. *Journal of Chromatography B-Analytical Technologies in the Biomedical and Life Sciences*, 877, 3695-3700.
- LIU, K. W., DAI, L. K. & JEAN, W. 2006. Metformin-related vitamin B12 deficiency. *Age and Ageing*, 35, 200-201.
- LIU, Q., LI, S., QUAN, H. & LI, J. 2014. Vitamin B-12 Status in Metformin Treated Patients: Systematic Review. *Plos One*, 9.
- LOIKAS, S., KOSKINEN, P., IRJALA, K., LOPPONEN, M., ISOAHO, R., KIVELA, S.-L. & PELLINIEMI, T.-T. 2007. Renal impairment compromises the use of total homocysteine and methylmalonic acid but not total vitamin B-12 and holotranscobalamin in screening for vitamin B-12 deficiency in the aged. *Clinical Chemistry and Laboratory Medicine*, 45, 197-201.
- LONG, A. & ATWELL, C. 2012. Vitamin B<sub>12</sub> Deficiency Associated With Concomitant Metformin and Proton Pump Inhibitor Use. *Diabetes Care*.
- LOUGH, W. & WAINER, I. 1995. *High Performance Liquid Chromatography: Fundamental Principles and Practice*, Blackie Academic & Professional.
- LOVELL, S. C., DAVIS, I. W., ADRENDALL, W. B., DE BAKKER, P. I. W., WORD, J. M., PRISANT, M. G., RICHARDSON, J. S. & RICHARDSON, D. C. 2003. Structure validation by C alpha geometry: phi,psi and C beta deviation. *Proteins-Structure Function and Genetics*, 50, 437-450.
- MADORE, F., LOWRIE, E. G., BRUGNARA, C., LEW, N. L., LAZARUS, J. M., BRIDGES, K. & OWEN, W. F. 1997. Anemia in hemodialysis patients: Variables affecting this outcome predictor. *Journal of the American Society of Nephrology*, 8, 1921-1929.
- MALINOWSKI, J. M. & BOLESTA, S. 2000. Rosiglitazone in the treatment of type 2 diabetes mellitus: A critical review. *Clinical Therapeutics*, 22, 1151-1168.
- MARCIL, V., HARMEL, E., SPAHIS, S., GRENIER, E., BENDJOUDI, A., ELCHEBLY, M., ZIV, E., LAVILLE, M., BEAULIEU, J.-F. & LEVY, E. 2013. Do AMP-Activated Protein Kinase

- (AMPK) and Metformin Play a Role in the Small Intestine in Normal and Pathophysiological Conditions? *Gastroenterology*, 144, S711-S712.
- MARKS, P. W., HARRIS, N. L., ZARGHAMEE-GAVAMI, M., ZUKERBERG, L. R., WEXLER, D. J. & AXELROD, L. 2004. A 37-year-old woman with paresthesias of the arms and legs - Anatomical diagnosis - Pernicious anemia with autoimmune gastritis and vitamin B12 deficiency. *New England Journal of Medicine*, 351, 1333-1341.
- MARQUES, M. A. S., SOARES, A. D., PINTO, O. W., BARROSO, P. T. W., PINTO, D. P., FERREIRA, M. & WERNECK-BARROSO, E. 2007. Simple and rapid method determination for metformin in human plasma using high performance liquid chromatography tandem mass spectrometry: Application to pharmacokinetic studies. *Journal of Chromatography B-Analytical Technologies in the Biomedical and Life Sciences*, 852, 308-316.
- MARTEL, F., GRUNDEMANN, D., CALHAU, C. & SCHOMIG, E. 2001. Apical uptake of organic cations by human intestinal Caco-2 cells: putative involvement of ASF transporters. *Naunyn-Schmiedeberg's Archives of Pharmacology*, 363, 40-49.
- MAYFIELD, J. A. & WHITE, R. D. 2004. Insulin therapy for type 2 diabetes: Rescue, augmentation, and replacement of beta-cell function. *American Family Physician*, 70, 489-500.
- MAZOKOPAKIS, E. E. 2012. The old Schilling test as a necessary criterion at present for the diagnosis of food-cobalamin malabsorption (FCM) syndrome. *Hellenic Journal of Nuclear Medicine*, 15, 262-263.
- MAZOKOPAKIS, E. E. & STARAKIS, I. K. 2012. Recommendations for diagnosis and management of metformin-induced vitamin B12 (Cbl) deficiency. *Diabetes Research and Clinical Practice*, 97, 359-367.
- MAZZONE, T., CHAIT, A. & PLUTZKY, J. 2008. Cardiovascular disease risk in type 2 diabetes mellitus: insights from mechanistic studies. *Lancet*, 371, 1800-1809.
- MCGUFFIN, L. J., BRYSON, K. & JONES, D. T. 2000. The PSIPRED protein structure prediction server. *Bioinformatics*, 16, 404-405.
- MEALEY, B. L. & OCAMPO, G. L. 2007. Diabetes mellitus and periodontal disease. *Periodontology 2000*, 44, 127-153.
- MENENDEZ, J. A., OLIVERAS-FERRAROS, C., CUFI, S., COROMINAS-FAJA, B., JOVEN, J., MARTIN-CASTILLO, B. & VAZQUEZ-MARTIN, A. 2012. Metformin is synthetically lethal with glucose withdrawal in cancer cells. *Cell Cycle*, 11, 2782-2792.
- MENON, D., THOMPSON, P. A., BLANEY, S. M., ADAMSON, P. C. & BARRETT, J. S. 2006. Population pharmacokinetic model of imatinib mesylate and its metabolite in children. *Journal of Clinical Pharmacology*, 46.
- MESSIER, H., BRICKNER, H., GAIKWAD, J. & FOTEDAR, A. 1993. A novel pou domain protein which binds to the t-cell receptor-beta enhancer. *Molecular and Cellular Biology*, 13, 5450-5460.
- MINOT, G. R. & MURPHY, W. P. 1926. Treatment of pernicious anemia by a special diet. *Journal of the American Medical Association*, 87, 470-476.
- MOESTRUP, S. K., BIRN, H., FISCHER, P. B., PETERSEN, C. M., VERRONST, P. J., SIM, R. B., CHRISTENSEN, E. I. & NEXO, E. 1996. Megalin-mediated endocytosis of transcobalamin-vitamin-B-12 complexes suggests a role of the receptor in vitamin-B-12 homeostasis. *Proceedings of the National Academy of Sciences of the United States of America*, 93, 8612-8617.
- MOLLIN, D. L., BOOTH, C. C. & BAKER, S. J. 1957. The Absorption Of Vitamin-B12 In Control Subjects, In Addisonian Pernicious Anaemia And In The Malabsorption Syndrome. *British Journal of Haematology*, 3, 412-428.
- MOORE, E., MANDER, A., AMES, D., CARNE, R., SANDERS, K. & WATTERS, D. 2012. Cognitive impairment and vitamin B12: a review. *International Psychogeriatrics*, 24, 541-556.

- MORIDANI, M. B.-P., SHANA. 2006. Laboratory Investigation of Vitamin B12 Deficiency.
- MOROVAT, A., JAMES, T. S., COX, S. D., REES, M. C., GALES, M. A. & TAYLOR, R. P. 2006. Comparison of Bayer Advia Centaur (R) immunoassay results obtained on samples collected in four different Becton Dickinson Vacutainer (R) tubes. *Annals of Clinical Biochemistry*, 43, 481-487.
- MOSS, D. M., LIPTROTT, N. J., CURLEY, P., SICCARDI, M., BACK, D. J. & OWEN, A. 2013. Rilpivirine Inhibits Drug Transporters ABCB1, SLC22A1, and SLC22A2 In Vitro. *Antimicrobial Agents and Chemotherapy*, 57, 5612-5618.
- MOSS, D. M., LIPTROTT, N. J., SICCARDI, M. & OWEN, A. 2015. Interactions of antiretroviral drugs with the SLC22A1 (OCT1) drug transporter. *Frontiers in Pharmacology*, 6.
- MOURITS-ANDERSEN, T. & DITZEL, J. 1983. Megaloblastic anemia caused by malabsorption of vitamin B12 during long-term metformin therapy. *Ugeskrift for laeger*, 145, 25-6.
- MULGAONKAR, A., VENITZ, J., GRUENDEMANN, D. & SWEET, D. H. 2013. Human Organic Cation Transporters 1 (SLC22A1), 2 (SLC22A2), and 3 (SLC22A3) as Disposition Pathways for Fluoroquinolone Antimicrobials. *Antimicrobial Agents and Chemotherapy*, 57, 2705-2711.
- MULLER, J., LIPS, K. S., METZNER, L., NEUBERT, R. H. H., KOEPEL, H. & BRANDSCH, M. 2005. Drug specificity and intestinal membrane localization of human organic cation transporters (OCT). *Biochemical Pharmacology*, 70, 1851-1860.
- MUNGALL, A. J., PALMER, S. A., SIMS, S. K., EDWARDS, C. A., ASHURST, J. L., WILMING, L., JONES, M. C., HORTON, R., HUNT, S. E., SCOTT, C. E., GILBERT, J. G. R., CLAMP, M. E., BETHEL, G., MILNE, S., AINSCOUGH, R., ALMEIDA, J. P., AMBROSE, K. D., ANDREWS, T. D., ASHWELL, R. I. S., BABBAGE, A. K., BAGGULEY, C. L., BAILEY, J., BANERJEE, R., BARKER, D. J., BARLOW, K. F., BATES, K., BEARE, D. M., BEASLEY, H., BEASLEY, O., BIRD, C. P., BLAKEY, S., BRAY-ALLEN, S., BROOK, J., BROWN, A. J., BROWN, J. Y., BURFORD, D. C., BURRILL, W., BURTON, J., CARDER, C., CARTER, N. P., CHAPMAN, J. C., CLARK, S. Y., CLARK, G., CLEE, C. M., CLEGG, S., COBLEY, V., COLLIER, R. E., COLLINS, J. E., COLMAN, L. K., CORBY, N. R., COVILLE, G. J., CULLEY, K. M., DHAMI, P., DAVIES, J., DUNN, M., EARTHROWL, M. E., ELLINGTON, A. E., EVANS, K. A., FAULKNER, L., FRANCIS, M. D., FRANKISH, A., FRANKLAND, J., FRENCH, L., GARNER, P., GARNETT, J., GHORI, M. J. R., GILBY, L. M., GILLSON, C. J., GLITHERO, R. J., GRAFHAM, D. V., GRANT, M., GRIBBLE, S., GRIFFITHS, C., GRIFFITHS, M., HALL, R., HALLS, K. S., HAMMOND, S., HARLEY, J. L., HART, E. A., HEATH, P. D., HEATHCOTT, R., HOLMES, S. J., HOWDEN, P. J., HOWE, K. L., HOWELL, G. R., HUCKLE, E., HUMPHRAY, S. J., HUMPHRIES, M. D., HUNT, A. R., JOHNSON, C. M., JOY, A. A., KAY, M., KEENAN, S. J., KIMBERLEY, A. M., KING, A., LAIRD, G. K., LANGFORD, C., LAWLOR, S., LEONGAMORNLETT, D. A., LEVERSHA, M., et al. 2003. The DNA sequence and analysis of human chromosome 6. *Nature*, 425, 805-U1.
- NAKAMURA, Y., GOJOBORI, T. & IKEMURA, T. 2000. Codon usage tabulated from international DNA sequence databases: status for the year 2000. *Nucleic Acids Research*, 28, 292-292.
- NATHAN, D. M., BALKAU, B., BONORA, E., BORCH-JOHNSEN, K., BUSE, J. B., COLAGIURI, S., DAVIDSON, M. B., DEFRONZO, R., GENUTH, S., HOLMAN, R. R., JI, L., KIRKMAN, S., KNOWLER, W. C., SCHATZ, D., SHAW, J., SOBNGWI, E., STEFFES, M., VACCARO, O., WAREHAM, N., ZINMAN, B., KAHN, R. & INT EXPERT, C. 2009a. International Expert Committee Report on the Role of the A1C Assay in the Diagnosis of Diabetes. *Diabetes Care*, 32, 1327-1334.
- NATHAN, D. M., BUSE, J. B., DAVIDSON, M. B., FERRANNINI, E., HOLMAN, R. R., SHERWIN, R. & ZINMAN, B. 2009b. Medical Management of Hyperglycemia in Type 2 Diabetes: A Consensus Algorithm for the Initiation and Adjustment of

- Therapy A consensus statement of the American Diabetes Association and the European Association for the Study of Diabetes. *Diabetes Care*, 32, 193-203.
- NATIONAL HEALTH SERVICE NHS. 2012. *Vitamins and minerals - B vitamins and folic acid* [Online]. [Accessed].
- NAUCK, M., BISSE, E. & WIELAND, H. 2001. Pre-analytical conditions affecting the determination of the plasma homocysteine concentration. *Clinical Chemistry and Laboratory Medicine*, 39, 675-680.
- NEWSTEAD, S., DREW, D., CAMERON, A. D., POSTIS, V. L. G., XIA, X. B., FOWLER, P. W., INGRAM, J. C., CARPENTER, E. P., SANSOM, M. S. P., MCPHERSON, M. J., BALDWIN, S. A. & IWATA, S. 2011. Crystal structure of a prokaryotic homologue of the mammalian oligopeptide-proton symporters, PepT1 and PepT2. *Embo Journal*, 30, 417-426.
- NEXO, E. & ANDERSEN, J. 1977. Unsaturated And Cobalamin Saturated Transcobalamin-I And Transcobalamin-Ii In Normal Human-Plasma. *Scandinavian Journal of Clinical & Laboratory Investigation*, 37, 723-728.
- NG, P. C. & HENIKOFF, S. 2001. Predicting deleterious amino acid substitutions. *Genome Research*, 11, 863-874.
- NIAFAR, M., HAI, F., PORHOMAYON, J. & NADER, N. D. 2015. The role of metformin on vitamin B12 deficiency: a meta-analysis review. *Internal and Emergency Medicine*, 10, 93-102.
- NIE, W. X., SWEETSER, S., RINELLA, M. & GREEN, R. M. 2005. Transcriptional regulation of murine Slc22a1 (Oct1) by peroxisome proliferator agonist receptor-alpha and -gamma. *American Journal of Physiology-Gastrointestinal and Liver Physiology*, 288, G207-G212.
- NIELSEN, F., CHRISTENSEN, M. M. H. & BROSEN, K. 2014. Quantitation of Metformin in Human Plasma and Urine by Hydrophilic Interaction Liquid Chromatography and Application to a Pharmacokinetic Study. *Therapeutic Drug Monitoring*, 36, 211-217.
- NIELSEN, R., SORENSEN, B. S., BIRN, H., CHRISTENSEN, E. I. & NEXO, E. 2001. Transcellular transport of vitamin B-12 in LLC-PK1 renal proximal tubule cells. *Journal of the American Society of Nephrology*, 12, 1099-1106.
- NIEMI, M. 2010. Transporter Pharmacogenetics and Statin Toxicity. *Clinical Pharmacology & Therapeutics*, 87, 130-133.
- NIES, A. T., HOFMANN, U., RESCH, C., SCHAEFFELER, E., RIUS, M. & SCHWAB, M. 2011a. Proton Pump Inhibitors Inhibit Metformin Uptake by Organic Cation Transporters (OCTs). *Plos One*, 6.
- NIES, A. T., KOESELL, H., DAMME, K. & SCHWAB, M. 2011b. Organic Cation Transporters (OCTs, MATes), In Vitro and In Vivo Evidence for the Importance in Drug Therapy. *Drug Transporters*, 105-167.
- NIES, A. T., KOESELL, H., WINTER, S., BURK, O., KLEIN, K., KERB, R., ZANGER, U. M., KEPPLER, D., SCHWAB, M. & SCHAEFFELER, E. 2009. Expression of Organic Cation Transporters OCT1 (SLC22A1) and OCT3 (SLC22A3) Is Affected by Genetic Factors and Cholestasis in Human Liver. *Hepatology*, 50, 1227-1240.
- O'LEARY, F., ALLMAN-FARINELLI, M. & SAMMAN, S. 2012. Vitamin B-12 status, cognitive decline and dementia: a systematic review of prospective cohort studies. *British Journal of Nutrition*, 108, 1948-1961.
- OBEID, R., JUNG, J., FALK, J., HERRMANN, W., GEISEL, J., FRIESENHAHN-OCHS, B., LAMMERT, F., FASSBENDER, K. & KOSTOPOULOS, P. 2013. Serum vitamin B12 not reflecting vitamin B12 status in patients with type 2 diabetes. *Biochimie*, 95, 1056-1061.
- OBERLEY, M. J. & YANG, D. T. 2013. Laboratory testing for cobalamin deficiency in megaloblastic anemia. *American Journal of Hematology*, 88, 522-526.

- OOSTERHUIS, W. P., NIESSEN, R., BOSSUYT, P. M. M., SANDERS, G. T. B. & STURK, A. 2000. Diagnostic value of the mean corpuscular volume in the detection of vitamin B12 deficiency. *Scandinavian Journal of Clinical & Laboratory Investigation*, 60, 9-18.
- PAI, M. P. & PALOUCEK, F. P. 2000. The origin of the "ideal" body weight equations. *Annals of Pharmacotherapy*, 34, 1066-1069.
- PATADE, G. & MARITA, A. 2014. Metformin: A Journey from countryside to the bedside. *Journal of Obesity and Metabolic Research*, 1, 127-130.
- PENN, L., WHITE, M., OLDROYD, J., WALKER, M., ALBERTI, K. G. M. M. & MATHERS, J. C. 2009. Prevention of type 2 diabetes in adults with impaired glucose tolerance: the European Diabetes Prevention RCT in Newcastle upon Tyne, UK. *Bmc Public Health*, 9.
- PENTIKAINEN, P. J., NEUVONEN, P. J. & PENTTILA, A. 1979. Pharmacokinetics Of Metformin After Intravenous And Oral-Administration To Man. *European Journal of Clinical Pharmacology*, 16, 195-202.
- PETTERSEN, E. F., GODDARD, T. D., HUANG, C. C., COUCH, G. S., GREENBLATT, D. M., MENG, E. C. & FERRIN, T. E. 2004. UCSF chimera - A visualization system for exploratory research and analysis. *Journal of Computational Chemistry*, 25, 1605-1612.
- PIETERS, B., STAALS, J., KNOTTNERUS, I., ROUHL, R., MENHEERE, P., KESSELS, A. & LODDER, J. 2009. Periventricular White Matter Lucencies Relate to Low Vitamin B12 Levels in Patients With Small Vessel Stroke. *Stroke*, 40, 1623-1626.
- PITT, J. J. 2009. Principles and applications of liquid chromatography-mass spectrometry in clinical biochemistry. *The Clinical biochemist. Reviews / Australian Association of Clinical Biochemists*, 30, 19-34.
- POLLASTRI, G., PRZYBYLSKI, D., ROST, B. & BALDI, P. 2002. Improving the prediction of protein secondary structure in three and eight classes using recurrent neural networks and profiles. *Proteins-Structure Function and Genetics*, 47, 228-235.
- PORTA, V., SCHRAMM, S. G., KANO, E. K., KOONO, E. E., ARMANDO, Y. P., FUKUDA, K. & SERRA, C. H. R. 2008. HPLC-UV determination of metformin in human plasma for application in pharmacokinetics and bioequivalence studies. *Journal of Pharmaceutical and Biomedical Analysis*, 46, 143-147.
- POWELL, J. R. & GOBBURU, J. V. S. 2007. Pharmacometrics at FDA: Evolution and impact on decisions. *Clinical Pharmacology & Therapeutics*, 82.
- PRESCRIBING AND PRIMARY CARE TEAM, H. A. S. C. I. C. 2013. Prescribing for Diabetes, England 2005-06 to 2012-13
- PROCTOR, W. R., BOURDET, D. L. & THAKKER, D. R. 2008. Mechanisms underlying saturable intestinal absorption of metformin. *Drug Metabolism and Disposition*, 36, 1650-1658.
- RAMACHANDRAN, G. N., RAMAKRISHNAN, C. & SASISEKHARAN, V. 1963. Stereochemistry Of Polypeptide Chain Configurations. *Journal of Molecular Biology*, 7, 95-&.
- REINSTATLER, L., QI, Y. P., WILLIAMSON, R. S., GARN, J. V. & OAKLEY, G. P. 2012. Association of Biochemical B-12 Deficiency With Metformin Therapy and Vitamin B-12 Supplements The National Health and Nutrition Examination Survey, 1999-2006. *Diabetes Care*, 35, 327-333.
- REYNOLDS, E. 2006. Vitamin B12, folic acid, and the nervous system. *Lancet Neurology*, 5, 949-960.
- REZNICHENKO, A., SINKELER, S. J., SNIEDER, H., VAN DEN BORN, J., DE BORST, M. H., DAMMAN, J., VAN DIJK, M. C. R. F., VAN GOOR, H., HEPKEMA, B. G., HILLEBRANDS, J.-L., LEUVENINK, H. G. D., NIESING, J., BAKKER, S. J. L., SEELLEN, M. & NAVIS, G. 2013. SLC22A2 is associated with tubular creatinine secretion

- and bias of estimated GFR in renal transplantation. *Physiological Genomics*, 45, 201-209.
- RICKES, E. L., BRINK, N. G., KONIUSZY, F. R., WOOD, T. R. & FOLKERS, K. 1948. CRYSTALLINE VITAMIN-B12. *Science*, 107, 396-397.
- ROBERT, F., FENDRI, S., HARY, L., LACROIX, C., ANDREJAK, M. & LALAU, J. D. 2003. Kinetics of plasma and erythrocyte metformin after acute administration in healthy subjects. *Diabetes & Metabolism*, 29, 279-283.
- RUDD, M. F., WILLIAMS, R. D., WEBB, E. L., SCHMIDT, S., SELICK, G. S. & HOULSTON, R. S. 2005. The predicted impact of coding single nucleotide polymorphisms database. *Cancer Epidemiology Biomarkers & Prevention*, 14, 2598-2604.
- SABOROWSKI, M., ELORANTA, J. J., FRIED, M. & KULLAK-UBLICK, G. A. 2005. The human organic cation transporter 1 gene (SLC22A1) is transactivated by the hepatocyte nuclear factor 4 alpha (HNF-4 alpha) and its coactivator p300, and suppressed by the small heterodimer partner (SHP). *Gastroenterology*, 128, A751-A752.
- SABOROWSKI, M., KULLAK-UBLICK, G. A. & ELORANTA, J. J. 2006. The human organic cation transporter-1 gene is transactivated by hepatocyte nuclear factor-4 alpha. *Journal of Pharmacology and Experimental Therapeutics*, 317, 778-785.
- SAIER, M. H. 2000. A functional-phylogenetic classification system for transmembrane solute transporters. *Microbiology and Molecular Biology Reviews*, 64, 354-+.
- SAKATA, T., ANZAI, N., KIMURA, T., MIURA, D., FUKUTOMI, T., TAKEDA, M., SAKURAI, H. & ENDOU, H. 2010. Functional Analysis of Human Organic Cation Transporter OCT3 (SLC22A3) Polymorphisms. *Journal of Pharmacological Sciences*, 113, 263-266.
- SALPETER, S. R., GREYBER, E., PASTERNAK, G. A. & SALPETER, E. E. 2003. Risk of fatal and nonfatal lactic acidosis with metformin use in type 2 diabetes mellitus - Systematic review and meta-analysis. *Archives of Internal Medicine*, 163, 2594-2602.
- SALTIEL, A. R. & OLEFSKY, J. M. 1996. Thiazolidinediones in the treatment of insulin resistance and type II diabetes. *Diabetes*, 45, 1661-1669.
- SAMBOL, N. C., CHIANG, J., OCONNER, M., LIU, C. Y., LIN, E. T., GOODMAN, A. M., BENET, L. Z. & KARAM, J. H. 1996. Pharmacokinetics and pharmacodynamics of metformin in healthy subjects and patients with noninsulin-dependent diabetes mellitus. *Journal of Clinical Pharmacology*, 36, 1012-1021.
- SAMBUY, Y., ANGELIS, I., RANALDI, G., SCARINO, M. L., STAMMATI, A. & ZUCCO, F. 2005. The Caco-2 cell line as a model of the intestinal barrier: influence of cell and culture-related factors on Caco-2 cell functional characteristics. *Cell Biology and Toxicology*, 21, 1-26.
- SAMUELSSON, U., LUDVIGSSON, J. & SUNDKVIST, G. 1994. Islet-cell antibodies (ica), insulin autoantibodies (iaa), islet-cell surface antibodies (icsa) and c-peptide in 1031 school-children in a population with a high background incidence of iddm. *Diabetes Research and Clinical Practice*, 26, 155-162.
- SANCHEZ-ALVAREZ, R., MARTINEZ-OUTSCHOORN, U. E., LAMB, R., HULIT, J., HOWELL, A., GANDARA, R., SARTINI, M., RUBIN, E., LISANTI, M. P. & SOTGIA, F. 2013. Mitochondrial dysfunction in breast cancer cells prevents tumor growth Understanding chemoprevention with metformin. *Cell Cycle*, 12, 172-182.
- SANGER, F., NICKLEN, S. & COULSON, A. R. 1977. Dna Sequencing With Chain-Terminating Inhibitors. *Proceedings of the National Academy of Sciences of the United States of America*, 74, 5463-5467.
- SAUER, H. & WILMANN, W. 1977. Cobalamin Dependent Methionine Synthesis And Methyl-Folate-Trap In Human Vitamin-B12 Deficiency. *British Journal of Haematology*, 36, 189-198.

- SCARPELLO, J. 2001. Optimal dosing strategies for maximising the clinical response to metformin in type 2 diabetes. *The British Journal of Diabetes and Vascular Disease*, 1, 28-36.
- SCHAFER, G. 1976. Some new aspects on interaction of hypoglycemia-producing biguanides with biological-membranes. *Biochemical Pharmacology*, 25, 2015-2024.
- SCHAFER, J. L. 1999. Multiple imputation: a primer. *Statistical Methods in Medical Research*, 8, 3-15.
- SCHEEN, A. J. 1996. Clinical pharmacokinetics of metformin. *Clinical Pharmacokinetics*, 30, 359-371.
- SCHEEN, A. J. 2012. A review of gliptins in 2011. *Expert Opinion on Pharmacotherapy*, 13, 81-99.
- SCHILLING, R. F. 1953. intrinsic factor studies .2. the effect of gastric juice on the urinary excretion of radioactivity after the oral administration of radioactive vitamin-b12. *Journal of Laboratory and Clinical Medicine*, 42, 860-866.
- SCHILLING, R. F., HARRIS, J. W. & CASTLE, W. B. 1951. Observations on the etiologic relationship of achylia gastrica to pernicious anemia .8. Hematopoietic activity of vitamin-b12a (vitamin b12b). *Blood*, 6, 228-232.
- SCHWABEDISSEN, H. E. M. Z., VERSTUYFT, C., KROEMER, H. K., BECQUEMONT, L. & KIM, R. B. 2010. Human multidrug and toxin extrusion 1 (MATE1/SLC47A1) transporter: functional characterization, interaction with OCT2 (SLC22A2), and single nucleotide polymorphisms. *American Journal of Physiology-Renal Physiology*, 298.
- SEELIGER, D. & DE GROOT, B. L. 2010. Ligand docking and binding site analysis with PyMOL and Autodock/Vina. *Journal of Computer-Aided Molecular Design*, 24, 417-422.
- SEETHARAM, B. 1999. Receptor-mediated endocytosis of cobalamin (vitamin B-12). *Annual Review of Nutrition*, 19, 173-195.
- SELHUB, J. 2002. Folate, vitamin B12 and vitamin B6 and one carbon metabolism. *The journal of nutrition, health & aging*, 6, 39-42.
- SELVAKUMAR, L. S. & THAKUR, M. S. 2012. Dipstick based immunochemiluminescence biosensor for the analysis of vitamin B-12 in energy drinks: A novel approach. *Analytica Chimica Acta*, 722, 107-113.
- SELVIN, E., MARINOPOULOS, S., BERKENBLIT, G., RAMI, T., BRANCATI, F. L., POWE, N. R. & GOLDEN, S. H. 2004. Meta-analysis: Glycosylated hemoglobin and cardiovascular disease in diabetes mellitus. *Annals of Internal Medicine*, 141, 421-431.
- SEMON, M., LOBRY, J. R. & DURET, L. 2006. No evidence for tissue-specific adaptation of synonymous codon usage in humans. *Molecular Biology and Evolution*, 23, 523-529.
- SHAH, P., VELLA, A., BASU, A., BASU, R., SCHWENK, W. F. & RIZZA, R. A. 2000. Lack of suppression of glucagon contributes to postprandial hyperglycemia in subjects with type 2 diabetes mellitus. *Journal of Clinical Endocrinology & Metabolism*, 85, 4053-4059.
- SHAW, S., JAYATILLEKE, E., BAUMAN, W. & HERBERT, V. 1993. Mechanism of b12 malabsorption and depletion due to metformin discovered by using serial serum holo-transcobalamin-ii (holotcii) (b12 on tcii) as a surrogate for serial schilling tests. *Blood*, 82, A432-A432.
- SHEINER, L. B. & BEAL, S. L. 1983. Evaluation Of Nonmem - A Method For Estimating Population Pharmacokinetic Parameters. *Clinical Pharmacology & Therapeutics*, 33, 202-202.
- SHU, Y., LEABMAN, M. K., FENG, B., MANGRAVITE, L. M., HUANG, C. C., STRYKE, D., KAWAMOTO, M., JOHNS, S. J., DEYOUNG, J., CARLSON, E., FERRIN, T. E.,

- HERSKOWITZ, I., GIACOMINI, K. M. & PHARMACOGENETICS MEMBRANE, T. 2003. Evolutionary conservation predicts function of variants of the human organic cation transporter, OCT1. *Proceedings of the National Academy of Sciences of the United States of America*, 100, 5902-5907.
- SHU, Y., SHEARDOWN, S. A., BROWN, C., OWEN, R. P., ZHANG, S. Z., CASTRO, R. A., IANCULESCU, A. G., YUE, L., LO, J. C., BURCHARD, E. G., BRETT, C. M. & GIACOMINI, K. M. 2007. Effect of genetic variation in the organic cation transporter 1 (OCT1) on metformin action. *Journal of Clinical Investigation*, 117, 1422-1431.
- SIGRIST, C. J. A., CERUTTI, L., HULO, N., GATTIKER, A., FALQUET, L., PAGNI, M., BAIROCH, A. & BUCHER, P. 2002. PROSITE: a documented database using patterns and profiles as motif descriptors. *Briefings in bioinformatics*, 3, 265-74.
- SIMHA, V. & GARG, A. 2008. Atypical Forms of Type 2 Diabetes. *Type 2 Diabetes Mellitus: an Evidence-Based Approach to Practical Management*, 413-431.
- SINGH, N., ARMSTRONG, D. G. & LIPSKY, B. A. 2005. Preventing foot ulcers in patients with diabetes. *Jama-Journal of the American Medical Association*, 293, 217-228.
- SLOTTA, K. H. & TSCHESCHE, R. 1929. On biguanides, II. The blood sugar-abating effect of biguanides. *Berichte Der Deutschen Chemischen Gesellschaft*, 62, 1398-1405.
- SNOW, C. F. 1999. Laboratory diagnosis of vitamin B-12 and folate deficiency - A guide for the primary care physician. *Archives of Internal Medicine*, 159, 1289-1298.
- SOMOGYI, A., STOCKLEY, C., KEAL, J., ROLAN, P. & BOCHNER, F. 1987. Reduction Of Metformin Renal Tubular Secretion By Cimetidine In Man. *British Journal of Clinical Pharmacology*, 23, 545-551.
- SONNHAMMER, E. L., VON HEIJNE, G. & KROGH, A. 1998. A hidden Markov model for predicting transmembrane helices in protein sequences. *Proceedings / ... International Conference on Intelligent Systems for Molecular Biology ; ISMB. International Conference on Intelligent Systems for Molecular Biology*, 6, 175-82.
- SRINIVASAN, B., TAUB, N., KHUNTI, K. & DAVIES, M. 2008. Diabetes: glycaemic control in type 2. *BMJ clinical evidence*, 2008.
- STEENTOFT, C., VAKHRUSHEV, S. Y., JOSHI, H. J., KONG, Y., VESTER-CHRISTENSEN, M. B., SCHJOLDAGER, K. T. B. G., LAVRSEN, K., DABELSTEEN, S., PEDERSEN, N. B., MARCOS-SILVA, L., GUPTA, R., BENNETT, E. P., MANDEL, U., BRUNAK, S., WANDALL, H. H., LEVERY, S. B. & CLAUSEN, H. 2013. Precision mapping of the human O-GalNAc glycoproteome through SimpleCell technology. *Embo Journal*, 32, 1478-1488.
- STOCKER, S. L., MORRISSEY, K. M., YEE, S. W., CASTRO, R. A., XU, L., DAHLIN, A., RAMIREZ, A. H., RODEN, D. M., WILKE, R. A., MCCARTY, C. A., DAVIS, R. L., BRETT, C. M. & GIACOMINI, K. M. 2013. The Effect of Novel Promoter Variants in MATE1 and MATE2 on the Pharmacokinetics and Pharmacodynamics of Metformin. *Clinical Pharmacology & Therapeutics*, 93, 186-194.
- STRACHAN, T. & READ, A. 2011. Human Molecular Genetics 4th Edition. *Human Molecular Genetics 4th Edition*, 1-781.
- STRATTON, I. M., ADLER, A. I., NEIL, H. A. W., MATTHEWS, D. R., MANLEY, S. E., CULL, C. A., HADDEN, D., TURNER, R. C., HOLMAN, R. R. & GRP, U. K. P. D. S. 2000. Association of glycaemia with macrovascular and microvascular complications of type 2 diabetes (UKPDS 35): prospective observational study. *British Medical Journal*, 321, 405-412.
- STUMVOLL, M., MITRAKOU, A., PIMENTA, W., JENSSEN, T., YKI-JARVINEN, H., VAN HAEFTEN, T., RENN, W. & GERICH, J. 2000. Use of the oral glucose tolerance test to assess insulin release and insulin sensitivity. *Diabetes Care*, 23, 295-301.
- SUM, C. F., WEBSTER, J. M., JOHNSON, A. B., CATALANO, C., COOPER, B. G. & TAYLOR, R. 1992. The Effect Of Intravenous Metformin On Glucose-Metabolism During Hyperglycemia In Type-2 Diabetes. *Diabetic Medicine*, 9, 61-65.

- SUN, Y., CONNORS, K. E. & YANG, D.-Q. 2007. AICAR induces phosphorylation of AMPK in an ATM-dependent, LKB1-independent manner. *Molecular and Cellular Biochemistry*, 306, 239-245.
- SUN, Y., LAI, M.-S. & LU, C.-J. 2005. Effectiveness of vitamin B12 on diabetic neuropathy: systematic review of clinical controlled trials. *Acta neurologica Taiwanica*, 14, 48-54.
- SUNYAEV, S., RAMENSKY, V., KOCH, I., LATHE, W., KONDRASHOV, A. S. & BORK, P. 2001. Prediction of deleterious human alleles. *Human Molecular Genetics*, 10, 591-597.
- TAL, S., SHAVIT, Y., STERN, F. & MALNICK, S. 2010. Association Between Vitamin B12 Levels and Mortality in Hospitalized Older Adults. *Journal of the American Geriatrics Society*, 58, 523-526.
- TANIHARA, Y., MASUDA, S., SATO, T., KATSURA, T., OYAWA, O. & INUI, K.-I. 2007. Substrate specificity of MATE1 and MATE2-K, human multidrug and toxin extrusions/H<sup>+</sup>-organic cation antiporters. *Biochemical Pharmacology*, 74, 359-371.
- TARASOVA, L., KALNINA, I., GELDNERE, K., BUMBURE, A., RITENBERGA, R., NIKITINAZAKE, L., FRIDMANIS, D., VAIVADE, I., PIRAGS, V. & KLOVINS, J. 2012. Association of genetic variation in the organic cation transporters OCT1, OCT2 and multidrug and toxin extrusion 1 transporter protein genes with the gastrointestinal side effects and lower BMI in metformin-treated type 2 diabetes patients. *Pharmacogenetics and Genomics*, 22.
- TESFAYE, S., CHATURVEDI, N., EATON, S. E. M., WARD, J. D., MANES, C., IONESCU-TIRGOVISTE, C., WITTE, D. R., FULLER, J. H. & COMPLICATIONS, E. P. 2005. Vascular risk factors and diabetic neuropathy. *New England Journal of Medicine*, 352, 341-350.
- TESFAYE, S., STEVENS, L. K., STEPHENSON, J. M., FULLER, J. H., PLATER, M., IONESCU-TIRGOVISTE, C., NUBER, A., POZZA, G. & WARD, J. D. 1996. Prevalence of diabetic peripheral neuropathy and its relation to glycaemic control and potential risk factors: The EURODIAB IDDM Complications Study. *Diabetologia*, 39, 1377-1384.
- THE HEALTH AND SOCIAL CARE INFORMATION CENTRE 2013. Prescription cost analysis England 2012.
- TIAN, Y., BREEDVELD, G. J., HUANG, S. Z., OOSTRA, B. A., HEUTINK, P. & LO, W. H. Y. 2002. Characterization of ZNF333, a novel double KRAB domain containing zinc finger gene on human chromosome 19p13.1. *Biochimica Et Biophysica Acta-Gene Structure and Expression*, 1577, 121-125.
- TING, R. Z. W., SZETO, C. C., CHAN, M. H. M., MA, K. K. & CHOW, K. M. 2006. Risk factors of vitamin B-12 deficiency in patients receiving metformin. *Archives of Internal Medicine*, 166, 1975-1979.
- TOMKIN, G. H. 1973. Malabsorption of vitamin-B12 in diabetic-patients treated with phenformin - comparison with metformin. *British Medical Journal*, 3, 673-675.
- TOMKIN, G. H., HADDEN, D. R., WEAVER, J. A. & MONTGOME.DA 1971. Vitamin-B12 Status Of Patients On Long-Term Metformin Therapy. *British Medical Journal*, 2, 685-&.
- TOYAMA, K., YONEZAWA, A., TSUDA, M., TERADA, T., KATSURA, T. & INUI, K.-I. 2011. Disruption of multidrug and toxin extrusion 1 (MATE1) causes metformin-induced lactic acidosis. *Drug Metabolism Reviews*, 43.
- TU, M., SUN, S., WANG, K., PENG, X., WANG, R., LI, L., ZENG, S., ZHOU, H. & JIANG, H. 2013. Organic cation transporter 1 mediates the uptake of monocrotaline and plays an important role in its hepatotoxicity. *Toxicology*, 311, 225-230.

- TUCKER, G. T., CASEY, C., PHILLIPS, P. J., CONNOR, H., WARD, J. D. & WOODS, H. F. 1981. METFORMIN KINETICS IN HEALTHY-SUBJECTS AND IN PATIENTS WITH DIABETES-MELLITUS. *British Journal of Clinical Pharmacology*, 12, 235-246.
- TURNER, R. C., HOLMAN, R. R., CULL, C. A., STRATTON, I. M., MATTHEWS, D. R., FRIGHI, V., MANLEY, S. E., NEIL, A., MCELROY, K., WRIGHT, D., KOHNER, E., FOX, C., HADDEN, D., MEHTA, Z., SMITH, A., NUGENT, Z., PETO, R., ADLEL, A. I., MANN, J. I., BASSETT, P. A., OAKES, S. F., DORNAN, T. L., ALDINGTON, S., LIPINSKI, H., COLLUM, R., HARRISON, K., MACINTYRE, C., SKINNER, S., MORTEMORE, A., NELSON, D., COCKLEY, S., LEVIEN, S., BODSWORTH, L., WILLOX, R., BIGGS, T., DOVE, S., BEATTIE, E., GRADWELL, M., STAPLES, S., LAM, R., TAYLOR, F., LEUNG, L., CARTER, R. D., BROWNLEE, S. M., FISHER, K. E., ISLAM, K., JELFS, R., WILLIAMS, P. A., WILLIAMS, F. A., SUTTON, P. J., AYRES, A., LOGIE, L. J., LOVATT, C., EVANS, M. A., STOWELL, L. A., ROSS, I., KENNEDY, I. A., CROFT, D., KEEN, A. H., ROSE, C., RAIKOU, M., FLETCHER, A. E., BULPITT, C., BATTERSBY, C., YUDKIN, J. S., STEVENS, R., STEARN, M. R., PALMER, S. L., HAMMERSLEY, M. S., FRANKLIN, S. L., SPIVEY, R. S., LEVY, J. C., TIDY, C. R., BELL, N. J., STEEMSON, J., BARROW, B. A., COSTER, R., WARING, K., NOLAN, L., TRUSCOTT, E., WALRAVENS, N., COOK, L., LAMPARD, H., MERLE, C., PARKER, P., MCVITTIE, J., DRAISEY, I., MURCHISON, L. E., BRUNT, A. H. E., WILLIAMS, M. J., PEARSON, D. W., PETRIE, X. M. P., LEAN, M. E. J., WALMSLEY, D., LYALL, F., CHRISTIE, E., CHURCH, J., THOMSON, E., FARROW, A., STOWERS, J. M., et al. 1998. Intensive blood-glucose control with sulphonylureas or insulin compared with conventional treatment and risk of complications in patients with type 2 diabetes (UKPDS 33). *Lancet*, 352, 837-853.
- TZVETKOV, M. V., VORMFELDE, S. V., BALEN, D., MEINEKE, I., SCHMIDT, T., SEHRT, D., SABOLIC, I., KOEPEL, H. & BROCKMOELLER, J. 2009. The Effects of Genetic Polymorphisms in the Organic Cation Transporters OCT1, OCT2, and OCT3 on the Renal Clearance of Metformin. *Clinical Pharmacology & Therapeutics*, 86, 299-306.
- UM, J. H., YANG, S., YAMAZAKI, S., KANG, H., VIOLLET, B., FORETZ, M. & CHUNG, J. H. 2007. Activation of 5'-AMP-activated kinase with diabetes drug metformin induces casein kinase I epsilon (CKI epsilon)-dependent degradation of clock protein mPer2. *Journal of Biological Chemistry*, 282, 20794-20798.
- UNIPROT 2015. Universal Protein Resource.
- VALENCIA, C. A., HUSAMI, A., QIAN, Y., ZHANG, K. & PERVAIZ, M. A. 2013. Sanger Sequencing Principles, History, and Landmarks. *Next Generation Sequencing Technologies in Medical Genetics*, 3-11.
- VAN BELLE, T. L., COPPIETERS, K. T. & VON HERRATH, M. G. 2011. Type 1 Diabetes: Etiology, Immunology, and Therapeutic Strategies. *Physiological Reviews*, 91, 79-118.
- VAN DE MERBEL, N. C., WILKENS, G., FOWLES, S., OOSTERHUIS, B. & JONKMAN, J. H. G. 1998. LC phases improve, but not all assays do: Metformin bioanalysis revisited. *Chromatographia*, 47, 542-546.
- VAN LEEUWEN, N., NIJPELS, G., BECKER, M. L., DESHMUKH, H., ZHOU, K., STRICKER, B. H. C., UITTERLINDEN, A. G., HOFMAN, A., VAN 'T RIET, E., PALMER, C. N. A., GUIGAS, B., SLAGBOOM, P. E., DURRINGTON, P., CALLE, R. A., NEIL, A., HITMAN, G., LIVINGSTONE, S. J., COLHOUN, H., HOLMAN, R. R., MCCARTHY, M. I., DEKKER, J. M., T HART, L. M. & PEARSON, E. R. 2012. A gene variant near ATM is significantly associated with metformin treatment response in type 2 diabetes: a replication and meta-analysis of five cohorts. *Diabetologia*, 55, 1971-1977.
- VECCHIO, S., GIAMPRETI, A., PETROLINI, V. M., LONATI, D., PROTTI, A., PAPA, P., ROGNONI, C., VALLI, A., ROCCHI, L., ROLANDI, L., MANZO, L. & LOCATELLI, C. A. 2014. Metformin accumulation: Lactic acidosis and high plasmatic metformin

- levels in a retrospective case series of 66 patients on chronic therapy. *Clinical Toxicology*, 52, 129-135.
- VESTERQVIST, O., NABBIE, F. & SWANSON, B. 1998. Determination of metformin in plasma by high-performance liquid chromatography after ultrafiltration. *Journal of Chromatography B*, 716, 299-304.
- VIALOU, V., AMPHOUX, A., ZWART, R., GIROS, B. & GAUTRON, S. 2004. Organic cation transporter 3 (Slc22a3) is implicated in salt-intake regulation. *Journal of Neuroscience*, 24, 2846-2851.
- VIDON, N., CHAUSSADE, S., NOEL, M., FRANCHISSEUR, C., HUCHET, B. & BERNIER, J. J. 1988. Metformin In The Digestive-Tract. *Diabetes Research and Clinical Practice*, 4, 223-229.
- VILSBOLL, T. & HOLST, J. J. 2004. Incretins, insulin secretion and Type 2 diabetes mellitus. *Diabetologia*, 47, 357-366.
- VINIK, A. I., MASER, R. E., MITCHELL, B. D. & FREEMAN, R. 2003. Diabetic autonomic neuropathy. *Diabetes Care*, 26, 1553-1579.
- WANG, D. S., JONKER, J. W., KATO, Y., KUSUHARA, H., SCHINKEL, A. H. & SUGIYAMA, Y. 2002. Involvement of organic cation transporter 1 in hepatic and intestinal distribution of metformin. *Journal of Pharmacology and Experimental Therapeutics*, 302, 510-515.
- WANG, Y. W., TANG, Y. B., GU, J. K., FAWCETT, J. P. & BAI, X. 2004. Rapid and sensitive liquid chromatography-tandem mass spectrometric method for the quantitation of metformin in human plasma. *Journal of Chromatography B-Analytical Technologies in the Biomedical and Life Sciences*, 808, 215-219.
- WANG, Z.-J., YIN, O. Q. P., TOMLINSON, B. & CHOW, M. S. S. 2008. OCT2 polymorphisms and in-vivo renal functional consequence: studies with metformin and cimetidine. *Pharmacogenetics and Genomics*, 18, 637-645.
- WASS, M. N., KELLEY, L. A. & STERNBERG, M. J. E. 2010. 3DLigandSite: predicting ligand-binding sites using similar structures. *Nucleic Acids Research*, 38, W469-W473.
- WEIR, D. G. & SCOTT, J. M. 1995. The Biochemical Basis Of The Neuropathy In Cobalamin Deficiency. *Baillieres Clinical Haematology*, 8, 479-497.
- WELCH, G. N. & LOSCALZO, J. 1998. Homocysteine and atherothrombosis. *New England Journal of Medicine*, 338, 1042-1050.
- WHO 2011. Use of glycated haemoglobin (HbA1c) in the diagnosis of diabetes mellitus. *Diabetes Research and Clinical Practice*, 93, 299-309.
- WIERNSPERGER, N. F. & BAILEY, C. J. 1999. The antihyperglycaemic effect of metformin - Therapeutic and cellular mechanisms. *Drugs*, 58, 31-39.
- WILCOCK, C., WYRE, N. D. & BAILEY, C. J. 1991. SUBCELLULAR-DISTRIBUTION OF METFORMIN IN RAT-LIVER. *Journal of Pharmacy and Pharmacology*, 43, 442-444.
- WILE, D. J. & TOTH, C. 2010. Association of Metformin, Elevated Homocysteine, and Methylmalonic Acid Levels and Clinically Worsened Diabetic Peripheral Neuropathy. *Diabetes Care*, 33, 156-161.
- WILLIAMS, R., AIREY, M., BAXTER, H., FORRESTER, J., KENNEDY-MARTIN, T. & GIRACH, A. 2004. Epidemiology of diabetic retinopathy and macular oedema: a systematic review. *Eye*, 18, 963-983.
- WINGENDER, E., CHEN, X., HEHL, R., KARAS, H., LIEBICH, I., MATYS, V., MEINHARDT, T., PRUSS, M., REUTER, I. & SCHACHERER, F. 2000. TRANSFAC: an integrated system for gene expression regulation. *Nucleic Acids Research*, 28, 316-319.
- WONG, C. W. 2015. Vitamin B-12 deficiency in the elderly: is it worth screening? *Hong Kong Medical Journal*, 21, 155-164.
- WORLD HEALTH ORGANIZATION 2014. Global status report on noncommunicable diseases 2014. *Global Status Report on Noncommunicable Diseases 2014*, VII-IX.

- WRIGHT, S. H. & DANTZLER, W. H. 2004. Molecular and cellular physiology of renal organic cation and anion transport. *Physiological Reviews*, 84, 987-1049.
- WULFFELE, M. G., KOOY, A., LEHERT, P., BETS, D., OGTEROP, J. C., VAN DER BURG, B. B., DONKER, A. J. M. & STEHOUWER, C. D. A. 2003. Effects of short-term treatment with metformin on serum concentrations of homocysteine, folate and vitamin B12 in type 2 diabetes mellitus: a randomized, placebo-controlled trial. *Journal of Internal Medicine*, 254, 455-463.
- XIA, L., ENGEL, K., ZHOU, M. & WANG, J. 2007. Membrane localization and pH-dependent transport of a newly cloned organic cation transporter (PMAT) in kidney cells. *American Journal of Physiology-Renal Physiology*, 292, F682-F690.
- YIN, Y., HE, X., SZEWCZYK, P., NGUYEN, T. & CHANG, G. 2006. Structure of the multidrug transporter EmrD from *Escherichia coli*. *Science*, 312, 741-744.
- YOON, H., CHO, H.-Y., YOO, H.-D., KIM, S.-M. & LEE, Y.-B. 2013. Influences of Organic Cation Transporter Polymorphisms on the Population Pharmacokinetics of Metformin in Healthy Subjects. *Aaps Journal*, 15, 571-580.
- YUE, P., MELAMUD, E. & MOULT, J. 2006. SNPs3D: Candidate gene and SNP selection for association studies. *Bmc Bioinformatics*, 7.
- YUEN, K. H. & PEH, K. K. 1998. Simple high-performance liquid chromatographic method for the determination of metformin in human plasma. *Journal of Chromatography B*, 710, 243-246.
- ZAIR, Z. M., ELORANTA, J. J., STIEGER, B. & KULLAK-UBLICK, G. A. 2008. Pharmacogenetics of OATP (SLC21/SLCO), OAT and OCT (SLC22) and PEPT (SLC15) transporters in the intestine, liver and kidney. *Pharmacogenomics*, 9, 597-624.
- ZARGHI, A., FOROUTAN, S. M., SHAFATI, A. & KHODDAM, A. 2003. Rapid determination of metformin in human plasma using ion-pair HPLC. *Journal of Pharmaceutical and Biomedical Analysis*, 31, 197-200.
- ZHANG, X. H., SHIRAHATTI, N. V., MAHADEVAN, D. & WRIGHT, S. H. 2005. A conserved glutamate residue in transmembrane helix 10 influences substrate specificity of rabbit OCT2 (SLC22A2). *Journal of Biological Chemistry*, 280, 34813-34822.
- ZHAO, L., LI, Q., LI, X., YIN, R., CHEN, X., GENG, L. & BI, K. 2012. Bioequivalence and Population Pharmacokinetic Modeling of Two Forms of Antibiotic, Cefuroxime Lysine and Cefuroxime Sodium, after Intravenous Infusion in Beagle Dogs. *Journal of Biomedicine and Biotechnology*.
- ZHOU, K., BELLENGUEZ, C., SPENCER, C. C. A., BENNETT, A. J., COLEMAN, R. L., TAVENDALE, R., HAWLEY, S. A., DONNELLY, L. A., SCHOFIELD, C., GROVES, C. J., BURCH, L., CARR, F., STRANGE, A., FREEMAN, C., BLACKWELL, J. M., BRAMON, E., BROWN, M. A., CASAS, J. P., CORVIN, A., CRADDOCK, N., DELOUKAS, P., DRONOV, S., DUNCANSON, A., EDKINS, S., GRAY, E., HUNT, S., JANKOWSKI, J., LANGFORD, C., MARKUS, H. S., MATHEW, C. G., PLOMIN, R., RAUTANEN, A., SAWCER, S. J., SAMANI, N. J., TREMBATH, R., VISWANATHAN, A. C., WOOD, N. W., HARRIES, L. W., HATTERSLEY, A. T., DONEY, A. S. F., COLHOUN, H., MORRIS, A. D., SUTHERLAND, C., HARDIE, D. G., PELTONEN, L., MCCARTHY, M. I., HOLMAN, R. R., PALMER, C. N. A., DONNELLY, P., PEARSON, E. R., GO, D. U. D. P., WELLCOME TRUST CASE CONTROL, C. & INVESTIGATORS, M. 2011. Common variants near ATM are associated with glycemic response to metformin in type 2 diabetes. *Nature Genetics*, 43, 117-U57.
- ZHOU, M., XIA, L. & WANG, J. 2007a. Metformin transport by a newly cloned proton-stimulated organic cation transporter (plasma membrane monoamine transporter) expressed in human intestine. *Drug Metabolism and Disposition*, 35, 1956-1962.
- ZHOU, M. Y. & WANG, J. 2006. Transport of metformin by a newly cloned polyspecific organic cation transporter PMAT. *Drug Metabolism Reviews*, 38, 385.

- ZHOU, M. Y., XIA, L., ENGEL, K. & WANG, J. 2007b. Molecular determinants of substrate selectivity of a novel organic cation transporter (PMAT) in the SLC29 family. *Journal of Biological Chemistry*, 282, 3188-3195.
- ZOLK, O. 2012. Disposition of metformin: Variability due to polymorphisms of organic cation transporters. *Annals of Medicine*, 44, 119-129.
- ZWART, R., VERHAAGH, S., BUITELAAR, M., POPP-SNIJDERS, C. & BARLOW, D. P. 2001. Impaired activity of the extraneuronal monoamine transporter system known as uptake-2 in *Orct3/Slc22a3*-deficient mice. *Molecular and Cellular Biology*, 21, 4188-4196.